VOLUME 84 NO. ST5
SEPTEMBER 1958
PART 1

JOURNAL of the

Structural Division

PROCEEDINGS OF THE

AMERICAN SOCIETY
OF CIVIL ENGINEERS

BASIC REQUIREMENTS FOR MANUSCRIPTS

This Journal represents an effort by the Society to deliver information to the reader with the greatest possible speed. To this end the material herein has none of the usual editing required in more formal publications.

Original papers and discussions of current papers should be submitted to the Manager of Technical Publications, ASCE. Authors should indicate the technical division to which the paper should be referred. The final date on which a discussion should reach the Society is given as a footnote with each paper. Those who are planning to submit material will expedite the review and publication procedures by complying with the following basic requirements:

1. Titles should have a length not exceeding 50 characters and spaces.

2. A 50-word summary should accompany the paper.

3. The manuscript (a ribbon copy and two copies) should be double-spaced on one side of 8½-in. by 11-in. paper. Papers that were originally prepared for oral presentation must be rewritten into the third person before being submitted.

4. The author's full name, Society membership grade, and footnote reference stating present employment should appear on the first page of the paper.

5. Mathematics are reproduced directly from the copy that is submitted. Because of this, it is necessary that capital letters be drawn, in black ink, ⅛-in. high (with all other symbols and characters in the proportions dictated by standard drafting practice) and that no line of mathematics be longer than 6½-in. Ribbon copies of typed equations may be used but they will be proportionately smaller on the printed version.

6. Tables should be typed (ribbon copies) on one side of 8½-in. by 11-in. paper with a 6½-in. by 10½-in. invisible frame. Small tables should be grouped within this frame. Specific reference and explanation should be made in the text for each table.

7. Illustrations should be drawn in black ink on one side of 8½-in. by 11-in. paper within an invisible frame that measures 6½-in. by 10½-in.; the caption should also be included within the frame. Because illustrations will be reduced to 69% of the original size, the capital letters should be ⅛-in. high. Photographs should be submitted as glossy prints in a size that is less than 6½-in. by 10½-in. Explanations and descriptions should be made within the text for each illustration.

8. Papers should average about 12,000 words in length and should be no longer than 18,000 words. As an approximation, each full page of typed text, table, or illustration is the equivalent of 300 words.

Further information concerning the preparation of technical papers is contained in the "Technical Publications Handbook" which can be obtained from the Society.

Reprints from this Journal may be made on condition that the full title of the paper, name of author, page reference (or paper number), and date of publication by the Society are given. The Society is not responsible for any statement made or opinion expressed in its publications.

This Journal is published monthly by the American Society of Civil Engineers. Publication office is at 2500 South State Street, Ann Arbor, Michigan. Editorial and General Offices are at 33 West 39 Street, New York 18, New York. $4.00 of a member's dues are applied as a subscription to this Journal. Second-class mail privileges are authorized at Ann Arbor, Michigan.

Journal of the

STRUCTURAL DIVISION

Proceedings of the American Society of Civil Engineers

STRUCTURAL DIVISION
EXECUTIVE COMMITTEE
Leo H. Corning, Chairman; George S. Vincent, Vice-Chairman;
Robert D. Dewell; Elmer K. Timby; Myle J. Holley, Jr., Secretary

COMMITTEE ON PUBLICATIONS
Nathan W. Morgan, Chairman; Mace H. Bell; Gerald F. Borrmann;
Edwin S. Elcock; Kurt H. Gerstle; Wayne C. Lewis; Alfred L. Parme;
Henry G. Schlitt; Philip A. Upp

CONTENTS

September, 1958

Papers

Number

Thermal Considerations in the Design of Concrete Shields
by Harold Davis 1755

An Analytical and Experimental Study of Helicoidal Girders
by Y. F. Young and A. C. Scordelis. 1756

Practical Aspects of Ultimate Strength Design
by Alfred L. Parme 1757

Numerical Analysis of Two-Hinged Arches
by Thomas D. Y. Fok and Tung Au 1758

High-Speed Computer Applied to Bridge Impact
by Charles T. G. Looney 1759

Causes of Deterioration and Protective Methods for Timber:
Progress Report of a Sub-Committee of the Committee on
Timber Construction of the Structural Division 1760

(Over)

Copyright 1958 by the American Society of Civil Engineers.

Number

Analysis of Rigid Frames by Successive Replacement
by Chen Loh-Kwan and Li Seung Ping 1761

Analysis of Continuous Beams by Carry-over Moments
by Jan J. Tuma 1762

General Considerations for Reactors and Related Plant Types
by John F. Stolz 1763

Analysis of Frames with Curved and Bent Members
by Jan J. Tuma, Kerry S. Havner and Frank Hedges 1764

Discussion 1787

Paper 1755 September, 1958 ST 5

Journal of the
STRUCTURAL DIVISION
Proceedings of the American Society of Civil Engineers

THERMAL CONSIDERATIONS IN THE DESIGN OF CONCRETE SHIELDS[a]

Harold S. Davis,[1] A. M. ASCE
(Proc. Paper 1755)

SYNOPSIS

The behavior and properties of concrete structures for shielding atomic power plants are discussed briefly. Methods are presented for estimating thermal effects associated with linear and non-linear distributions of temperature, nuclear heating, and shield cooling. These data and procedures are subsequently used for analyzing several design problems and thermal criteria.

INTRODUCTION

Portland cement concrete has been used successfully for constructing numerous shielding structures during the past 15 years. In order to protect concrete from the harmful effects of intense nuclear radiations and high temperatures, elaborate and expensive "thermal" shields are often interposed between the reactor core and the concrete shield. Justifiable conservatism prevails in the design of these shields due to the lack of design data and specific experience. However, if the cost of atomic power is to become competitive with other sources of electricity in the United States, conservatism must be replaced with a realistic appraisal of material properties and a more efficient use of construction materials, including concrete. Since thermal considerations often limit how and where concrete can be used, a discussion of the subject is in order.

Presented below is a review of the effects which radiation and temperatures have on the physical properties of concrete. This is followed by a

Note: Discussion open until February 1, 1959. To extend the closing date one month, a written request must be filed with the Executive Secretary, ASCE. Paper 1755 is part of the copyrighted Journal of the Structural Division, Proceedings of the American Society of Civil Engineers, Vol. 84, No. ST 5, September 1958.

a. This paper is similar to the paper sponsored by the ASCE and presented by the author at the 1958 Nuclear Congress held March 17-21, 1958 in Chicago, Ill.

1. Senior Engr., Hanford Atomic Products Operation, General Electric Co., Richland, Wash.

discussion of certain thermal factors which should be considered during the design of a concrete shield. It is emphasized that the discussion is directed to the engineer who is responsible for the conceptual or preliminary design, and that the approach may appear rather crude at times. However, it must be remembered that before one can analyze a structure or prepare a detailed cost estimate, the dimensions and material properties must be defined. Also, the methods described in this paper for estimating temperatures and thermal stresses are intended to give scale (order of magnitude), and are probably as accurate as present methods for estimating rates of heat generation and flux levels in the shield. It is hoped that the criteria and data presented herein will reduce the time and effort required to design radiation shields and that they will assist the engineer in utilizing concrete effectively in shield construction.

Radiation Damage to Concrete

The shield designer is constantly beset with the question of how much radiation a concrete shield can stand without serious damage. Unfortunately, only limited data are available for answering this question. Experiments performed at BEPO indicate that concrete will have a life of at least ten years in a flux of 10^{11} neutrons/cm^2-sec.(1) Experiments carried out in this country indicate that portland cement concrete may be damaged if subjected to an integrated flux in excess of 3×10^{20} neutrons and gammas/cm^2.(2) This is equivalent to ten years at a combined flux of 10^{12} neutrons and gammas/cm^2-sec. These data are not conclusive due to the limited number of tests performed and the few types of concrete studied. In some cases, the loss in compressive strength observed for irradiated specimens can be attributed primarily to temperature effects. It is believed that damage to concrete caused by related thermal effects is greater than that due to radiation. However, this observation is based upon radiation levels somewhat lower than those given above. Additional tests for evaluating radiation damage to concrete are needed and should be performed in such a manner as to distinguish between thermal damage and radiation damage.

Temperature Effects on the Properties of Concrete

In general, exposure to temperatures greater than about 73° F has a detrimental effect on the physical and shielding properties of concrete. However, for constant exposure at temperatures up to 150 or 200° F, the loss in strength is quite small; and for temperatures as high as 500 to 600° F, the deterioration in structural properties is ordinarily tolerable. The loss in strength for specimens of concrete subjected to wide fluctuations in temperature has been observed to be two or three times as great as for constant exposure to high temperature, depending upon the severity of the thermal cycle. Unfortunately, there is very little information published on thermal cycling of concrete, so that the shield designer must proceed cautiously in this direction.

Of interest are the data presented in Tables 1 and 2 for mortars and concrete made with heavy aggregates processed from hydrous iron ore obtained from the Running Wolf deposits in Montana. Approximately 9.6 and 7 bags of Type II portland cement were used per cubic yard of mortar and

TABLE 1

EFFECT OF HEATING ON PHYSICAL PROPERTIES OF MORTAR MADE WITH RUNNING WOLF SAND AND PORTLAND CEMENT

		2 x 2 x 11-in. Mortar Bars					
Curing Condition	Age (Days)	% Weight Change	% Length Change	Dyn. Mod. Elast. psi x 10-6	Mod. of Rupt. psi	Compressive Strength 2 in. Cubes (psi)	Tensile Strength Briquets (psi)
Moist	28	1.2	0.009	5.84	1164	6894	848
Lab. Air	90	-1.2	-0.040	5.71	1209	6894	1053
185° F	105	-4.7	-0.074	4.58			
185° F	120	-4.9	-0.076	4.71*	1701	6475	1167
390° F	120	-5.8	-0.161	3.89**	1505	6112	877
660° F	120	-8.0	-0.359	2.92	1364	6175	810
1110° F						4200	

* 4.78×10^6 psi after 30 thermal cycles 70° - 185° F

** 3.56×10^6 psi after an additional 20 cycles at 70° - 390° F

TABLE 2

PHYSICAL PROPERTIES OF CONCRETE "G"
MADE WITH RUNNING WOLF AGGREGATES

Specimen*	Age (Days)	28	90	106**	106**
a, b, c	Storage Condition	Moist	Lab. Air	185°F	660°F
a, b	Unit Weight (pcf)	224	221	218	209
a	Compressive Strength (psi)	6910	8910		6850
b	Modulus of Rupture (psi)	965	930	1015	840
c	Bond Strength (psi)				
	0.00005 in. Slippage	1200	1120		320
	0.0005 in. Slippage	1550	1430		880
	0.0015 in. Slippage	1580	Steel Failed		1300
a	Thermal Diffusivity (ft^2/hr)		0.32	0.34	
b	% Length Change	+0.002		-0.020	-0.111
b	% Weight Change	0.4		-2.4	-6.6
b	Coef. of Thermal Expansion ($in/in/^oF)(10^6$)	5.2		5.3	4.6
a	Mod. of Elasticity (psi x 10^{-6})(Taken at 3000 psi)	7.42	8.33		4.00

* Specimens: (a) 6-in. x 12-in. cylinders (b) 6-in. x 6-in. x 12-in. beams
(c) 9-in. cube with 3/4-in. steel bar

** All specimens cured 28 days in fog room followed by two months in laboratory air. Specimens heated two weeks at 185° F or 660° F, respectively.

concrete, respectively. The distinction between mortar and concrete rests in the fact that the mortar specimens were made with fine aggregate passing the 1/4 inch screen; whereas, the concrete specimens contain both fine and coarse aggregates. Both types had a water/cement ratio of 0.57 by weight. The data presented in Tables 1 and 2 are for a particular type of high density concrete made with exceedingly strong aggregates. It is noted that the modulus of elasticity, tensile and bonding properties of concrete are reduced more than compressive strength by exposure to high temperatures. The effect of temperature on the amount of water retained hydrous iron ore is shown in Fig. 1.

Exposure of concrete to temperatures above normal accelerates drying of the concrete and the removal of water required by the chemical processes of hydration and hardening. At temperatures above 200° F, some of the water of hydration is removed from the hardened paste in addition to the free, or evaporable, water. The amount of water retained in concrete is primarily a function of temperature and relative humidity, and is lower for high temperatures and dry surroundings. The amount of water retained by a hardened paste of portland cement is shown in Fig. 2. It is noted that specimens which were heated after being moist-cured for several months retained more water than the 28-day specimens. Also, the strength and density of heated specimens can be expected to be greater for well-cured concrete in which hydration is fairly complete. For this reason, it is desirable to moist-cure concrete continuously from the time it is placed until it has attained the desired structural and shielding properties.

As discussed above, dehydration of concrete decreases concrete strength in compression, flexure, tension and bond. Any loss in strength follows the loss in hydrated water from the hardened cement paste. Once equilibrium is reached in water content, corresponding to existing conditions of vapor pressure and temperature, no more strength is apparently lost, even after long periods of exposure. Loss of water also reduces the density of the concrete, as well as its coefficient of expansion and thermal conductivity. Upon loss of water, concrete also tends to shrink; and if restrained, cracking may occur. In some cases, thermal expansion offsets shrinkage effects. Volume changes (shrinkage and/or expansion) may be very important in some designs. High density concrete made with hydrous iron ore (limonite or goethite) will shrink more at elevated temperatures than concrete made with magnetite or barite. The coefficient of expansion for barite concrete is 1.5 to 2 times as great as that for other types of concrete.

It is well to point out that loss-of-strength data have usually been obtained by heating small specimens, and that these data may or may not be indicative of what takes place in a large concrete structure. Because of the nature of radiation heating within a shield and since heat sources are usually located near the inner portion of a shield, any damage will usually be restricted to the first foot or so of concrete. Also, it may take years for the water to diffuse through a thick concrete shield. Concrete is not a good heat conductor; the thermal conductivity ranges from about 0.9 to 2.7 B/ft-hr-° F.[3] If the first few inches of concrete are subjected to high temperatures, the concrete in this region loses some of its thermal conductivity and serves to protect the concrete in the interior of the wall. For these reasons, long exposure to moderately high temperatures is required to materially affect the strength and shielding properties of the concrete located in the middle and outside

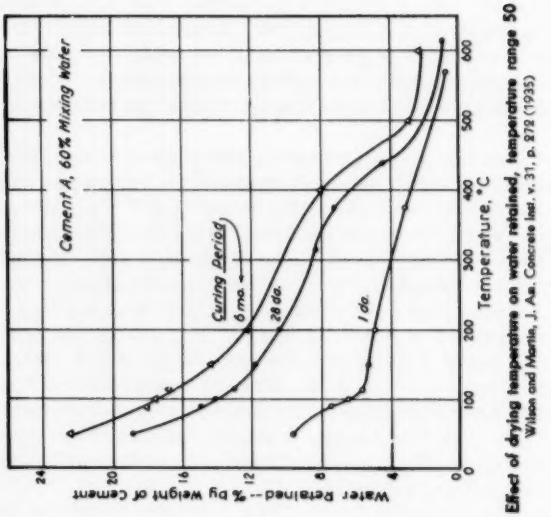

Fig 2 - Effect of drying temperature on water retained, temperature range 50 to 600C
Wilson and Mamis, J. Am. Concrete Inst. v. 31, p. 278 (1935)

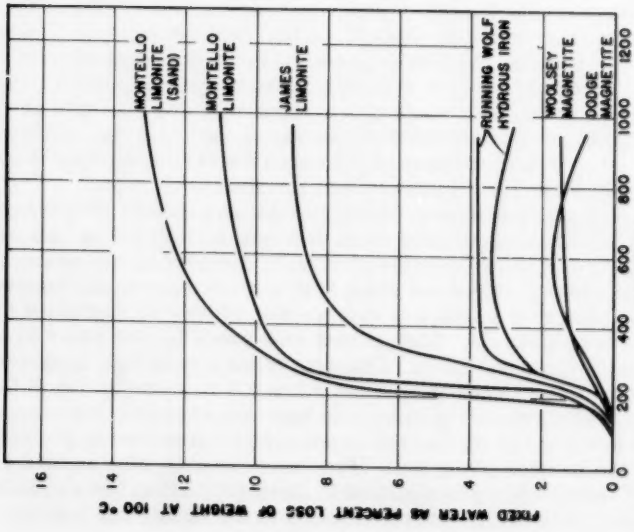

FIGURE 1
AVERAGE VALUES OF FIXED WATER CONTENT
FOR HEAVY AGGREGATES

portions of a concrete shield. (This may not be the case for an end shield pierced by numerous coolant pipes containing hot liquids.)

Attenuation Properties of Heated Concrete

Loss of water at high temperature decreases the attenuation effectiveness of concrete for neutrons and gamma radiation. Absorption coefficients for gamma rays of around 3 Mev vary almost directly with the density of the concrete, so that they may be decreased 5 to 10 per cent by heating, depending upon the weight of water lost. Attenuation effectiveness for fast neutrons is more sensitive to changes in water content since it depends upon hydrogen content as well as density. Equilibrium values of relaxation lengths for fast neutrons are summarized in Table 3 for heated slabs of high density concrete. These data were obtained in a shielding facility at HAPO, and correspond to static temperature exposures of 85 to 600° F. Although the density decreased about 5 per cent, the neutron relaxation lengths increased about 30 per cent. Both types of concrete were found to possess adequate moderating and absorption properties at these temperatures for slow, intermediate and fast neutrons.(4) Computed values of the neutron relaxation lengths based upon effective removal cross sections are summarized in Table 4 for conventional concrete containing 10 to less than 0.1 per cent water. In this example, the relaxation length for fast neutrons increased 35 per cent when the concrete was dehydrated.

TABLE 3

FAST NEUTRON ATTENUATION DATA FOR HEATED CONCRETE SLABS (a)

Bake Temp. °C	Iron-Masonite		Iron-Limonite		Magn.-Limonite		Magnetite		Ordinary	
	g/cm³	λ, cm.	g/cm³	λ, cm.	g/cm³	λ, cm.	g/cm³	λ, cm.	g/cm³	λ, cm.
Initial(b)	4.27	7.03	4.23	7.4	3.39	8.9	3.29	8.75	2.35	12.06
100			4.14	7.9	3.33	9.7	3.27	9.52	2.29	12.80
175			4.04	9.0	3.24	10.8				
200							3.25	9.75		
300							3.21	10.10		
320			4.05	9.4	3.26	10.9				

Note: (a) Values of density and fast neutron relaxation lengths are from "A Summary of Neutron Attenuation in Materials Tested at Hanford", by R. M. Fryar and E. G. Peterson, August, 1958.

(b) "As-cured" condition.

TABLE 4

NEUTRON ATTENUATION DATA
FOR CONVENTIONAL CONCRETE

(Computed Values Based Upon Effective
Neutron Removal Cross-Sections)

Unit Wt. (pcf)	Percent Water	W/C Ratio	Σ (cm^{-1})	Relaxation Length (cm)
153	10	0.742 (a)	0.0949	10.5
150	8	0.582	0.0896 (d)	11.2
147 (b)	6	0.427	0.0845	11.8
143	4	0.278	0.0796	12.5
141 (c)	2	0.136	0.0749	13.3
139	1	0.067	0.0726	13.7
138	0	0.0	0.0704	14.2

NOTE:

(a) Initial W/C Ratio - 0.60 with 6 bags of portland cement/ cu. yd.

(b) Corresponds to well cured, moist concrete at about 70° F.

(c) Corresponds to concrete dried at about 300° F.

(d) Σ = 0.0884 cm^{-1} reported in ORNL-2193, with a water content of 7.48 percent. See this document for typical composition.

Approximating Thermal Stresses in Slab Shields (Linear Temperature Distributions)

When considering thermal effects, analytical and graphical procedures can be used to define upper and lower limits of stress and strain which can then be used as a basis for applying engineering judgment. Judgment is required since the restraint present in a given structure is usually unknown and difficult to evaluate accurately. Likewise, the concrete may yield locally (plastic flow) or it may crack, both of which tend to alleviate thermal stresses.

It is noted that linear temperature variations in an isotropic, homogeneous body do not produce thermal stresses unless movements are restrained, either externally or internally. However, a free-standing wall of concrete is not "ideally" isotropic or homogeneous, so that linear temperature variations probably produce some thermal stresses. Also, a concrete wall is somewhat restrained at its base and along its edges. These conditions are usually neglected in analyzing ordinary concrete structures, but may be important in concrete shields subjected to severe heat loads.

Temperature stresses in a concrete wall can be studied by taking a vertical section of unit width as shown in Fig. 3-a. When the wall is heated on the inside, the internal fibers lengthen as shown in Fig. 3-c, assuming that the ends of the section are not restrained. A horizontal plane in the member moves from AB to AC, through a small angle-change ($\Delta\phi = \alpha t/h$), and the member bends to a circular curvature without producing thermal stress. In the above expression, α is the coefficient of expansion, and t is the temperature difference across a wall thickness of h.

If the ends of the member are prevented from rotating or moving vertically, the plane section remains at AB, while the end restraint produces the compression stress distribution corresponding to line CA in Fig. 3-c. The maximum temperature stress in this case will be equal to αtE, where E is the modulus of elasticity and αt is a measure of the restrained strains on the hot side. If the ends of the member are prevented from rotating only, section AB moves to the horizontal position ED as indicated in Fig. 3-d. In this case, compression stresses are produced on the hot side, and tensile stresses on the cold side of the member; the maximum stresses being equal to $\alpha Et/2$.

It is evident from the above discussion that the actual position of a plane section after heating can be somewhere between lines AB and ED and inclined at some angle between the horizontal and line AC, depending upon the type and amount of restraint provided at the ends of the member. In general, if plastic flow or cracking does not occur, temperature stresses can be estimated by multiplying the restrained strains in the member by the modulus of elasticity. If all four edges of a wall or slab are prevented from rotating, the magnitude of the thermal stress can be approximated by multiplying values of thermal stress obtained in the above manner by the factor: 1/(1−Poisson's ratio). Poisson's ratio for concrete ranges from 0.1 to about 0.25.

The effects of various types of end restraint on thermal stresses are illustrated in Fig. 4. It is assumed that each wall is subjected to a linear temperature distribution (t) through its thickness, and that t is uniform along its length. In examples e and f, lateral shearing forces are produced as well as bending.

The thermal moment required to prevent the rotation of the ends of a "fixed" beam or a section of a wall is equal to:

$$M_t = EI\,(\alpha t/h), \qquad (1)$$

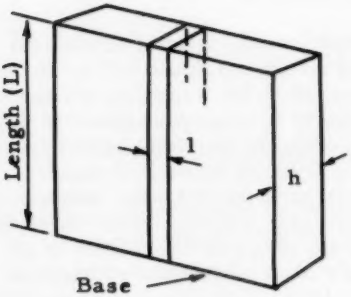

(a) Wall Dimensions

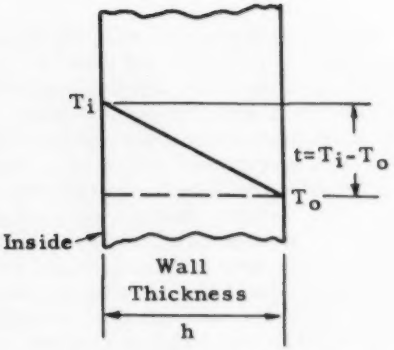

(b) Temperature Distribution Across Wall

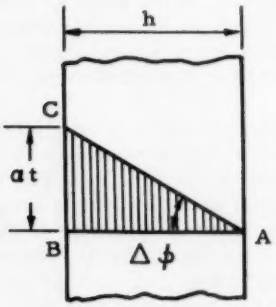

(c) Elongation of Fibers

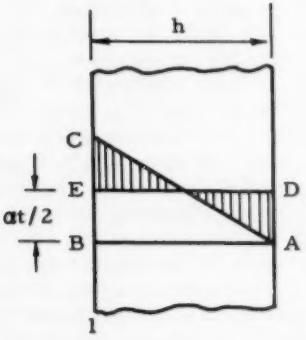

(d) Restrained Strains for No Rotation

NOTE:
αt is very small compared with h so that $\Delta\phi = \alpha t/h$

FIGURE 3
TEMPERATURE AND STRAIN DISTRIBUTIONS
(Linear Case)

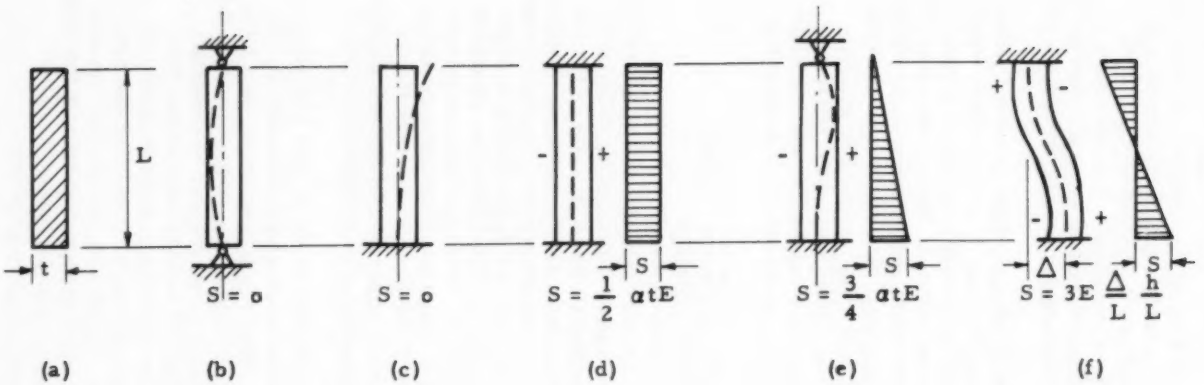

NOTE:

(a) Rectangular distribution of temperature difference t assumed for each case except (f). No restraint vertically. $\Delta\phi = \alpha t/h$.
(b) Free-standing wall, unrestrained at base and top.
(c) Free-standing wall, fixed at base.
(d) Wall fixed at base and top.
(e) Wall fixed at base and hinged at top.
(f) Ends fixed against rotation. Ends moved laterally a distance Δ.
(g) If vertical expansion is prevented, add a compressive stress of $\alpha tE/2$.

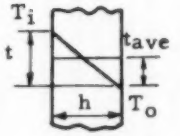

FIGURE 4
VARIOUS TYPES OF END RESTRAINT

where I is the moment of inertia of the section about its neutral axis and the other terms are as defined above. It is noted that the thermal moment M_t is independent of the length of the member as long as the temperature difference (t) varies symmetrically with respect to the mid-length of the member. If symmetrical, the average value of temperature (t_a) should be used in the above equation as indicated in Fig. 5. If unsymmetrical, it is necessary to determine the distribution of angle-changes ($\Delta\phi = \alpha t/h$) along the member's length and the corresponding fixed-end moments required to prevent end rotation.

In some cases, fixed-end moments can be obtained from tabulated values corresponding to known distributions of angle-changes (or moments), which are interpreted as being produced by imaginary loads on a simple supported beam. An inspection of the simple diagrams shown in Fig. 5 should convince the reader of the similarity between temperature distributions, angle-changes, and moments in fixed-end beams. It is noted that the area beneath the solid curve must equal that beneath the dashed curve, for a particular example, since the summation of angle-changes along a fixed beam must equal zero. In case the ends of a member are only partially restrained, the end-moments corresponding to given values of end rotation can be determined accordingly.

Approximating Thermal Stresses in Concrete Frames (Linear Temperature Distributions)

In the examples discussed above, thermal stresses are caused by restraint applied "externally" at the top and bottom edges. Temperature differences through some structures will produce thermal stresses by virtue of the "internal" restraint developed when they try to deform. For example, when the inner surface of a hollow cylinder is hotter than the outside, the concrete near the inside tends to expand more than the outside, but is restrained in order to maintain a cylindrical shape without cracking. The restrained strains for this case are similar to those shown in Fig. 3-d, while the thermal moment M_t is given by Eq. (1). (Due to edge effects, maximum stresses near the top and bottom of a hollow cylinder are about 25 per cent greater than that obtained using M_t.[5] However, the temperature difference (t) through the walls of a cylindrical shield will usually be much greater near mid-length than at the top or bottom.)

Thermal stresses in rigid frames can be determined by first computing the fixed-end moments corresponding to the temperature difference (t_a) for each member of the frame. (See Fig. 5) Unbalanced moments at each joint can then be distributed until the frame is in equilibrium. Depending upon the rigid frame being analyzed, length changes of members may be important. Space does not permit a complete discussion of various computation procedures; however, attention is called to the equilibrium thermal moments (M_e) developed in the simple frames shown in Fig. 6. It is noted that when a relatively thin wall is connected to a thick (rigid) wall, the thermal moment produced in the thin wall may be several times greater than its own fixed-end moment, M_t.

Non-Linearities in Temperature Distribution

When considering thermal effects in the design of concrete shields, a number of problems in non-linear mechanics may arise for the following reasons:

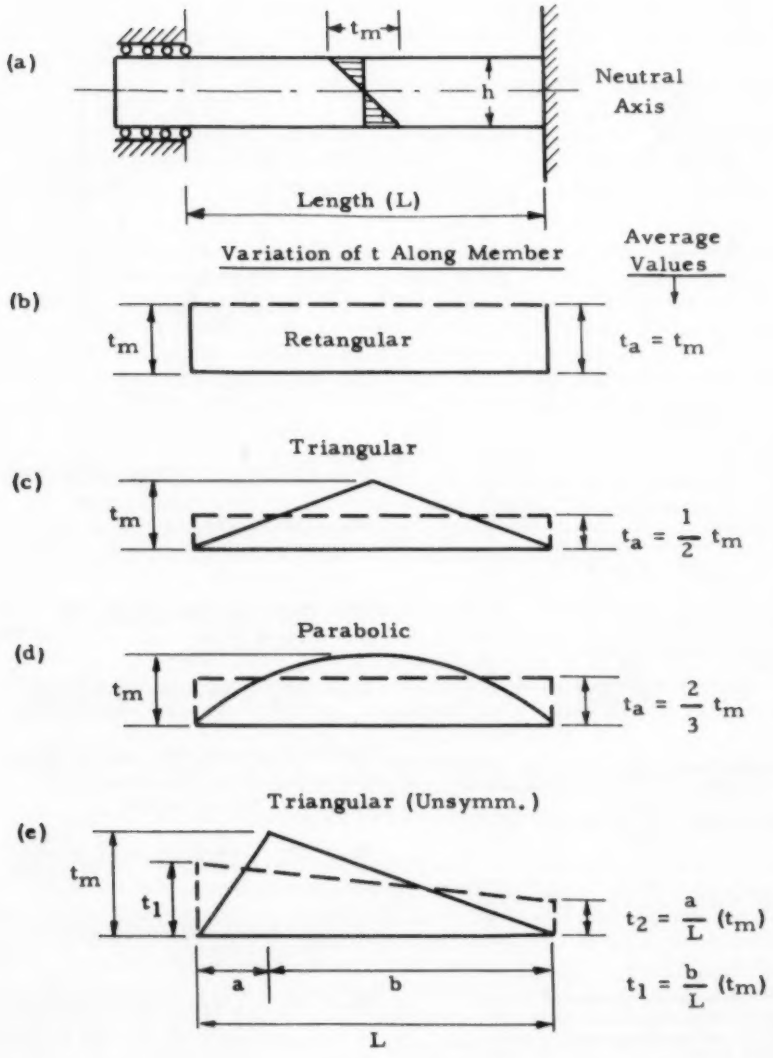

FIGURE 5
AVERAGE VALUES OF TEMPERATURE (t_a)
DISTRIBUTION FOR COMPUTING $M_t = EI\alpha t/h$

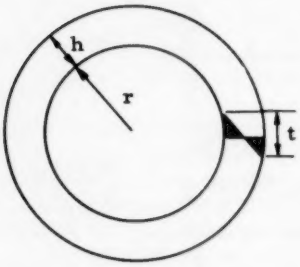

(a) $M_e = M_t = EI \frac{\alpha t}{h}$

$h \ll r$

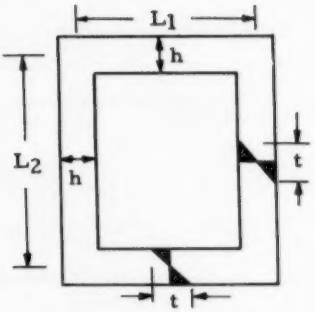

(b) $M_e = M_t = EI \frac{\alpha t}{h}$

(c)

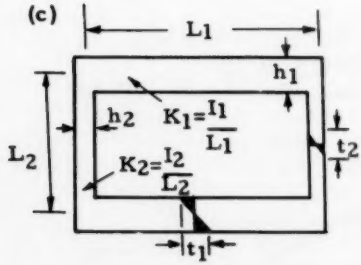

Fixed End Moments (c, d, e)

$$M_1 = EI_1 \frac{\alpha t_1}{h_1} = EI_1 \frac{\alpha q}{k}$$

$$M_2 = EI_2 \frac{\alpha t_2}{h_2} = EI_2 \frac{\alpha q}{k}$$

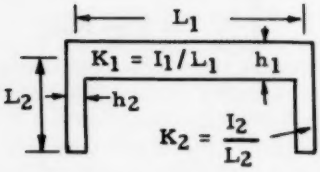

(d) and (e)

(c) Uniform Thermal Moment

$$M_e = M_1 - (M_1 - M_2) \frac{K_1}{K_1 + K_2}$$

(d) Thermal Moments for Fixed Base

$$M_e = M_1 - (M_1 - M_2) \frac{K_1}{K_1 + 2K_2}$$

Uniform along top, and then changing linearly along both sides to M_b at base:

$$M_b = M_2 - \frac{1}{2}(M_1 - M_2) \frac{2K_2}{K_1 + 2K_2}$$

(e) Thermal Moments for Hinged Bases

$$M_e = M_1 - (M_1 - \frac{3}{2} M_2) \frac{K_1}{K_1 + \frac{3}{2}K_2}$$

Uniform along top, and then decreasing linearly to zero at base.

FIGURE 6
THERMAL MOMENTS IN SIMPLE FRAMES

(1) Most of the heat is generated within the first foot or so of concrete, resulting in a non-linear temperature distribution across the shield.
(2) Part of the structure may be hotter than another due to variations in the heat flux impinging upon the shield.
(3) Connected components may operate at different temperatures, or cool at different rates.
(4) Non-linear distributions of temperature (and stress) are likely to occur in the shield whenever the reactor is shut down or started up.
(5) Thermal shock may be present; that is, rapid changes or cyclic variations in temperatures.

Some of these problems can be analyzed adequately by applying corrections to the results obtained by the elastic theory, or by developing expressions based upon assumed conditions and a non-linear theory of mechanics.[6,7] However, detailed analytical procedures are apt to be time-consuming. Due to the uncertainties involved in making most thermal stress computations, a sketching procedure suggested by Professor Frank Baron[6] is usually as accurate as need be. This procedure is utilized in the example of Fig. 7.

It is assumed that the temperature distribution shown in Fig. 7 is known, and that the shield is simple supported along its edges. If the wall does not crack, a horizontal plane AB before heating will remain plane (flat) after heating. The problem is now to locate the position taken by plane AB corresponding to the given temperature distribution. First, it must be raised vertically so that its neutral axis corresponds to the average temperature, t_{ave}, shown in Fig. 7-b. This can be done by "eye" by making the shaded area above the horizontal line through point g equal to that below. The correct slope of this plane is given by points F and E, Fig. 7-c, on the basis that the shaded areas must vanish, i.e., equal zero, as well as their moments. These shaded areas also correspond to the restrained strains across the wall thickness required to keep plane AB flat after heating. Corresponding values of thermal stress are shown in Fig. 7-d. To satisfy the requirements of statics, the summation of these thermal stresses across the section and their moments must equal zero; thereby, justifying the procedure described above. If additional precision is required, the above steps can be carried out graphically or analytically.

It is also noted that the equilibrium criteria for thermal stresses are similar to criteria for determining fixed-end moments in beams. In the latter case, angle-changes along a fixed beam must equal zero, as well as the summation of their moments about either end of the beam. Thus, it is sometimes convenient to determine thermal stresses caused by non-linearity in temperature distribution in terms of fixed-end moments, since the latter are already tabulated for numerous cases. Several cases have been depicted in Fig. 5; however, the length of the member in this case, should be taken as the wall thickness h and not L. As an example, consider the parabolic distribution of temperature shown in Fig. 5. The restrained strains (and corresponding thermal stresses) are indicated by the vertical distance between the horizontal dashed line and the solid temperature curve. The maximum compressive stress in this example occurs at the center and is equal to $\alpha E t_m/3$, while maximum tensile stresses of $2\ \alpha E t_m/3$ occur at the inside and outside surfaces of the wall.

Temperature difference t, defined in Fig. 7-c, is used for determining angle-changes ($\Delta\phi = \alpha t/h$) along the wall length. If the ends are not restrained, this temperature difference produces no thermal stress in the

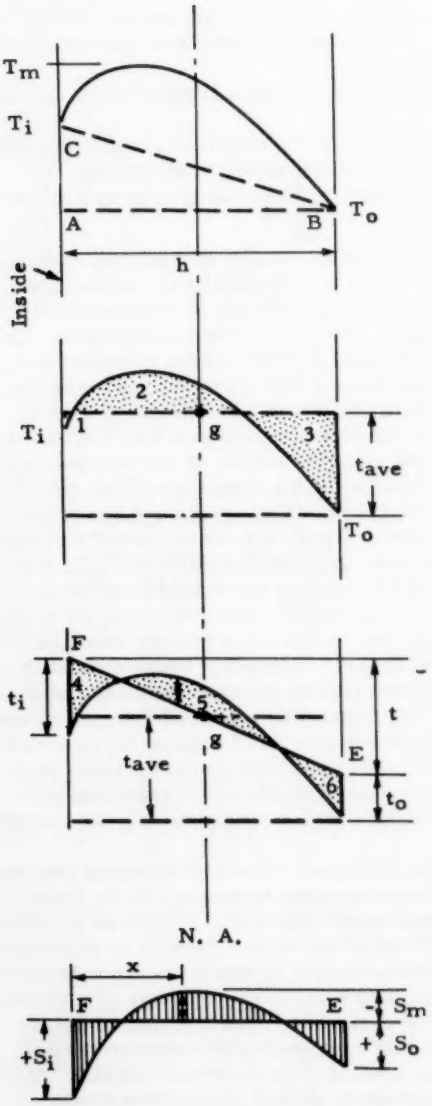

(a) Non-linear temperature distribution through wall. (Wall is free to rotate at top and bottom)

(b) Determine average temperature through wall thickness h.

Area 1 plus area 3 equals area 2.

(c) Rotate line EF about point (g) so that:
1- Area 4 plus area 6 equals area 5.
2- Summation of moments of these areas vanish.

(d) Distribution of thermal stresses due to non-linear distribution of temperature.

FIGURE 7
PROCEDURE FOR DETERMINING THERMAL STRESSES ASSOCIATED WITH NON-LINEAR TEMPERATURE DISTRIBUTIONS

member. (However, thermal stresses indicated in Fig. 7-d exist in this example because of non-linearity in temperature distribution.) If the ends are fixed or partially restrained, the temperature difference t is used for determining the thermal moment, $M_t = EI\alpha t/h$, in beams and members of a rigid frame. The total thermal stress at a given location is found by adding stresses due to non-linear temperature distributions (Fig. 7-d, for example) to those associated with the thermal moment, M_t, (Figs. 3, 4 and 6) based upon a linear temperature distribution. In the above examples, it has been assumed that the magnitude of thermal stress is less than the material's proportional limit. Allowance can also be made in the above procedures for determining thermal stresses arising from non-linearity in the stress-strain relationship; however, a discussion of this subject is not within the scope of this paper. (See References 7 and 8).

Heat Generation

For preliminary design, heat generation in a concrete shield may be assumed to be caused entirely by gamma rays that are absorbed, releasing their entire energy as heat at the point of absorption. If appropriate energy absorption coefficients are not available, it is sufficiently accurate to use total absorption coefficients in the computations.[9] In the example shown in Fig. 8, an infinite slab is subjected to a collimated beam of I_o gamma photons per cm^2-sec, having an average energy of E Mev/photon. During steady state conditions, the temperature distribution through the concrete slab is given by the equation:

$$k \frac{d^2T}{dx^2} = -\frac{EI_o}{\lambda} e^{-x/\lambda} = -\frac{q_o}{\lambda} e^{-x/\lambda} \qquad \text{Eq. (2)}$$

The heat flux q_o through the shield may be expressed in engineering units (B/ft^2-hr) by multiplying Mev/cm^2-sec by 5×10^{-10}. In this case, the relaxation length λ (or mean free path distance required to reduce the intensity by a factor of e = 2.718) must be expressed in feet.

Eq. (2) can be integrated to obtain an expression for temperature distribution through an infinite slab.[10] However, an approximate equation can be obtained readily when it is realized that Eq. (2) is similar in form to the differential equation for determining loads, shears and moments in a beam having a length equal to the wall thickness. In this analogy, loads, shears and moments along the fictitious beam correspond to the heat generation rate, heat flux, and temperature distribution through the wall, respectively. The engineer who is more familiar with the computation of moments in beams than with heat transfer problems may wish to proceed as indicated in Fig. 9. This method is especially useful for determining temperatures when the heat generation is discontinuous through the slab or difficult to express in simple algebraic terms. Likewise, the effects of different types and distributions of heat deposition can be estimated quickly. The method can also be used for determining the most effective way for cooling a shield, since the heat flux removed at a sump is treated as a concentrated load acting upward on the fictitious beam.

If all the heat generated in the slab shown in Fig. 9 is removed from the inside of the slab, the ficticious beam is a cantilever beam, with its support at the inside. The maximum temperature rise can be determined from the

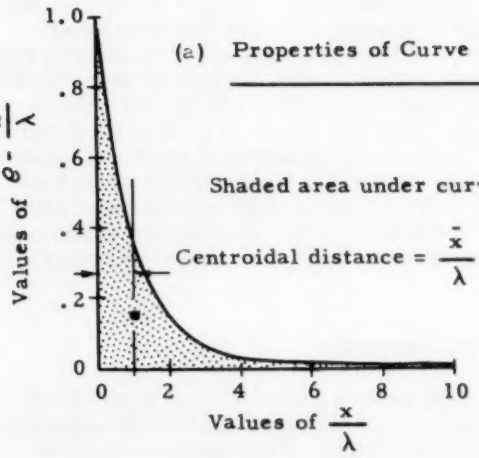

(a) Properties of Curve $\varepsilon^{-x/\lambda}$

Shaded area under curve = $\lambda\left\{1 - \varepsilon^{-x/\lambda}\right\} \approx \lambda$

Centroidal distance = $\frac{\bar{x}}{\lambda} = 1$

(b)

Heat Distribution in an Infinite Slab		Moments Along a Ficticious Beam
Wall thickness - h		Beam length - h
$k\frac{d^2T}{dx^2} = -q_x/\lambda = -Q_x$	Heat Gen. Rate / Unit Load	$\frac{d^2M}{dx^2} = -W_x$
$Q_o = \frac{q_o}{\lambda} = \frac{B/ft^2 - hr}{ft}$		W_x = lb/ft
$k\frac{dT}{dx}$	Heat Flux / Shear	$\frac{dM}{dx}$
q_o = B/ft^2 - hr		V = lb
k t = B/ft - hr	Temperature / Moment	M = lb - ft
t = T = ^oF		

FIGURE 8
RELATIONSHIPS IN MOMENT - TEMPERATURE ANALOGY

Load ficticious beam, having a constant area A, with heat generation curve Q_x in B/ft^3 - hr. The total load on beam, i.e. heat flux q_o, is equal to area beneath curve.

Assume temperature of outside and inside faces of wall to be equal to zero for reference. In this case, moments at ends of beam will be zero. The end shears correspond to the heat flux arriving at the inside and outside faces, respectively.

When h/λ is greater than 3, the cross-hatched area beneath the shear curve can be neglected. In this case:

$$kt_m = q_o \frac{\lambda}{h} \left\{ h - \lambda \ln \frac{h}{\lambda} \right\}$$

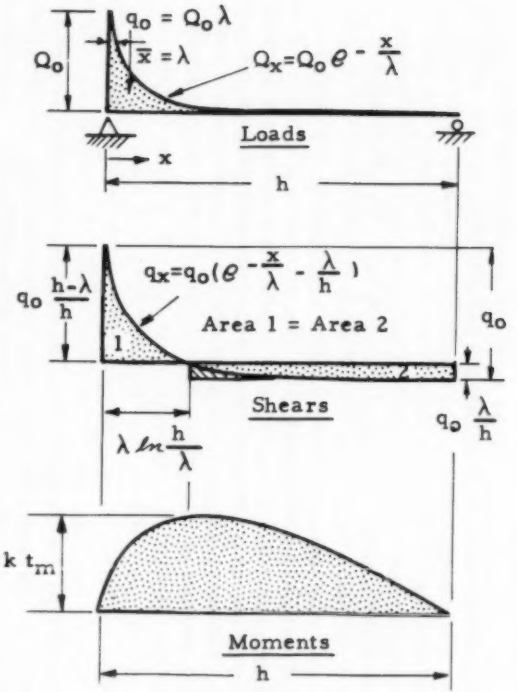

FIGURE 9
DETERMINING TEMPERATURE DISTRIBUTION DUE TO HEAT GENERATION IN INFINITE SLAB BY MOMENT - TEMPERATURE ANALOGY

moment at the support, or $kt_m = \lambda q_o$. If all the heat generated in the slab is removed at the outside surface, the ficticious cantilever beam is supported at the outside and is loaded with the total heat flux q_o placed a distance λ from the inside. The maximum temperature rise in this case can be very large since the moment (kt) at the outside support is equal to $q_o (h - \lambda)$. In the example of Fig. 9, the temperature of the inside face was assumed the same as the outside of the slab. If these temperatures are not the same, the final temperature distribution may look like that shown in Fig. 7-a. To provide for this condition in the analogy, a downward load equal to the additional heat flux $q = kt/h$, should be applied to the left support in addition to a moment equal to $kt = qh$. The additional moment curve corresponds to a linear temperature distribution defined by $t = T_i - T_o$.

When desired, corrections can be factored into the procedure to allow for radiations which are not collimated, or for shield geometries other than an infinite slab. In general, the methods discussed above are extremely useful for estimating thermal effects under a wide range of conditions and for determining design criteria.

Design Criteria

The effects of high temperature on the physical and shielding properties of concrete have been discussed above, as well as rapid methods for estimating temperatures in shielding structures. These items will assist in establishing design criteria for a particular shield and for obtaining answers to the following questions:

(1) What is the maximum temperature to be allowed in the shield?
(2) What temperature differential can be tolerated in a particular design?
(3) Will cooling be required? If so, how much and where?
(4) Is the concrete likely to crack? How can steel reinforcement be used most effectively to minimize cracking?

High values of temperature should be avoided in concrete structures, if possible. However, this may not be feasible in some designs. If adequate allowances are made for shrinkage, loss of strength and reduction in shielding effectiveness, temperatures as high as 500 or 600° F may possibly be tolerated in some concrete shields. If the concrete contains limonite aggregate, the maximum temperature should be kept below 350° F so that the water of hydration will not be driven off. Such high values of temperature can be permitted only if the whole shield is maintained essentially at the same temperature. To avoid cracking of the concrete, the restrained strains produced during heating and cooling of the shield, or when the reactor is operating at full power, should not produce stresses greater than the tensile strength of the concrete.

Lacking data for a particular type of concrete, the tensile strength can be taken as one-tenth of the compressive strength (f'_c) and the modulus of elasticity as 1000 f'_c. For these values, cracking can be expected when the restrained strain exceeds 10^{-4}. Setting αt_r equal to 10^{-4}, the critical temperature (t_r) at which cracking starts is equal to 15° F, if α equals 6.7×10^{-6}. It is admitted that this temperature limit is quite restrictive, and that a value of at least 20° F can usually be justified for t_r on the following bases:

(1) Plastic flow may relieve the restrained strains. (This behavior is more pronounced in damp concrete at early ages than for dry concrete several years old. Also, concrete which is slightly cracked may tend to "heal" if sufficiently damp.)
(2) The exact unit strain at which cracking occurs is unknown, but is probably somewhat greater than 10^{-4}.
(3) The value of the modulus of elasticity for concrete, when subjected to high temperatures, decreases a greater amount proportionately, than corresponding values of the tensile strength and expansion coefficient.
(4) If cracking occurs, reinforcing steel will minimize the damage.

The temperature and stress distributions given above may be used as a guide for determining the maximum heat flux that a concrete wall can handle without cracking. For a free-standing wall, non-linear temperature distributions resulting from gamma ray heating produce maximum tensile stresses at the inside face. (See Fig. 10) If tensile cracking is to be avoided, the total heat flux impinging on the inside face should be less than 125 B/ft^2-hr. If the top and bottom edges of the wall are prevented from rotating, the total heat flux can be increased to around 200 B/ft^2-hr. In this case, the end restraint produces compression at the inside face, so that the maximum tensile stress occurs at the outside. In both of these examples, approximately 95 per cent of the heat flux must be removed from the inside face by forced cooling.

In the more general case, where the inside face is hotter than the outside, the maximum tensile stress occurs at the outside face and is equal to $\alpha t_{ave} E$. (See Fig. 7-c and 10) Applying this criteria to the wall described in Fig. 3-d and 4-d, the permissible temperature differential (t) across the wall is 40° F. Corresponding to this temperature differential, the limiting value of heat flux for a magnetite concrete shield, 6 feet thick with fixed ends is obtained as follows:

$$q_o = k\,t/h = 1.5(40)/6 = 10 \text{ B/ft}^2\text{-hr.} \qquad \text{Eq. (3)}$$

This heat is assumed to be conducted to the concrete wall from an interior thermal shield and then removed at the outside of the wall. If the heat is caused by gamma rays near the inside face and then removed at the outside, the total heat flux, corresponding to a temperature difference of 40° F, is equal to:

$$q_o = k\,t_w/(h - \lambda) = 1.5(40)/5.67 = 10.6 \text{ B/ft}^2\text{-hr.} \qquad \text{Eq. (4)}$$

The above data indicate that the inside surface of this shield must be cooled when the combined heat flux from conduction and gamma heating exceeds about 10 B/ft^2-hr. This corresponds to an energy level of 2 x 10^{10} Mev/cm^2-sec. In general, sufficient cooling should be provided so that the average temperature (t_{ave}) through the shield thickness, measured above the temperature of the cold side (T_o) is less than 20° F. Otherwise, the concrete is likely to craze or crack locally.

Since concrete is weak in tension, it is usually reinforced. By incorporating a nominal amount of steel in a concrete shield, the permissible temperature drop, if linear, can be increased from 40 to around 120° F and the allowable heat flux raised accordingly. (See Eq. 6) If the temperature distribution is not linear, the temperature drop should be somewhat less than 100° F, depending upon the severity of the temperature gradients in the concrete. If

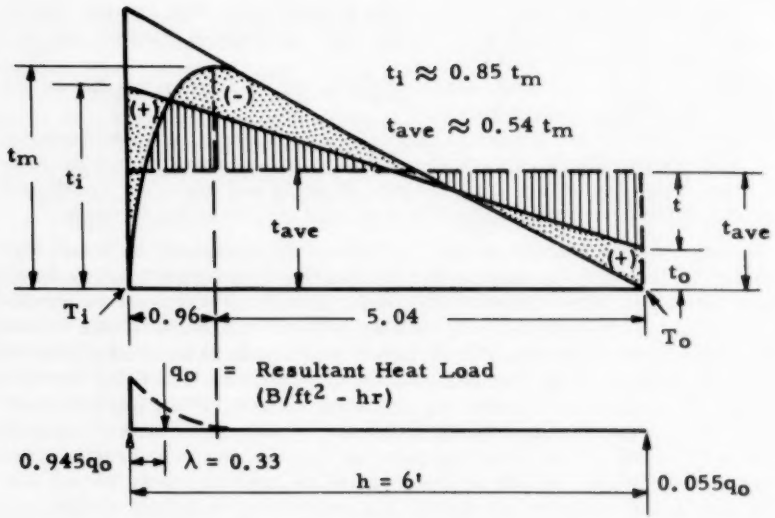

For a High-Density Concrete Shield:

h = 6 ft
$\mu = 0.10\ cm^{-1}$
$\lambda = 0.33$ ft
$T_i = T_o$
k = 1.5 B/ft - hr - °F
W = 220 pcf
t_i = 20 °F
Aggregates: Hydrous Iron Ore
No edge restraint

$\therefore h/\lambda = 18.3 \quad \ln \frac{h}{\lambda} = 2.90$

$\lambda \ln h/\lambda = 0.96$ ft

$t_m = \frac{0.055}{1.5} q_o(5.04) = 0.185 q_o$

$\therefore q_o = \frac{t_m}{0.185} = \frac{20}{0.85(.185)} = \underline{\underline{127}}$

$\approx 2.5 \times 10^{11}$ Mev/cm^2 - sec

If the top and bottom edges cannot rotate, additional bending stresses (shown cross-hatched) must be added to those (shown shaded) caused by the non-linear temperature distribution.
In this case, the maximum tensile stress is defined by:

t_{ave} = 20 °F = 0.54 t_m

$\therefore q_o = \frac{t_m}{0.185} = \frac{20}{0.54(0.185)} = \underline{\underline{200}}$

$\approx 4 \times 10^{11}$ Mev/cm^2 - sec

FIGURE 10
DETERMINING PERMISSIBLE HEAT LOADS

subjected to numerous thermal cycles and severe temperature gradients, it is desirable to keep temperature differentials below 40 or 50° F, or as required to minimize tensile cracking.

Reinforcement of Concrete Shields

The amount of steel reinforcement and its proper location in a concrete shield are open to question, depending upon the type of shield being designed. The right amount of steel prevents detrimental cracking by (a) reducing the width and length of cracks that tend to develop, and (b) distributing these hair-line cracks more or less evenly over the surface of the concrete wall. Ordinarily, the location and spacing of reinforcing bars are more important than using a large amount of temperature steel.

Theoretically, reinforcement may not be required in a free-standing concrete wall; however, a small amount of reinforcement is usually provided to take care of local strains associated with shrinkage during hardening or small temperature differences. If a free-standing wall is submitted to a substantial temperature differential, non-linear in distribution, reinforcement is needed in areas subjected to tensile strain. (See Fig. 10) If the edges of the wall are restrained, reinforcement will be required when the associated strain (or stress) in the concrete approaches values which cause tensile cracking. The procedures described above for determining temperature and stress distributions will assist the engineer in determining the location and amount of reinforcement required for a particular shield. In the case of thick concrete walls, it is not always feasible to neglect tension in the concrete when determining the amount of reinforcement.

Consider a concrete wall having its top and bottom edges fixed and which is subjected to a linear temperature drop of t° F. Lacking specific criteria, Eq. (5) can be used to determine the "nominal" percentage of primary steel required near the cold side. This relationship is obtained by making the resisting moment of the tensile steel (neglecting tension in the concrete) equal to the ultimate moment of the uncracked section of concrete.

$$p_n = \frac{f_t}{6 f_s} (100\%) \qquad \text{Eq. (5)}$$

In the above equation, f_t is the ultimate tensile strength (or modulus of rupture) of the concrete, and f_s is the allowable steel stress. For example, if f_t equals 300 psi and f_s is 18,000 psi, the nominal reinforcement would be 0.28 per cent. Specifications usually require that at least 0.2 per cent of temperature steel be used in a direction normal to the primary reinforcement. If all four edges of the wall are restrained, equal amounts of reinforcement should be provided in each direction. Although these values represent minimum percentages of reinforcement, it may be impractical to provide this much steel in a concrete wall, 8 or 9 feet thick. To reduce steel requirements, a thick wall can sometimes be constructed in smaller sections and free edges or expansion joints provided.

When the amount of temperature steel is known, the permissible temperature differential, if linear, can be computed from the equation:

$$t = \frac{f_s}{\alpha E_s} \left\{ \frac{d}{d - Kd} \right\} = \frac{100}{1 - K} \qquad \text{Eq. (6)}$$

A steel stress of 18,000 psi is used to obtain the factor on the right side, α is the coefficient of thermal expansion, E_S is the modulus of elasticity for steel, Kd is the distance from the inside surface of the shield to the neutral axis, and d is the distance from the inside surface to the centroid of the tensile reinforcement. Eq. (6) corresponds to a linear stress or strain distribution across a narrow section of wall having its top and bottom fixed. If all four edges of a wall are fixed, t will be about 90 percent of that obtained from Eq. (6). If a concrete shield is subjected to structural loads in addition to temperature gradients, f_s in the above equation should be taken equal to the difference between 18,000 psi and the tensile stress in the steel produced by the structural loads.

An attempt is sometimes made to increase the permissible temperature drop across a concrete shield by utilizing large amounts of reinforcement. The optimum steel percentage in this case corresponds to that for "balanced" reinforcement or 1.6 per cent when E_S/E_C equals 10, f_c equals 1350 psi and f_s equals 18,000 psi. Since the location of the neutral axis changes slowly with increases in steel area, a substantial increase in steel is required to raise the permissible temperature differential (t) appreciably. In the above example, increasing the steel percentage from 0.2 to 1.6 per cent raises t from 125 to 175° F. Then too, it is often difficult if not impractical, to place large amounts of reinforcing in a shielding wall, especially when it is penetrated by numerous process pipes or test holes. In some designs, it will be more economical to add steel to an interior thermal shield rather than to the surrounding concrete.

Practical Considerations

Very little information is available on the maximum temperature gradient which a concrete shield can safely withstand. Steep gradients can occur when a shield is heated or cooled rapidly, or when subjected to high rates of gamma heat generation. Procedures described in Fig. 7 can be used effectively for determining the amount and location of tensile reinforcement in such cases. In general, sufficient steel should be provided so that if cracking of the concrete should start, it will not continue through the shield or develop into a few wide cracks. A vulnerable point for spalling is one in which a few inches of concrete covers a large steel structural member or a series of large, closely-spaced reinforcing bars. In such cases, wire mesh can be integrated into the encasing layer or concrete; or better still, means taken to protect the concrete surface from the intense heat load or to reduce the thermal gradient. A steel liner is sometimes placed on the inside face for this purpose. Refractory material or an aluminum heat reflector may be useful, or other means taken to reduce the heat load being conducted to the concrete shield. The temperature differential through the shield can be decreased by using concrete with a higher thermal conductivity, by making the wall thinner, or by cooling the hot side in order to reduce the heat load through the shield. In some designs, it may be desirable to construct concrete shields in layers separated by insulation or water.

The above discussion applies primarily to massive concrete walls which are not penetrated by numerous coolant channels. In case a concrete shield is penetrated by tubes containing reactor coolant at temperatures of 300 to 600° F, it may not be feasible to cool the shield. In this case, the concrete is

usually enclosed in a load-carrying steel structure. The interaction between the concrete and steel at high temperatures may be a serious problem, depending upon the temperature conditions and the relative expansion of the steel and concrete. To alleviate this situation, the coefficient of expansion for the concrete should be about the same as, or slightly greater than, that of the steel forms. Likewise, the ingredients, mix proportions and concrete placement should be such as to produce concrete with minimum shrinkage at high temperatures.

It is admitted that general criteria cannot be formulated which will be applicable to all concrete shields that might be constructed in the future. For example, the behavior of a free-standing wall subjected to no loads other than its own weight will be different from the behavior of a rigid frame subjected to live loads in addition to its own weight. However, in most shielding structures, thermal effects are not of "secondary" importance; in fact, they may be the major load to which a shield is subjected. Recognition of this fact will assist the engineer in utilizing concrete effectively and economically in shield construction.

BIBLIOGRAPHY

1. Halliday, D. B., Heat Release in Concrete Reactor Shields, AERE R/R 1963; Atomic Energy Research Establishment, Harwell, Berks; May 1956.
2. Rockwell, T., Reactor Shielding Design Manual, McGraw-Hill Book Company, Inc., 1956, p. 451.
3. Davis, H. S., F. L. Browne and H. C. Witter, "Properties of High-Density Concrete Made with Iron Aggregate", Journal of the American Concrete Institute, V. 27, No. 7, March 1956.
4. Bunch, W. L., Attenuation Properties of High-Density Portland Cement Concretes as a Function of Temperature, HW-54656; General Electric Company, Hanford Atomic Products Operation, January 22, 1958. p. 42.
5. Timoshenko, S., Strength of Materials, Vol. II, D. Van Nostrand Company, Inc., August 1941, p. 176.
6. Baron, F., Lectures presented in graduate courses during 1948 at Northwestern Technological Institute, Evanston, Illinois.
7. Baron, F., "A Pressure Line Concept for Inelastic Bending", Proceedings of the American Society of Civil Engineers, Separate 1157, January 1957.
8. Baron, F., and H. S. Davis, "The Pressure Line and the Inelastic Buckling of Columns", Proceedings of the American Society of Civil Engineers, Separate 1424, October 1957.
9. Grotenhuis, M., and J. W. Butler, Experimental Boiling Water Reactor (EBWR) Shield Design, ANL-5544, Argonne National Laboratory, August 1956.
10. Glasstone, S., Principles of Nuclear Reactor Engineering, D. Van Nostrand Company, Inc., 1955, p. 665.

Paper 1756 September, 1958 ST 5

Journal of the
STRUCTURAL DIVISION
Proceedings of the American Society of Civil Engineers

AN ANALYTICAL AND EXPERIMENTAL STUDY OF HELICOIDAL GIRDERS

Y. F. Young,[1] and A. C. Scordelis,[2] J. M. ASCE
(Proc. Paper 1756)

SYNOPSIS

A study of the helicoidal girder, fixed at the ends, subtending a horizontal angle of 180 degrees, and having a slope of 30 degrees is presented. Four girders, each having a different uniform rectangular cross-section throughout its length, are investigated. The determination of influence lines for end reactions due to vertical load is illustrated using analytical and experimental methods and final results are presented in tabulated and graphical form. End reactions under uniform load over half and full span are also given. The effect of width-depth ratio of cross-section on end reactions and internal forces is discussed.

INTRODUCTION

In recent years a number of helicoidal staircases, supported only at the ends, have been designed and built.[1,2] This architecturally fascinating structure may be visualized as being a circular bow girder with one end displaced vertically out of the plane of the other.

A problem which immediately confronts the designer of such a structure is the elementary one of determining end reactions. Bergman[3] suggests that for design purposes it may be adequate to determine the end reactions by reducing the girder to its horizontal projection and thus analyze it as a bow girder. This simplification neglects the inherent strength of the three-dimensional structure. In the case of a helicoidal staircase built for the showroom of the General Motors Building in Antwerp, Belgium, Magnel[1] obtained

Note: Discussion open until February 1, 1959. To extend the closing date one month, a written request must be filed with the Executive Secretary, ASCE. Paper 1756 is part of the copyrighted Journal of the Structural Division, Proceedings of the American Society of Civil Engineers, Vol. 84, No. ST 5, September, 1958.

1. Engr.-Structures, North American Aviation, Inc., Fresno, Calif.
2. Associate Prof. of Civ. Eng., Univ. of California, Berkeley, Calif.

experimental data, as a basis for design, by test loading a full scale model. The test results, however, failed to substantiate his computed values. Analytical studies have been presented by Fuchssteiner,[12] Gedizli,[13] and Cohen,[14] but as yet little work has been done experimentally to verify the applicability of the theories being used.

Because of the lack of knowledge regarding the behavior of this type of structure the study reported in this paper was conducted with the purpose of investigating the following items:

a. The nature of the end reactions, and the means by which they may be evaluated using both analytical and experimental approaches.
b. A comparison between the end reactions obtained for the structure by analyzing its horizontal projection as a bow girder and by analyzing it as a true helicoid.
c. The effect of the width-depth ratio of the cross-section on the end reactions.
d. The applicability of the analytical solution to structures with large transverse dimensions, since the analysis does not take into account the additional resistance provided by slab action.

The geometry of a helicoidal girder may be defined physically, as shown in Fig. 1, in terms of its radius, R; horizontal angle, ϕ; helix angle, α; width, b; and depth, h. Four girders were analyzed in this study, all having the same horizontal angle, $\phi = 180^0$, and the same helix angle, $\alpha = 30^0$, but each having a different width-depth ratio, b/h. The nominal width-depth ratios of the girders investigated were 1:1, 4:1, 8:1, 16:1.

Analytical Solution

The helicoidal girder fixed at the ends, under vertical load, is a structure which is statically indeterminate to the sixth degree. It may be analyzed by considering the six reactions at one end, Fig. 2, as redundants. Then using the principle of superposition, the following equations known as the Maxwell-Mohr equations may be written.

$$\delta_{xo} + X_x\delta_{xx} + X_y\delta_{xy} + X_z\delta_{xz} + X_t\delta_{xt} + X_p\delta_{xp} + X_r\delta_{xr} = 0 \quad (1)$$

$$\delta_{yo} + X_x\delta_{yx} + X_y\delta_{yy} + X_z\delta_{yz} + X_t\delta_{yt} + X_p\delta_{yp} + X_r\delta_{yr} = 0 \quad (2)$$

$$\delta_{zo} + X_x\delta_{zx} + X_y\delta_{zy} + X_z\delta_{zz} + X_t\delta_{zt} + X_p\delta_{zp} + X_r\delta_{zr} = 0 \quad (3)$$

$$\delta_{to} + X_x\delta_{tx} + X_y\delta_{ty} + X_z\delta_{tz} + X_t\delta_{tt} + X_p\delta_{tp} + X_r\delta_{tr} = 0 \quad (4)$$

$$\delta_{po} + X_x\delta_{px} + X_y\delta_{py} + X_z\delta_{pz} + X_t\delta_{pt} + X_p\delta_{pp} + X_r\delta_{pr} = 0 \quad (5)$$

$$\delta_{ro} + X_x\delta_{rx} + X_y\delta_{ry} + X_z\delta_{rz} + X_t\delta_{rt} + X_p\delta_{rp} + X_r\delta_{rr} = 0 \quad (6)$$

In the above equations:

X_x, X_y, X_z represent the redundant forces in the direction of the x, y, and z axes respectively

X_t, X_r, X_p represent the redundant moments acting about the x, y, and z axes respectively

δ_{xo}, δ_{yo}, etc., displacements due to load P with redundants equal to zero.

δ_{xx}, δ_{yx}, etc., displacements due to $X_x = 1$.

R = radius
ϕ = central angle
α = helix angle
b = width
h = depth

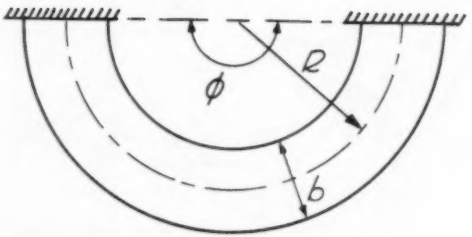

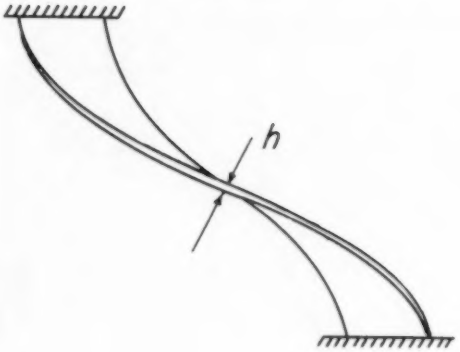

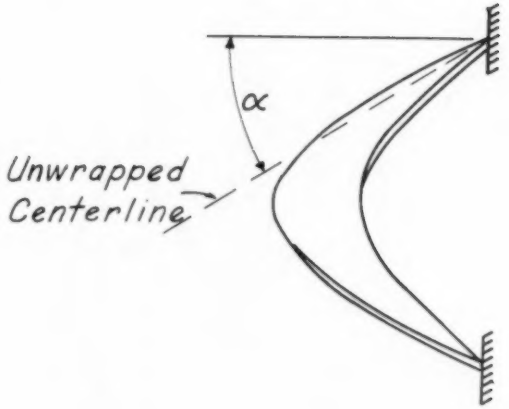

Fig. 1 Left-Hand Helicoidal Girder

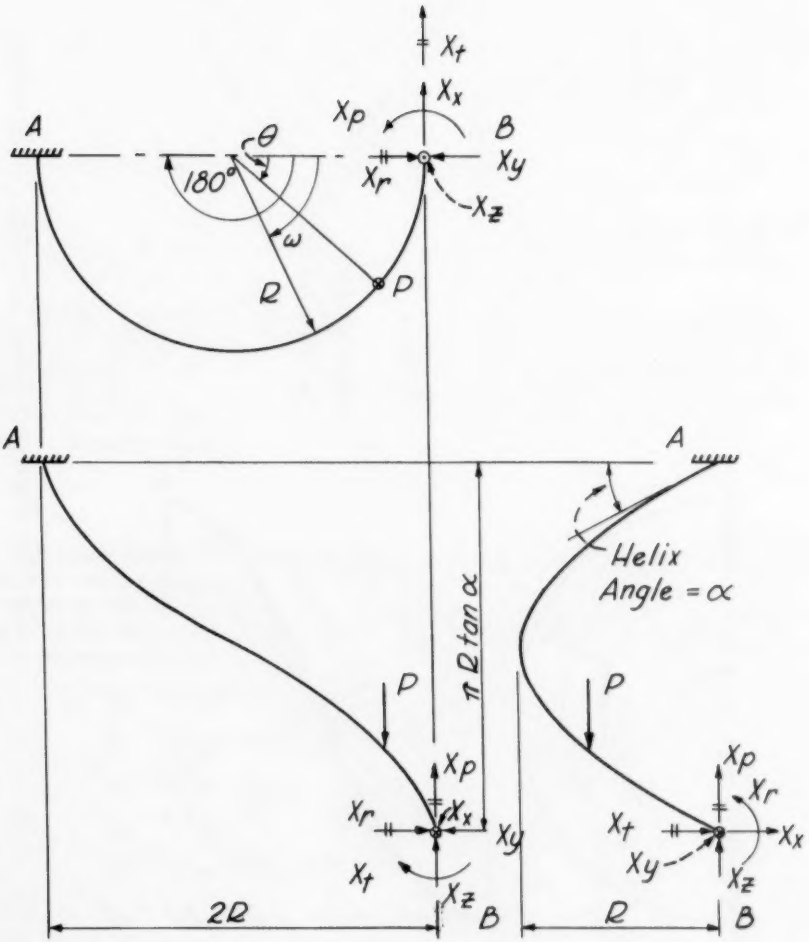

Fig. 2 -- Positive Direction of Redundants in Helicoidal Girder

δ_{xy}, δ_{yy}, etc., displacements due to $X_y = 1$.
δ_{xz}, δ_{yz}, etc., displacements due to $X_z = 1$.
δ_{xt}, δ_{yt}, etc., displacements due to $X_t = 1$.
δ_{xp}, δ_{yp}, etc., displacements due to $X_p = 1$.
δ_{xr}, δ_{yr}, etc., displacements due to $X_r = 1$.

The term displacement is understood to mean angular as well as linear displacement.

In order to obtain a solution for the redundants the displacements must be evaluated. There are 42 displacements in the equations, but using Maxwell's law of reciprocal displacements ($\delta_{xy} = \delta_{xy}$, etc.) this number reduces to 27. These displacements may be determined using the method of virtual work. For example:

$$\delta_{xy} = \delta_{yx} = \int \frac{M_{rx} M_{ry} ds}{EI_r} + \int \frac{M_{sx} M_{sy} ds}{EI_s} + \int \frac{T_x T_y ds}{GJ_e}$$

M_{rx}, M_{sx}, T_x represent bending and torsional moments in girder due to $X_x = 1$.

M_{ry}, M_{sy}, T_y represent bending and torsional moments in girder due to $X_y = 1$.

EI_r, EI_s, represent bending stiffnesses about r and s axes respectively, see Fig. 3.

GJ_e torsional stiffness about e axis, see Fig. 3.

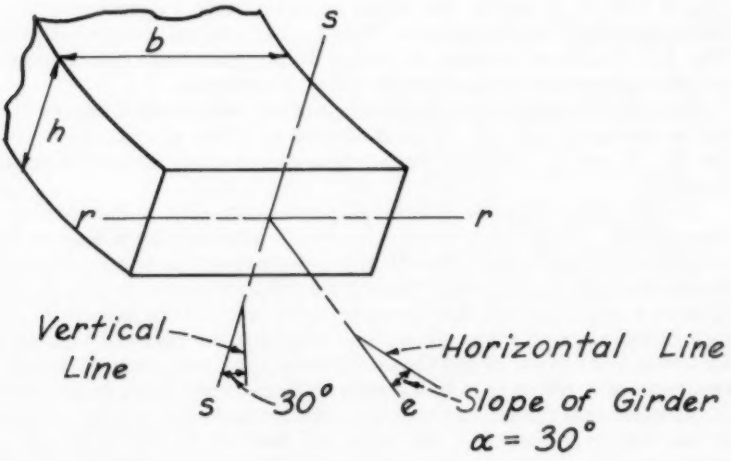

Fig. 3 -- Bending and Torsional Axes Indicated on Section Cut Normal to Longitudinal Axis of Girder

After the displacement coefficients have been evaluated they may be substituted into Eqs. (1) through (6) and the redundants found by solving these simultaneous equations.

Formulae for each of the necessary 27 displacements have been derived and are given in the appendix to this paper. The equations given are for a girder having a horizontal angle $\phi = 180$ degrees. They are expressed in terms of the load position, θ; the helix angle, α; the radius, R; and the bending and torsional stiffnesses. An inspection of these equations will reveal that they are quite lengthy and complex and care must be exercised in evaluating them numerically for a specific case.

In order to compare the results of an analytical solution with an experimental solution the four girders used in the model analysis, described later, were analyzed using the equations shown in the appendix together with Eqs. (1) through (6). All girders had the same helix angle of 30 degrees and were of rectangular cross-section. The cross-sectional dimensions of these girders, together with the bending and torsional stiffnesses, are given in Table 1. The models were made of plexiglas which had a modulus of elasticity, E, of 462 kips per sq. in. and a modulus of elasticity in shear, G, of 162 kips per sq. in. These physical constants of the material were obtained experimentally. The equivalent polar moments of inertia, J_e, of the cross-sections were obtained by means of the expression $J_e = k_1 bh^3$ in which k_1 is a constant depending on the width-depth ratio. The values of k_1 were obtained from Timoshenko and Goodier[4] p. 277.

End reactions for each girder were obtained analytically for a concentrated vertical load placed successively at five locations along the girder. Thus a total of twenty solutions were involved in obtaining the influence ordinates shown in Table 2. Influence lines for end reaction are shown graphically in Fig. 4, 5, 6, 7, 8, and 9. The signs given in Table 2 correspond to the positive direction of redundants given in Fig. 2. For convenience in the plotting of Fig. 4, 5, and 8 the positive direction of the redundants has been reversed. A key is given with these figures to avoid confusion.

In order to compare the foregoing results with those found by analyzing the horizontal projection of the structure as a bow girder, the influence lines for X_z, X_t, and X_r obtained from a bow-girder analysis are shown in Fig. 6, 7, and 8.

These three reactions are the only ones that exist in the case of a planar bow girder. Tabulated ordinates for these influence lines may be found in a number of publications [5,6,7,8]. It is interesting that in the case of the bow girder analysis the results obtained for the four girder cross-sections differ by such a small amount that for practical purposes the same influence lines may be used for all four. Thus, it is seen that the relative bending and torsional stiffnesses of the cross-sections have very little effect on the end reactions of a 180 degree bow girder. On the other hand, it can be seen that in the helicoidal girder analysis the relative stiffnesses have a marked effect on the end reactions. It is also apparent that any further increase in the width-depth ratio of the cross-section would result in theoretical influence lines which differ only slightly from those obtained for the 16:1 girder.

It might be well, at this point, to emphasize the assumptions that are inherent in an analysis of the type just described.

1. The material is elastic and homogeneous.
2. The bending and torsional stiffnesses of a warped girder (therefore a helicoidal surface) may be defined by those of a straight prismatic member.

TABLE 1

Sectional Properties of Helicoidal Girders

Nominal b/h	Actual b (in)	Actual h (in)	Actual b/h	$I_r \times 10^4$ (in^4)	$I_s \times 10^4$ (in^4)	k_1	$J_e \times 10^4$ (in^4)	EI_r (kip in^2)	EI_s (kip in^2)	GJ_e (kip in^2)
1:1	.256	.245	1.04	3.15	3.43	.146	5.50	.146	.158	.089
4:1	1.033	.244	4.22	12.6	224.	.283	42.8	.582	10.3	.693
8:1	1.987	.244	8.14	24.1	1590.	.304	87.6	1.11	73.5	1.42
16:1	4.000	.249	16.04	51.7	13,300	.333	207.	2.39	614.	3.35

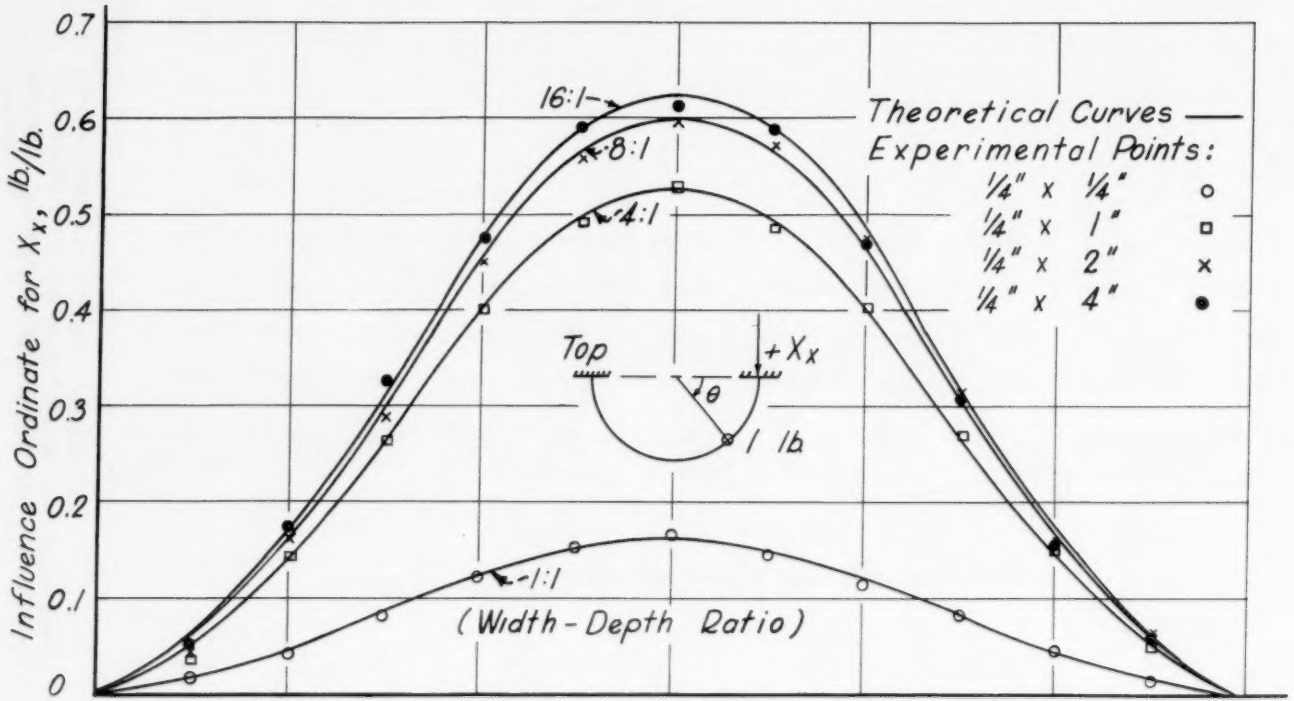

Fig. 4 -- Influence Lines for Reaction X_x

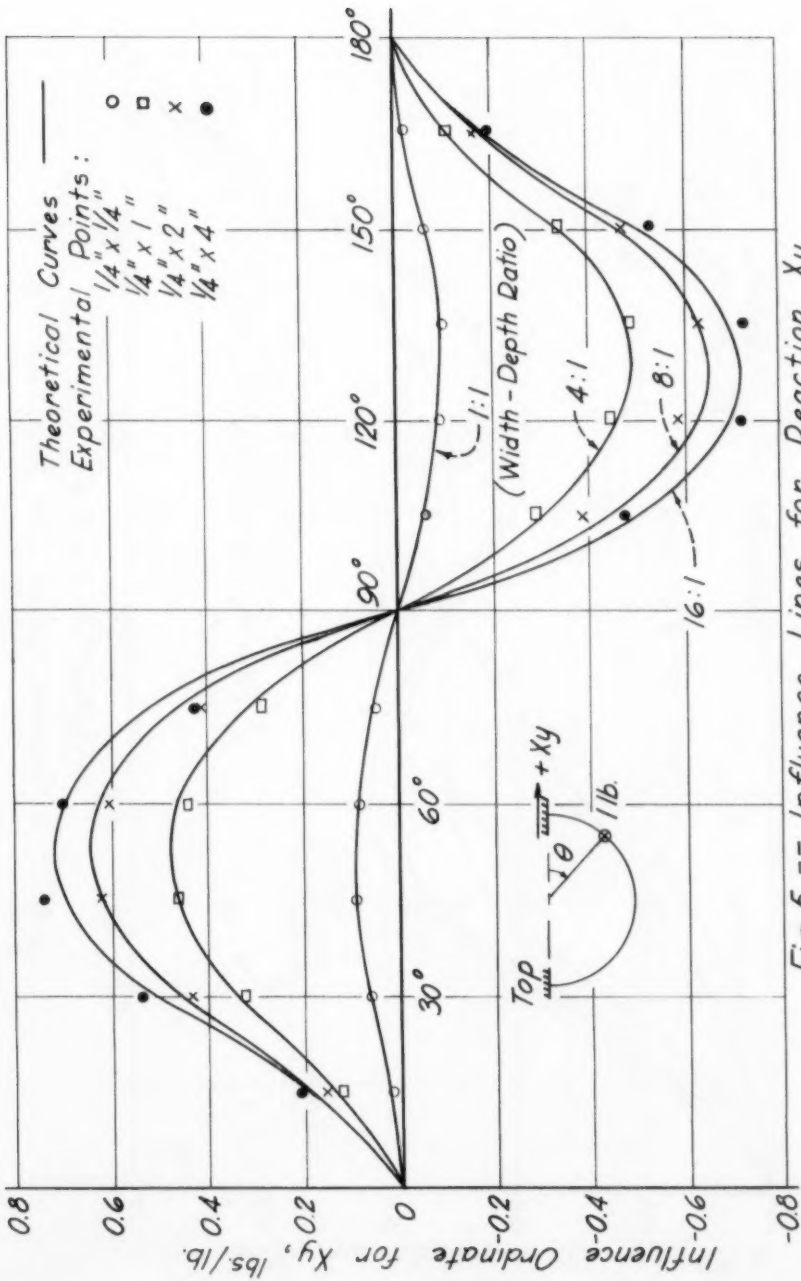

Fig. 5 -- Influence Lines for Reaction Xy

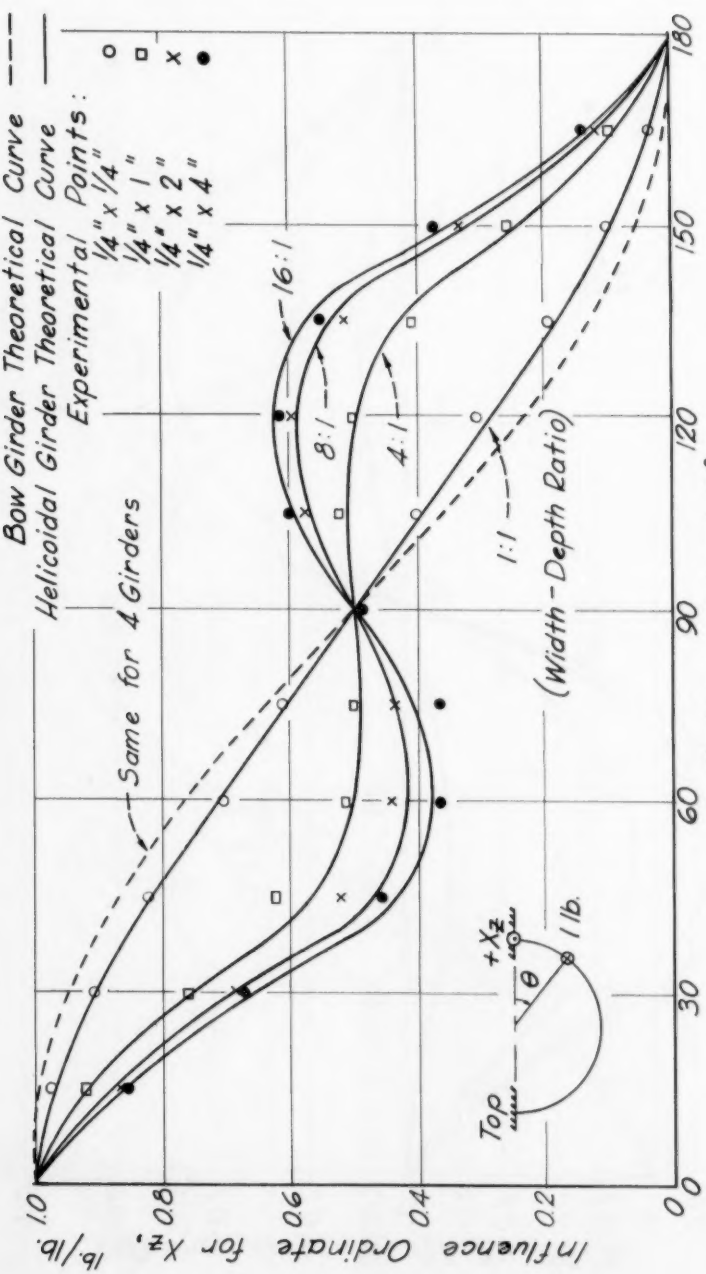

Fig. 6 -- Influence Lines for Reaction X_z

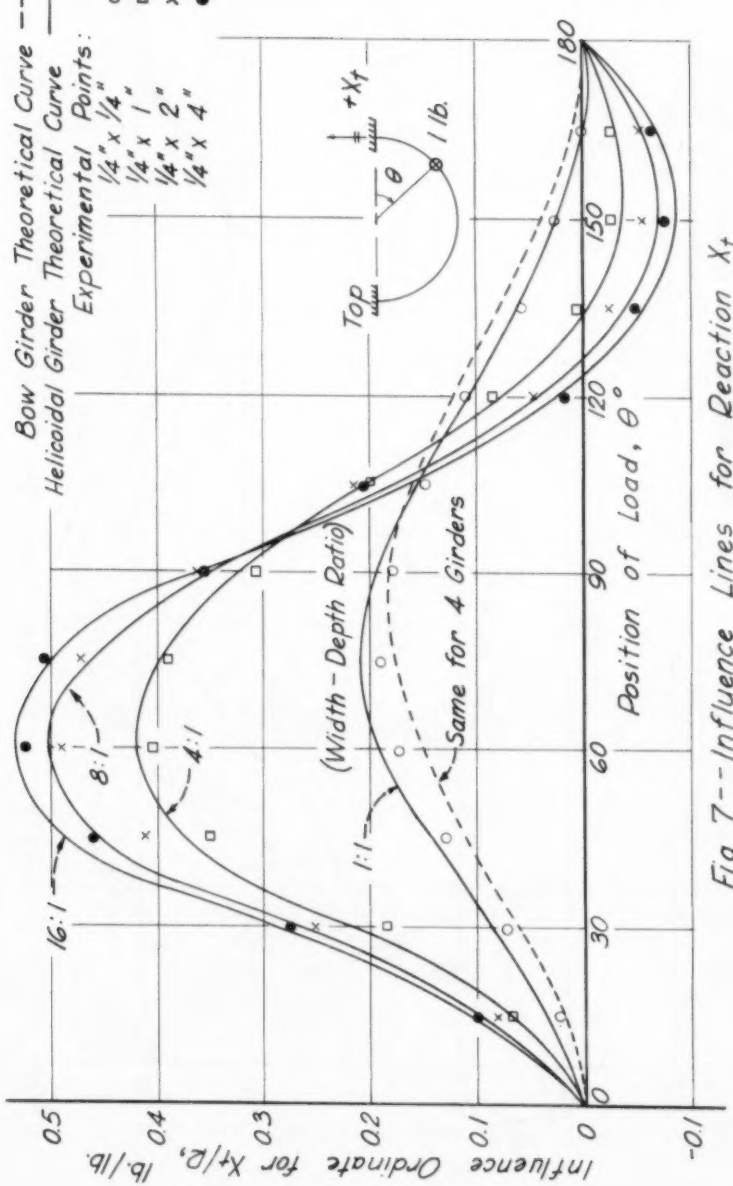

Fig 7--Influence Lines for Reaction X_f

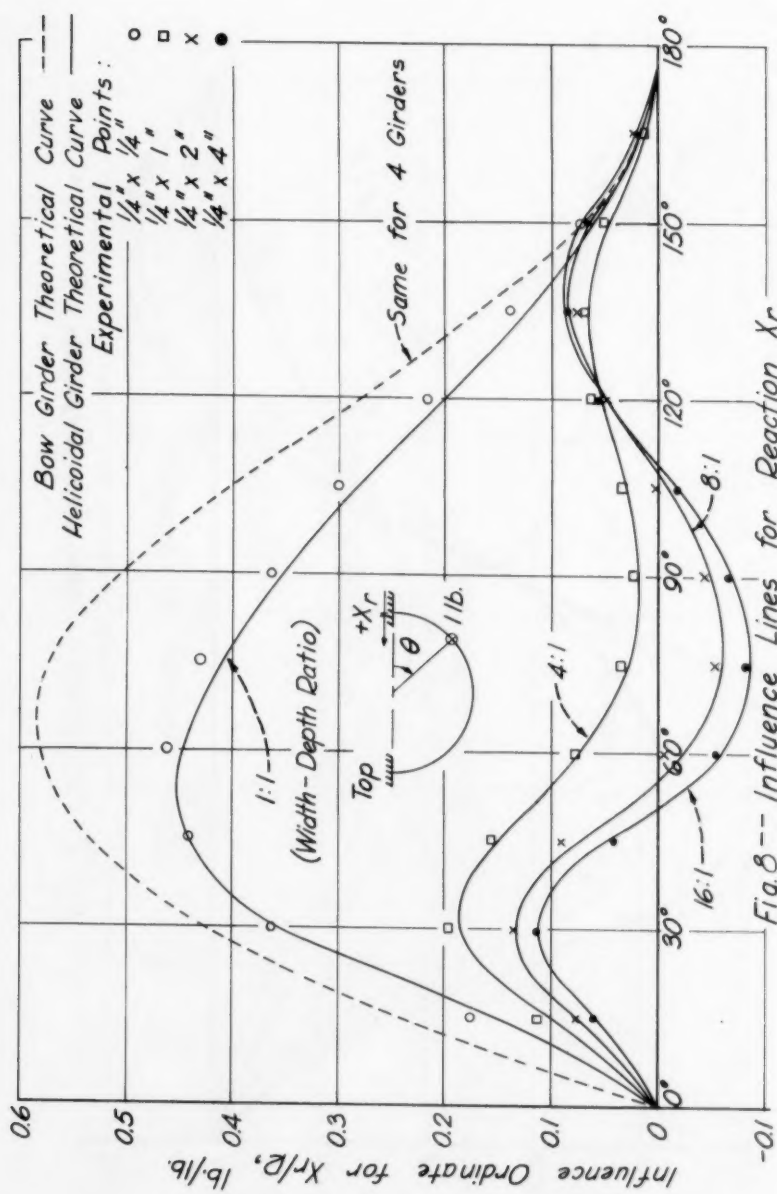

Fig. 8 -- Influence Lines for Reaction X_r

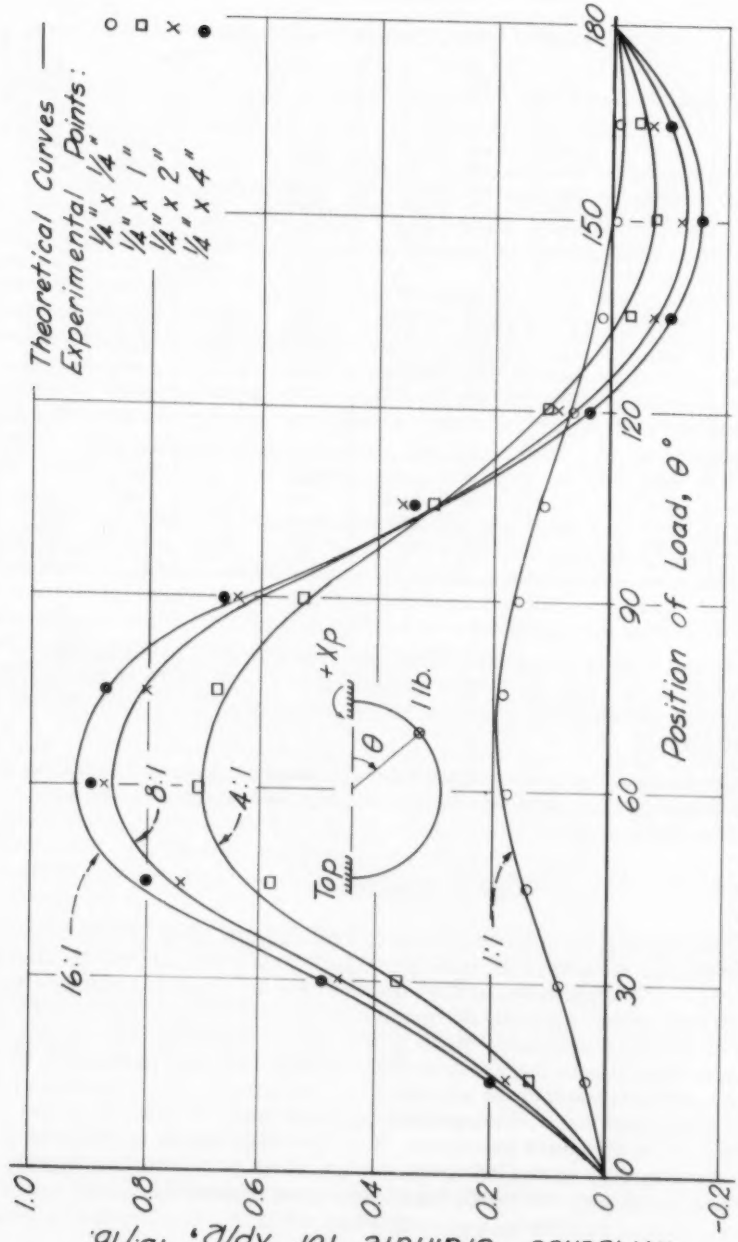

Fig. 9 -- Influence Lines for Reaction Xp

TABLE 2

Influence Line Ordinates for Reactions at Bottom

End of Helicoidal Girder Produced by a Concentrated Vertical Load

Nominal $\frac{b}{h}$	1:1	4:1	8:1	16:1	1:1	4:1	8:1	16:1
Load at θ	X_x				$X_{t/R}$			
30°	-.0446	-.1448	-.1649	-.1716	.0873	.2179	.2684	.2893
60°	-.1276	-.4072	-.4630	-.4813	.1937	.4240	.5041	.5356
90°	-.1674	-.5314	-.6041	-.6277	.1938	.3247	.3528	.3621
120°	-.1276	-.4072	-.4630	-.4813	.1068	.0770	.0403	.0229
150°	-.0446	-.1448	-.1649	-.1716	.0234	-.0359	-.0709	-.0863
	X_y				$X_{r/R}$			
30°	-.0665	-.3387	-.4586	-.5091	-.3599	-.1874	-.1347	-.1141
60°	-.0917	-.4645	-.6286	-.6973	-.4388	-.0736	.0243	.0606
90°	.0000	.0000	.0000	.0000	-.3482	-.0181	.0479	.0693
120°	+.0917	+.4645	+.6286	+.6973	-.1959	-.0538	-.0504	-.0536
150°	+.0665	+.3393	+.4593	+.5099	-.0593	-.0501	-.0665	-.0750
	X_z				$X_{p/R}$			
30°	.9046	.7526	.6867	.6592	.0869	.3605	.4570	.4964
60°	.7103	.5022	.4118	.3740	.1860	.7029	.8632	.9252
90°	.5000	.5000	.5000	.5000	.1674	.5314	.6042	.6279
120°	.2898	.4978	.5882	.6260	.0691	.1115	.0629	.0375
150°	.0955	.2477	.3138	.3417	.0021	-.0712	-.1276	-.1531

3. The unit load is distributed uniformly over the width of the girder.
4. The structure may be studied by neglecting any slab effects and analyzing only the elastic line defined by the longitudinal centroidal axis of the girder.

In order to investigate the validity of these assumptions and the results obtained in the analytical solution, the model analysis described in the next section was undertaken.

Experimental Solution

The experimental solution involved a model analysis using the displacement method based on the Muller-Breslau principle. This principle may be stated as follows:(9) "The ordinates of the influence line for any force element (such as axial force, shear, moment, or reaction) of any structure are proportional to those of the deflection curve which is obtained by removing only the restraint corresponding to that element from the structure and introducing in its place a deformation into the structure that remains". The advantage of this type of analysis over other methods becomes more pronounced as the complexity of the structure increases. It is especially useful in analyzing a space structure, such as the helicoidal girder, which is relatively complex geometrically and also has a high degree of indeterminacy.

Apparatus and Procedure

The experimental analysis was conducted with the aid of the apparatus shown in Fig. 10. Part of the apparatus was required to induce end displacements in the models, and the remainder was required to measure the resulting deflections. The apparatus was designed by Gerstle[10] and had been used by him in earlier studies on the bow girder and the cantilevered scissors stairway. With minor revisions it was adapted to the analysis of the helicoidal girder.

Corresponding to the condition for which the structures were analyzed, the left abutment of the deformeter apparatus provided a fixed support, while the right abutment was movable. This movable right abutment through which all but one of the displacements were introduced is the principal feature of the apparatus and is shown in detail in Fig. 11. An 8-in. milling machine turntable provided for translations in the direction of the y and z-axis and for a rotation about the x-axis. A 4-in. channel-arm swinging between ball-bearing pillow blocks permitted the necessary rotation about the y-axis. Translation in the direction of the x-axis was achieved by removing or inserting spacer blocks between the turntable and pillow blocks. Rotation about the z-axis was introduced at the left support while the right abutment was kept fixed. This rotation was accomplished by rotating the upper portion of the frame at the left support through a prescribed amount and then bolting it back to the main frame.

Some play was present in the controls of the milling-machine turntable so that the graduations provided thereon were not sufficiently accurate to measure the induced displacements. Instead, the end movements were measured by means of dial gages which had a least count of 0.001 in. Two dial gages were used for a check. Cantilevered arms, the ends of which rested on dial gages, were used to measure rotations.

Vertical displacements along the length and width of the models were measured from a steel plate which could be accurately leveled. The actual measuring device consisted of a movable overhanging arm, on the end of which was an adjustable vertical rod and a micrometer gage reading to 0.001 in.

An extremely useful device was the "Magic Eye" tube contact indicator which served to indicate the instant of contact between the micrometer on the measuring rod and the model. When contact was established, a gap in the fluorescent tube closed. Aquadag, trade name for a collidal water-soluble graphite solution, was brushed on the plastic models to make the surfaces conductive.

End displacements were induced in such a manner that one-half of the total was introduced in opposite directions in order to compensate for geometrical errors which result from large displacements. Large displacements were deemed necessary to insure sufficient accuracy in making the various measurements. Readings were taken at 15 degree intervals of horizontal angle along the centerline of the models.

Plastic Models

From earlier work in this field[10] it was known that plexiglas, a clear plastic, possessed several desirable model qualities. Among these are flexibility and workability. It is far more flexible than steel or aluminum, the

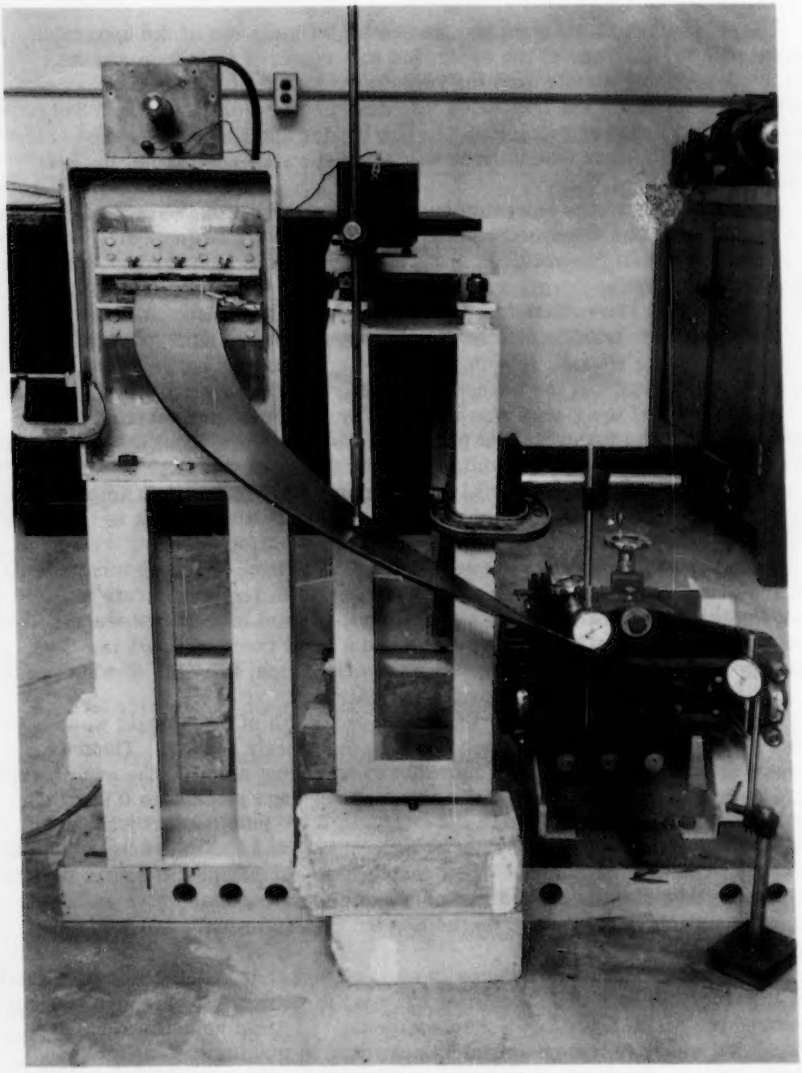

Fig. 10 Over-all experimental setup showing 1/4 x 4 in. Plexiglas model mounted in position

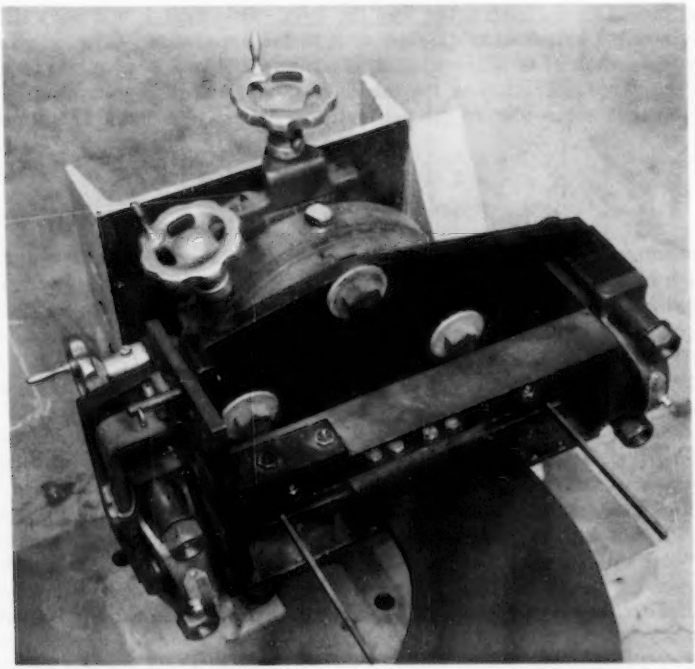

Fig. 11 Detail of movable abutment of deformeter apparatus

modulus of elasticity being on the order of one-half million lbs per sq. in. Furthermore, the plastic can be easily formed into any shape when heated to a pliable state at about 300° F. Plastics have the undesirable property of creeping under stress; however, this property is of secondary importance in displacement models, since the elastic curve resulting from an induced displacement is independent of the modulus of elasticity of the structure as long as the modulus is constant throughout the structure.

Although the helicoidal girder may be visualized as being a circular bow girder with one end displaced vertically out of the plane of the other, a true helicoidal surface is non-developable, that is, it cannot be obtained by cutting a flat sheet and then lifting or bending it into shape. Accordingly, the plexiglas models had to be formed between two relatively rigid helicoidal surfaces.

These two surfaces were obtained by first constructing a pattern of the 4-in.-wide model having a centerline radius of 12 in. using gypsum cement reinforced with expanded metal. This pattern in turn was used to cast an aluminum model of the helicoidal girder. The aluminum model may be used at a future date in stress investigations. Two rigid surfaces were now available to form the plastic models. This was achieved by heating a 1/4-in. flat sheet of plastic to the proper temperature and forming it to the desired shape by clamping it between the gypsum-cement pattern and the aluminum casting.

The first model thus constructed was the 4-in.-wide model, and very little difficulty was experienced in displacing it in the apparatus. Subsequently three more models of smaller widths, (2, 1, and 1/4 in.) were made by performing the same operation as for the 4-in. model and then trimming the edges from both sides toward the centerline. All models had a 12-in. centerline radius.

Model Analysis Results

The results of the model analyses are plotted on Fig. 4, 5, 6, 7, 8 and 9. Experimental values may be compared with influence lines obtained from the theoretical analyses. Agreement is generally good and seems to justify the assumptions made in the theoretical analysis. No systematic order of deviations is apparent, the deviations varying in nature from curve to curve for a particular model. A summary of the maximum differences between experimental and theoretical ordinates is given in Table 3.

Influence lines for reactions resulting from concentrated vertical loads acting along the centerline of the girder have been shown in Fig. 4 through 9. In slab-like structures these influence lines should extend across the width of the structure as well as through the length of the structure so that influence surfaces can be plotted. In the case of the 4-in.-wide model experimental influence ordinates were obtained at the inner and outer edges of the girder as well as along the centerline. These values are not recorded in this paper, but it is important to note that a linear relationship existed for the influence ordinates across the width of the structure, the ordinate at the centerline being the average ordinate at any radial section. Inasmuch as these structures are normally designed for a load in lbs per sq. ft. of horizontal projected area it is apparent that a centerline analysis is sufficient for design purposes.

End Reactions Under Distributed Load

Having obtained influence lines for end reactions, it is a relatively simple task to obtain end reactions under any distributed loading condition by simply determining the area under the influence line between the two limits of the distributed load. In design the three cases of a uniformly distributed load over the whole span, the bottom half, and the top half are perhaps of greatest importance. For this reason curves for reactions at the bottom end versus width-depth ratio of girder cross-section are given in Fig. 12, 13, and 14 for the three cases mentioned above. Sign convention is as illustrated in Fig. 2. A study of these curves reveals in almost all cases a rapid initial change of end reactions with increasing width-depth ratios between 1 and 4, but a relatively small change between 8 and 16. A reinspection of Table 1, which gives section properties of the various girders, shows that between the 8:1 and 16:1 ratios the EI_r/EI_s ratio changes considerably while there is only a small change in the EI_r/GJ_e ratio. Apparently the controlling factor in the behavior of the girder, after I_s has reached a sufficiently large value, is the ratio of EI_r/GJ_e.

It should be pointed out that in designing a slab like structure the resultant of a uniform load across any radial width will have a small eccentricity with respect to the centerline of the girder, since the inner circumference of the girder is smaller than the outer circumference. The effect of this eccentricity

TABLE 3

Maximum Differences between Experimental and Theoretical

Influence Ordinates for End Reactions of Helicoidal Girders

Girders	Maximum Difference for Entire Curve				Max. Theor. Ordinate for Curve		Maximum Difference for Entire Curve				Max. Theor. Ordinate for Curve	
	Position	Theor.	Exper.	Diff.	Position	Theor.	Position	Theor.	Exper.	Diff.	Position	Theor.
	X_x						$X_{t/R}$					
1:1	90°	.167	.172	.015	90°	.167	60°	.194	.174	.020	75°	.208
4:1	150°	.145	.152	.007	90°	.531	30°	.218	.188	.030	60°	.424
8:1	120°	.463	.476	.013	90°	.604	30°	.268	.252	.016	60°	.504
16:1	150°	.172	.162	.010	90°	.628	30°	.289	.276	.013	60°	.536
	X_y						$X_{r/R}$					
1:1	120°	.092	.090	.002	48°	.097	120°	.196	.221	.025	53°	.449
4:1	120°	.465	.444	.021	53°	.480	120°	.054	.065	.011	30°	.187
8:1	120°	.629	.582	.047	53°	.650	60°	.024	.003	.021	30°	.135
16:1	90°	.000	.032	.032	53°	.720	60°	.061	.051	.010	30°	.114
	X_z						$X_{p/R}$					
1:1	120°	.290	.312	.022	0°	1.000	60°	.186	.179	.007	72°	.191
4:1	60°	.502	.516	.014	0°	1.000	60°	.703	.710	.007	60°	.703
8:1	60°	.412	.440	.028	0°	1.000	90°	.604	.650	.046	60°	.863
16:1	150°	.342	.373	.031	0°	1.000	90°	.628	.670	.042	60°	.925

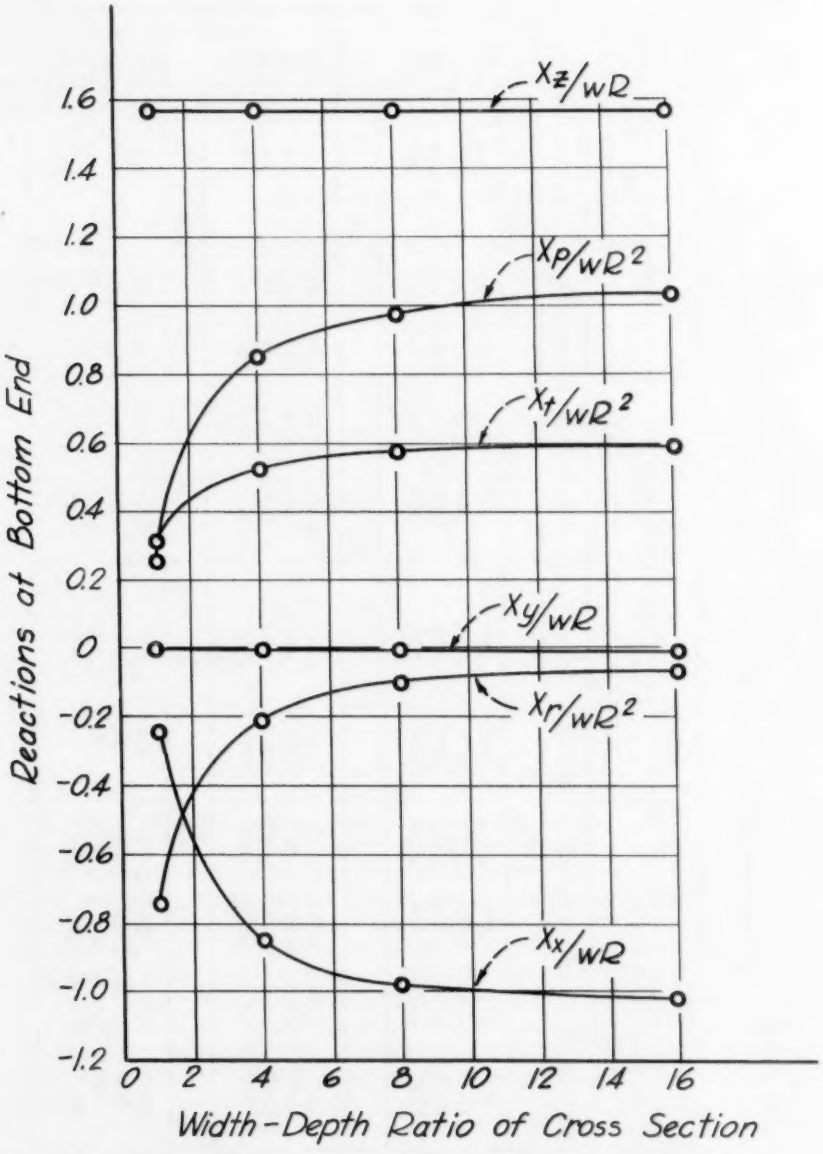

Fig. 12--End Reactions at Bottom of Helicoidal Girder Due to Uniform Load of "w" on Whole Span

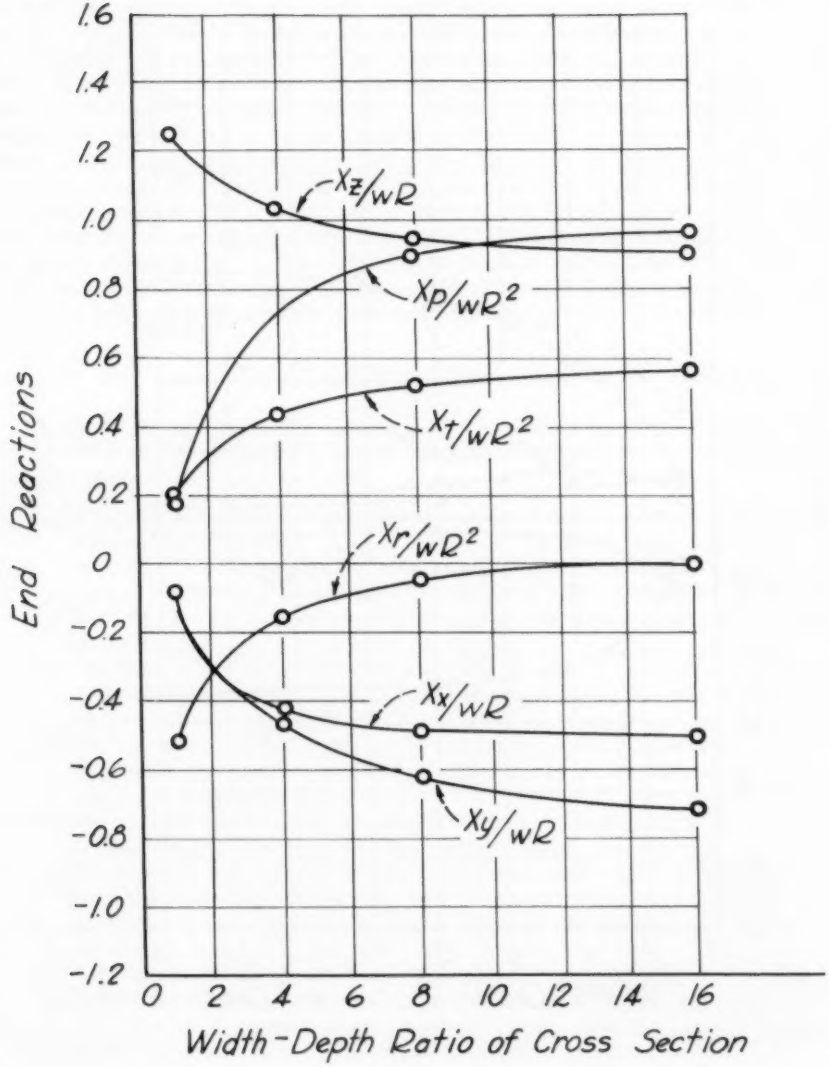

Fig. 13 -- End Reaction at Bottom of Helicoidal Girder Due to Uniform Load of "w" on Bottom Half

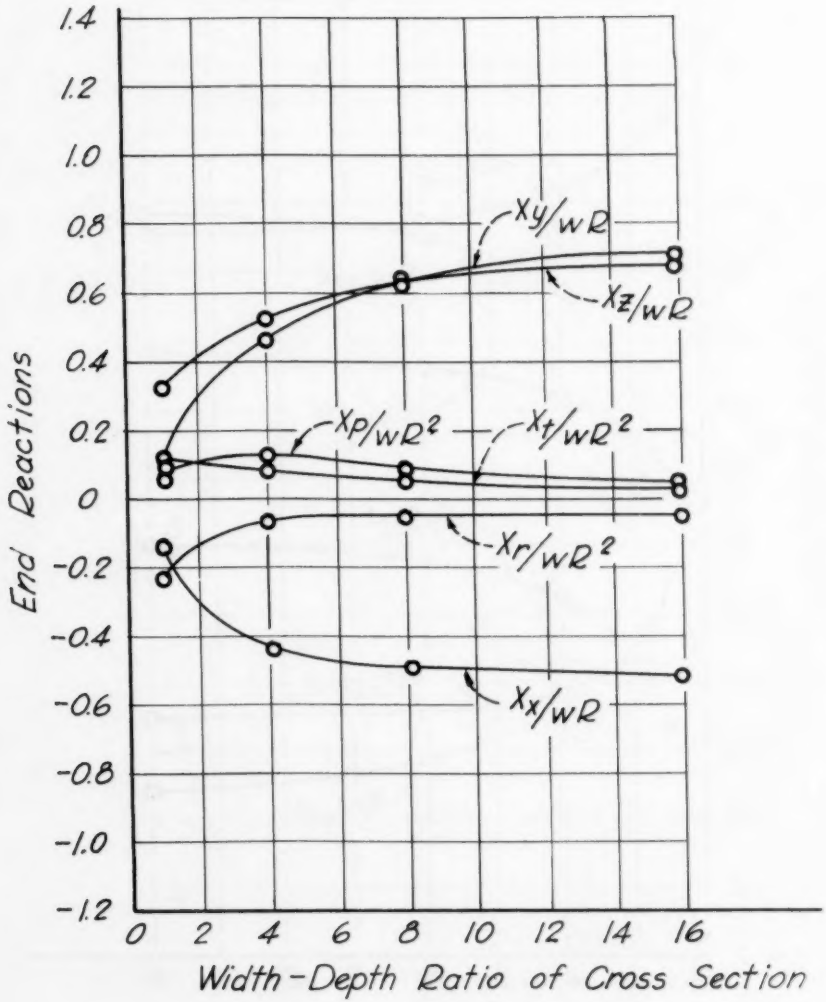

Fig. 14 -- End Reactions at Bottom of Helicoidal Girder Due to Uniform Load of "w" on Top Half

of load was negligible in the cases considered in this paper and the resultant load could be assumed as acting on the centerline of the girder.

Once the end reactions are known the bending moments, torsional moment, shears, and axial force at any section may be obtained by simple statics. A plot of the bending moments about the r and s axes and torsional moments about the e axis (see Fig. 3) for the four girders under a uniformly distributed load may be found in a discussion of a paper by one of the authors.(11) It was found, as might be expected, that the moments about the r and e axes decreased tremendously with increasing width-depth ratio while the moments about the s-axis increased somewhat. The net result indicates that for a given depth of cross-section the stresses due to bending and torsional moments will rapidly get smaller up to a width-depth ratio of 8:1 after which there will be a much smaller decrease in stresses.

CONCLUSIONS

On the basis of the study reported in this paper the following conclusions may be drawn regarding the behavior and analysis of a semi-circular helicoidal girder under vertical load.

1. For girders with rectangular cross sections having a width-depth ratio between 1 and 16 and a ratio of centerline radius to width between 3 and infinity, sufficiently accurate results for the end reactions to be used in design may be obtained by analyzing only the elastic line defined by the longitudinal centroidal axis of the girder, thus neglecting slab effects.
2. The bending and torsional stiffnesses to be used in the analysis may be taken as those defined for a straight prismatic member of the same cross-section.
3. The influence ordinates across the width of a girder have a linear relationship, the ordinate at the centerline being the average ordinate at any radial section.
4. For a cross-section of given depth there is little change in the end reactions for increasing width-depth ratios beyond about 6 to 8.
5. For girders subjected to a uniformly distributed load over the whole span the stresses in the girder will decrease rapidly with increasing width-depth ratio up to about 6 to 8, after which there will be little change.
6. A design based on the internal moments and torques obtained by analyzing the horizontal projection of the helicoid as a bow girder under uniform load will, in most cases, be grossly conservative since it neglects the inherent strength of the three-dimensional structure.

Obviously a determination of the end reactions is only a first step in the design of this type of a structure. Once the end reactions are known the internal forces and moments at any cut section may be obtained, but a knowledge of stress distribution is still lacking. This later problem requires further study. However, in reinforced concrete structures the proportioning of sections and reinforcement must in all probability be based on approximate methods rather than "exact" stress formulas.

REFERENCES

1. Magnel, G., "Revolutionary Staircase Built of Prestressed Concrete", Civil Engineering, v. 21, No. 9, Sept. 1951, pp 25-27, with discussions in No. 11, Nov. 1951, p 56; v. 22, No. 2; Feb. 1952, p 52, and No. 5, May 1952, p 56.
2. Bourne, N. B., "Rapid Concrete Construction in Spain", Concrete and Constructional Engineering (London), v. 45, No. 10, Oct. 1950, pp 357-362.
3. Bergman, V. R., "Helicoidal Staircases of Reinforced Concrete", Journal ACI, v. 28, No. 4, Oct. 1956, pp 403-412.
4. Timoshenko, S. and Goodier, J. N., "Theory of Elasticity", McGraw Hill Book Co., Inc., New York, 2nd Edition, 1951.
5. Michalos, J. P., "Numerical Analysis of Frames with Curved Girders", Transactions, ASCE, v. 121, 1956, pp 521-543.
6. Hogan, M. B., "The Solution of Closed Circular Rings by the Conjugate Ring Method", Bulletin of the University of Utah, v. 38, No. 14, Jan. 1948. (Contains extensive bibliography.)
7. Moorman, R. B. B. and Tate, M. B., "Influence Lines for Horizontally Curved Fixed-End Beams of Circular Arc Plan", University of Missouri Bulletin, v. 48, No. 26, Oct. 1947.
8. Gibson, A. H. and Ritchie, E. G., "A Study of the Circular Arc Bow Girder," D. Van Nostrand and Co., New York, 1915.
9. Wilbur, J. B. and Norris, C. H., "Elementary Structural Analysis", McGraw Hill Book Company, Inc., New York, 1st Edition, 1948.
10. Gerstle, K. H. and Clough, R. W., "Model Analyses of Three-Dimensional Slab Structures", Proc. Society for Experimental Stress Analysis, v. 13, No. 2, 1955.
11. Scordelis, A. C., Discussion of reference 3, Journal ACI, v. 28, No. 12, June 1957.
12. Fuchssteiner, W., "Die freitragende Wendeltreppe (Spannungsberechnung und Bewehrung)," Beton- und Stahlbetonbau (Berlin), V. 49, No. 11, 1954, pp 256-258.
13. Gedizli, H. S., Discussion:"Die freitragende Wendeltreppe," Beton- und Stahlbetonbau (Berlin), V. 50, No. 9, Sept. 1955, p 247.
14. Cohen, J. S., "Design of Helical Staircases," Concrete and Construction Engineering (London), V. 50, No. 5, May 1955, pp 181-194.

APPENDIX

The following equations express the displacements at the bottom end of a helicoidal girder subtending a horizontal angle, ϕ, equal to 180 degrees due to a vertical concentrated load P. Terms used in equations are defined as follows: See Fig. 2

- R horizontal radius
- α helix angle, slope of girder
- EI_r, EI_s bending stiffnesses about r and s axes respectively
- GJ_e torsional stiffness about e axis
- θ horizontal angle from bottom end to position of concentrated load P

$$\delta_{xx}=\frac{R^3}{EI_r}\left[\frac{\tan^2\alpha}{\cos\alpha}\right]\left[\frac{\pi^3}{6}+\frac{\pi}{4}\right]+\frac{R^3}{EI_s}\left[\frac{1}{\cos\alpha}\right]\left[(\cos^2\alpha)\left(\frac{3\pi}{2}\right)+(\sin^2\alpha)\left(\frac{5\pi}{2}\right)\right.$$
$$\left.+(\sin\alpha\tan\alpha)^2\left(\frac{\pi^3}{6}-\frac{\pi}{4}\right)\right]+\frac{R^3}{GJ_e}\left[\frac{1}{\cos\alpha}\right]\left[(\sin^2\alpha)\left(\frac{\pi^3}{6}-\frac{5\pi}{4}\right)\right]$$

$$\delta_{xy}=\delta_{yx}=\frac{R^3}{EI_r}\left[\frac{\tan^2\alpha}{\cos\alpha}\right]\left[\frac{\pi^2}{4}\right]+\frac{R^3}{EI_s}\left[\frac{1}{\cos\alpha}\right]\left[2\cos^2\alpha-2\sin^2\alpha\right.$$
$$\left.-(\sin\alpha\tan\alpha)^2\left(\frac{\pi^2}{4}\right)\right]+\frac{R^3}{GJ_e}\left[\frac{\sin^2\alpha}{\cos\alpha}\right]\left[4-\frac{\pi^2}{4}\right]$$

$$\delta_{xz}=\delta_{zx}=\frac{R^3}{EI_r}\left[-\frac{\tan\alpha}{\cos\alpha}\right]\left[\frac{\pi}{4}\right]+\frac{R^3}{EI_s}\left[\sin\alpha\right]\left[\frac{3\pi}{2}+(\tan^2\alpha)\left(\frac{5\pi}{4}\right)\right]$$
$$+\frac{R^3}{GJ_e}\left[-\sin\alpha\right]\left[\frac{\pi}{4}\right]$$

$$\delta_{xp}=\delta_{px}=\frac{R^2}{EI_s}\left[\cos\alpha\right]\left[\pi+(\tan^2\alpha)(\pi)\right]$$

$$\delta_{xr}=\delta_{rx}=\frac{R^2}{EI_r}\left[\frac{\tan\alpha}{\cos\alpha}\right]\left[\frac{\pi^2}{4}\right]+\frac{R^2}{EI_s}\left[\sin\alpha\right]\left[(\tan^2\alpha)\left(\frac{\pi^2}{4}\right)+2\right]$$
$$+\frac{R^2}{GJ_e}\left[\sin\alpha\right]\left[\frac{\pi^2}{4}-2\right]$$

$$\delta_{xt}=\delta_{tx}=\frac{R^2}{EI_r}\left[\frac{\tan\alpha}{\cos\alpha}\right]\left[\frac{\pi}{4}\right]+\frac{R^2}{EI_s}\left[-\sin\alpha\right]\left[\frac{\pi}{2}+(\tan^2\alpha)\left(\frac{\pi}{4}\right)\right]$$
$$+\frac{R^2}{GJ_e}\left[\sin\alpha\right]\left[\frac{\pi}{4}\right]$$

$$\delta_{yy}=\frac{R^3}{EI_r}\left[\frac{\tan^2\alpha}{\cos\alpha}\right]\left[\frac{\pi^3}{6}-\frac{\pi}{4}\right]+\frac{R^3}{EI_s}\left[\frac{1}{\cos\alpha}\right]\left[(\cos^2\alpha)\left(\frac{\pi}{2}\right)\right.$$
$$\left.-(\sin^2\alpha)\left(\frac{\pi}{2}\right)+(\sin\alpha\tan\alpha)^2\left(\frac{\pi^3}{6}+\frac{\pi}{4}\right)\right]+\frac{R^3}{GJ_e}\left[\frac{\sin^2\alpha}{\cos\alpha}\right]\left[\frac{\pi^3}{6}+\frac{5\pi}{4}\right]$$

$$\delta_{yz}=\delta_{zy}=\frac{R^3}{EI_r}\left[-\frac{\tan\alpha}{\cos\alpha}\right]\left[\frac{\pi^2}{4}\right]+\frac{R^3}{EI_s}\left[\sin\alpha\right]\left[2-2\tan^2\alpha\right.$$
$$\left.-(\tan^2\alpha)\left(\frac{\pi^2}{4}\right)\right]+\frac{R^3}{GJ_e}\left[-\sin\alpha\right]\left[4+\frac{\pi^2}{4}\right]$$

$$\delta_{yp}=\delta_{py}=\frac{R^2}{EI_s}\left[2(\cos\alpha-\sin\alpha\tan\alpha)\right]+\frac{R^2}{GJ_e}\left[\frac{4\sin^2\alpha}{\cos\alpha}\right]$$

$$\delta_{yr}=\delta_{ry}=\frac{R^2}{EI_r}\left[\frac{\tan\alpha}{\cos\alpha}\right]\left[\frac{\pi}{4}\right]+\frac{R^2}{EI_s}\left[\sin\alpha\right]\left[\frac{\pi}{2}-(\tan^2\alpha)\left(\frac{\pi}{4}\right)\right]$$
$$+\frac{R^2}{GJ_e}\left[-\sin\alpha\right]\left[\frac{3\pi}{4}\right]$$

$$\delta_{yt}=\delta_{ty}=\frac{R^2}{EI_r}\left[\frac{\tan\alpha}{\cos\alpha}\right]\left[\frac{\pi^2}{4}\right]+\frac{R^2}{EI_s}\left[(\sin\alpha\tan^2\alpha)\left(\frac{\pi^2}{4}\right)\right]$$
$$+\frac{R^2}{GJ_e}\left[(\sin\alpha)\left(\frac{\pi^2}{4}\right)\right]$$

$$\delta_{zz}=\frac{R^3}{EI_r}\left[\left(\frac{1}{\cos\alpha}\right)\left(\frac{\pi}{2}\right)\right]+\frac{R^3}{EI_s}\left[\frac{\sin^2\alpha}{\cos\alpha}\right]\left[\frac{3\pi}{2}\right]+\frac{R^3}{GJ_e}\left[(\cos\alpha)\left(\frac{3\pi}{2}\right)\right]$$

$$\delta_{zp}=\delta_{pz}=\frac{R^2}{EI_s}\left[(\sin\alpha)(\pi)\right]+\frac{R^2}{GJ_e}\left[(-\sin\alpha)(\pi)\right]$$

$$\delta_{zr}=\delta_{rz}=\frac{R^2}{EI_s}\left[\frac{2\sin^2\alpha}{\cos\alpha}\right]+\frac{R^2}{GJ_e}\left[2\cos\alpha\right]$$

$$\delta_{zt}=\delta_{tz}=\frac{R^2}{EI_r}\left[\left(-\frac{1}{\cos\alpha}\right)\left(\frac{\pi}{2}\right)\right]+\frac{R^2}{EI_s}\left[\left(-\frac{\sin^2\alpha}{\cos\alpha}\right)\left(\frac{\pi}{2}\right)\right]+\frac{R^2}{GJ_e}\left[(-\cos\alpha)\left(\frac{\pi}{2}\right)\right]$$

$$\delta_{pp} = \frac{R}{EI_s}\left[(\cos\alpha)(\pi)\right] + \frac{R}{GJ_e}\left[\left(\frac{\sin^2\alpha}{\cos\alpha}\right)(\pi)\right]$$

$$\delta_{pr} = \delta_{rp} = \frac{R}{EI_s}\left[2\sin\alpha\right] + \frac{R}{GJ_e}\left[-2\sin\alpha\right]$$

$$\delta_{pt} = \delta_{tp} = 0$$

$$\delta_{rr} = \frac{R}{EI_r}\left[\left(\frac{1}{\cos\alpha}\right)\left(\frac{\pi}{2}\right)\right] + \frac{R}{EI_s}\left[\left(\frac{\sin^2\alpha}{\cos\alpha}\right)\left(\frac{\pi}{2}\right)\right] + \frac{R}{GJ_e}\left[(\cos\alpha)\left(\frac{\pi}{2}\right)\right]$$

$$\delta_{rt} = \delta_{tr} = 0$$

$$\delta_{tt} = \frac{R}{EI_r}\left[\left(\frac{1}{\cos\alpha}\right)\left(\frac{\pi}{2}\right)\right] + \frac{R}{EI_s}\left[\left(\frac{\sin^2\alpha}{\cos\alpha}\right)\left(\frac{\pi}{2}\right)\right] + \frac{R}{GJ_e}\left[(\cos\alpha)\left(\frac{\pi}{2}\right)\right]$$

$$\delta_{xo} = \frac{PR^3}{EI_r}\left[-\frac{\tan\alpha}{\cos\alpha}\right]\left[\left(\frac{\cos\theta}{4}\right)\left(\theta\cos 2\theta - \frac{1}{2}\sin 2\theta - \pi\right) - \left(\frac{\sin\theta}{4}\right)\left(\frac{1}{2}\right.\right.$$
$$\left.\left. + \pi^2 - \theta^2 - \theta\sin 2\theta - \frac{\cos 2\theta}{2}\right)\right] + \frac{PR^3}{EI_s}\left[-\sin\alpha\right]\left[(\pi-\theta) + (\tan^2\alpha)\right.$$
$$\left.(\pi - \sin\theta + \theta\cos\theta) + (\cos\theta)\left(\frac{\pi}{2} - \frac{\theta}{2} - \frac{\sin 2\theta}{4}\right) + \left(\frac{\sin\theta}{4}\right)(\cos 2\theta - 1)\right.$$
$$\left. - \left(\frac{\tan^2\alpha}{4}\right)(\cos\theta)\left(\theta\cos 2\theta - \frac{1}{2}\sin 2\theta - \pi\right) - \left(\frac{\tan^2\alpha}{4}\right)(\sin\theta)\right.$$
$$\left.\left(\pi^2 - \frac{1}{2} - \theta^2 + \theta\sin 2\theta + \frac{\cos 2\theta}{2}\right)\right] + \frac{PR^3}{GJ_e}\left[-\sin\alpha\right]$$
$$\left[\theta - \frac{5}{8}\sin\theta + \frac{1}{4}(\theta^2 - \pi^2)\sin\theta + \frac{3}{2}\theta\cos\theta - \frac{\pi}{4}\cos\theta\right.$$
$$+ \frac{3}{8}\cos\theta\sin 2\theta - \frac{3}{8}\sin\theta\cos 2\theta - \frac{\theta}{4}\sin\theta\sin 2\theta$$
$$\left. - \frac{\theta}{4}\cos\theta\cos 2\theta\right]$$

$$\delta_{yo} = \frac{PR^3}{EI_r}\left[\frac{\tan\alpha}{\cos\alpha}\right]\left[\left(\frac{\cos\theta}{4}\right)\left(\pi^2 - \frac{1}{2} - \theta^2 + \theta\sin 2\theta + \frac{\cos 2\theta}{2}\right)\right.$$
$$\left. - \frac{\sin\theta}{4}\left(\theta\cos 2\theta - \frac{1}{2}\sin 2\theta - \pi\right)\right] + \frac{PR^3}{EI_s}\left[-\sin\alpha\right]\left[1 + \cos\theta\right.$$
$$\left. - \left(\tan^2\alpha\right)\left(1 + \cos\theta + \theta\sin\theta\right) - \left(\frac{\cos\theta}{4}\right)\left(\cos 2\theta - 1\right) - \left(\frac{\sin\theta}{2}\right)\right.$$
$$\left.\left(\pi - \theta + \frac{\sin 2\theta}{2}\right) - \left(\frac{\tan^2\alpha}{4}\right)\left(\cos\theta\right)\left(\frac{1}{2} + \pi^2 - \theta^2 - \theta\sin 2\theta\right.\right.$$
$$\left.\left. - \frac{\cos 2\theta}{2}\right) - \left(\frac{\tan^2\alpha}{4}\right)\left(\sin\theta\right)\left(\theta\cos 2\theta - \frac{1}{2}\sin 2\theta - \pi\right)\right]$$
$$+ \frac{PR^3}{GJ_e}\left[-\sin\alpha\right]\left[-\left(1 + \cos\theta + \theta\sin\theta\right) - \left(1 + \cos\theta\right) - \left(\frac{\cos\theta}{4}\right)\right.$$
$$\left.\left(\frac{3}{2} + \pi^2 - \theta^2 - \theta\sin 2\theta - \frac{3}{2}\cos 2\theta\right) - \left(\frac{\sin\theta}{4}\right)\left(\theta\cos 2\theta\right.\right.$$
$$\left.\left. - \frac{3}{2}\sin 2\theta - 3\pi + 2\theta\right)\right]$$

$$\delta_{zo} = \frac{PR^3}{EI_r}\left[-\frac{1}{\cos\alpha}\right]\left[\left(\frac{\cos\theta}{2}\right)\left(\pi - \theta + \frac{\sin 2\theta}{2}\right) - \left(\frac{\sin\theta}{4}\right)\left(\cos 2\theta - 1\right)\right]$$
$$+ \frac{PR^3}{EI_s}\left[-\frac{\sin^2\alpha}{\cos\alpha}\right]\left[\pi - \theta + \left(\frac{\cos\theta}{2}\right)\left(\pi - \theta - \frac{\sin 2\theta}{2}\right) + \left(\frac{\sin\theta}{4}\right)\right.$$
$$\left.\left(\cos 2\theta - 1\right)\right] + \frac{PR^3}{GJ_e}\left[-\cos\alpha\right]\left[\pi - \theta + \left(\frac{\cos\theta}{2}\right)\left(\pi - \theta - \frac{\sin 2\theta}{2}\right)\right.$$
$$\left. + \left(\frac{\sin\theta}{4}\right)\left(\cos 2\theta - 1\right)\right]$$

$$\delta_{po}=\frac{PR^2}{EI_s}\left[-\sin\alpha\right]\left[(\pi-\theta)-\sin\theta\right]+\frac{PR^2}{GJ_e}\left[\sin\alpha\right]\left[(\pi-\theta)-\sin\theta\right]$$

$$\delta_{ro}=\frac{PR^2}{EI_r}\left[-\frac{1}{\cos\alpha}\right]\left[\left(\frac{\cos\theta}{4}\right)(\cos 2\theta-1)-\left(\frac{\sin\theta}{2}\right)\left(\pi-\theta-\frac{\sin\theta}{2}\right)\right]$$
$$+\frac{PR^2}{EI_s}\left[-\frac{\sin^2\alpha}{\cos\alpha}\right]\left[1+\cos\theta-\left(\frac{\cos\theta}{4}\right)(\cos 2\theta-1)-\left(\frac{\sin\theta}{2}\right)\right.$$
$$\left.\left(\pi-\theta+\frac{\sin 2\theta}{2}\right)\right]+\frac{PR^2}{GJ_e}\left[-\cos\alpha\right]\left[1+\cos\theta-\left(\frac{\cos\theta}{4}\right)(\cos 2\theta-1)\right.$$
$$\left.-\left(\frac{\sin\theta}{2}\right)\left(\pi-\theta+\frac{\sin 2\theta}{2}\right)\right]$$

$$\delta_{to}=\frac{PR^2}{EI_r}\left[\frac{1}{\cos\alpha}\right]\left[\left(\frac{\cos\theta}{2}\right)\left(\pi-\theta+\frac{\sin 2\theta}{2}\right)-\left(\frac{\sin\theta}{4}\right)(\cos 2\theta-1)\right]$$
$$+\frac{PR^2}{EI_s}\left[-\frac{\sin^2\alpha}{\cos\alpha}\right]\left[-\sin\theta-\left(\frac{\cos\theta}{2}\right)\left(\pi-\theta-\frac{\sin 2\theta}{2}\right)-\left(\frac{\sin\theta}{4}\right)\right.$$
$$\left.(\cos 2\theta-1)\right]+\frac{PR^2}{GJ_e}\left[-\cos\alpha\right]\left[-\sin\theta-\left(\frac{\cos\theta}{2}\right)\left(\pi-\theta-\frac{\sin 2\theta}{2}\right)\right.$$
$$\left.-\left(\frac{\sin\theta}{4}\right)(\cos 2\theta-1)\right]$$

Paper 1757 September, 1958 ST 5

Journal of the
STRUCTURAL DIVISION
Proceedings of the American Society of Civil Engineers

PRACTICAL ASPECTS OF ULTIMATE STRENGTH DESIGN

Alfred L. Parme,[1] A.M. ASCE
(Proc. Paper 1757)

SYNOPSIS

Time-saving design charts for the rapid selection of the critical-load-factor combination are presented. The paper also includes studies comparing the loads and area of reinforcement as obtained by the ultimate-strength procedure to that obtained by conventional methods.

More than any other method, ultimate strength design procedure directs the attention of the engineer to the two primary considerations involved in any design. The first of these is that of providing a sufficient margin of safety against (a) overloading, (b) uncertainties in the method of analysis and (c) variations in the strength of materials. The second consideration is that of securing satisfactory behavior at service loads. Ultimate strength design satisfies the first requirement by relating the margin of safety directly to overload factors which can be varied to accomodate the conditions of a particular situation. More specifically, the ultimate strength of a section is equated to the stresses produced by multiples of the service loads.

Critical Load Combinations

In its recently published report the Joint ASCE-ACI Committee on Ultimate Strength Design recommends that four critical load combinations be investigated for bending and for combined bending and axial load. For bending the four combinations are shown in Fig. 1 in which , as defined in the report published as ASCE Proceedings Paper No. 809,

U = ultimate strength of section,

B = effect of basic load consisting of dead load

Note: Discussion open until February 1, 1959. To extend the closing date one month, a written request must be filed with the Executive Secretary, ASCE. Paper 1757 is part of the copyrighted Journal of the Structural Division, Proceedings of the American Society of Civil Engineers, Vol. 84, No. ST 5, September, 1958.

1. Cons. Engr., Portland Cement Assn., Chicago, Ill.

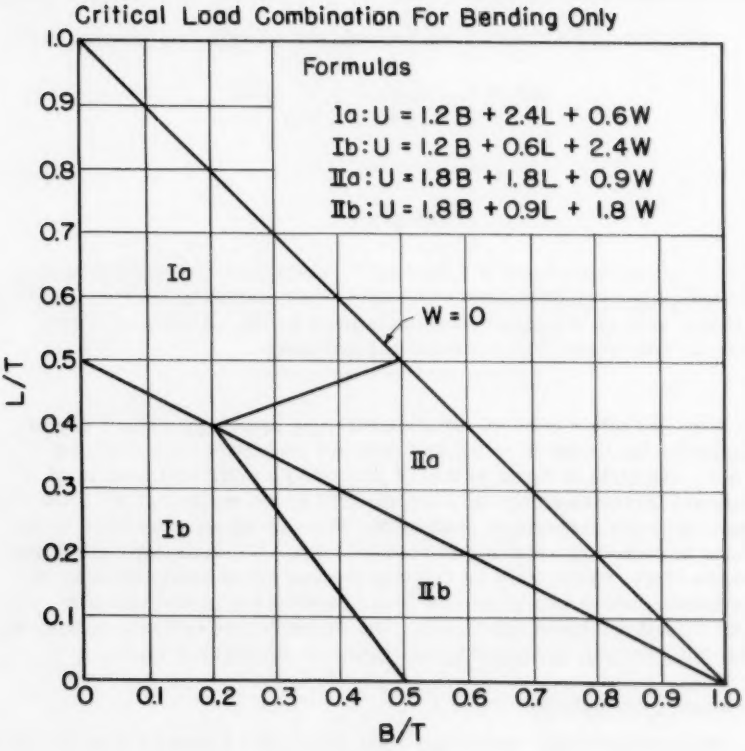
Critical Load Combination For Bending Only
Formulas
Ia: U = 1.2 B + 2.4L + 0.6W
Ib: U = 1.2 B + 0.6L + 2.4W
IIa: U = 1.8B + 1.8L + 0.9W
IIb: U = 1.8 B + 0.9L + 1.8 W
Ia
Ib
W = 0
IIa
IIb
L/T
B/T
0
0.1
0.2
0.3
0.4
0.5
0.6
0.7
0.8
0.9
1.0

Fig. 1

plus volume change due to plastic and elastic actions, shrinkage and temperature change,

L = effect of live load plus impact,
W* = effect of wind load,
T** = effect of all loads.

Throughout this paper the symbols B, L, W and T will be referred to loosely as basic, live, wind and total load. However, it should be understood that it is the effect and not the actual loads that is intended. By definition then

$$W = T - B - L \tag{1}$$

Replacing W by its value as expressed in equation (1), the four equations in Fig. 1 can be rewritten as

$$U_{Ia} = 0.6B + 1.8L + 0.6T \tag{2a}$$

$$U_{Ib} = -1.2B - 1.8L + 2.4T \tag{2b}$$

$$U_{IIa} = 0.9B + 0.9L + 0.9T \tag{2c}$$

$$U_{IIb} = -0.9L + 1.8T \tag{2d}$$

with the subscript for U denoting the particular combination. For a given set of ratios of basic and live load to total load, there is one formula which yields the maximum value. The particular formula which controls can be readily obtained by first determining the ratios at which any two formulas give equal ultimate moment. Taking U_{Ia} equal to U_{Ib}, then subtracting equation (2b) from (2a), gives

$$1.8B + 3.6L - 1.8T = 0 \tag{3a}$$

which reduces to

$$L/T = -0.5B/T + 0.5 \tag{3b}$$

In a similar manner, subtracting equation (2c) from (2a) with $U_{Ia} = U_{IIa}$

$$L/T = 0.33B/T + 0.33 \tag{3c}$$

Subtracting equation (2d) from (2c) gives

$$L/T = -0.5B/T + 0.5 \tag{3d}$$

* For structures subject to earthquakes, substitute E for W.
** This symbol not included in Joint Committee Report.

and subtracting equation (2d) from (2b) gives

$$L/T = -1.33B/T + 0.67 \qquad (3e)$$

The plot of the four equations (3b) to (3e) on a single graph as in Fig. 1 for bending only defines the limits of the area of application of each combination. Except near the boundaries, the particular formula to be used can be determined by mental arithmetic.

The same type of design aid is presented in Fig. 2 for combined bending and axial load. However, in this case, two separate investigations must be made, one to determine the combination yielding the maximum thrust and one to determine the combination giving the maximum moment. Even then this two fold examination can only act as a guide since the critical moment-thrust value may not be given by the maximum value of either the thrust or moment.

Overall Factor of Safety

One of the first questions that enters the mind of engineers familiarizing themselves with ultimate strength design is how does the overall margin of safety provided by this procedure compare to that given by the straightline theory and allowable working stresses, hereafter referred to as the conventional method. Such a comparison to be exact entails for indeterminate structures a complete analysis by the two methods even to the extent of making separate frame analyses. The reason for this is that the maximum moments in an indeterminate structure require loading of specific areas or bays. Since the ultimate strength method for some load combinations assigns a higher overload factor to live load than to dead load, it imposes a loading that is more severe than the conventional procedure which places only one live load on contributing areas. However, to shed some light on this question, Fig. 3 is presented. In this figure the overall factor F has been computed by dividing the ultimate capacity as given by formulas Ia to IIb by the sum of the basic load, live load and wind load, which always yields a conservative value.

If it is assumed that the overall factor by the conventional method of design is 2, it is evident from Fig. 3 that when no wind load is involved and the ratio of basic load to live load is less than 0.5, the ultimate strength recommendations are more severe. When the basic load is large, giving a ratio of basic load to live load of more than 0.5, the ultimate strength recommendations are more liberal. This difference in overall factors is justified by the fact that the live loads are less predictable quantities and are beyond the designer's control while dead load is a fixed determinate quantity unchanging throughout the life of the structure.

When the wind load is more than 25 per cent of the sum of the basic load and live load, the overall factor given by ultimate strength equations is larger than that obtained by the conventional method which, by permitting a one-third increase in allowable stresses, reduces the overall factor from 2 to 1.5. Hence, for most conditions involving wind load, ultimate strength requirements are more critical.

The graphical presentation of the overall factor in Fig. 3 is to some extent marred by the difficulty of interpolating for ratios of wind load to the sum of basic and live load greater than 0.25. A superior chart is possible by altering the form of the parameters to ratios of the individual loads to the

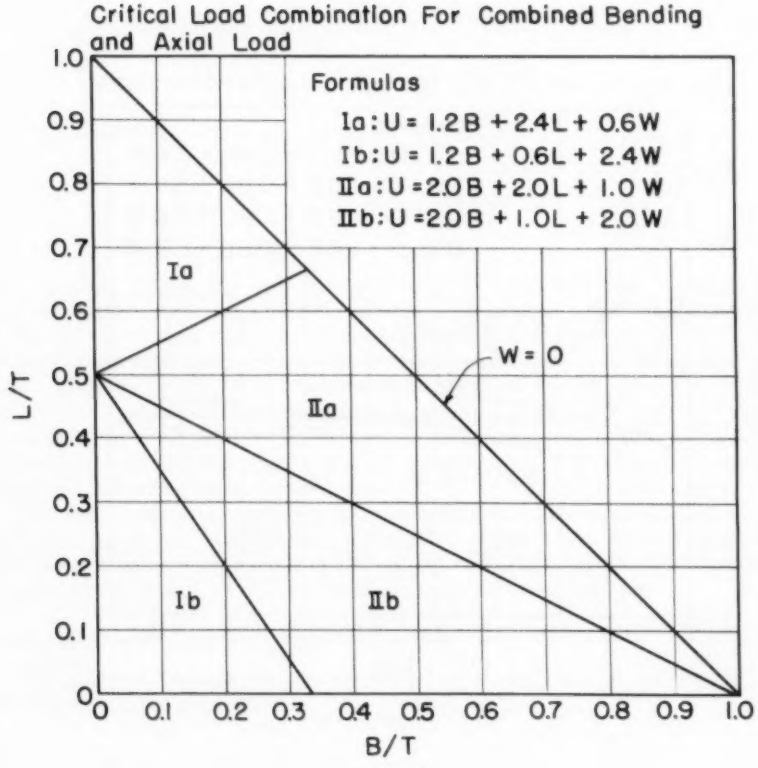
Critical Load Combination For Combined Bending and Axial Load
Formulas
Ia: U = 1.2B + 2.4L + 0.6W
Ib: U = 1.2B + 0.6L + 2.4W
IIa: U = 2.0B + 2.0L + 1.0W
IIb: U = 2.0B + 1.0L + 2.0W
Ia
IIa
Ib
IIb
W = 0
L/T
B/T
0
0.1
0.2
0.3
0.4
0.5
0.6
0.7
0.8
0.9
1.0

Fig. 2

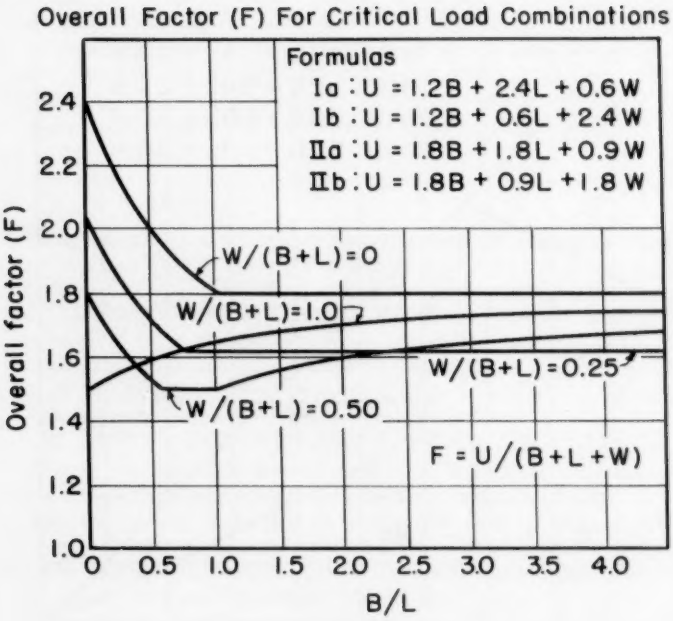
Overall Factor (F) For Critical Load Combinations
Formulas
Ia : U = 1.2B + 2.4L + 0.6W
Ib : U = 1.2B + 0.6L + 2.4W
IIa : U = 1.8B + 1.8L + 0.9W
IIb : U = 1.8B + 0.9L + 1.8W
W/(B+L)=0
W/(B+L)=1.0
W/(B+L)=0.25
W/(B+L)=0.50
F = U/(B+L+W)
Overall factor (F)
2.4
2.2
2.0
1.8
1.6
1.4
1.2
1.0
0
0.5
1.0
1.5
2.0
2.5
3.0
3.5
4.0
B/L

Fig. 3

total load as in Fig. 4, which is obtained by plotting modified forms of equations (2a) to (2d). For example, the overall factor expressed by equation (2a) is

$$F = \frac{0.6B + 1.8L + 0.6T}{B+L+W} = \frac{0.6B + 1.8L + 0.6T}{T} \quad (4a)$$

$$= 0.6\ B/T + 1.8\ L/T + 0.6 \quad (4b)$$

Hence, transposing terms and factoring gives

$$L/T = -0.33\ B/T - 0.33 + 0.56F \quad (4c)$$

For constant values of F this equation plots as a straight line. This process must be repeated for the other three equations to obtain the completed figure. In Fig. 4, the overall factors are represented by the heavy solid lines. The diagonal dash line designated as W/T = 0.25 marks the upper boundary of the area within which the overall factor is 1.5 by the conventional method. Since the overall factors by ultimate strength method shown below this line are equal to or more than 1.5 it is evident as mentioned previously that the recommended overload factors lead to more conservative designs when the wind load effect is large.

The use of the overall factor as a measure of significant difference between ultimate strength procedure and the conventional method represents only part of the difference. In addition, the flexural capacities of a given section as computed by the procedures must be taken into account.

Beams Without Compression Reinforcement

The flexural capacity of a beam of rectangular cross-section by the ultimate strength method is

$$M_u = f'_c bd^2 q(1 - 0.59q) \quad (5a)$$

in which $q = pfy/f'_c$

By the conventional method, assuming that the capacity of the section is controlled by compression,

$$M_s = f'_c bd^2 c_1 \left(\frac{0.45kj}{2}\right) \quad (5b)$$

in which c_1 equals 1.0 with no wind load and 1.33 when the effect of wind load equals or is greater than 33 per cent of the effect of the sum of the dead and live load. Since F designates the overall factor, then

$$F(B+L+W)_u = FT_u = M_u \quad (6a)$$

Overall Factor (F) For Critical Load Combinations

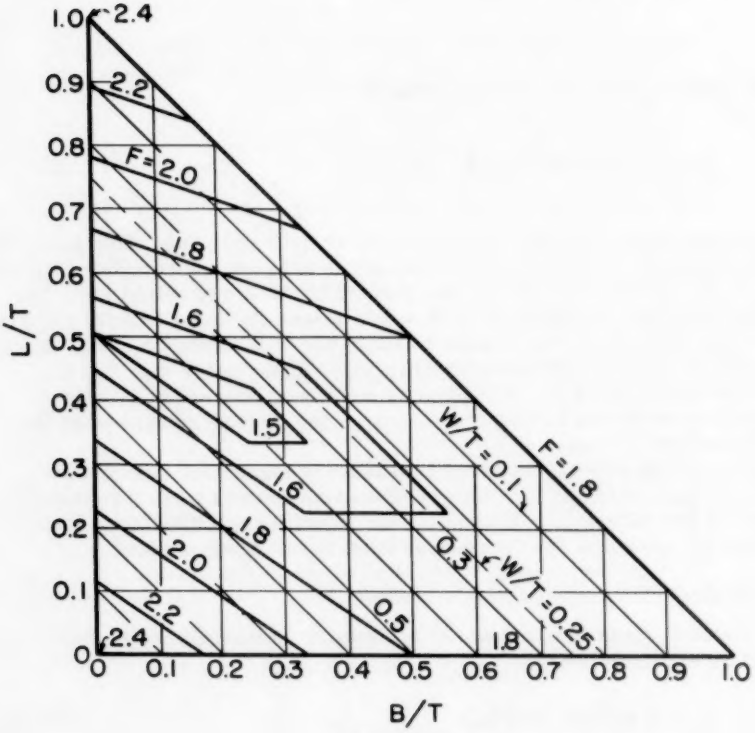

Bending Only

Fig.4a

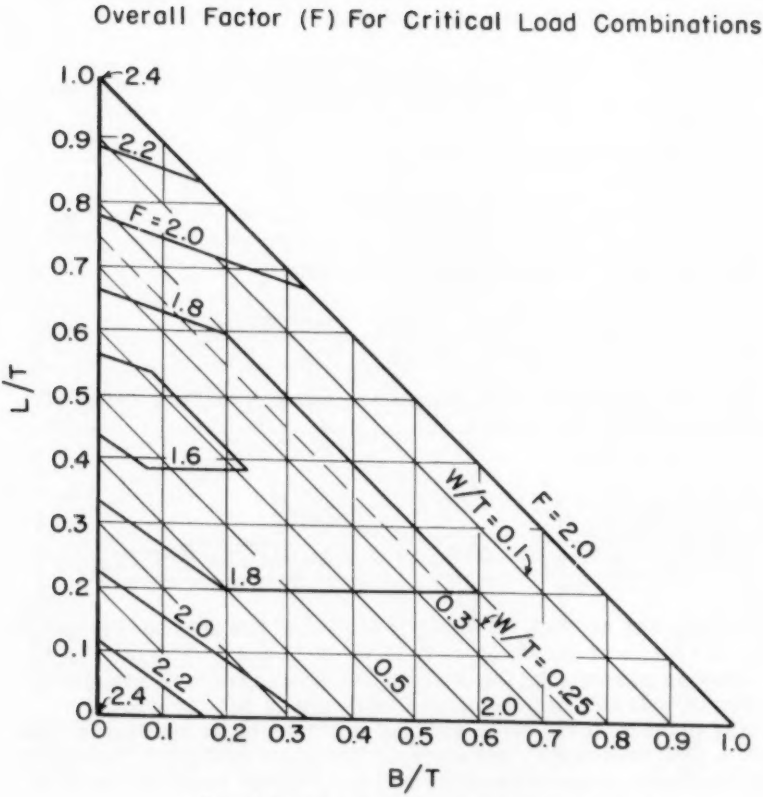

Combined Bending and Axial Load

Fig. 4b

in which the subscript u designates the service load given by the ultimate strength procedure. By the conventional method

$$(B + L + W)_s = T_s = M_s \tag{6b}$$

in which the subscript s designates the service load given by the straightline method and allowable stresses. The ratio of the two loads being equal to equation (6a) divided by equation (6b) is therefore

$$\frac{T_u}{T_s} = \frac{M_u}{FM_s} = \frac{q(1-0.59q)}{c_1F(0.225\,kj)} \tag{7}$$

By the straight-line theory

$$k = \sqrt{2np + (np)^2} - np \tag{8a}$$

with $n = E_s/E_c$. If E_c is assumed as equal to $1000\,f'_c$,

$$np = \frac{E_s}{1000f'_c} \cdot \frac{q_s f'_c}{2f_s} = \frac{15{,}000\,q_s}{f_s} \tag{8b}$$

Substituting the expression for np as given by equation (8b) in equation (7) and letting f_s = 20,000 psi, yields

$$\frac{T_u}{T_s} = \frac{\frac{1}{c_1F}\left[\frac{f_y}{40{,}000}\,q_s\left(1-0.59q_s\,\frac{f_y}{40{,}000}\right)\right]}{\left(\frac{\sqrt{1.5\,q_s+(0.75q_s)^2}-0.75q_s}{4.44}\right)\left(1-\frac{\sqrt{1.5\,q_s+(0.75q_s)^2}-0.75q_s}{3}\right)} \tag{9}$$

Values computed by equation (9) with fy = 40,000 psi are presented graphically in Fig. 5 in terms of the variables B/L, W/(B+L) and q. The ratio of the service loads as computed by the two methods is determined by entering the figure from the left side with the appropriate value of B/L, proceeding horizontally to the W/(B+L) curve and then vertically to the specified q value. The ratio is then read at the right margin. For other values of f_y, the ratio of the service loads is approximately equal to $f_y/40{,}000$ times that given by ordinates on the right margin of the chart.

It is evident that for normal and economical percentages of reinforcement represented by $q = p\frac{f_y}{f'_c} - 0.18$, the difference in service loads between the two methods amounts to only about 10 per cent. For values of q greater than 0.18, a marked increase in the ratio of the service loads is obtained. However, comparison in this range is somewhat unrealistic because by the conventional theory it is not advantageous to increase the load carrying capacity of beams by the addition of tensile reinforcement above q = 0.18. It is more advantageous to provide compression reinforcement. Hence, a more realistic comparison of the two methods should be based on including compressive reinforcement in the section designed by the conventional procedure.

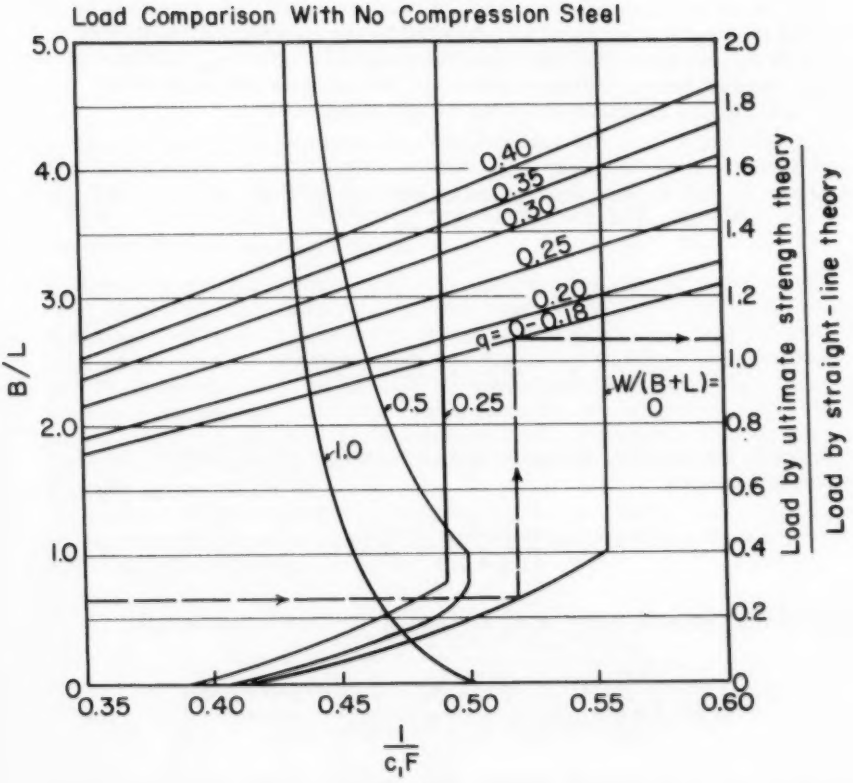
Load Comparison With No Compression Steel
B/L
5.0
4.0
3.0
2.0
1.0
0
0.35
0.40
0.45
0.50
0.55
0.60
$\frac{1}{c_1 F}$
0.40
0.35
0.30
0.25
0.20
q= 0-0.18
1.0
0.5
0.25
W/(B+L)= 0
2.0
1.8
1.6
1.4
1.2
1.0
0.8
0.6
0.4
0.2
0
Load by ultimate strength theory / Load by straight-line theory

Fig.5

Beams with Compression Reinforcement

In making a comparison with compression reinforcement included, it is not desirable to determine the relative load carrying capacity of a given section with the same amount of tensile reinforcement as was done in the previous instance. Such a comparison would be difficult to interpret because both the total amount of reinforcement and the magnitude of the service loads would vary. A better approach is to compare the total amount of reinforcement as computed by the two methods for a member carrying the same service loads.

To determine the relative amounts of reinforcement, it is expedient to express the resisting moment as computed by the conventional method in terms of A'_S, the area of compressive reinforcement, and A_{Sb}, the area of tensile reinforcement sufficient to balance the compressive area of the concrete. Taking moments about the tensile reinforcement

$$M_s = \left[A_{sb} f_s j d + \frac{A'_s f_s 2(k - d'/d)(1 - d'/d)d}{1 - k}\right] c_1 \qquad (10)$$

but

$$A_t = A_{sb} + A'_s \left[1 + \frac{2(k - d'/d)}{1 - k}\right] \qquad (11)$$

in which A_t equals sum of tensile and compressive reinforcement. Transposing terms,

$$A'_s = \frac{(A_t - A_{sb})(1 - k)}{1 - k + 2(k - d'/d)} \qquad (11b)$$

Substituting this expression of A'_S in equation (10) and factoring $f_S d$

$$M_s = c_1 f_s d \left[A_{sb} j + \frac{(A_t - A_{sb}) 2(k - d'/d)(1 - d'/d)}{1 - k + 2(k - d'/d)}\right] \qquad (12)$$

Inserting this expression in equation (6b) and utilizing the previous relationships given by equations (5a) and (6a)

$$\frac{1}{F} = \frac{c_1 f_s d \left[A_{sb} j + \frac{(A_t - A_{sb}) 2(k - d'/d)(1 - d'/d)}{1 - k + 2(k - d'/d)}\right]}{f'_c b d^2 q(1 - 0.59q)} \qquad (13)$$

which can be factored to

$$\frac{A_t}{A_u} = \frac{\frac{f_y}{c_1 F f_s}(1-0.59q) - \frac{q_b}{q}\left[j - \frac{2(k-d'/d)(1-d'/d)}{1-k+2(k-d'/d)}\right]}{\frac{2(k-d'/d)(1-d'/d)}{1-k+2(k-d'/d)}} \qquad (14)$$

in which q_b is the value of q_s for balanced reinforcement by the straight-line theory and A_u equals area of steel by ultimate strength theory. For $d'/d = 0.1$, $f_y = 2f_s$ and k computed as before in terms of q_b, equation (14) reduces to

$$\frac{A_t}{A_u} = \frac{4.452}{c_1 F}(1 - 0.59q) - \frac{0.1682}{q} \qquad (15)$$

Fig. 6 is a plot of the values given by equation (15). Here again it is evident that large savings in reinforcement are made by ultimate strength design only when shallow sections are necessary and high values of q are used.

Combined Bending and Axial Load

From the preceding discussion it is apparent that except when the yield point of the steel is considerably greater than 40,000 psi and when the percentage of reinforcement is greatly in excess of that given by $q = 0.18$, there is little choice between the two methods as far as the design of an individual section is concerned. This similarity, however, does not hold for the case of combined bending and axial load. Because of the marked variations in the factor of safety resulting from the conventional method, substantial differences in the load-carrying capacity of a given section as computed by the two methods can result.

When e/t is less than 0.67, the allowable service load on a rectangular tied column subject to combined bending and axial load according to Section 1109 of the ACI Building Code is

$$N = f'_c A_g \frac{0.8\left(0.225 + (f_s/f'_c)p_g\right)}{1 + \left[\frac{\left(0.225 + (f_s/f'_c)p_g\right)0.8}{\left(\frac{1}{6} + \frac{n-1}{2}p_g g^2\right)0.45}\right]\frac{e}{t}} \qquad (16a)$$

with e measured from the centroidal axis. By the ultimate strength procedure, the ultimate axial load is

$$P_u = \frac{A'_s f_y}{\frac{1}{2} + \frac{e}{d-d'}} + \frac{b t f'_c}{\frac{3te}{d^2} + 1.18} \qquad (16b)$$

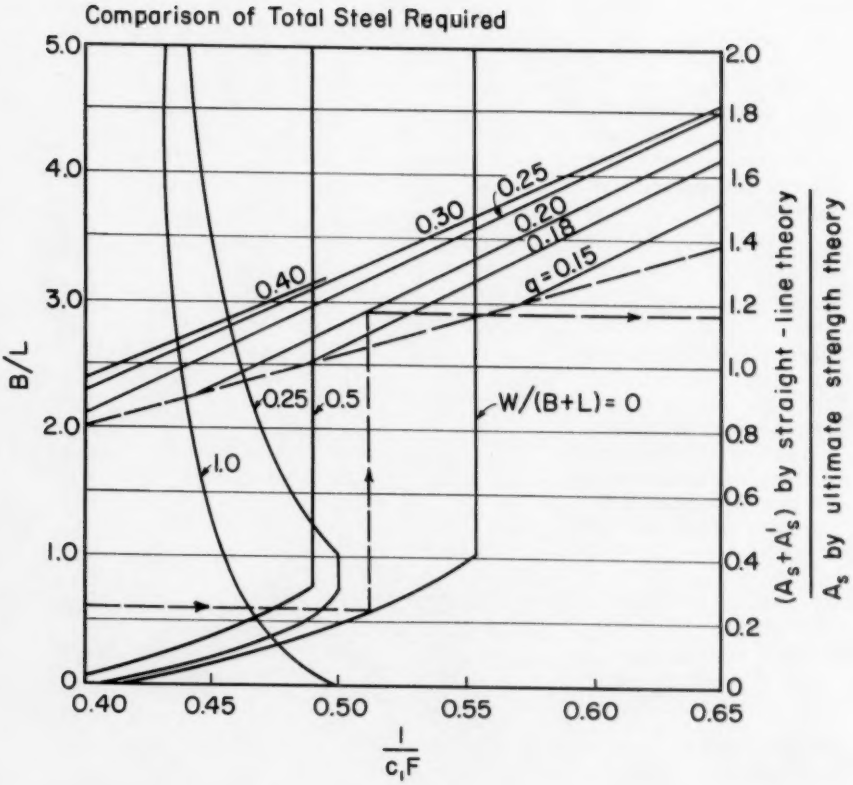
Comparison of Total Steel Required
B/L
5.0
4.0
3.0
2.0
1.0
0
0.40
0.45
0.50
0.55
0.60
0.65
1/c1F
2.0
1.8
1.6
1.4
1.2
1.0
0.8
0.6
0.4
0.2
0
(As+A's) by straight-line theory / As by ultimate strength theory
0.40
0.30
0.25
0.20
0.18
q=0.15
0.25
0.5
1.0
W/(B+L)= 0

Fig.6

Since it has been shown that the value of P_u as computed by equation (16b) agrees closely with test results, the ratio given by dividing equation (16b) by equation (16a) represents the factor of safety by the conventional method of design. Such values are shown on the left side of Fig. 7 for f'_c = 3000 psi, f_s = 20,000 psi, $f_y = 2f_s$ and d = 0.9t for e/t ranging from 0.1 to 1.0, and various percentages of reinforcement. For values of e/t less than 0.1, the ultimate strength values have been decreased in accordance to the recommendations made in the ultimate strength design report. Fig. 7 indicates that for the percentages of reinforcement permitted by the ACI Code, the factor of safety can vary from an extravagantly high value of 4 for e/t = 0.1 to a low value of 1.5 for e/t = 1.0 which was the limiting value in the 1951 ACI Code.

Inasmuch as the ordinate on the left side of Fig. 7 represents the ultimate load capacity divided by the allowable load, the ratio of the service loads as computed by the two methods can be obtained by dividing the ordinate by the overall factor. This is done graphically on the right hand portion of Fig. 7. The ratio of the loads is read as the abscissa at the bottom of the figure as shown by the dash lines. For the particular values of e/t, p and overall factor chosen, an 80 per cent increase in service loads is indicated.

To illustrate in a more vivid manner the savings possible by ultimate strength design, the size of columns required for a given load for two percentages of reinforcement and for two eccentricities are shown in Fig. 8. In this comparison, the values of e/t for the sections determined by the ultimate strength method were made larger than the value used for the ACI design to maintain the same moment. As could be expected from the curves in Fig. 7, the reduction in size for the smaller eccentricity is much greater than that obtained for the larger eccentricity.

Deflections

Because by ultimate strength design procedure the value of balanced reinforcement is greater than that obtained by the conventional method, the ASCE-ACI Joint Committee Report suggests that whenever q is greater than 0.18, the deflection of the member should be investigated. This is tantamount to saying that whenever the ratio of reinforcement used is greater than balanced reinforcement according to the conventional method the deflection should be computed. Fortunately, the ultimate strength design formulas lend themselves to a rapid evaluation of deflections. For the condition at service loads, the long time deflection of a member can be based on the amount of inertia of the homogeneous section and a reduced modulus of elasticity. For a beam of constant depth, uniformly loaded, the deflection at the center ignoring the effects of the end moments is:

$$\Delta_s = \frac{5wL^4}{384EI} \tag{17a}$$

The deflection at midspan due to end moments is

$$\Delta_m = \frac{24}{384}\frac{L^2}{EI}(M_{AB} + M_{BA}) \tag{17b}$$

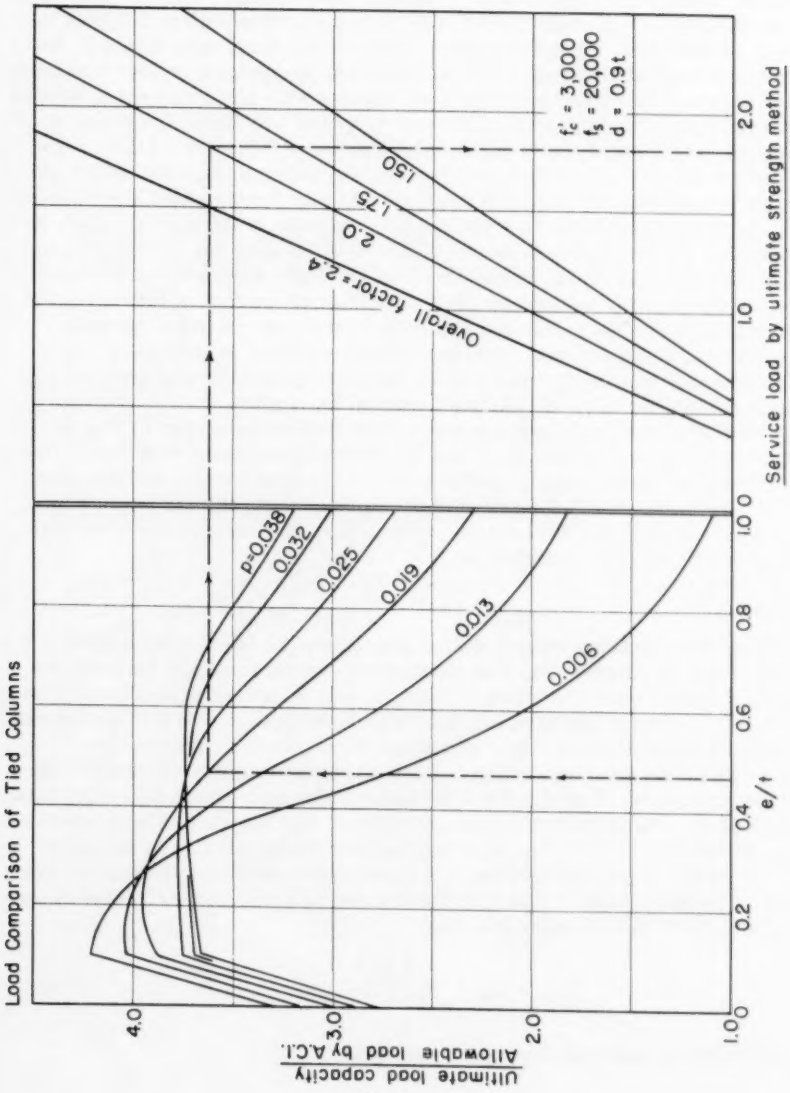
Load Comparison of Tied Columns
Ultimate load capacity / Allowable load by A.C.I.
4.0
3.0
2.0
1.00
0.2
0.4
e/t
0.6
0.8
1.0
p=0.038
0.032
0.025
0.019
0.013
0.006
Overall factor = 2.4
2.0
1.75
1.50
f'c = 3,000
fs = 20,000
d = 0.9t
1.0
2.0
Service load by ultimate strength method / Service load by A.C.I. column formula

Fig. 7

Comparison Of Column Sizes

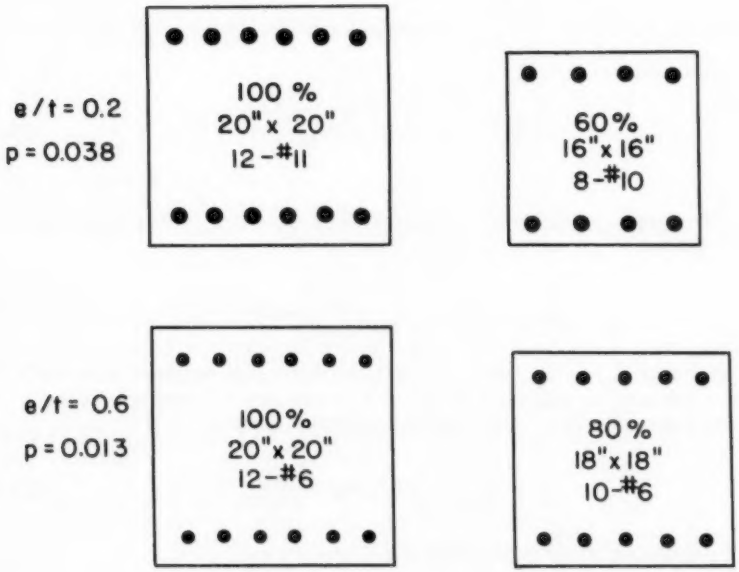

Fig. 8

Taking

$$r_1 M_{AB}^F = \left(\frac{M_{AB} + M_{BA}}{2}\right) \tag{17c}$$

in which r, equals the ratio of the average of the end moments to the fixed end moment.
And with

$$M_{AB}^F = -\frac{wL^2}{12} \tag{17d}$$

Substituting the value of M_{AB}^F given by equation (17d) in (17c) gives

$$-\frac{2r_1 wL^2}{12} = M_{AB} + M_{BA} \tag{17e}$$

Substituting equation (17e) in equation (17b) and adding this to equation (17a) the net deflection Δ is

$$\Delta = \Delta_s + \Delta_m = \frac{wL^4}{384EI}(5 - 4r_1) \tag{17f}$$

Assuming that r_m is the ratio of long time deflection to short time deflection and that increase in long time deflection is due only to dead load, then separating the effects of dead and live load, we have

$$\Delta = \frac{L^4}{384EI}(r_m w_d + w_L)(5 - 4r_1) \tag{17g}$$

but if w_t is the total service load, then

$$w_L = w_t - w_d \tag{17h}$$

therefore

$$\Delta = \frac{L^4}{384EI}\left((r_m - 1)\, w_d + w_t\right)(5 - 4r_1) \tag{17i}$$

Letting r_2= ratio of dead load to live load, equation (17i) reduces to

$$\Delta = \frac{w_t L^4}{384EI}\left((r_m - 1)\, r_2 + 1\right)(5 - 4r_1) \tag{17j}$$

At the support

$$M_u = \left(\frac{w_t L^2}{12} r_1 r_3\right) F \tag{18a}$$

in which r_3 is the ratio of the larger of the two end moments to the average of the end moments, and F is the overall factor.
At midspan

$$M_u = \left[\frac{w_t L^2}{12}(1.5 - r_1)\right] F \tag{18b}$$

The moment at the support will be greater than the midspan moment whenever

$$r_1 > \frac{1.5}{1 + r_3}$$

Substituting for M_u its value as expressed in equation (5a) and transposing terms gives for the value of q at the support

$$w_t = \frac{f'_c b d^2 q(1 - 0.59q)12}{L^2 r_1 r_3 F} \tag{19a}$$

and for the value of q at midspan

$$w_t = \frac{f'_c b d^2 q(1 - 0.59q)12}{L^2(1.5 - r_1)F} \tag{19b}$$

Substituting in equation (17j) the values of w_t given by equations (19a) and (19b) and assuming $E = 10000 f'_c$ and factoring common terms gives for the value of q at the support

$$\frac{r_3 \Delta}{L} = \frac{3}{8000} \frac{(L/t)q(1 - 0.59q)(5 - 4r_1)\left[r_2(r_m - 1) + 1\right](d/t)^2}{r_1 F} \tag{20a}$$

and for the value of q at midspan

$$\frac{\Delta}{L} = \frac{3}{8000} \frac{(L/t)q(1 - 0.59q)(5 - 4r_1)\left[r_2(r_m - 1) + 1\right](d/t)^2}{(1.5 - r_1) F} \tag{20b}$$

In order to facilitate the rapid determination of the deflection of a member as given by equations (20a) and (20b), the composite graph in Fig. 9 may be used. The graph is based on $r_m = 3.0$. The solid lines representing the ratio of the average of the end moments to the fixed end moments apply to q at the support while the long-dash lines in the same quadrant apply to q at midspan. The dash lines with directional arrows illustrate the procedure through the chart which is entered with the given value of q and proceeding to the value of $r_3 \Delta/L$ or Δ/L in the lower left scale.

Comparison of actual deflections obtained in the field generally agree quite well with values computed on the basis of uncracked sections provided due account is taken of the effect of creep. However, comparisons have been mainly limited to percentages of reinforcement with q less than 0.18. Consequently, because greater values of q may involve the formation of more cracks especially when steel having a high yield point is used, there has been some uncertainty regarding the validity of applying the usual methods for determining deflections in the range of q above 0.18.

Long Time Deflection Of Uniformly Loaded Beams

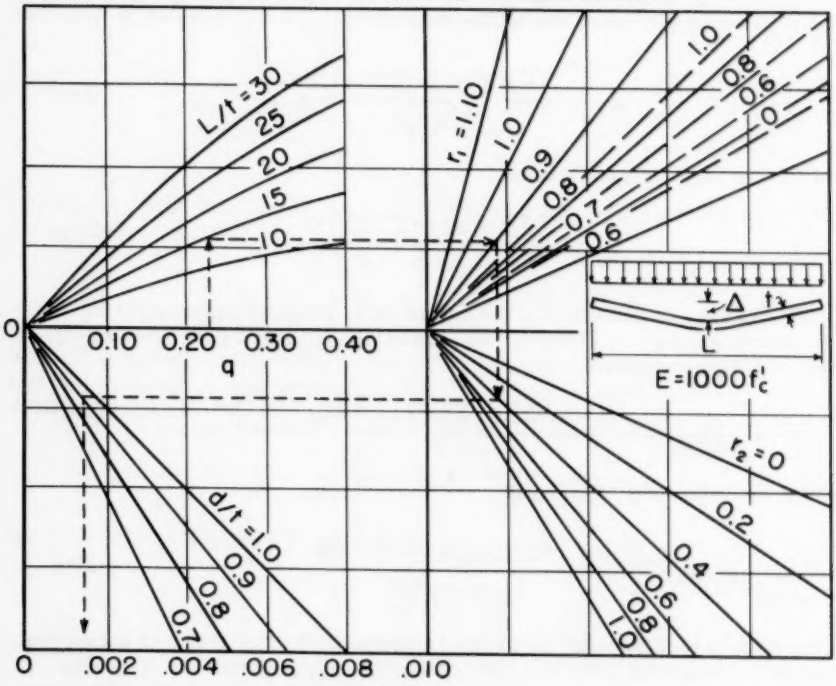

Δ/L for q at midspan

r_3 Δ/L for q at supports

Fig. 9

To answer this question, the Research and Development Division of the Portland Cement Association subjected two frames to sustained load. The frames were identical in every respect except for the percentages of reinforcement. In one frame designed according to the provisions of the ACI Building Code and the straightline theory, the percentage of reinforcement was limited to make $q = 0.18$. The corresponding service load was 7,100 lb. The other frame designed by ultimate strength procedure with an overload factor of 1.8 was reinforced with a percentage of reinforcement making $q = 0.40$. To provide this large amount of reinforcement and still maintain the proper spacing of bars, steel having a yield point strength of 60,000 psi was used. Because of the larger percentage of reinforcement used in the second frame, its service load was 15,700 lb. In spite of the large difference in amount of reinforcement, the deflections of the frames are almost directly proportional to the applied loads as shown in Fig. 10.

The measured deflections at 186 days adjusted for vertical displacements of the supports were 0.249 and 0.500 in. as compared with computed deflections of 0.21 and 0.46 in. respectively for the 7100-lb load and $q = 0.18$ and for the 15,700-lb load and $q = 0.40$ with $r_m = 3$. The difference between the measured and computed deflections are minor and it should be noted that the deflections are virtually stabilized.

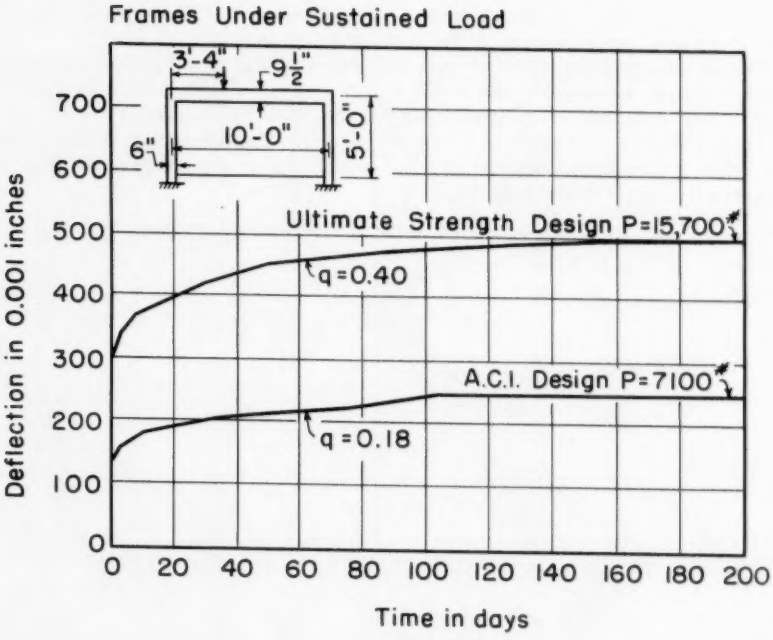
Frames Under Sustained Load
3'-4"
9 1/2"
10'-0"
5'-0"
6"
Ultimate Strength Design P=15,700
q=0.40
A.C.I. Design P=7100
q=0.18
Deflection in 0.001 inches
0
100
200
300
400
500
600
700
0 20 40 60 80 100 120 140 160 180 200
Time in days

Fig. 10

Paper 1758 September, 1958 ST 5

Journal of the
STRUCTURAL DIVISION
Proceedings of the American Society of Civil Engineers

NUMERICAL ANALYSIS OF TWO-HINGED ARCHES

Thomas D. Y. Fok,[1] A. M. ASCE, and Tung Au,[2] A. M. ASCE
(Proc. Paper 1758)

SYNOPSIS

The paper presents a numerical solution for the influence ordinates of the horizontal reaction in a two-hinged arch of variable section. The procedure consists of the application of Newmark's numerical method for the integration of the terms in the horizontal reaction obtained by the conventional theory of consistent deformation. The entire operation can be carried out in a compact tabulation most suitable for design offices.

INTRODUCTION

The analysis of two-hinged arch of variable section often involves laborious integration or summation by segments. When the curve of the arch axis can be represented by a simple equation and the variation of the moment of inertia of the section along the same axis is also amenable to a simple equation, the integrals can be evaluated without difficulty. If the equation representing the arch axis is not simple, or there exist abrupt changes in the moment of inertia of the section along the arch axis, the process of summation becomes rather tedious. The subject has been treated extensively in literature and many methods of analysis are available. However, this paper presents a simple numerical procedure which is believed to have reduced the amount of computations to a minimum without sacrificing the precision required in ordinary engineering design. The idea is not new, but it is here treated in complete generality and presented in a form most suitable for design offices.

Note: Discussion open until February 1, 1959. To extend the closing date one month, a written request must be filed with the Executive Secretary, ASCE. Paper 1758 is part of the copyrighted Journal of the Structural Division, Proceedings of the American Society of Civil Engineers, Vol. 84, No. ST 5, September, 1958.

1. Design Engr., Richardson, Gordon & Associates, Pittsburgh, Pa.
2. Visiting Associate Prof. of Civ. Eng., Carnegie Institute of Technology, Pittsburgh, Pa.

Since a two-hinged arch is a statically indeterminate structure of one degree, the horizontal reaction is usually taken as the redundant. With reference to Fig. 1(a), the horizontal reaction H can be determined by the following equation:[3]

$$H = -\frac{\delta_a'}{\delta_{aa}} = -\frac{\int \frac{M'm\,ds}{EI}}{\int \frac{m^2 ds}{EI}} \qquad (1)$$

where

δ_a' = the horizontal displacement at support A due to given loading, horizontal reaction being removed.

δ_{aa} = the horizontal displacement at support A due to H = unity, acting alone.

M' = moment at any point of the arch due to given loading, horizontal reaction being removed.

m = moment at any point of the arch due to H = unity, acting alone.

E = modulus of elasticity of the material.

I = moment of inertia along the arch axis.

ds = element along the arch axis.

When the influence ordinates of the horizontal reaction are desired, the given loading is a unit moving load acting vertically downward. Thus, δ_a' represents the horizontal displacement at support A due to a vertical unit load at a point B of the arch axis, and M' is the moment at any point C of the arch due to a vertical unit load at point B of the arch axis, horizontal reaction being removed. Note also that the moment diagram M' shown in Fig. 1(b) is identical to an influence line for the bending moment at point B of the basic structure without horizontal reaction. The moment at any point C of the arch due to H = unity as shown in Fig. 1(c) is m = Y = (y - xh/L). Consequently, the product M'm ds/EI = (m ds/EI)M' is the bending moment at point B due to a vertical load (m ds/EI) acting through point C. By the method of elastic loads,[4] δ_a' due to a unit load at any point on the arch can be conceived as the bending moment at the projection of the same point on a horizontal conjugate beam having the same span length as the arch with the (m ds/EI) diagram as vertical elastic loads.

Since the (m ds/EI) diagram involves numerical integration along the arch axis, a modification to replace ds by dx will simplify the process. Let the "horizontal component" of the moment of inertia of a section be denoted by I_b, and be related to the moment of inertia I of that section along the arch axis as follows:

$$I_b = I\frac{dx}{ds} \qquad (2)$$

3. See for instance "Analysis of Statically Indeterminate Structures" by J. I. Parcel and R. B. B. Moreman, John Wiley & Sons, Inc., 1955, p. 461.
4. Ibid, footnote 3, p. 68.

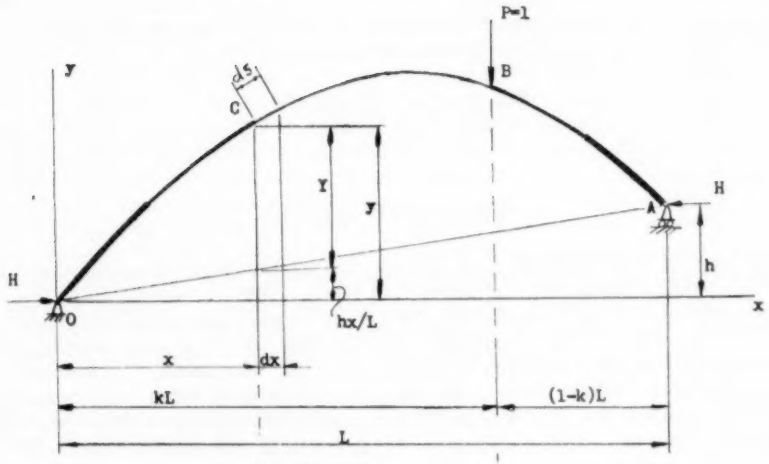

(a) The Arch

(b) Moment M' due to P = 1 at B

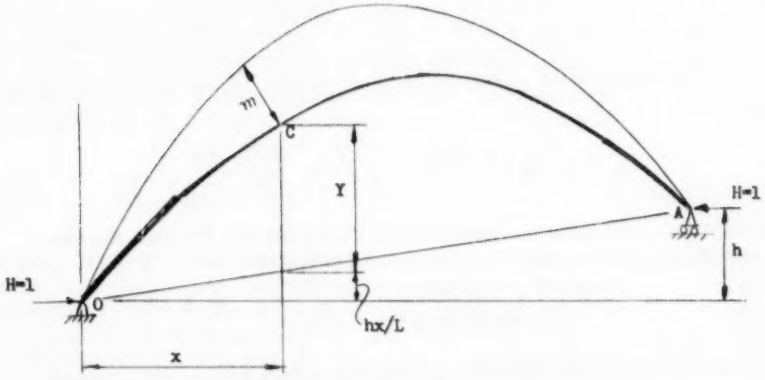

(c) Moment m due to H = 1 at A

Figure 1. GENERAL RELATION IN THE ANALYSIS OF THE ARCH

Then, (m ds/EI) becomes (m dx/EI$_b$), which represents a moment diagram m projected on x-axis and divided by EI$_b$. Consequently, δ'_a due to a unit load at any point of the arch equals numerically the bending moment at the corresponding point of the conjugate beam with (m dx/EI$_b$) diagram as vertical elastic loads, and δ_{aa} can be obtained accordingly. Thus,

$$\delta_{aa} = \int \frac{Y^2 dx}{E I_b} \tag{3}$$

Simple Beam Analogy

We may, at this point, digress into an analogy which gives some physical meaning to the "horizontal component" of the moment of inertia and at the same time leads to an independent check of the numerical value obtained by Eq. (3). Imagine a simply supported beam having the same span length L as the arch and the same moment of inertia I_b as the "horizontal component" of I along the arch. What then will be the load w(x) on such beam which will have a bending moment m = Y = (y - xh/L) at a section of distance x from the left support? Since the loading intensity of a beam is the second derivative of the moment, for downward w(x) as positive, it leads to

$$w(x) = -\frac{d^2 Y}{dx^2} = -\frac{d^2 y}{dx^2} \tag{4}$$

Hence, δ'_a can be visualized as the deflection curve of an analogous simply supported beam.

Such digression would seem trivial but for the fact that it leads to another interpretation of δ_{aa}. Since $\delta_{aa} = \int m^2 ds/EI = \int (m\, ds/EI)m$ for the arch, the summation of the products of the angle change (m ds/EI) at any point and the moment m at the same point due to H = unity represents the total change of internal energy in the arch due to work done by the external force H = unity. Similarly, $\delta_{aa} = \int m^2 dx/EI_b$ is the total change of internal energy of the analogous beam, which must equal the total work done by the external load on the beam, or

$$\delta_{aa} = \int \delta'_a w(x)\, dx = -\int \delta'_a \frac{d^2 y}{dx^2}\, dx \tag{5}$$

This equation can be used as an independent check for Eq. (3) and, for the case of parabolic arches, leads to a very simple expression for δ_{aa}.

The Numerical Procedure

Since only the influence ordinates at discrete points are usually needed, the span of the arch can be divided into equal panels in the horizontal direction to facilitate the computations. Once the section properties at various

panels of the arch are computed, the influence ordinates can be obtained by a numerical method.[5]

In the numerical procedure, finite segments instead of infinite elements are considered, and the arc lengths along the arch axis are approximated by the chord lengths. Hence, the accuracy of the method depends to a certain extent on the number of panels used. The points of abrupt changes of the moment of inertia of the section along the arch axis are chosen as panel points so that the moment of inertia remains constant within a panel. If the moment of inertia of the section changes gradually along the arch axis, the span can still be divided into small segments and the average value of the moment of inertia of the section in each segment may be used.

As shown in Fig. 2(a), the span L of the arch is divided into q equal segments of length λ each. The ordinates y of the arch axis can be computed from the equation of the arch axis for all panel points. The moments of inertia I at various sections are given. Let n be the particular panel point under consideration such as n = 3 in the figure. For $\Delta x = \lambda$, $x = n\lambda$, then

$\Delta y_n = y_n - y_{n-1}$ and $\Delta s_n = \sqrt{(\Delta y_n)^2 + \lambda^2}$.

The section properties of the arch, or of the analogous beam shown in Fig. 2(b), are derived from Eq. (2).

$$\frac{I}{I_{bn}} = \frac{\Delta s_n}{I_n \lambda} \tag{6}$$

Since the vertical distances Y of the arch are the ordinates of the moment diagram m, they can be obtained as follows:

$$m_n = Y_n = y_n - \frac{nh}{q} \tag{7}$$

For segments of arch with different moments of inertia, the m dx/EI$_b$ diagram consists of broken curves as shown in Fig. 2(c). At the nth panel point, for instance, the ordinate is Y_n/EI_{bn} to the left of the panel point and is $Y_n/EI_b(n+1)$ to the right of the same panel point. Consequently, the equivalent concentration of the angle change at the nth panel point ϕ_n can be approximated by the formula for polygonal curve as follows:[6]

$$\phi_n = \frac{\lambda}{6E}\left[(Y_{n-1} + 2Y_n)/I_{bn} + (2Y_n + Y_{n+1})/I_{b(n+1)}\right] \tag{8}$$

If more accurate result is desired, the number of segments in the span should be doubled and the concentrated angle changes can be obtained by the formula for smooth curve.[6] The deflection $(\delta'_a)_n$ at the nth panel point can be determined by taking moment at that point due to the concentrated angle changes as elastic weights. Finally, Eq. (3) can be expressed in the following form:

$$\delta_{aa} = \sum_{n=0}^{n=q} Y_n \phi_n \tag{9}$$

5. "Numerical Procedure for Computing Deflections, Moments and Buckling Loads" by N. M. Newmark. Transactions, ASCE, vol. 108, 1943, pp. 1161-1234.

6. Ibid, footnote 5, pp. 1165-1167.

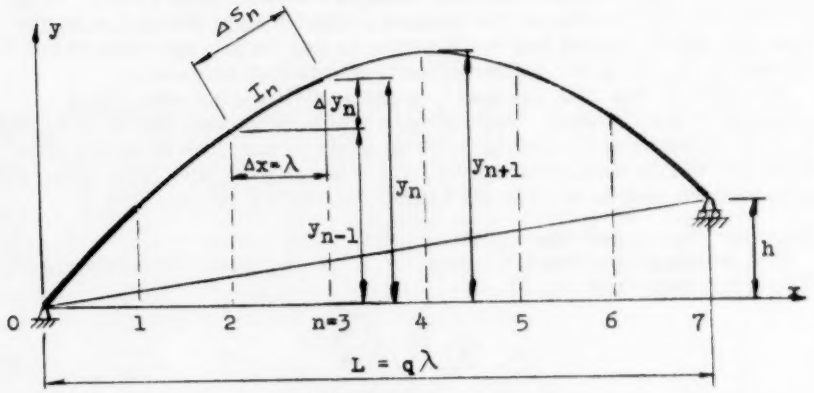

(a) The Arch

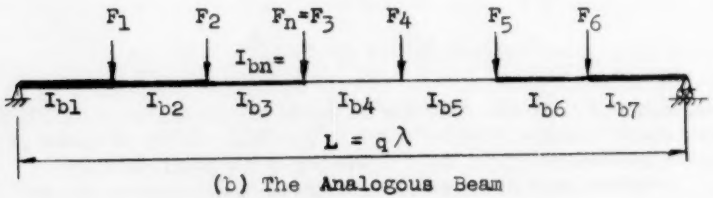

(b) The Analogous Beam

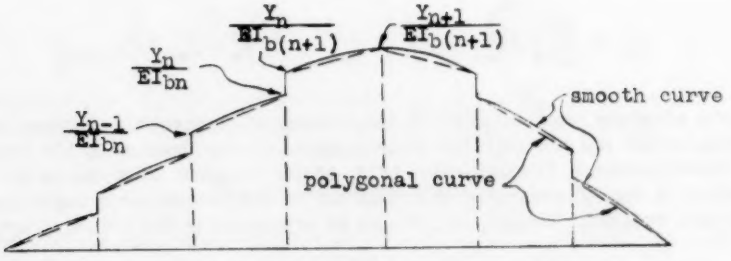

(c) $\int M\,dx/EI_b$ Diagram

FIGURE 2. RELATION IN FINITE SEGMENTS

The loading intensity w(x) on the analogous beam can also be replaced by concentrated loads F_n at the panel points. Thus, from Eq. (4),

$$F_n = -\left(\frac{\Delta^2 y_n}{\Delta x^2}\right)(\Delta x) = -\left[\frac{y_{n+1} - y_n}{\lambda} - \frac{y_n - y_{n-1}}{\lambda}\right]$$

or by denoting $\Delta' y_n = \Delta y_{n+1} - \Delta y_n$ and $\Delta y_n = y_n - y_{n-1}$,

$$F_n = -\frac{\Delta y_{n+1} - \Delta y_n}{\lambda} = -\frac{\Delta' y_n}{\lambda} \tag{10}$$

Consequently, δ_{aa} can be obtained from Eq. (5) as follows:

$$\delta_{aa} = \sum_{n=0}^{n=q} F_n (\delta_a')_n = -\frac{1}{\lambda} \sum_{n=0}^{n=q} \Delta' y_n (\delta_a')_n \tag{11}$$

Second Degree Parabola as a Special Case

Since second degree parabolas are often used for arch axes, it may be treated here as a special case. Moreover, it can be checked by a series of integrations to verify the numerical solution as it has been done for the example in this paper. Consider a symmetrical two-hinged arch whose axis is represented by the equation:

$$y = \frac{4f}{L^2} x (L - x) \tag{12}$$

where f is the rise of the crown of the arch. For $L = q\lambda$ and $x = n\lambda$, the equation becomes:

$$y_n = \frac{4f}{q^2} n (q - n) \tag{13}$$

Then, from Eq. (10), δ_{aa} can be derived by letting Y = y because of symmetry. Hence,

$$\delta_{aa} = \frac{4f}{q} \sum_{n=0}^{n=q} n (q - n) \phi_n \tag{14}$$

Note that in this case $w(x) = -d^2y/dx^2 = 8\,f/L^2$ is a constant. The concentrated loads at all panel points of the analogous beam are the same, i.e., $F_n = 8f\lambda/L^2 = 8f/q^2\lambda$. Consequently, the term δ_{aa} can be derived from Eq. (11) as follows:

$$\delta_{aa} = \frac{8f}{q^2 \lambda} \sum_{n=0}^{n=q} (\delta_a')_n \tag{15}$$

Illustrative Examples

Two numerical examples are given in Figs. 3 and 4 as illustration. In Fig. 3, an unsymmetrical semi-cubical parabola is treated while Fig. 4 deals with a symmetrical second degree parabola. Since the numerical work involves the difference of two quantities of the same order of magnitude, it is

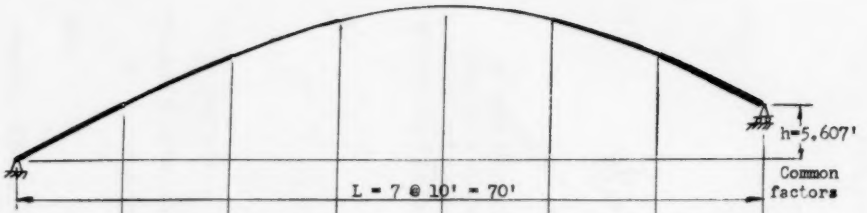

(1) Moment of inertia I_n	4	3	2	1	1	2	3	I_c	
(2) Ordinate y_n	0	5.607	10.343	14.000	16.000	14.000	10.343	5.607	
(3) $\Delta y_n = y_n - y_{n-1}$		5.607	4.736	3.657	2.000	-2.000	-3.657	-4.736	
(4) $\Delta' y_n = \Delta y_{n+1} - \Delta y_n$		-0.871	-1.079	-1.657	-4.000	-1.657	-1.079		
(5) $\lambda^2 + (\Delta y_n)^2$		131.442	122.428	113.372	104.000	104.000	113.372	122.428	
(6) $\Delta s_n = \sqrt{\lambda^2 + (\Delta y_n)^2}$		11.465	11.065	10.648	10.198	10.198	10.648	11.065	
(7) $1/I_{bn} = \Delta s_n / I_n \lambda$		0.2866	0.3688	0.5324	1.0198	1.0198	0.5324	0.3688	
(8) hq/n	0	0.801	1.602	2.403	3.204	4.005	4.806	5.607	
(9) $m_n = Y_n = y_n - hq/n$	0	4.806	8.741	11.597	12.796	9.995	5.537	0	
(10) $m_n(\Delta s_n)/EI_n\lambda = m_n/E I_{bn}$	0	-1.378.	-3.224.	-6.174.	-13.050.	-10.193.	-2.948.		$1/EI_c$
		-1.773	-4.654	-11.827	-13.050	-5.321	-2.042	0.	
(11) Concentrated angle change ϕ_n		-9.524	-23.702	-53.705	-74.219	-47.025	-15.300		$\lambda/6EI_c$
(12) Assumed average slope		100.000	90.476	66.774	13.069	-61.150	-108.175	-123.475	"
(13) Trial deflection	0	100.000	190.476	257.250	270.319	209.169	100.994	-22.481	$\lambda^2/6EI_c$
(14) Linear Correction		3.212	6.424	9.635	12.847	16.058	19.270	22.481	"
(15) Final deflection $(\delta'_a)_n$	0	103.212	196.900	266.885	283.166	225.227	120.264	0	"
(16) $-(\delta'_a)_n \Delta' y_n / \lambda$		89.90	212.46	442.23	1132.66	373.20	129.76	0	$\lambda/6EI_c$
(17) $H_n = -(\delta'_a)_n / \delta_{aa}$	0	-0.4336	-0.8272	-1.1213	-1.1897	-0.9663	-0.5053	0	
		$\delta_{aa} = \Sigma -(\delta'_a)_n \Delta' y_n / \lambda = 2380.21\ \lambda/6EI_c$							
For check:									
(18) $Y_n \phi_n$	0	45.77	207.18	622.82	949.71	470.01	84.72	0	$\lambda/6EI_c$
		$\delta_{aa} = \Sigma Y_n \phi_n = 2380.21\ \lambda/6EI_c$							

FIGURE 3. UNSYMMETRICAL SEMI-CUBICAL PARABOLIC ARCH

desirable to perform the computations with the aid of a desk calculator in order to obtain the required degree of accuracy.

The solution of both examples are given in tabulated form. The steps for determining the section properties of the arch have been fully explained. The remaining steps outline the process of numerical integration which is identical to obtaining the deflections of the analogous simple beam by Newmark's method.[5]

In Fig. 3, the arch axis is represented by a semi-cubical parabola as follows:

$$y = \begin{cases} 16\left[1 - \left(1 - \frac{x}{40}\right)^{3/2}\right] & \text{for } x \leq 40 \\ 16\left[1 - \left(\frac{x}{40} - 1\right)^{3/2}\right] & \text{for } x \geq 40 \end{cases} \qquad (16)$$

With L = 70 ft. and h = 5.607 ft., the span is divided into 7 equal segments, which have different values of I as multiples of I_c, the moment of inertia of the section at the center segment. The influence ordinates are given in line 17 of the table. A check for δ_{aa} is shown in line 18.

Fig. 4 shows a second degree parabolic arch whose axis is given by Eq. (12). With L = 90 ft. and f = 18 ft., the span is divided into 9 equal segments with different values of I as indicated. Because of symmetry, only the computations for half of the arch are shown. The influence ordinates are given in line 15 of the table, and a check for δ_{aa} is shown in line 16.

CONCLUSION

While the method of analysis is based on Eq. (1), it can also be used when the effects of rib-shortening, change of temperature, and yielding of supports are considered. For such factors influencing the analysis, additional terms[3] must be added to both the numerator and the denominator of the expression in Eq. (1). These additional terms can be incorporated in the solution after the terms in Eq. (1) are evaluated by the method suggested in this paper.

The method can also be applied to the determination of the arch deflection due to dead load or live load, and to the analysis of the arch by the deflection theory.

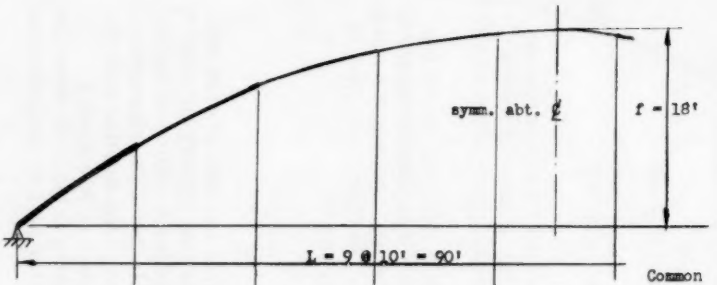

														Common factors
(1) Moment of inertia I_n	.	3.0	.	2.5	.	2.0	.	1.5	.	1.0	.			I_c
(2) Point n	0		1		2		3		4		5			
(3) $(q - n)$	9		8		7		6		5		4			
(4) $n(q - n)$	0		8		14		18		20		20			
(5) $y_n = n(q - n)(4f)/q^2$	0		7.111		12.444		16.000		17.778		17.778			
(6) $\Delta y_n = y_n - y_{n-1}$	.	7.111	.	5.333	.	3.556	.	1.778	.	0	.			
	.		.		.		.		.		.			
(7) $\lambda^2 + (\Delta y_n)^2$	.	150.568	.	128.444	.	112.642	.	103.160	.	100.000	.			
	.		.		.		.		.		.			
(8) $\Delta s_n = \sqrt{(\Delta y_n)^2 + \lambda^2}$	.	12.271	.	11.333	.	10.613	.	10.157	.	10.000	.			
(9) $1/I_{bn} = \Delta s_n / I_n \lambda$	.	0.4090	.	0.4533	.	0.5306	.	0.6771	.	1.0000	.			$1/I_c$
(10) $m_n = y_n$	.		8		14		18		20		20			$4f/q^2$
(11) $m_n(\Delta s_n)/EI_n\lambda = m_n/EI_{bn}$	.0	-3.272.		-6.346.		-9.552.		-13.543.						$4f/q^2EI_c$
	.		-3.627		-6.349		-12.188		-20.000		-20.			
(12) Concentrated angle change ϕ_n	.		-20.144		-40.730		-64.452		-99.274		-99.274			$4f\lambda/6q^2EI_c$
(13) Average slope	.	224.600	.	204.456	.	163.726	.	99.274	.	0	.			
(14) Deflection $(\delta'_a)_n$	0		224.600		429.056		592.782		692.056		692.056			$4f\lambda^2/6q^2EI_c$
	.		.		.		.		.		.			
(15) $H_n = -(\delta'_a)_n / \delta_{aa}$	0		-0.3259		-0.6225		-0.8601		-1.0040		-1.0040			
	.		.		.		.		.		.			
		$\delta_{aa} = (8f/q^2\lambda)\sum(\delta'_a)_n = (689.24)(4f\lambda)/6q^2EI_c$												
For check:	.		.		.		.		.		.			
(16) $n(q - n)\phi_n$	0		161.15		570.22		1160.14		1985.48		1985.48			$4f\lambda/6q^2EI_c$
		$\delta_{aa} = (4f/q^2\lambda)\sum n(q - n)\phi_n = (689.24)(4f\lambda)/6q^2EI_c$												

FIGURE 4. SYMMETRICAL SECOND-DEGREE PARABOLIC ARCH

Paper 1759 September, 1958 ST 5

Journal of the
STRUCTURAL DIVISION
Proceedings of the American Society of Civil Engineers

HIGH-SPEED COMPUTER APPLIED TO BRIDGE IMPACT

Charles T. G. Looney,[1] M. ASCE
(Proc. Paper 1759)

SYNOPSIS

The analysis and results of a study of the impact on highway bridges is described. The analysis was made on the IBM 704 high speed digital computer. The programming of this analysis was done by means of Fortran, an automatic coding system written in language closely resembling ordinary mathematical language and specially designed for engineering work. The effect of different bridge and truck characteristics are presented, and a dimensionless representation of all the variables.

A comprehensive research program on impact is now being conducted by universities and state highway departments. A report of this research, recently published by the Highway Research Board,[2] gives the results of some of the field tests. A number of bridges were tested, including both simple and continuous spans, and most of those studied were constructed with steel girders with a concrete deck. Data were obtained for static loads to determine the load distribution between the slab and stringers and the composite action of the slab and stringers. This composite action had previously been noted in tests carried out by A. H. Fuller and R. A. Caughey in 1922 and a more recent article[3] by A. H. Fuller describes the behaviour of the same bridge after twenty-eight years of service. The Highway Research Board tests revealed that trucks, with their smoothly rolling loads, caused considerable impact, just as had been observed in the case of the railroads when tests were made of the movement of diesel locomotives over railroad bridges.

Note: Discussion open until February 1, 1959. To extend the closing date one month, a written request must be filed with the Executive Secretary, ASCE. Paper 1759 is part of the copyrighted Journal of the Structural Division, Proceedings of the American Society of Civil Engineers, Vol. 84, No. ST 5, September, 1958.

1. Prof. and Head, Dept. of Civil Eng., Univ. of Maryland, College Park, Md.
2. Highway Research Board, Bulletin 124, 1956.
3. "Skunk River Bridge Exhibits Composite Action after 28 Years of Service," ASCE CIVIL ENGINEERING, July, 1951.

These latest tests were made by running trucks at various speeds to find a relation between speed and the natural frequency of the bridge. A series of axle loads with equal spacing can subject the bridge to a series of impulses equally spaced with respect to time and forced vibrations are therefore possible. The tests showed evidence of synchronism between this series of impulses and the natural frequency of the bridge.

By far the most spectacular results were those derived from tests made to determine the effect of obstructions. Excellent deflection records are shown in these reports. Tests were conducted at various speeds with obstructions provided by boards of different heights (1 x 2, 2 x 4). In one set of tests, strain gages placed on the axle of the truck were calibrated to determine the axle loads. Tests were made of a truck running over a board and a comparison was made of the amplitude of vibration and the variation of the axle load.

The reports described in the Highway Research Board, Bulletin 124 contain a substantial amount of impact data of an exploratory nature and call attention to some important factors. The reports are useful too, in indicating the need for and direction of further impact studies.

Considerable progress has been made on the subject of impact on railroad bridges. Experience gained there, both analytical and experimental in nature, forms an excellent background for determining the best approach to the study of highway impact. The question of highway impact is a much more difficult problem than that of railroad impact. The chief difficulty lies in the number of types of highway bridges and floor systems and in the variety of vehicle axle spacings and loadings. The complexity of the problem demands careful analytical studies of these variables. Analysis can provide basic data for the planning of field tests and for the interpretation of field data on the effect of moving vehicles on highway bridges. Analysis could also be used to derive an impact allowance for inclusion in the specifications. A limited number of field tests would be required to provide correlation and scale.

The analysis of the oscillations due to a series of axle loads is ideally suited to the use of digital computers. The proposed method has been programmed for both the IBM 704 and 650 computers. This paper will describe this application of high-speed digital computers to a difficult engineering problem. It will show the results which can be obtained from a study of the variables involved in impact on highway bridges.

The investigation described here will be limited to simply supported deck girder spans. This type was chosen because it is a common type and because the short spans have a high impact under present specifications. An analytical study was made of the impact due to a series of smoothly rolling axle loads on a number of spans ranging from short to long. The variables for the bridge are the span length, the weight per foot, and the stiffness. The vehicle axle loads and spacing used in the study correspond to the present AASHO specification requirements. Both two-axle, H, and three-axle, HS, loadings are used. In the case of the three-axle loading a study was made of the effect of the variable axle spacing between the rear axle of the tractor and the trailer.

Description of Analysis

The analysis to be used in this investigation is the same as that described in Bulletin 352, University of Illinois[4] (see Articles 17 through 22).

4. "Impact on Railway Bridges," C. T. G. Looney, Bulletin 352, University of Illinois.

For a series of smoothly rolling loads, Equation 8 on page 34 becomes:

$$a''\left[\left(\frac{\Delta t}{2}\right)^2 - \left(\frac{\pi^2 \dot{x}_p^2}{L^2}\right)\left(\frac{\Delta t}{2}\right)^2 A'' + A'' + \frac{1}{2}\,\frac{wL}{K}\,\frac{1}{g} + \left(2\,\frac{\pi}{L}\,\dot{x}_p\right)\left(\frac{\Delta t}{2}\right) B''\right]$$

$$= d''_{ST} - d'\left[1 - \left(\frac{\pi^2 \dot{x}_p^2}{L^2}\right) A''\right] - V'\left[\Delta t - \Delta t\left(\frac{\pi^2 \dot{x}_p^2}{L^2}\right) A'' + \left(2\,\frac{\pi}{L}\,\dot{x}_p\right) B''\right]$$

$$- a'\left[\left(\frac{\Delta t}{2}\right)^2 - \left(\frac{\pi^2 \dot{x}_p^2}{L^2}\right)\left(\frac{\Delta t}{2}\right)^2 A'' + \left(2\,\frac{\pi}{L}\,\dot{x}_p\right)\left(\frac{\Delta t}{2}\right) B''\right]$$

where

- a = center acceleration of bridge (a' at time t and a'' at time t + Δt)
- d = total center deflection (dynamic + static)
- dst = static center deflection (live load considered as a static force)
- g = acceleration of gravity (386 inches per second per second used in this analysis)
- K = modulus of the bridge; the number of pounds at the center necessary to make the center deflect one inch
- L = span length of bridge
- P = any axle load of truck
- Δt = small interval of time
- v = center velocity of bridge
- w = weight per foot, assumed to be uniformly distributed
- $\dot{x}_p$ = constant horizontal component of velocity of any axle load P
- x_p = horizontal distance of any axle load P from left end of bridge

$$A = \sum \frac{P}{K}\,\frac{1}{g}\,\sin^2\frac{\pi x_p}{L} = \sum \frac{P}{K}\,\frac{1}{g}\left(1 - \cos\frac{2\pi x_p}{L}\right)$$

$$B = \sum \frac{P}{K}\,\frac{1}{g}\,\sin\frac{\pi x_p}{L}\cos\frac{\pi x_p}{L} = \frac{1}{2}\sum \frac{P}{K}\,\frac{1}{g}\sin\frac{2\pi x_p}{L}$$

$$d_{ST} = \sum \frac{P}{K}\left[3\,\frac{x_p}{L} - 4\left(\frac{x_p}{L}\right)^3\right]$$

Equation 8 can be written in dimensionless form by dividing by $\frac{1}{2}\,\frac{wL}{K}\,\frac{1}{g}$. Certain revisions have been made for convenience in programming the analysis for a digital computer. Let c be a fraction of the span length L, and $\Delta t = c\,\frac{L}{\dot{x}_p}$ a fraction of the time required by the truck to traverse the span.

Measure the distance of any axle load P from the left end by a number of small equal distances which are called steps. Let the small distance, or step, equal cL, and the number of steps from the left end be n. Therefore the distance of any axle load P from the left end $x_p = ncL$. Making these substitutions and dividing both sides by $\frac{1}{2}\frac{wL}{K}\frac{1}{g}$, the revised Equation 8 becomes:

$$a''\left[\frac{1}{2}c^2g\frac{\left(\frac{L}{\dot{x}_p}\right)^2}{\frac{wL}{K}} - \frac{1}{4}\pi^2c^2\sum\frac{P}{wL}(1-\cos 2\pi nc)'' + \sum\frac{P}{wL}(1-\cos 2\pi nc)'' + 1 + \pi c\sum\frac{P}{wL}(\sin 2\pi nc)''\right]$$

$$= 2g\sum\frac{P}{wL}\left[3nc - 4(nc)^3\right]$$

$$- d'\frac{1}{\left(\frac{1}{2}c\frac{L}{\dot{x}_p}\right)^2}\left[\frac{1}{2}c^2g\frac{\left(\frac{L}{\dot{x}_p}\right)^2}{\frac{wL}{K}} - \frac{1}{4}\pi^2c^2\sum\frac{P}{wL}(1-\cos 2\pi nc)''\right]$$

$$- v'\frac{1}{\left(\frac{1}{2}c\frac{L}{\dot{x}_p}\right)}\left[2\left\{\frac{1}{2}c^2g\frac{\left(\frac{L}{\dot{x}_p}\right)^2}{\frac{wL}{K}} - \frac{1}{4}\pi^2c^2\sum\frac{P}{wL}(1-\cos 2\pi nc)''\right\} + \pi c\sum\frac{P}{wL}(\sin 2\pi nc)''\right]$$

$$- a'\left[\frac{1}{2}c^2g\frac{\left(\frac{L}{\dot{x}_p}\right)^2}{\frac{wL}{K}} - \frac{1}{4}\pi^2c^2\sum\frac{P}{wL}(1-\cos 2\pi nc)'' + \pi c\sum\frac{P}{wL}(\sin 2\pi nc)''\right]$$

In this analysis, the truck is moved across the bridge from left to right in a series of equal steps, the length of the step being determined by the value of c. The time interval for one step, Δt, is therefore c times the time required by the truck to traverse the span which is $L/\dot{x}_p$.

If a', v' and d' are known for any position of the truck at t', the acceleration a", after a time interval Δt, during which the truck has moved forward

one step, can be computed by means of this equation. With a" known, values of v" and d" can also be found for the new position of the truck by means of the equations

$$v'' - v' \cong a' \frac{\Delta t}{2} + a'' \frac{\Delta t}{2}$$

$$d'' - d' \cong v \frac{\Delta t}{2} + v'' \frac{\Delta t}{2}$$

These values of a", v" and d" then become a', v' and d' values for the next step.

The programming of this analysis for the IBM 704 was done by means of Fortran, an automatic coding system. Fortran is a library program for the 704 computer which will accept a program written in language closely resembling ordinary mathematical language and will then translate it into the machine language required by the 704. The complete program in Fortran language is shown in Table 1. Fortran has the advantage of allowing the programmer to think in terms of arithmetic formulas and logical statements which differ little from common usage. The translation into machine language is done by the machine itself. The writing of Fortran is very similar to the writing used to instruct an analyst who is to use a hand calculator. This "analyst" is, however, most unusual: "he" is an automaton with no ability to reason and "he" will do exactly as he is told, no more and no less. The general features of this program can be presented to the reader in sufficient detail to make clear the advantages of the Fortran system.

The revised Equation 8 can be written

$$\begin{aligned} &APP''[FCAP - HCAP \times ACAP'' + ACAP'' + 1 + BCAP''] \\ &= CCAP'' - DP'[FCAP - HCAP \times ACAP''] \\ &\quad - VP'[2\,(FCAP - HCAP \times ACAP'') + BCAP''] \\ &\quad - AP'[FCAP - HCAP \times ACAP'' + BCAP''] \end{aligned}$$

When this equation is solved for APP" it becomes Equation 600 of the Fortran program. The two equations which follow 600 determine v" and d". The equation for the change in velocity when divided by $\frac{\Delta t}{2}$ and transposed becomes

$$\frac{v''}{\frac{\Delta t}{2}} = a'' + a' + \frac{v'}{\frac{\Delta t}{2}}$$

which is written

$$V\,PP = APP + AP + VP$$

and similarly the equation for the change of deflection when divided by $\left(\frac{\Delta t}{2}\right)^2$ and transposed become

$$\frac{d}{\left(\frac{\Delta t}{2}\right)^2} = \frac{v''}{\frac{\Delta t}{2}} + \frac{v'}{\frac{\Delta t}{2}} + \frac{d'}{\left(\frac{\Delta t}{2}\right)^2}$$

which is written

$$DPP = VPP + VP + DP$$

Table 1

Fortran Source Program

```
    THE VIBRATION OF HIGHWAY BRIDGES,CTGL
    REWIND 2
304 READ 165, ENPRIN
165 FORMAT (F3.0)
    READ 170, HCAP, C, SPAN, FREE
170 FORMAT (2E15.8, 2F5.0)
250 READ 3, P10WL, P20WL, P30WL, FCAP, AXLE1, AXLE2
  3 FORMAT (3E15.8 / E15.8,2F5.0)
    IF (SENSE SWITCH 1) 306,305
305 IF (P10WL) 304,304,301
301 WRITE OUTPUT TAPE 2, 1, P10WL, P20WL, P30WL, FCAP, AXLE1, AXLE2
  1 FORMAT (38H ANALYSIS FOR THE FOLLOWING PARAMETERS/7H P1/WL=E15.8.
   18H  P2/WL=E15.8,8H  P3/WL=E15.8/6H  FCAP=E15.8,8H  AXLE1=F4.0,
   28H  AXLE2=F4.0/1H)
    PIE=3.14159265
    TWOG=772.0
    EN=1.0
    AP=0.
    VP=0.
    DP=0.
    P1ACAP=0.
    P2ACAP=0.
    P3ACAP=0.
    P1BCAP=0.
    P2BCAP=0.
    P3BCAP=0.
    P1CCAP=0.
    P2CCAP=0.
    P3CCAP=0.
100 IF (EN-SPAN) 110,110,200
110 P1ACAP=P10WL*(1.0-COSF(2.0*PIE*EN*C))
    P1BCAP=C*PIE*P10WL*(SINF(2.0*PIE*EN*C))
    IF (EN-(SPAN/2.0)) 120,120,130
120 P1CCAP=TWOG*P10WL*(3.0*EN*C-4.0*((EN*C)**3.0))
    GO TO 200
130 P1CCAP=TWOG*P10WL*(3.0*(SPAN-EN)*C-4.0*(((SPAN-EN)*C)**3.0))
200 IF (EN-(SPAN+AXLE1)) 210,210,300
210 IF (EN-AXLE1) 550,220,220
220 P2ACAP=P20WL*(1.0-COSF(2.0*PIE*(EN-AXLE1)*C))
    P2BCAP=C*PIE*P20WL*(SINF(2.0*PIE*(EN-AXLE1)*C))
    IF (EN-(SPAN/2.0+AXLE1)) 230,230,240
230 P2CCAP=TWOG*P20WL*(3.0*(EN-AXLE1)*C-4.0*(((EN-AXLE1)*C)**3.0))
    GO TO 300
240 P2CCAP=TWOG*P20WL*(3.0*(SPAN-EN+AXLE1)*C
  1          -4.0*(((SPAN-EN+AXLE1)*C)**3.0))
300 IF (EN-(SPAN+AXLE1+AXLE2)) 310,310,400
310 IF (EN-(AXLE1+AXLE2)) 550,320,320
```

Table 1 (Cont'd)

Fortran Source Program

```
320 P3ACAP=P30WL*(1.0-COSF(2.0*PIE*(EN-AXLE1-AXLE2)*C))
    P3BCAP=C*PIE*P30WL*(SINF(2.0*PIE*(EN-AXLE1-AXLE2)*C))
    IF (EN-(SPAN/2.0+AXLE1+AXLE2)) 330,330,340
330 P3CCAP=TWOG*P30WL*(3.0*(EN-AXLE1-AXLE2)*C
   1          -4.0*(((EN-AXLE1-AXLE2)*C)**3.0))
    GO TO 550
340 P3CCAP=TWOG*P30WL*(3.0*(SPAN-EN+AXLE1+AXLE2)*C
   1          -4.0*(((SPAN-EN+AXLE1+AXLE2)*C)**3.0))
    GO TO 550
400 IF (EN-(SPAN+AXLE1+AXLE2+FREE)) 500,500,700
500 ACAP=0.
    BCAP=0.
    CCAP=0.
    GO TO 600
550 ACAP=P1ACAP+P2ACAP+P3ACAP
    BCAP=P1BCAP+P2BCAP+P3BCAP
    CCAP=P1CCAP+P2CCAP+P3CCAP
600 APP=(CCAP-DP*(FCAP-HCAP*ACAP)-VP*(2.0*(FCAP-HCAP*ACAP)+BCAP)
   1 -AP*(FCAP-HCAP*ACAP+BCAP))/(FCAP-HCAP*ACAP+ACAP+1.0+BCAP)
    VPP=APP+AP+VP
    DPP=VPP+VP+DP
    AP=APP
    VP=VPP
    DP=DPP
    IF (MODF(EN, ENPRIN)) 160,161,160
161 WRITE OUTPUT TAPE 2, 4, EN,AP,VP,DP,CCAP
  4 FORMAT (3H N=F5.0,10H          ACC=E15.8,
   110H          VEL=E15.8,11H          DEFL=E15.8,13H          STATIC=E15.8)
160 EN=EN+1.0
    GO TO 100
700 WRITE OUTPUT TAPE 2,302
302 FORMAT (1H1)
    GO TO 250
306 END FILE 2
    REWIND 2
    STOP 77777
```

Input Data

```
02
0.30461742E-03  0.11111111E-01  0090 0045
0.27397260E-01  0.10958904E 00  0.10958904E 00
0.31653947E-02  0018  0018
```

The computation of ACAP, BCAP and CCAP is made for each axle load. Statements 110 through 130 determine these values for the first axle P1. Statements 220 through 240 and 320 through 340 determine ACAB, BCAP and CCAP for axles two and three. The summation is accomplished by statement 550. The statements between 100 and 400, beginning with IF, are for the purpose of determining the position of the axle loads. For example, statement 100 identifies the position of axle one. When EN = 0 the first axle is at the left end. When EN is less than SPAN the first axle is on the bridge (SPAN being the number of steps in the span length and is equal to the reciprocal of c). When EN is equal to SPAN the first axle is at the right end. And when EN is greater than SPAN, axle one has left the right end and is off the bridge. The IF statements make possible a three-way direction for the analysis. When the quantity in the parenthesis is negative, the direction is to the first numbered statement; when the quantity is zero, the direction is to the second numbered statement; and when the quantity is positive, the direction is to the third numbered statement. The position of the axle loads is important in the computation of ACAP, BCAP and CCAP.

The various statements direct the analysis as follows:

1. Start with the first axle P1 at left end of bridge.
   Initial condition are:
   AP = VP = DP = 0 EN = 0.
   P1ACAP, P1BCAP, P1CCAP . . . . . P3CCAP = 0
2. Move one step EN = 1.

Statements 100 to 400 identify the positions of axles one, two and three and compute components of ACAP, BCAP and CCAP for each axle.

3. Statements 550 add the values for each axle to obtain the summation.
4. Statement 600 determines the new acceleration APP and the two following statements determine VPP and DPP.

This completes one cycle ready to start the next. AP = APP, VP = VPP, DP = DPP, EN is increased by one and the analysis is started again at statement 100. Other statements have reference to the input and output of data. A typical set of input data cards are shown on page 10.[5] The first line, 02, determines the answers recorded and printed in the output. The 02 indicates that the values of EN, AP, VP, DP and CCAP will be recorded for EN = 0, 2, 4 . . . . . Number 01 would result in the above answers being recorded for EN = 0, 1, 2 . . . . . .

The second line gives the values of HCAP, C, SPAN (number of steps to the span length) and FREE, the distance of computation of free vibrations after all axles have passed over the bridge.

---

5. Input and output data are for one H20-S16 truck crossing a 105 foot span at 120 feet per second.
   Span length 105 feet
   Stiffness 72.5 kips per inch
   Total weight 458 kips
   Truck P1 = 8K, P2 = 32K, P3 = 32K
   Axle spacing 14 feet and 14 feet
   Value of c = 1/90
   Number of steps to span = 90

The third line gives the values of P1/WL, P2/WL and P3/WL: the ratio of the three axle loads to the weight of the bridge.

The fourth line gives values of FCAP, AXLE 1 and AXLE 2, the latter giving the distance between the first and second and the second and third axles expressed in steps.

A typical output data sheet is shown in Table 2. This is a record of N = EN, AP = ACC, VP = VEL, DP = DEFL and CCAP = STATIC for every step.[6] EN is the position of the first axle P1 of the truck from the left end of the bridge expressed in steps. The number of steps in the span length is determined by the value of c. ACC is the acceleration of the center of the bridge in inches per second per second. VEL is the velocity of the center in inches per second divided by a factor $\left(\frac{1}{2}\ c\ \frac{L}{\dot{x}_p}\right)$. DEFL is the total center deflection in inches divided by a factor $\left(\frac{1}{2}\ c\ \frac{L}{\dot{x}_p}\right)^2$. STATIC is the static center deflection in inches divided by a factor $\left(\frac{1}{2}\ \frac{wL}{K}\ \frac{1}{g}\right)$. Therefore the ratio of the total center deflection to the static center deflection, the magnification factor, is equal to $\text{DEFL}\left(\frac{1}{2}\ c\ \frac{L}{\dot{x}_p}\right)^2 / \text{STATIC}\left(\frac{1}{2}\ \frac{wL}{K}\ \frac{1}{g}\right)$ which is equal to (DEFL/STATIC)FCAP. Thus a relationship can be expressed between the magnification factor (impact) and the dimensionless parameters FCAP and P/WL, which permits a systematic study of the relation between the variables.

In addition to the printed output as shown it is possible to retain the data on magnetic tape as an input to the 704 for further analytical studies. It is also possible to punch the output cards as input data for the IBM 704 or 650. The data can also be projected on a screen for a complete graph of EN vs ACC (or VEL, DEFL, STATIC) which can be photographed against a background grid.

The illustrated Fortran program, punched on cards, is read into the 704 computer which computes the machine instructions from these statements. Approximately 2000 machine instructions were produced by the 704 from this Fortran program. These machine instructions, punched on cards, are the instructions for performing the analysis. In order to make an analysis the instructions are first read into the machine and stored. The instructions are followed by data cards which the machine reads and computes, storing the answers on magnetic tape. The answers on tape are removed from the 704 and printed on a separate tape-to-print machine. The 704 can take in data at the rate of 1000 numbers per minute and perform arithmetic steps at approximately 10,000 per second. The slowest operation is the printing of the answers which is performed at the rate of 150 lines per minute.

The speed with which these computers will perform arithmetic analysis requires a revision in the thinking of civil engineers. Numbers are the means whereby we measure what we are designing and describe the phenomena with which we are dealing. We must often resort to numerical methods in our analyses and most of us have faced situations where analyses were feasible but were impractical because of shortage of time and manpower

6. All numbers are in floating point arithmetic.

0.12345678 E 00 = 0.12345678
0.12345678 E - 01 = 0.012345678
0.12345678 E + 01 = 1.2345678

Table 2

ANALYSIS FOR THE FOLLOWING PARAMETERS
P1/WL= 0.27397259E-01 P2/WL= 0.10958903E-00 P3/WL= 0.10958903E-00
FCAP= 0.31653947E-02 AXLE1= 18. AXLE2= 18.

N= 2.	ACC= 0.13950611E 01	VEL= 0.28002391E 01	DEFL= 0.42054172E 01	STATIC= 0.14091171E 01
N= 4.	ACC= 0.27101164E 01	VEL= 0.11040325E 02	DEFL= 0.30571491E 02	STATIC= 0.28126638E 01
N= 6.	ACC= 0.38700396E 01	VEL= 0.24248175E 02	DEFL= 0.99988571E 02	STATIC= 0.42050692E 01
N= 8.	ACC= 0.48090804E 01	VEL= 0.41668903E 02	DEFL= 0.23088368E 03	STATIC= 0.55807631E 01
N= 10.	ACC= 0.54746355E 01	VEL= 0.62310087E 02	DEFL= 0.43817610E 03	STATIC= 0.69341749E 01
N= 12.	ACC= 0.58300320E 01	VEL= 0.85000194E 02	DEFL= 0.73244127E 03	STATIC= 0.82597336E 01
N= 14.	ACC= 0.58561615E 01	VEL= 0.10845587E 03	DEFL= 0.11193272E 04	STATIC= 0.95518693E 01
N= 16.	ACC= 0.55519164E 01	VEL= 0.13135338E 03	DEFL= 0.15992500E 04	STATIC= 0.10805011E 02
N= 18.	ACC= 0.49334839E 01	VEL= 0.15239943E 03	DEFL= 0.21673740E 04	STATIC= 0.12013588E 02
N= 20.	ACC= 0.93812701E 01	VEL= 0.18115927E 03	DEFL= 0.28300436E 04	STATIC= 0.18808499E 02
N= 22.	ACC= 0.13173212E 02	VEL= 0.22646390E 03	DEFL= 0.36414980E 04	STATIC= 0.25525422E 02
N= 24.	ACC= 0.16081941E 02	VEL= 0.28521775E 03	DEFL= 0.46619526E 04	STATIC= 0.32136505E 02
N= 26.	ACC= 0.17955805E 02	VEL= 0.35356455E 03	DEFL= 0.59376432E 04	STATIC= 0.38613895E 02
N= 28.	ACC= 0.18724392E 02	VEL= 0.42720382E 03	DEFL= 0.74984113E 04	STATIC= 0.44929739E 02
N= 30.	ACC= 0.18394703E 02	VEL= 0.50171018E 03	DEFL= 0.93565688E 04	STATIC= 0.51056183E 02
N= 32.	ACC= 0.17039954E 02	VEL= 0.57282226E 03	DEFL= 0.11506988E 05	STATIC= 0.56965377E 02
N= 34.	ACC= 0.14783765E 02	VEL= 0.63667662E 03	DEFL= 0.13928242E 05	STATIC= 0.62629467E 02
N= 36.	ACC= 0.11782622E 02	VEL= 0.68997443E 03	DEFL= 0.16584545E 05	STATIC= 0.68020599E 02
N= 38.	ACC= 0.12721983E 02	VEL= 0.73919678E 03	DEFL= 0.19441947E 05	STATIC= 0.78747390E 02
N= 40.	ACC= 0.12811974E 02	VEL= 0.79047458E 03	DEFL= 0.22501200E 05	STATIC= 0.89123236E 02
N= 42.	ACC= 0.12089556E 02	VEL= 0.84047272E 03	DEFL= 0.25763817E 05	STATIC= 0.99098003E 02
N= 44.	ACC= 0.10630579E 02	VEL= 0.88608541E 03	DEFL= 0.29218392E 05	STATIC= 0.10862155E 03
N= 46.	ACC= 0.85351482E 01	VEL= 0.92456225E 03	DEFL= 0.32841782E 05	STATIC= 0.11764399E 03
N= 48.	ACC= 0.59178957E 01	VEL= 0.95358384E 03	DEFL= 0.36600691E 05	STATIC= 0.12612074E 03
N= 50.	ACC= 0.28961834E 01	VEL= 0.97129904E 03	DEFL= 0.40453478E 05	STATIC= 0.13401259E 03
N= 52.	ACC=-0.42237346E-00	VEL= 0.97630849E 03	DEFL= 0.44352011E 05	STATIC= 0.14128053E 03
N= 54.	ACC=-0.39449330E 01	VEL= 0.96761458E 03	DEFL= 0.48243380E 05	STATIC= 0.14788558E 03

Table 2 (Cont'd)

N= 56.	ACC=-0.75953323E 01	VEL= 0.94455781E 03	DEFL= 0.52071375E 05	STATIC= 0.15378874E 03
N= 58.	ACC=-0.11313798E 02	VEL= 0.90675029E 03	DEFL= 0.55777708E 05	STATIC= 0.15895101E 03
N= 60.	ACC=-0.15055023E 02	VEL= 0.85401366E 03	DEFL= 0.59302977E 05	STATIC= 0.16333341E 03
N= 62.	ACC=-0.18785245E 02	VEL= 0.78632688E 03	DEFL= 0.62587388E 05	STATIC= 0.16689694E 03
N= 64.	ACC=-0.22478084E 02	VEL= 0.70378760E 03	DEFL= 0.65571309E 05	STATIC= 0.16960353E 03
N= 66.	ACC=-0.26096480E 02	VEL= 0.60661361E 03	DEFL= 0.68195729E 05	STATIC= 0.17143647E 03
N= 68.	ACC=-0.29589652E 02	VEL= 0.49520355E 03	DEFL= 0.70402856E 05	STATIC= 0.17240041E 03
N= 70.	ACC=-0.32904250E 02	VEL= 0.37016410E 03	DEFL= 0.72136905E 05	STATIC= 0.17250092E 03
N= 72.	ACC=-0.35981579E 02	VEL= 0.23232519E 03	DEFL= 0.73344961E 05	STATIC= 0.17174355E 03
N= 74.	ACC=-0.38754563E 02	VEL= 0.82767638E 02	DEFL= 0.73977919E 05	STATIC= 0.17013390E 03
N= 76.	ACC=-0.41145390E 02	VEL=-0.77138465E 02	DEFL= 0.73991568E 05	STATIC= 0.16767751E 03
N= 78.	ACC=-0.43064073E 02	VEL=-0.24568766E 03	DEFL= 0.73347835E 05	STATIC= 0.16437998E 03
N= 80.	ACC=-0.44408270E 02	VEL=-0.42078966E 03	DEFL= 0.72016226E 05	STATIC= 0.16024686E 03
N= 82.	ACC=-0.45064147E 02	VEL=-0.59992190E 03	DEFL= 0.69975460E 05	STATIC= 0.15528466E 03
N= 84.	ACC=-0.44894782E 02	VEL=-0.78006538E 03	DEFL= 0.67215316E 05	STATIC= 0.14952123E 03
N= 86.	ACC=-0.43745577E 02	VEL=-0.95761016E 03	DEFL= 0.63738816E 05	STATIC= 0.14300577E 03
N= 88.	ACC=-0.41468840E 02	VEL=-0.11283380E 04	DEFL= 0.59564643E 05	STATIC= 0.13578843E 03
N= 90.	ACC=-0.37938380E 02	VEL=-0.12874790E 04	DEFL= 0.54729480E 05	STATIC= 0.12791933E 03
N= 92.	ACC=-0.32100102E 02	VEL=-0.14278950E 04	DEFL= 0.49292894E 05	STATIC= 0.12085773E 03
N= 94.	ACC=-0.24915551E 02	VEL=-0.15422579E 04	DEFL= 0.43345404E 05	STATIC= 0.11323907E 03
N= 96.	ACC=-0.16458489E 02	VEL=-0.16253074E 04	DEFL= 0.37001816E 05	STATIC= 0.10510793E 03
N= 98.	ACC=-0.69039008E 01	VEL=-0.16722757E 04	DEFL= 0.30397096E 05	STATIC= 0.96508858E 02
N= 100.	ACC= 0.34554207E 01	VEL=-0.16793276E 04	DEFL= 0.23683530E 05	STATIC= 0.87486421E 02
N= 102.	ACC= 0.14201742E 02	VEL=-0.16440482E 04	DEFL= 0.17026033E 05	STATIC= 0.78085190E 02
N= 104.	ACC= 0.24799918E 02	VEL=-0.15659329E 04	DEFL= 0.10595472E 05	STATIC= 0.68349725E 02
N= 106.	ACC= 0.34623930E 02	VEL=-0.14468087E 04	DEFL= 0.45601650E 04	STATIC= 0.58324592E 02
N= 108.	ACC= 0.43004302E 02	VEL=-0.12911077E 04	DEFL=-0.92404813E 03	STATIC= 0.48054354E 02
N= 110.	ACC= 0.54089129E 02	VEL=-0.10964154E 04	DEFL=-0.57101791E 04	STATIC= 0.43220045E 02
N= 112.	ACC= 0.62799004E 02	VEL=-0.86195910E 03	DEFL=-0.96356378E 04	STATIC= 0.38207477E 02
N= 114.	ACC= 0.68480363E 02	VEL=-0.59857027E 03	DEFL=-0.12562378E 05	STATIC= 0.33038934E 02

Table 2 (Cont'd)

N= 116.	ACC= 0.70611730E 02	VEL=-0.31944744E 03	DEFL=-0.14400544E 05	STATIC= 0.27736700E 02
N= 118.	ACC= 0.68869749E 02	VEL=-0.39494451E 02	DEFL=-0.15116686E 05	STATIC= 0.22323053E 02
N= 120.	ACC= 0.63184269E 02	VEL= 0.22558622E 03	DEFL=-0.14738817E 05	STATIC= 0.16820277E 02
N= 122.	ACC= 0.53772206E 02	VEL= 0.46038058E 03	DEFL=-0.13357472E 05	STATIC= 0.11250655E 02
N= 124.	ACC= 0.41141754E 02	VEL= 0.65092798E 03	DEFL=-0.11122224E 05	STATIC= 0.56364688E 01
N= 126.	ACC= 0.26062654E 02	VEL= 0.78583531E 03	DEFL=-0.82336186E 04	STATIC= 0.
N= 128.	ACC= 0.15550897E 02	VEL= 0.86932668E 03	DEFL=-0.49127829E 04	STATIC= 0.
N= 130.	ACC= 0.42565082E 01	VEL= 0.90906728E 03	DEFL=-0.13447006E 04	STATIC= 0.
N= 132.	ACC=-0.72520985E 01	VEL=-0.90305708E 03	DEFL= 0.22910566E 04	STATIC= 0.
N= 134.	ACC=-0.18395727E 02	VEL= 0.85159855E 03	DEFL= 0.58115114E 04	STATIC= 0.
N= 136.	ACC=-0.28613551E 02	VEL= 0.75728145E 03	DEFL= 0.90394893E 04	STATIC= 0.
N= 138.	ACC=-0.37391335E 02	VEL= 0.62485250E 03	DEFL= 0.11812534E 05	STATIC= 0.
N= 140.	ACC=-0.44287317E 02	VEL= 0.46097647E 03	DEFL= 0.13991088E 05	STATIC= 0.
N= 142.	ACC=-0.48954444E 02	VEL= 0.27390078E 03	DEFL= 0.15465510E 05	STATIC= 0.
N= 144.	ACC=-0.51157830E 02	VEL= 0.73040433E 02	DEFL= 0.16161596E 05	STATIC= 0.
N= 146.	ACC=-0.50786586E 02	VEL=-0.13149583E 03	DEFL= 0.16044313E 05	STATIC= 0.
N= 148.	ACC=-0.47859396E 02	VEL=-0.32941429E 03	DEFL= 0.15119567E 05	STATIC= 0.
N= 150.	ACC=-0.42523576E 02	VEL=-0.51075424E 03	DEFL= 0.13433894E 05	STATIC= 0.
N= 152.	ACC=-0.35047664E 02	VEL=-0.66638936E 03	DEFL= 0.11072130E 05	STATIC= 0.
N= 154.	ACC=-0.25807901E 02	VEL=-0.78848697E 03	DEFL= 0.81531386E 04	STATIC= 0.
N= 156.	ACC=-0.15269299E 02	VEL=-0.87090224E 03	DEFL= 0.48238216E 04	STATIC= 0.
N= 158.	ACC=-0.39622357E 01	VEL=-0.90948744E 03	DEFL= 0.12517352E 04	STATIC= 0.
N= 160.	ACC= 0.75442356E 01	VEL=-0.90230069E 03	DEFL=-0.23833475E 04	STATIC= 0.
N= 162.	ACC= 0.18671026E 02	VEL=-0.84970368E 03	DEFL=-0.58984830E 04	STATIC= 0.
N= 164.	ACC= 0.28858157E 02	VEL=-0.75434347E 03	DEFL=-0.91167644E 04	STATIC= 0.
N= 166.	ACC= 0.37592938E 02	VEL=-0.62101926E 03	DEFL=-0.11876224E 05	STATIC= 0.
N= 168.	ACC= 0.44435771E 02	VEL=-0.45644089E 03	DEFL=-0.14037987E 05	STATIC= 0.
N= 170.	ACC= 0.49042276E 02	VEL=-0.26889113E 03	DEFL=-0.15493257E 05	STATIC= 0.

coupled with prohibitive cost. The computers can make a tremendous difference.

The results to be described here, derive from a preliminary study of the effect of several variables on the oscillation of highway bridges. Analyses were made of 150 problems, each involving a truck or trucks passing over a bridge at a given velocity. One man, using a calculator, would have needed approximately 300 weeks to do the calculations required in these analyses: obviously an impractical effort. The 704 made the analyses at an average of about 15 seconds each for a total of about 40 minutes computing time. The time required for writing the program from which these computations were made would obviously depend on the skill and experience of the programmer.

Since I propose to recommend this analysis as a practical tool for use by civil engineers in research and in office practice, it is appropriate to indicate the special preparation needed. The reader, being a graduate engineer with some experience in numerical analysis would find a one-semester course in programming for computers a sufficient training in programming for the 650 and in programming by the Fortran system for the 704. At a conservative estimate, the present study required about 100 hours to write the described program, to punch the cards, to test and to de-bug.

Description of Analytical Studies

Several analytical studies were made to investigate the nature of the problem of impact on highway bridges. It was decided to investigate the effect of multiple axle loads. Field test data showed evidence that the oscillation due to the individual axle loads at certain speeds would accumulate and at other speeds would interfere. The effect of the mass of the axle loads on the oscillation was also investigated.

Fig. 1 shows the center deflection due to three 20 kip axle loads spaced 15 feet apart. At a velocity of 40 feet per second the truck moves a distance equal to the axle spacing (15 feet) in a time equal to twice the natural period of the bridge. If the mass of the axle loads does not affect the natural frequency appreciably, then the oscillations due to the separate axle loads should be in phase and should add successive equal increments to the amplitude as the axle loads come on to the bridge. The effect of the three 20 kip axle loads on the natural frequency is small. Fig. 1 shows the dynamic center of deflection increasing by approximately equal steps as each axle load comes on to the span. The magnitude of the oscillations obtained by this analysis as shown are 0.0064 inches (total-static) and 0.0057 inches (maximum semi-amplitude).

At a velocity of 80 feet per second the truck moves a distance equal to the axle spacing in a time equal to the natural period of the bridge. Therefore the oscillations due to the separate axle loads should again be in phase. Fig. 1 shows that such is the case. The magnitude of the oscillations obtained by this analysis, as shown, are 0.0114 inches (total-static) and 0.0101 inches (maximum semi-amplitude).

At a velocity of 53-1/3 feet per second the truck moves a distance equal to the axle spacing in 1-1/2 times the natural period. At this velocity the oscillations due to the first and second axles are 180° out of phase and should cancel, while the subsequent oscillations should be due to the third axle alone. Fig. 1 shows the interference of the oscillations due to the first and second axles and the remaining oscillations due to the third axle. The magnitude of

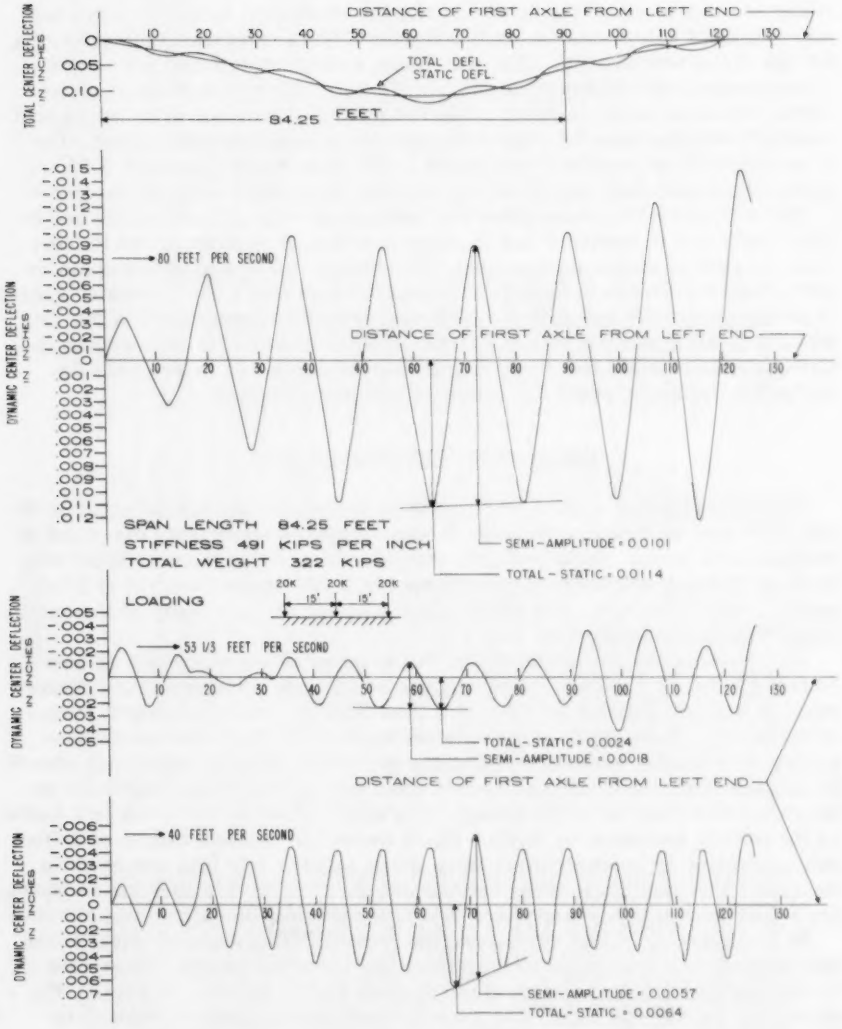
TOTAL CENTER DEFLECTION IN INCHES
DISTANCE OF FIRST AXLE FROM LEFT END
TOTAL DEFL.
STATIC DEFL.
84.25 FEET
DYNAMIC CENTER DEFLECTION IN INCHES
80 FEET PER SECOND
DISTANCE OF FIRST AXLE FROM LEFT END
SPAN LENGTH 84.25 FEET
STIFFNESS 491 KIPS PER INCH
TOTAL WEIGHT 322 KIPS
SEMI-AMPLITUDE = 0.0101
TOTAL - STATIC = 0.0114
LOADING
20K 20K 20K
15' 15'
53 1/3 FEET PER SECOND
TOTAL - STATIC = 0.0024
SEMI-AMPLITUDE = 0.0018
DISTANCE OF FIRST AXLE FROM LEFT END
40 FEET PER SECOND
SEMI-AMPLITUDE = 0.0057
TOTAL - STATIC = 0.0064

Figure 1. Oscillations Due to Three Axle Loads

the oscillations shown on Fig. 1 are 0.0024 inches (total-static) and 0.0018 inches (maximum semi-amplitude).

Using the analysis for a moving force,[7] the maximum amplitude of oscillation was computed at a range of velocities. The results of this analysis for three 20 kip forces spaced 15 feet apart is shown on Fig. 2. The upper line is the maximum amplitude which occurs when the deflections due to the individual forces are in phase and consequently add together. This occurs at velocities of 80, 40, 26-2/3, 20 . . . . . (1 : 1/2 : 1/3 : 1.4 . . .) feet per second. The lower line represents the minimum amplitude which occurs when the deflection due to the first and second forces are 180° out of phase and cancel. The total deflection is due to the third force. This occurs at velocities of 160, 53-1/3, 32, 22-6/7 . . . . . (2 : 2/3 : 2/5 : 2/7) . . . . . 80 FPS = 1).

Above 80 feet per second, the deflections due to the individual forces become out of phase and this tends to decrease the amplitude of the oscillations. The increase of velocity, however, tends to increase the amplitude. At velocities above 80 feet per second, there will be a decrease of amplitude but at high speeds, the amplitude will eventually increase.

This analysis provides evidence which explains the results of field tests. Data from tests show a linear increase of impact with velocity up to a certain level of velocity with no apparent increase above that level.[8,9]

The inteference of the deflections due to the several axles can cause a scattering of the data. The spacing of the axles will affect the slope of the line of maximum amplitude: the closer the spacing the steeper the line. The relative magnitude of the axle loads will affect the scatter of the measured values: two equal axle loads 15 feet apart and moving at 53-1/3 feet per second have a theoretical zero dynamic deflection. A small change in the velocity of a test can bring about a marked change in the amplitude of the oscillations. For this reason the velocity must be very closely controlled in the field tests and perhaps the velocity of the test should be varied in small intervals in the range of apparent maximum amplitude.

In these analyses the ratio of live to dead load is approximately 0.2. A number of analyses were made to investigate the influence of the mass of the live load on the oscillations. A series of four analyses were made of bridges with span lengths of 90, 70, 50 and 30 feet whose ratio of live to dead load is 0.4, 0.5, 0.7, and 1.2 for one H20 truck loading. The results of these analyses for a velocity of 80 feet per second are shown on Figs. 3, 4, 5, and 6. The oscillations produced by moving forces of constant magnitude are superimposed on the oscillations computed by the analysis described, which includes the effect of the mass of the axle loads. A comparison of these oscillations for the same axle loads and spacings shows that analysis for a moving force is not adequate for these ratios of live to dead load.

These preliminary analyses show that although the theory of a moving force, which ignores the effect of the mass of the load on the oscillations, is useful in a qualitative sense in describing the phenomenon, it is inadequate, for analytical purposes, for computing the oscillations. A series of analyses

7. "Mathematical Treatise on Vibrations of Railroad Bridges," C. E. Inglis. Cambridge University Press, London, 1934.
8. "Impact in Railroad Bridges," E. J. Ruble, ASCE Separate No. 736, 1955.
9. "Live-load Stress Measurements on Fort Loudon Bridge," Neil Van Eenan, Highway Research Board Proc., 1952.

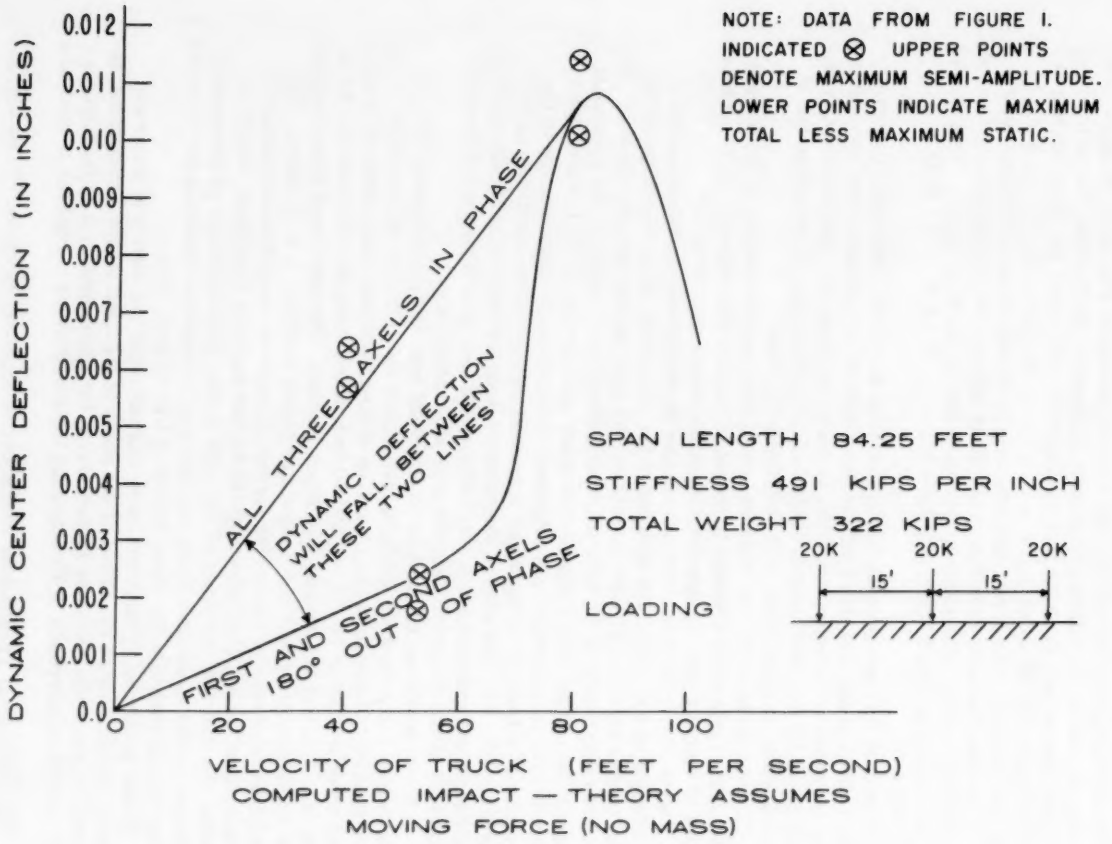

Figure 2. Maximum and Minimum Amplitude Due to Three Axle Loads

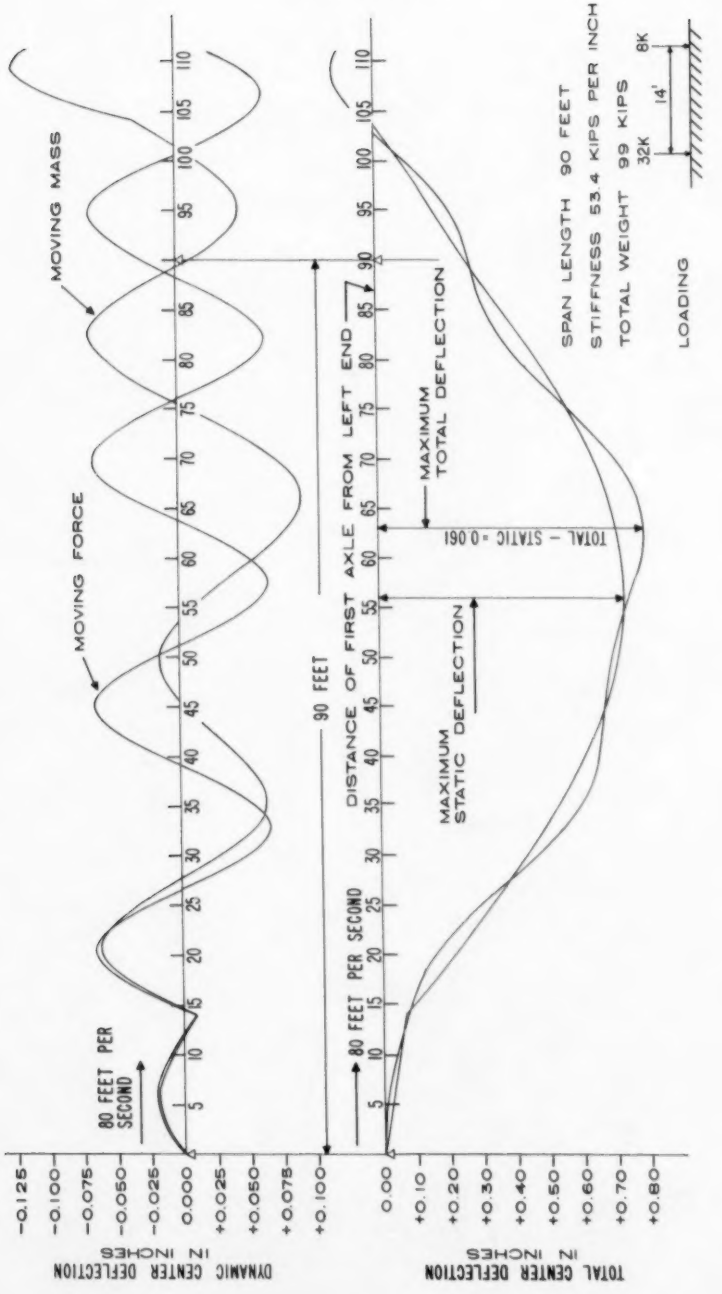

Figure 3. Deflection Due to One H20 Truck ; Ratio LL:DL 0.4

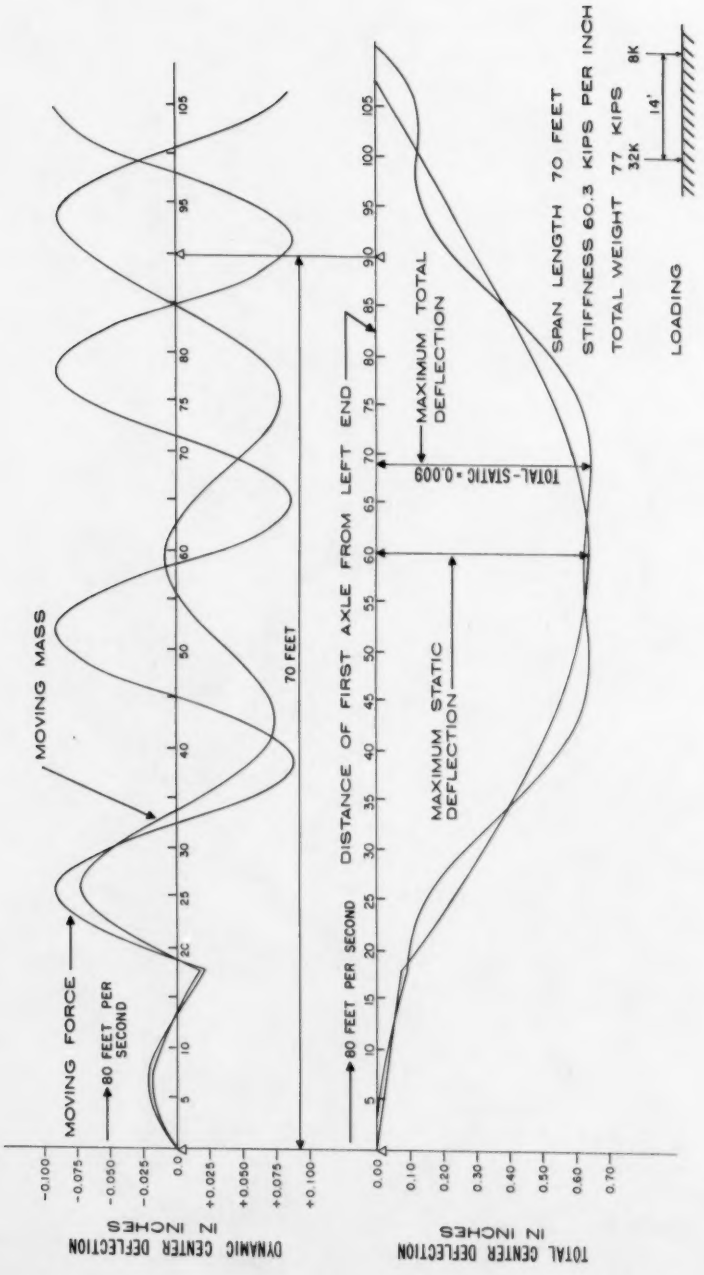

Figure 4. Deflection Due to One H20 Truck : Ratio LL:DL 0.5

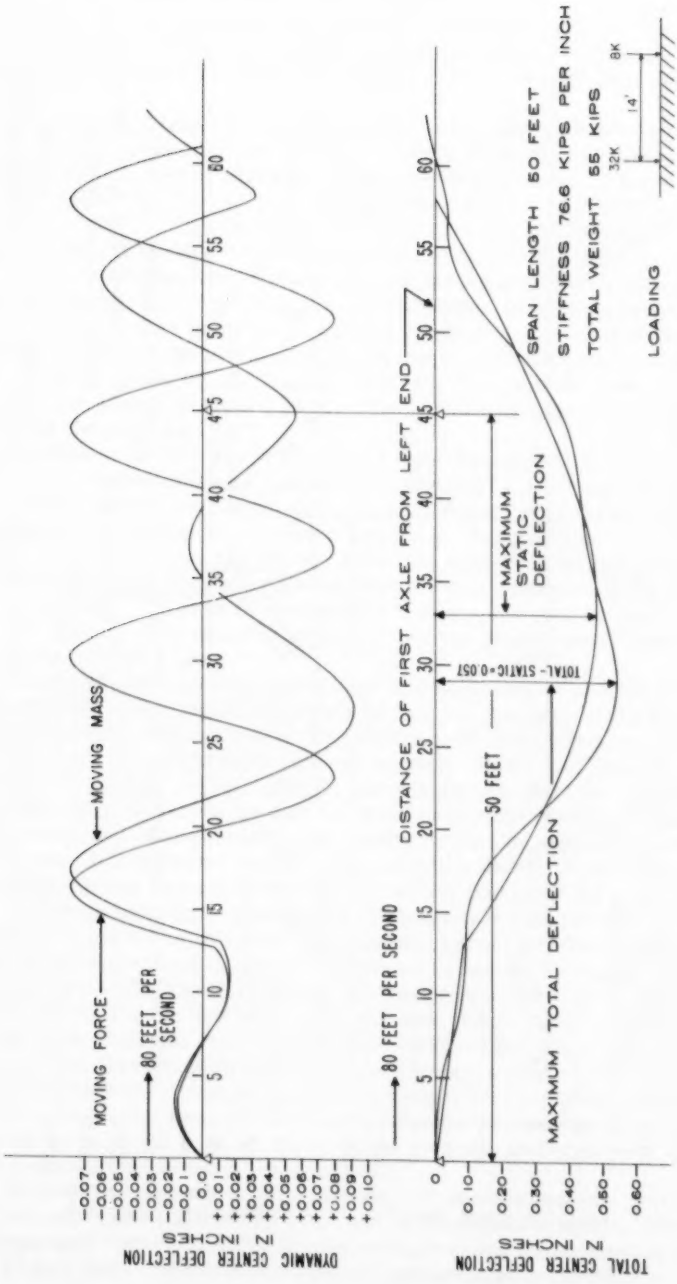

Figure 5. Deflection Due to One H20 Truck : Ratio LL:DL 0.7

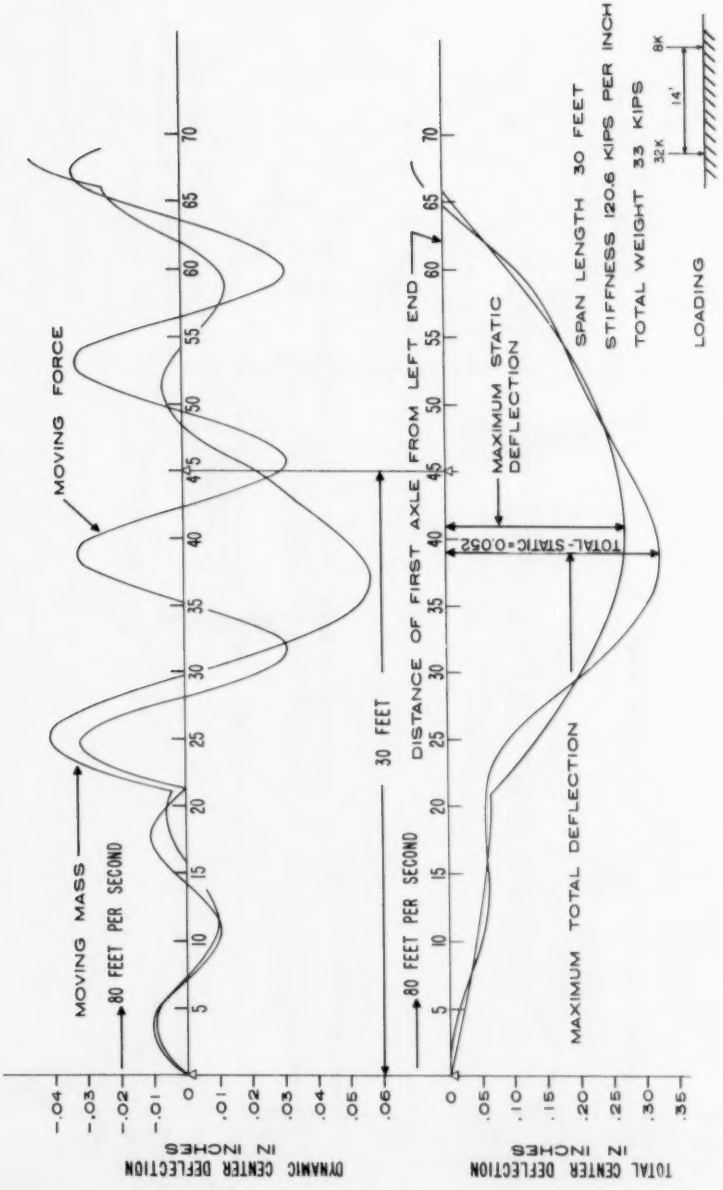

Figure 6. Deflection Due to One H20 Truck : Ratio LL:DL 1.2

were made using the described theory which includes the effect of the mass of the axle loads. These analyses were designed to provide for a systematic investigation of the variables in this problem. Although a considerable number of analyses were made, the results are still preliminary in scope. These analyses show that much valuable information can be obtained by a systematic study.

Analyses were made of the oscillations due to an H20 truck and to an H20-S16 truck on several simple span bridges. Information on the bridges was obtained from the Standard Plans for Highway Bridge Superstructures BPR. Span lengths of 30, 45, 70, 105 and 140 feet were chosen. The velocity of the truck was varied from approximately 20 to a maximum of 120 feet per second. For each bridge, velocities were selected which would cause both maximum and minimum oscillations according to the theory for a moving force. The computed velocities at which the truck will move the distance between the axles (14 feet) in a time equal to the natural frequencies are as follows for the five spans: 90, 62, 39, 28 and 20 feet per second for the span lengths, in ascending order, of 30, 45, 70, 105 and 140.feet. The results of the first set of analyses are shown on Figs. 7 to 11. The stiffnesses shown were computed for the steel beams alone.

The percentage impact was computed as the maximum total center deflection minus the maximum static deflection expressed as a percentage of the static. The velocities were chosen to obtain maximum and minimum values of the oscillation. Although the results are not in close agreement with the theory for a moving force, velocities chosen did exhibit an irregular amplitude of oscillation and showed the marked effect of a change of a few feet per second in velocity. All span lengths exhibit a sharp increase in impact above 60 feet per second. The upper limit of 120 feet per second has a marked effect on the maximum impact.

Fig. 12 summarizes all data and a limit line is drawn. The data show that there is considerable irregularity below 60 feet per second and the impact is a low 15% or less. With velocities ranging from 60 to a maximum of 120 feet per second there is a marked increase in impact. This upper limit of impact percentage will change considerably in accordance with the limit placed on the velocity. Fig. 13 shows perhaps the most interesting result of these analyses. The decrease of impact with span length, which, in present specifications was patterned after railroad bridge impact specifications, is not borne out.

The analyses just described were based on one H20 truck on a two-lane bridge. Although the impact percentage is higher than that allowed in present specifications, the static live-load stresses are lower than the design stresses. In order to increase the static live-load stress, a second series of analyses were made for two H20 trucks. These analyses were identical to the set just described except for the use of double truck axle loads. The impact percentages were approximately the same as those reported for one truck. This indicates that the dynamic deflection increased in proportion to the axle loads so that the percentage increase based on the static live load was approximately the same. The greatest difference between the two sets of analyses is found in the analysis of short spans where the ratio of live to dead load is markedly changed by doubling the live load.

The percentage impact for all spans, Fig. 14, shows the same characteristics as before. The 15% limit up to 60 feet per seond is adequate. The upper limit is changed from 50 to 60% largely because of the higher impact recorded for the 30 foot span. The maximum impact percentages recorded for two

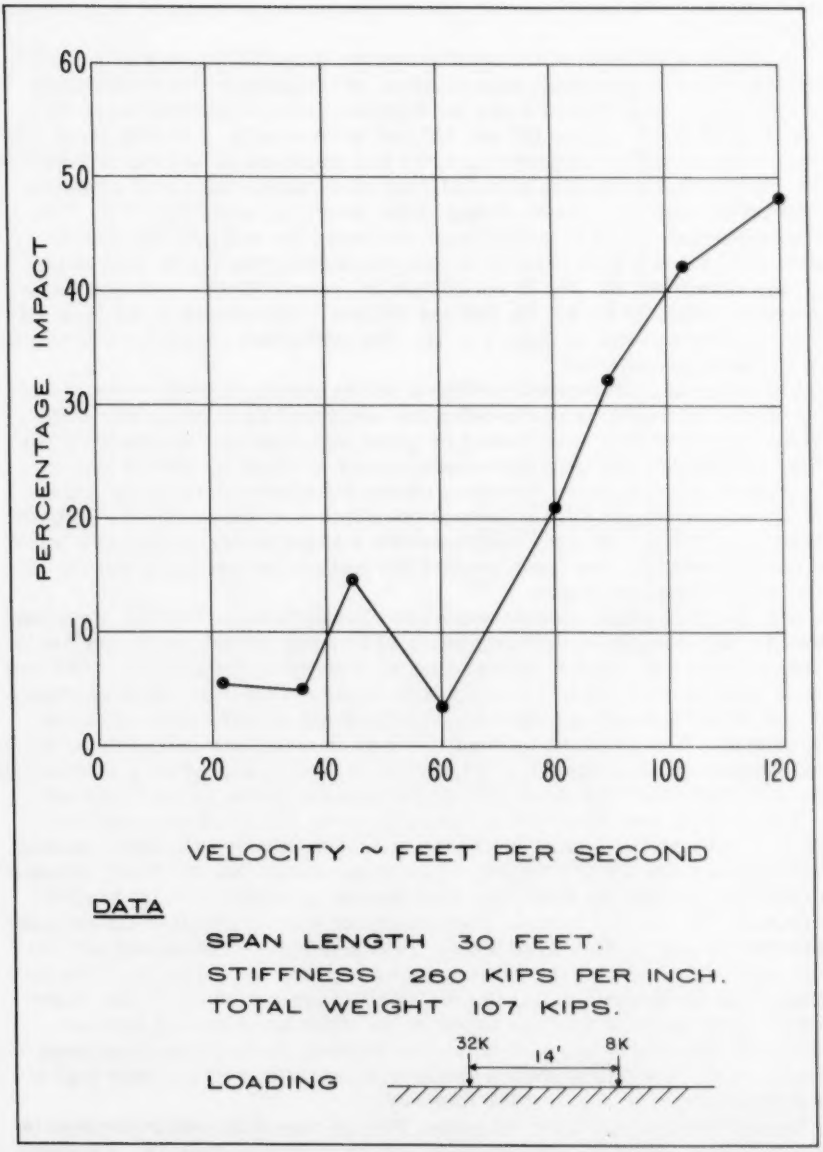

Figure 7. Variation of Impact with Velocity : One H20 Truck;Span 30 ft.

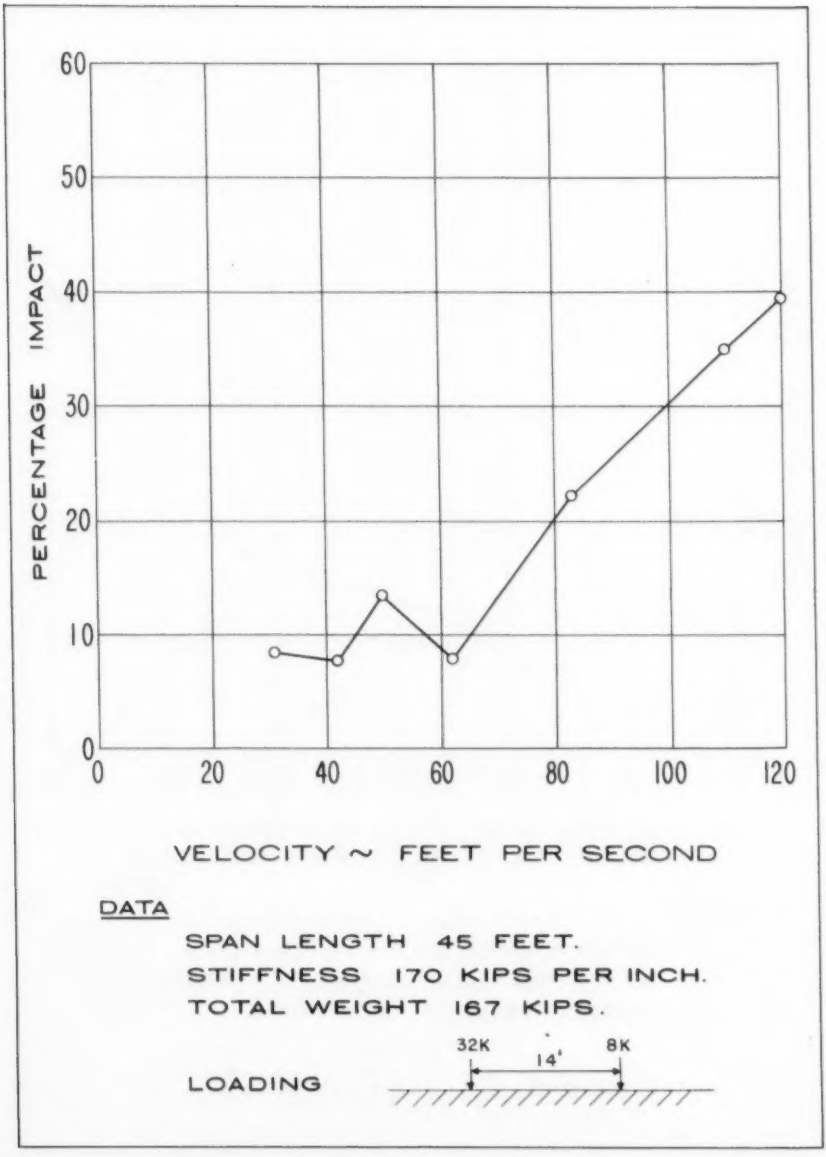

Figure 8. Variation of Impact with Velocity : One H20 Truck;Span 45 ft.

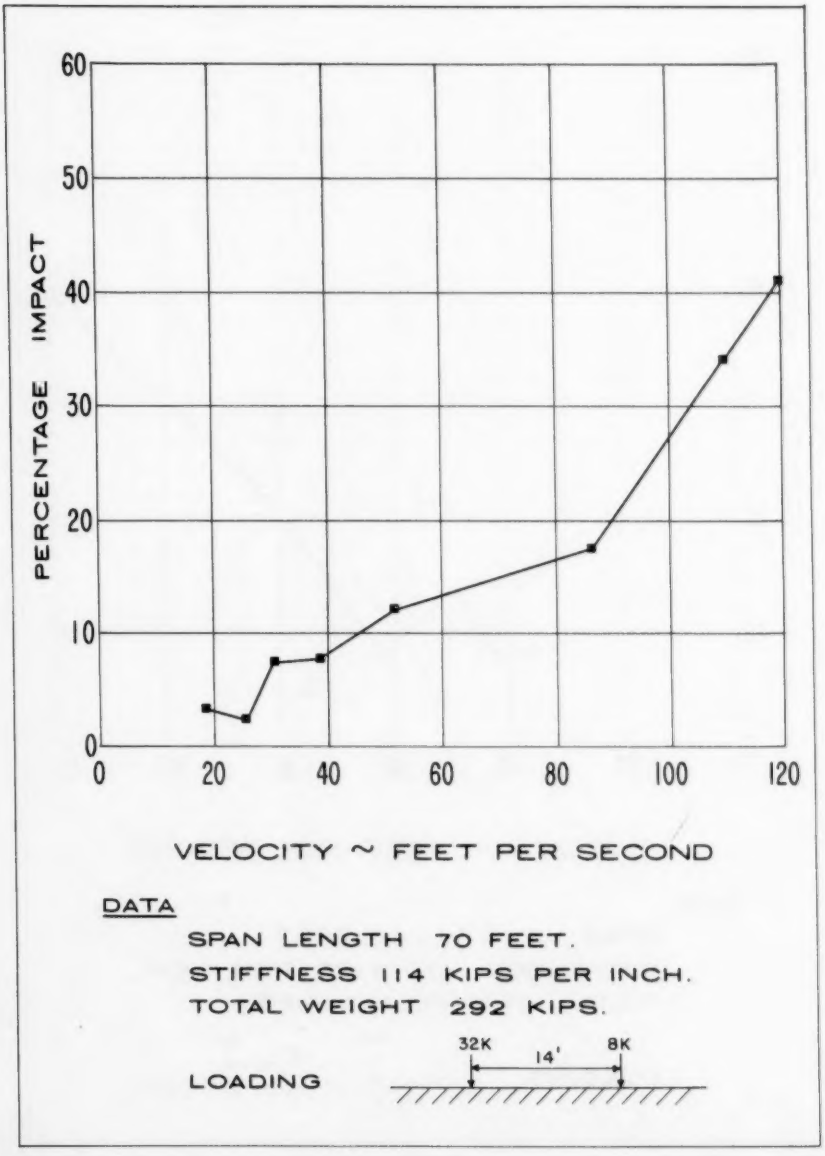

Figure 9. Variation of Impact with Velocity : One H20 Truck ; Span 70 ft.

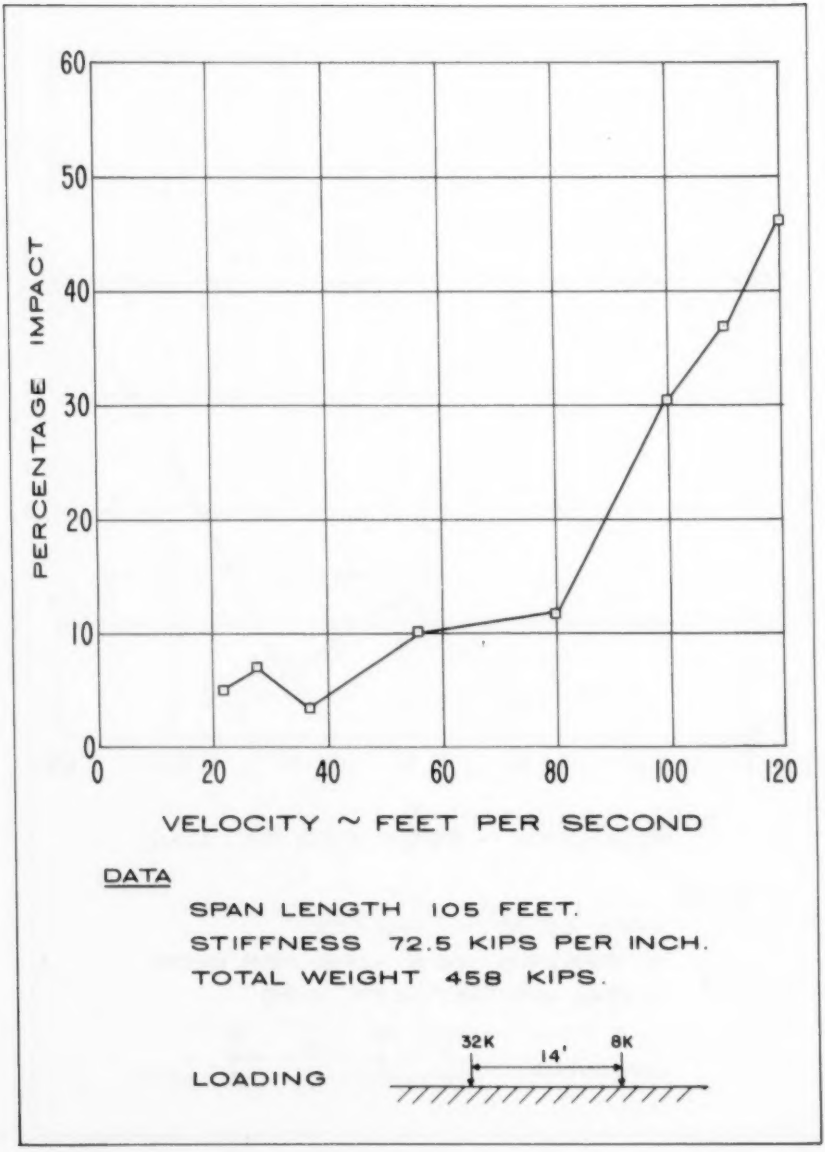

Figure 10. Variation of Impact with Velocity : One H20 Truck; Span 105 ft.

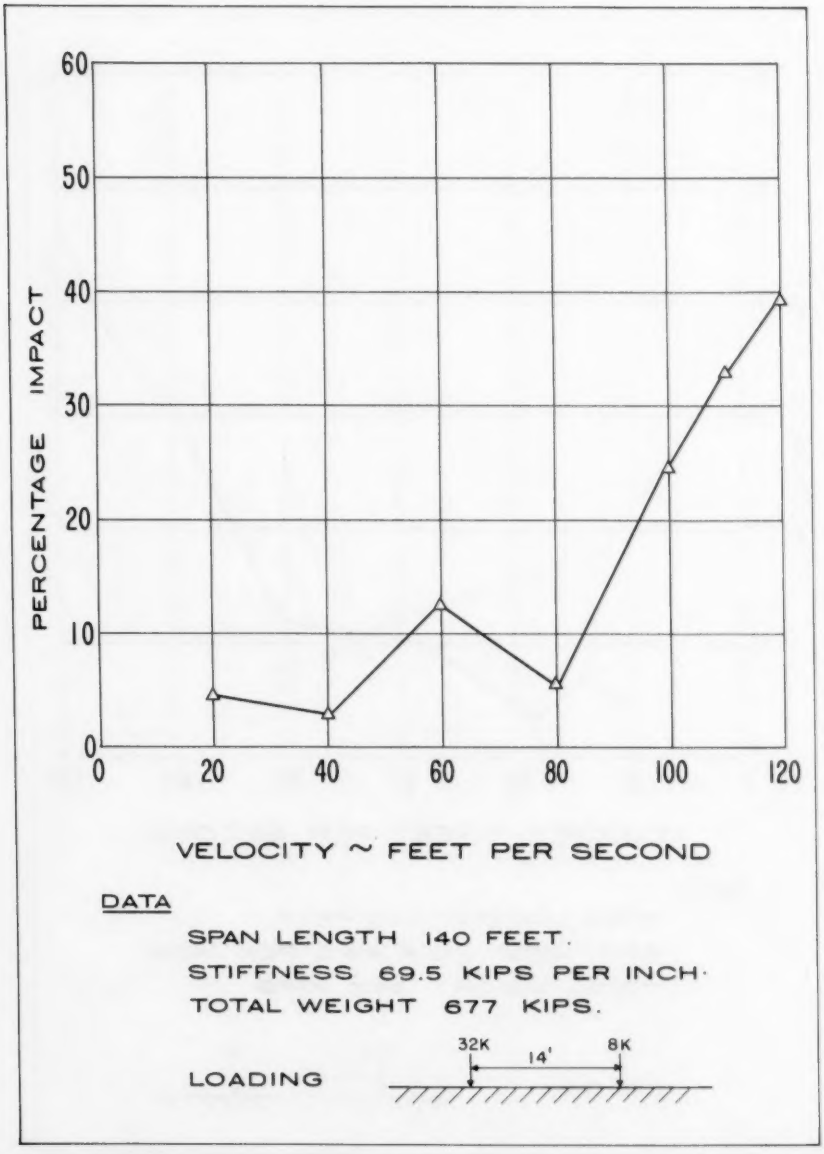

Figure 11. Variation of Impact with Velocity : One H20 Truck; Span 140 ft.

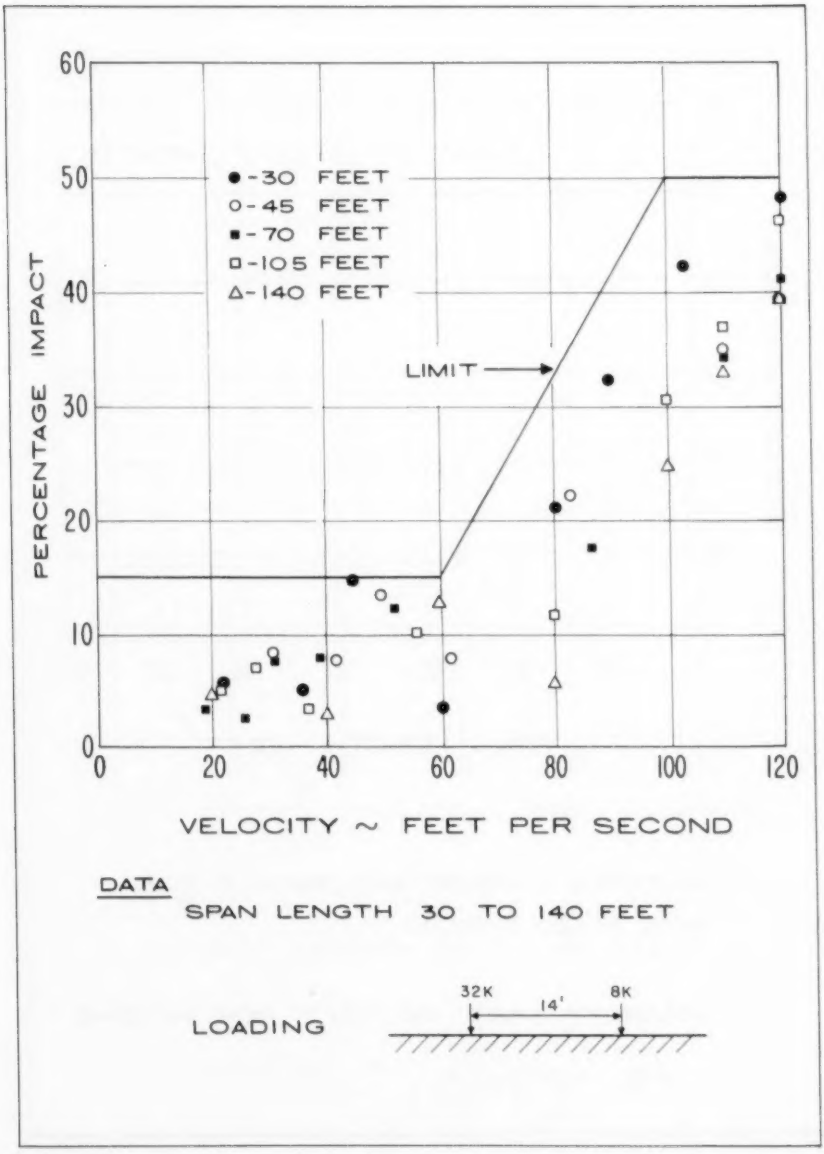

Figure 12. Impact VS Velocity : One H20 Truck; 30 to 140 ft. Span

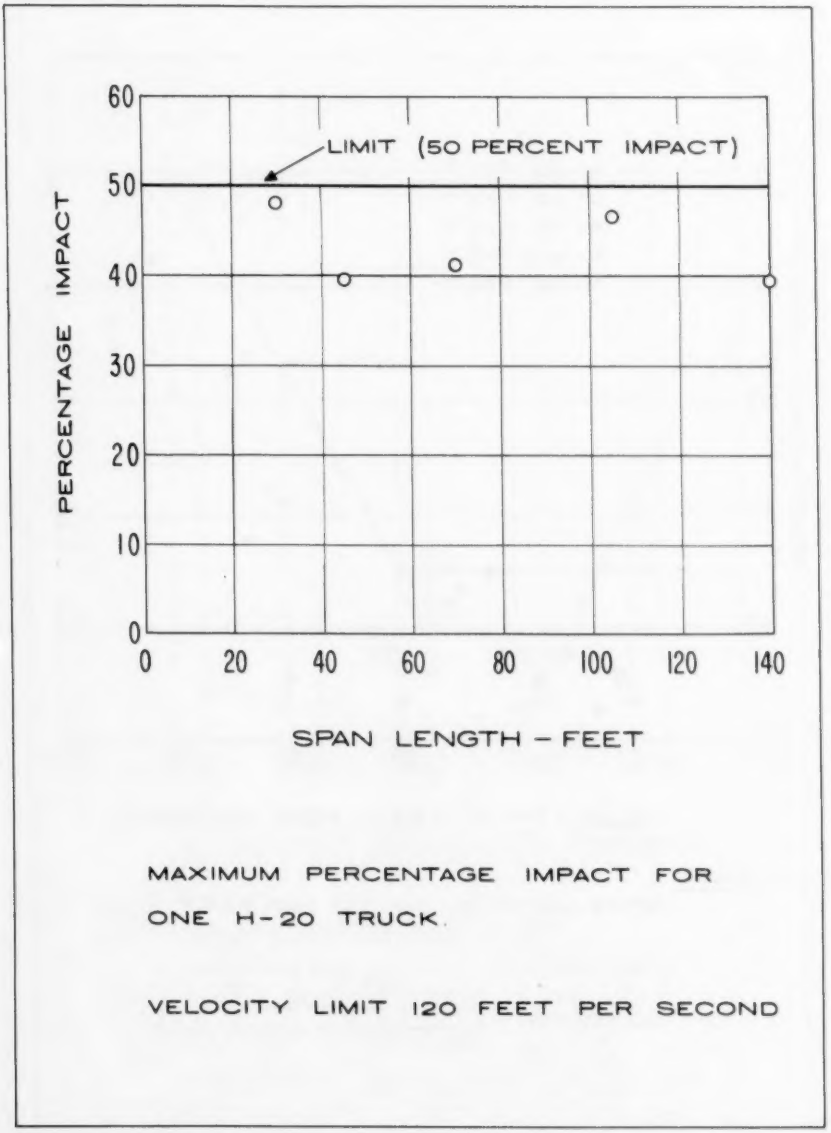

Figure 13. Impact VS Span Length : One H20 Truck; Maximum Velocity 120 fps

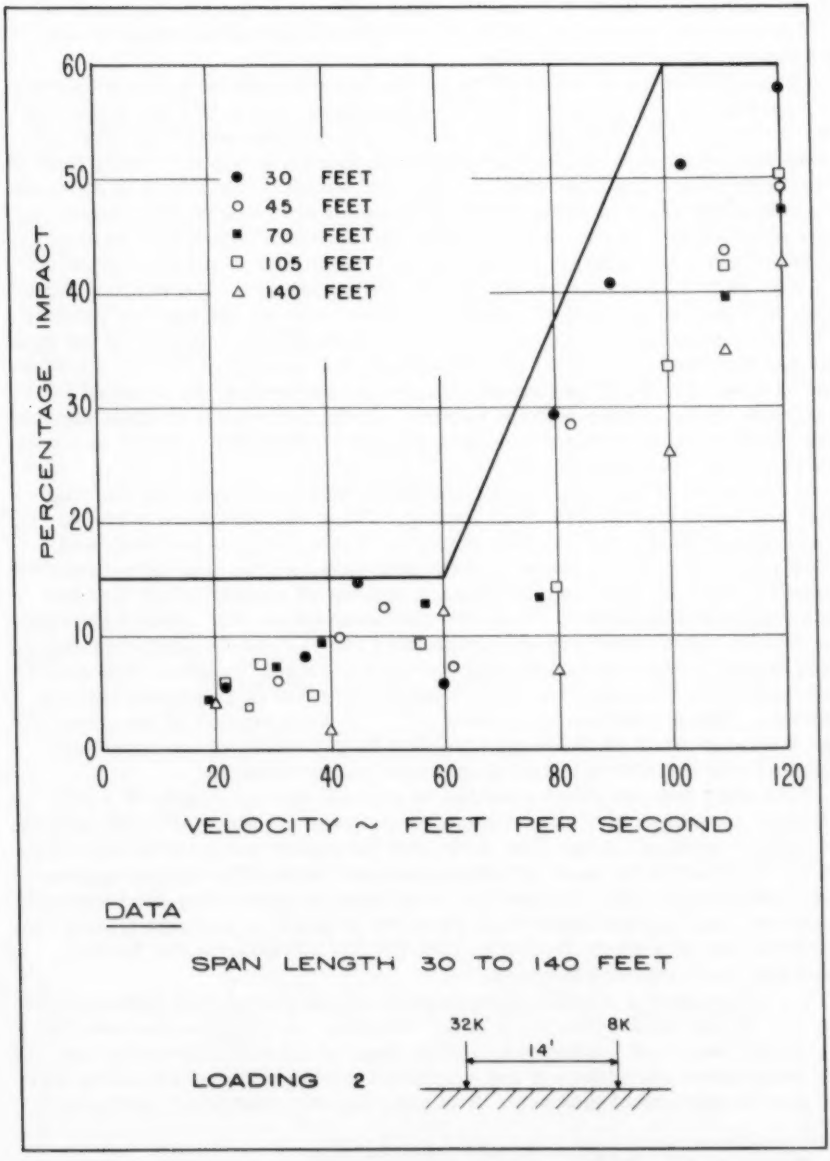

Figure 14. Impact VS Velocity : Two H20 Trucks; 30 to 140 ft. Span

trucks, shown on Fig. 15, are about 10% higher and there is some tendency for impact to decrease in proportion as the span length increases. The evidence for impact decrease coupled to increase of span length is not, however, conclusive. The higher impact on the 30 foot span tilts the maximum line downward to the right. It is possible that a change in the velocity limit of 120 feet per second would change both the magnitude and the slope of this maximum impact percentage line.

The effect of the stiffness of the bridge was investigated in a third series of analyses by repeating the first set of analyses for one H20 truck with the stiffness doubled. Data obtained from the standard designs of the BPR and from measured static deflections show that composite design roughly doubles the stiffness and has little effect on the dead weight. The change in stiffness, K, affects the value of FCAP in the analysis. If the value of the velocity, $\dot{x}_p$, is multiplied by $\sqrt{2}$ when K is doubled, the value of FCAP will remain unchanged and consequently the computed deflection will remain unchanged.[10]

Fig. 16 to 22 show the results of this set of analyses. The marked reduction of impact is due to the limitation of the velocity to 120 feet per second. At 120 feet per second the impact on the spans with stiffness doubled is the same as that recorded on the first set of analyses at a velocity of $120 \div \sqrt{2} = 85$ feet per second. At 85 feet per second, the impact on the first set is small but all values increase rapidly with the velocity. In the analyses of bridges with stiffness doubled, a small change in the maximum velocity would result in a large change in the maximum impact.

A fourth set of analyses were made to investigate the effect of the rear axle spacing of an H20-S16 truck loading. These analyses were made for three spans, 30, 70, and 140 feet in length. The velocity of the truck was constant at 120 feet per second and the rear axle spacing was varied over the specified 14 to 30 feet. On each span, a spacing of approximately four feet was analyzed to simulate a truck with dual rear axles. The results are shown on Fig. 23. These analyses are exploratory and the results limited in scope. Only the rear axle was varied whereas the impact will, in actual fact, also be affected by the spacing of the tractor axles, the relative axle loads, and the velocity. These analyses do, however, show that the spacing of the axle loads has a marked effect on the impact and that larger values of the impact are possible with the H20-S16 loading than with the H20 loading.

This study has described a method of analysis and the results of a preliminary investigation of the relations between the variables affecting impact on highway bridges. It has also shown that the digital computer is very valuable in facilitating the study of engineering problems. The Fortran system described is especially designed for programming engineering and technical problems, enabling the engineer to write the program in language closely resembling that of mathematics. The IBM 704 itself translates the Fortran statements into machine language.

The advantages of a preliminary analysis in advance of field tests are obvious from the results described in the foregoing. A complete analysis for any bridge and truck loading over a wide range of velocities would be a simple and inexpensive operation and test conditions could be chosen with the analytical data to supplement judgment. It is quite possible that fewer tests would

---

10. Values of DP = DEFL = $\dfrac{\text{TOTAL DEFLECTION}}{\left(\frac{1}{2}\, c\, \frac{L}{\dot{x}_p}\right)^2}$

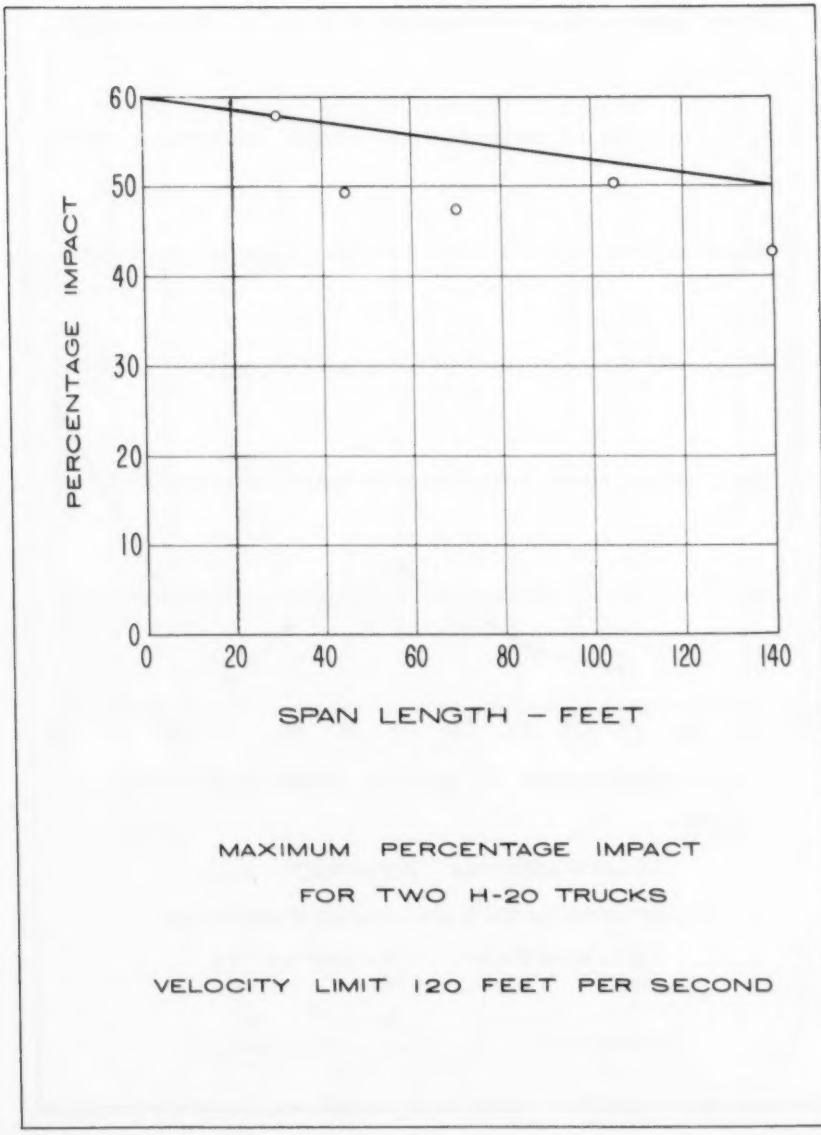

Figure 15. Impact VS Span Length : Two H20 Trucks; Maximum Velocity 120 fps

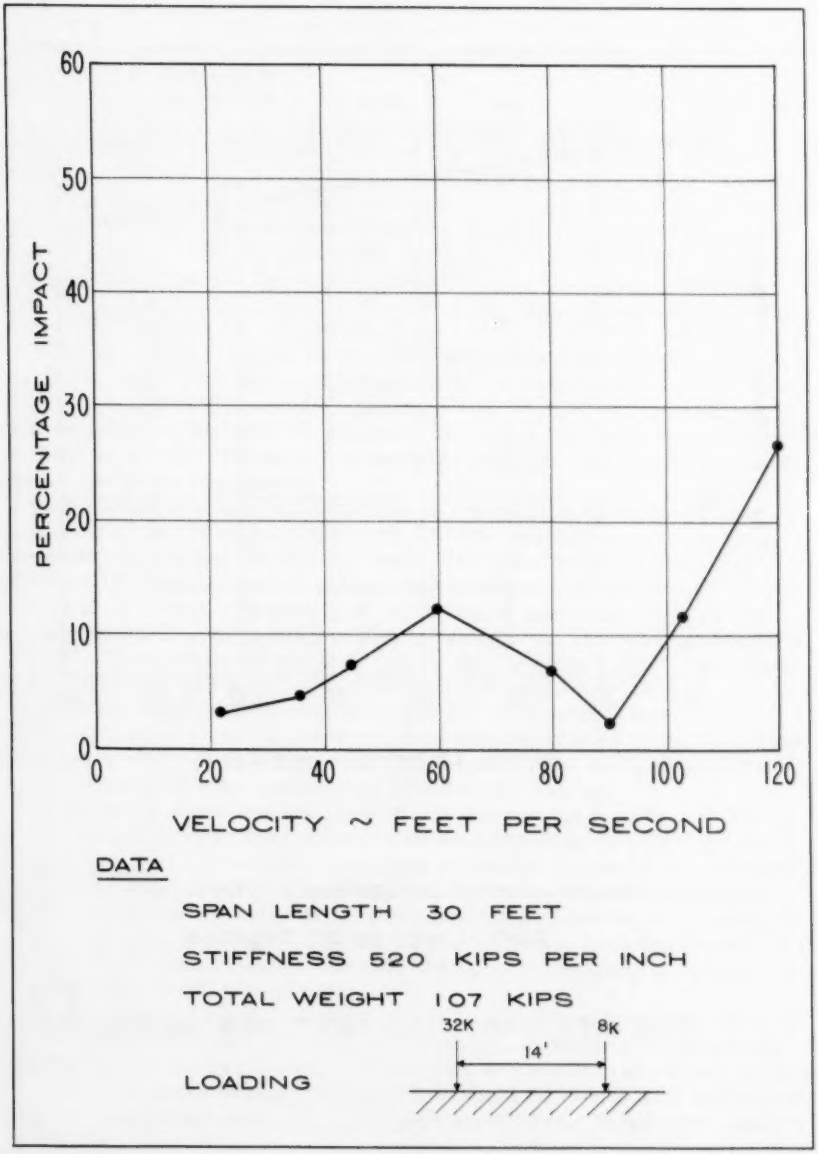

Figure 16. Variation of Impact with Velocity : One H20 Truck; Span 30 ft. (Double Stiffness)

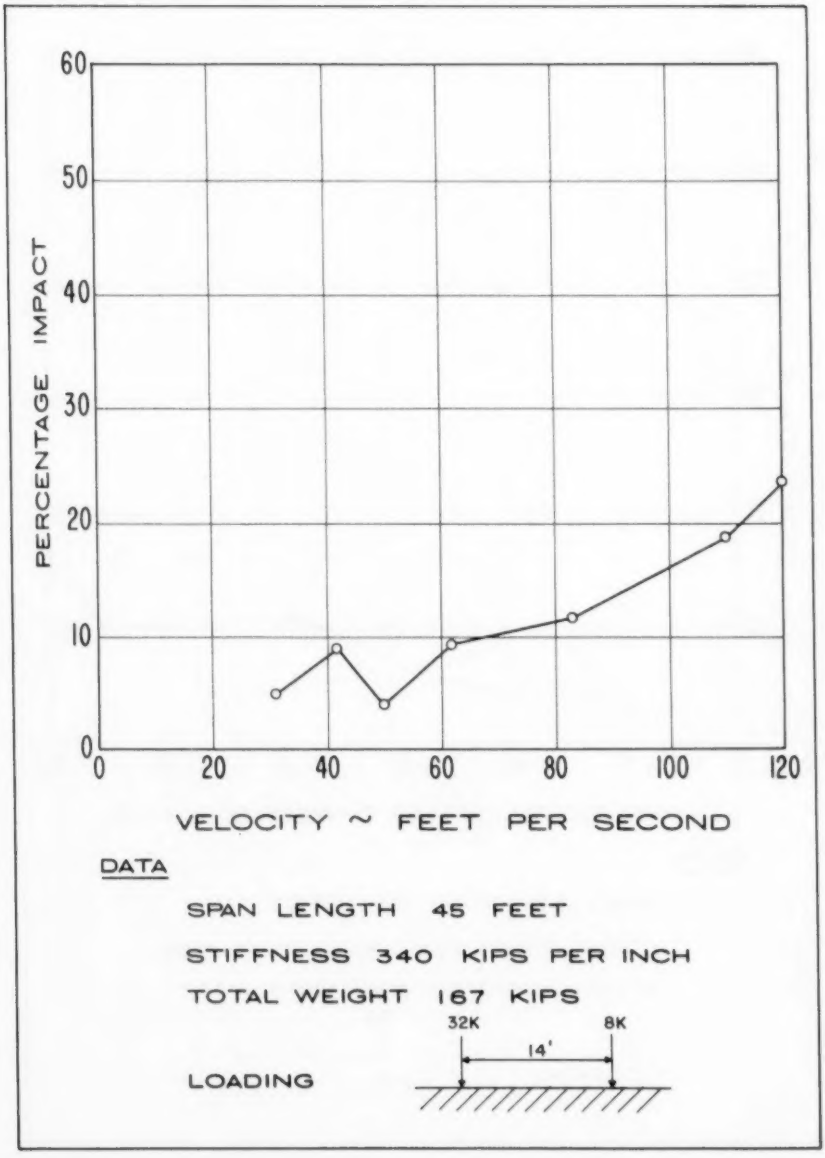

Figure 17. Variation of Impact with Velocity : One H20 Truck; Span 45 ft. (Double Stiffness)

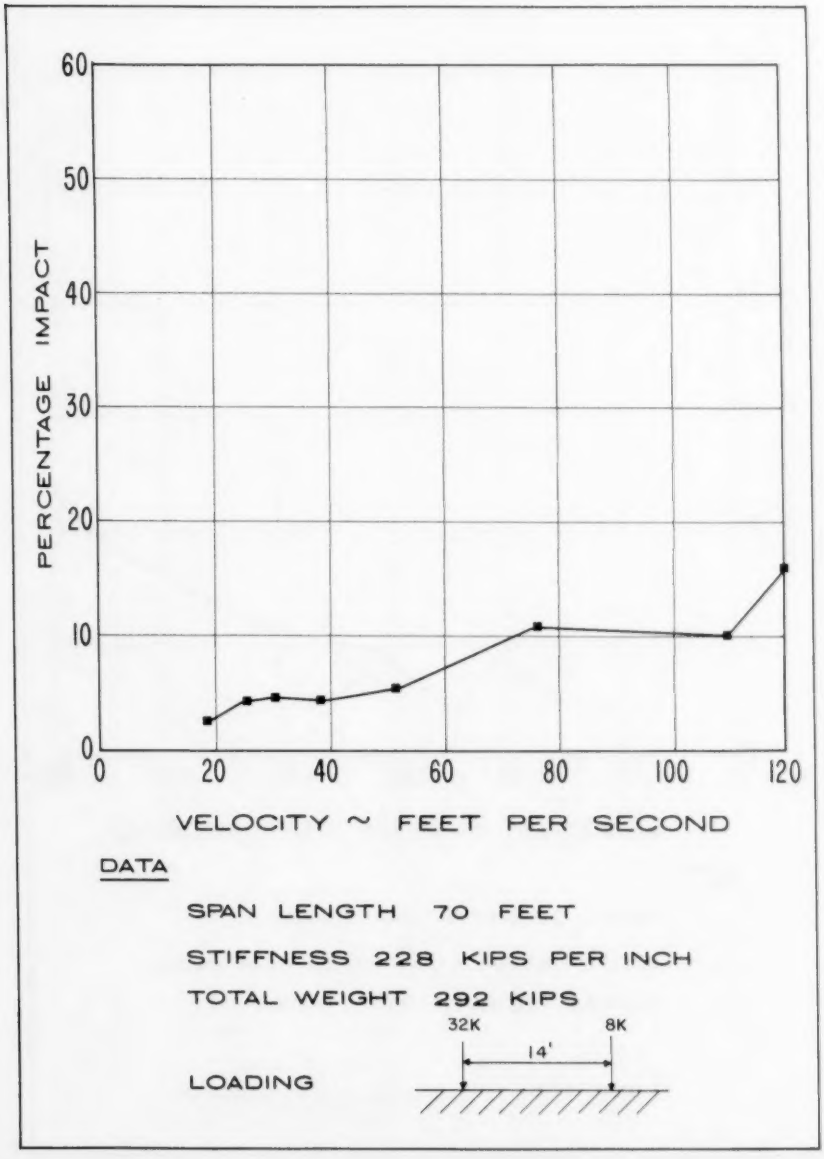

Figure 18. Variation of Impact with Velocity : One H20 Truck; Span 70 ft. (Double Stiffness)

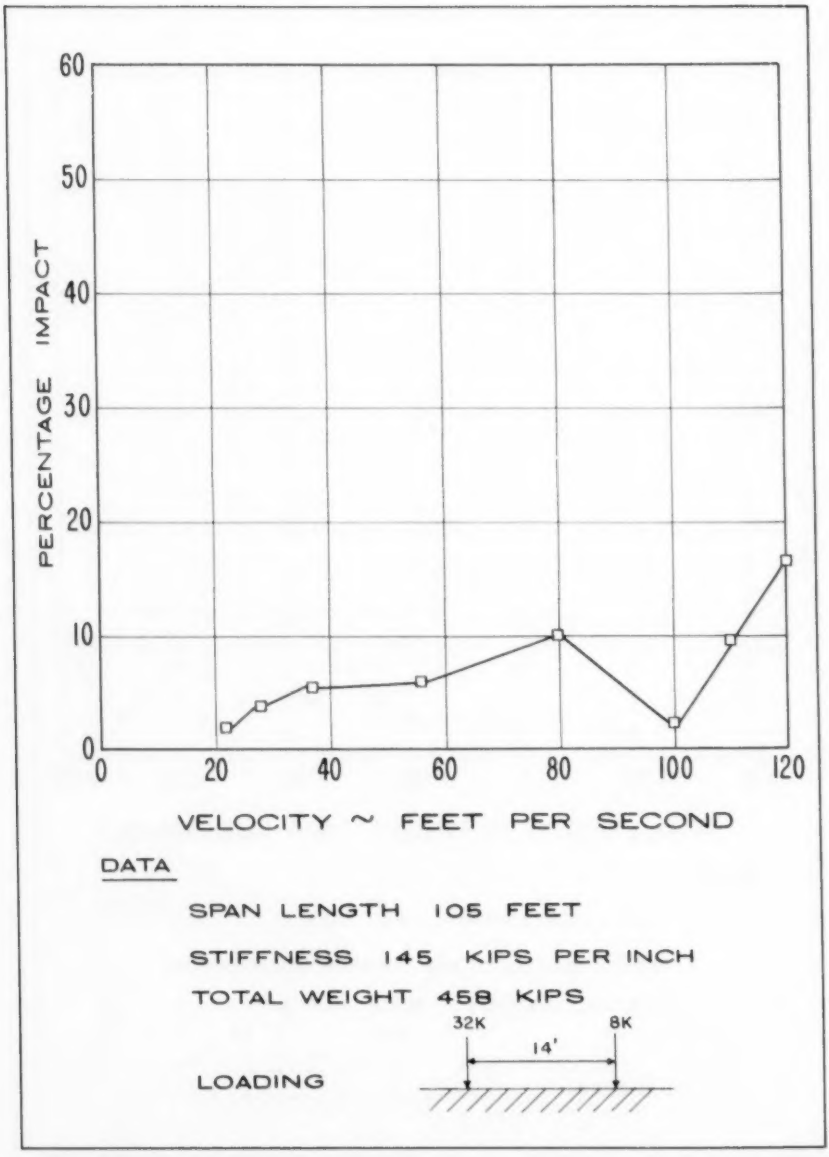

Figure 19. Variation of Impact with Velocity : One H20 Truck; Span 105 ft. (Double Stiffness)

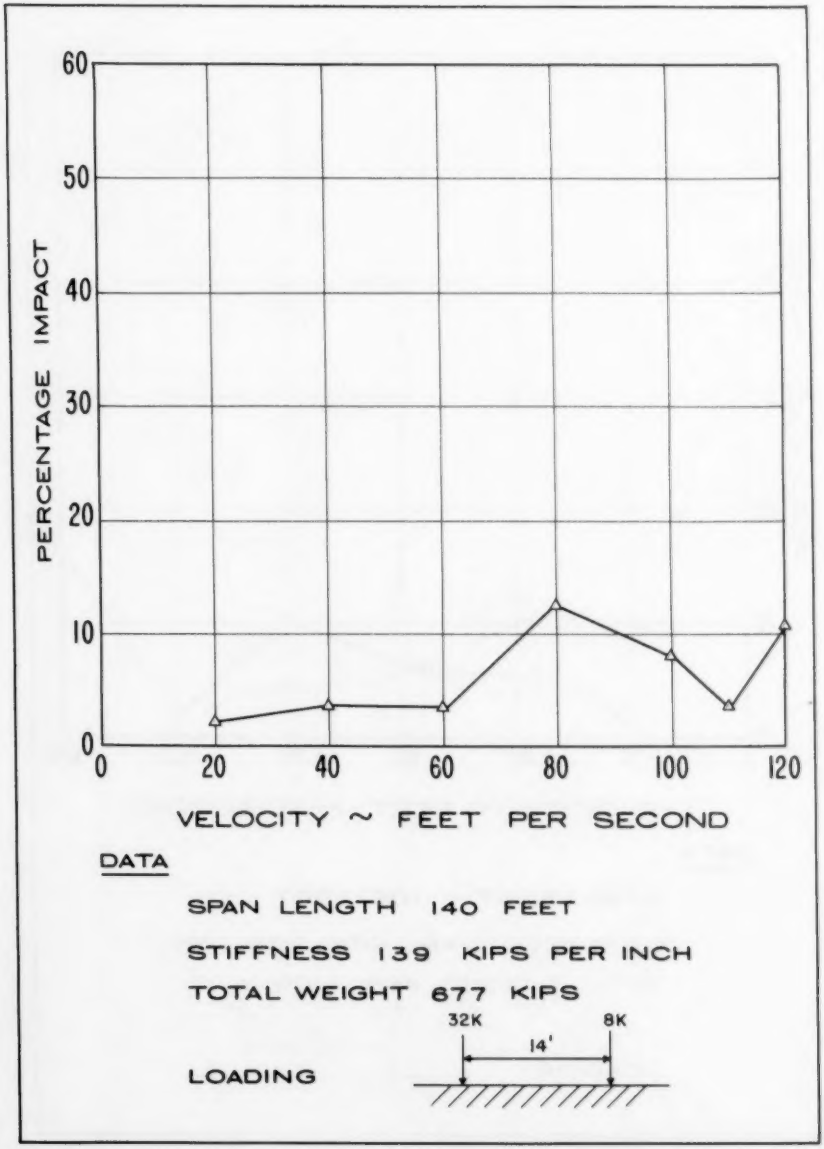

Figure 20. Variation of Impact with Velocity : One H20 Truck; Span 140 ft. (Double Stiffness)

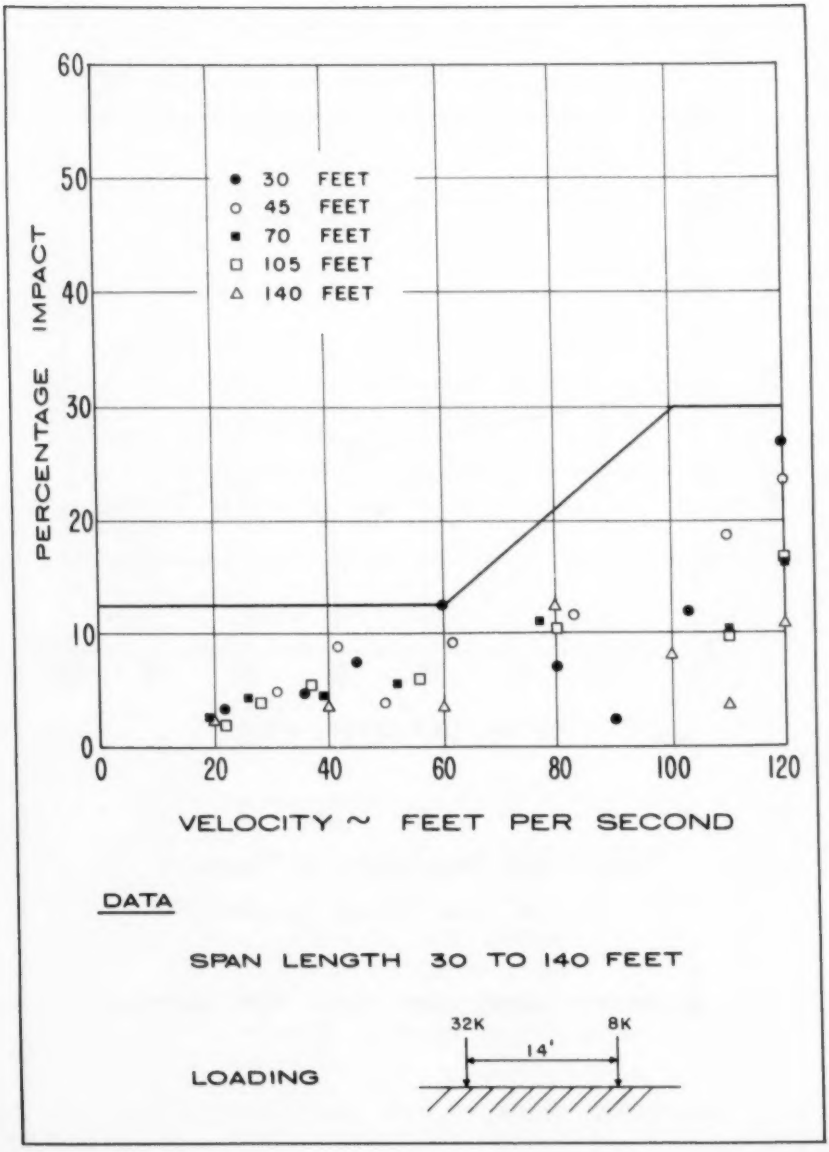

Figure 21. Impact VS Velocity : One H20 Truck; 30 to 140 ft. Span (Double Stiffness)

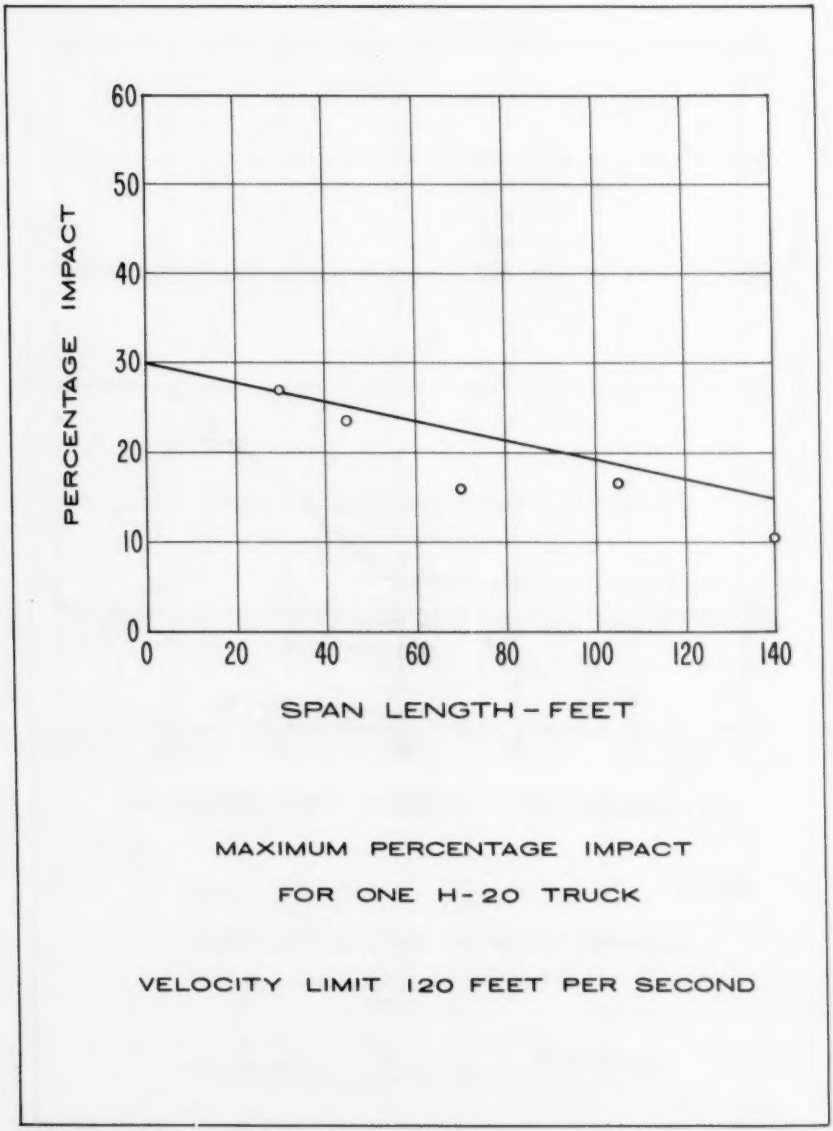

Figure 22. Impact VS Span Length : One H20 Truck; Maximum Velocity 120 fps (Double Stiffness)

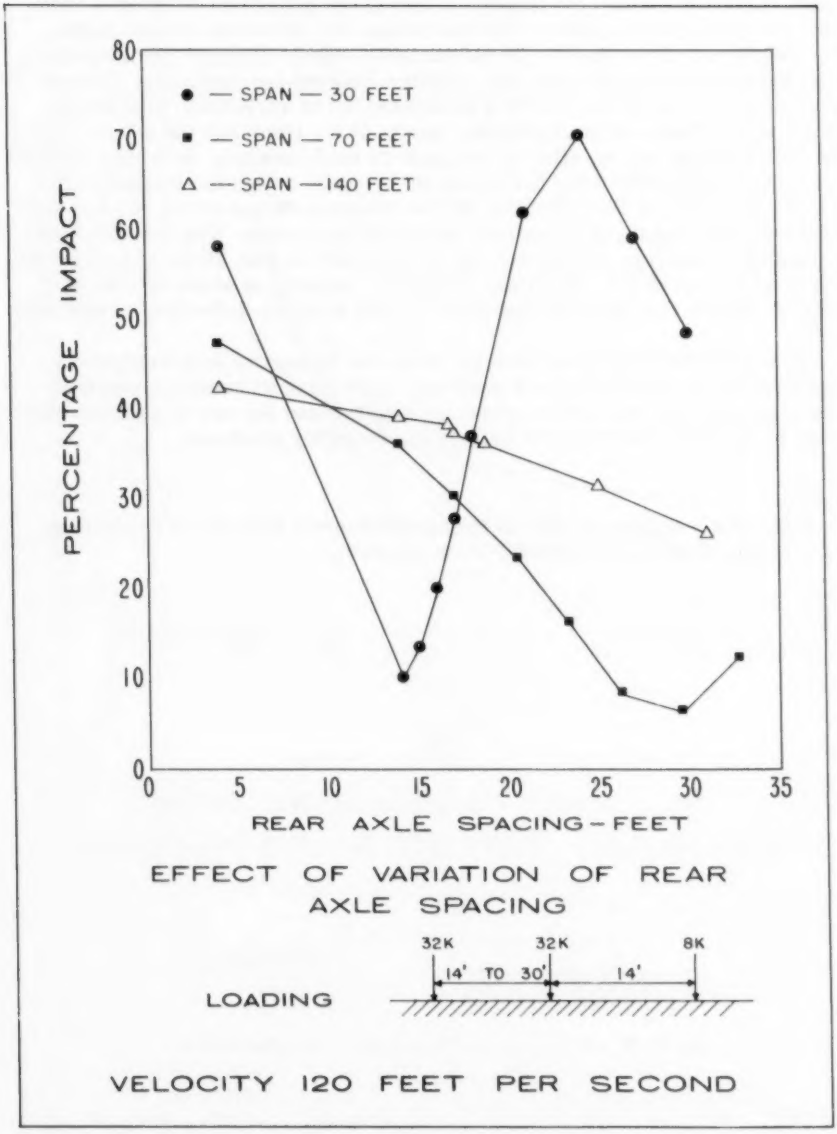

Figure 23. Impact Due to One H20-S16 Truck : Effect of Varying Rear Axle Spacing

be needed and that they would serve primarily as sources for basic data for the analysis and as a means for providing scale for analytical results.

An elaborate analysis of the relations between variables will be required and the analysis described here is especially adapted to this purpose. The truck variables include the number of axles, the magnitude of the axle loads, and the spacing of the axles. For the bridge, the variables are the length, the weight and the stiffness. These variables can be grouped into dimensionless parameters to represent the relations between the variables. Certain quantities must be invariant for a particular set of variables. The number of axles, the distribution of the total weight of the truck and the ratio between the axle spacing and the span length must be held constant. It is then possible to plot the ratio of the total deflection to the static deflection (magnification factor) vs values of $(L/\dot{x}_p)^2 / (wL/K)$ for different values of the ratio of the total weight of the truck to the total weight of the bridge. The data for these preliminary analyses are plotted, as an example, on Fig. 24 for values of the abscissa from 0 to 0.6. For these values the velocity is above 60 feet per second. Below this velocity, the ratio of total to static deflection is less than 1.15.

An analytical relation between the variables is particularly valuable in interpreting the results of field tests and in deriving an impact allowance. The proposed approach to the problems involved and the use of a digital computer to facilitate the task will be found to be highly practical.

Credit

This work was done in part at the Massachusetts Institute of Technology Computation Center, Cambridge, Massachusetts.

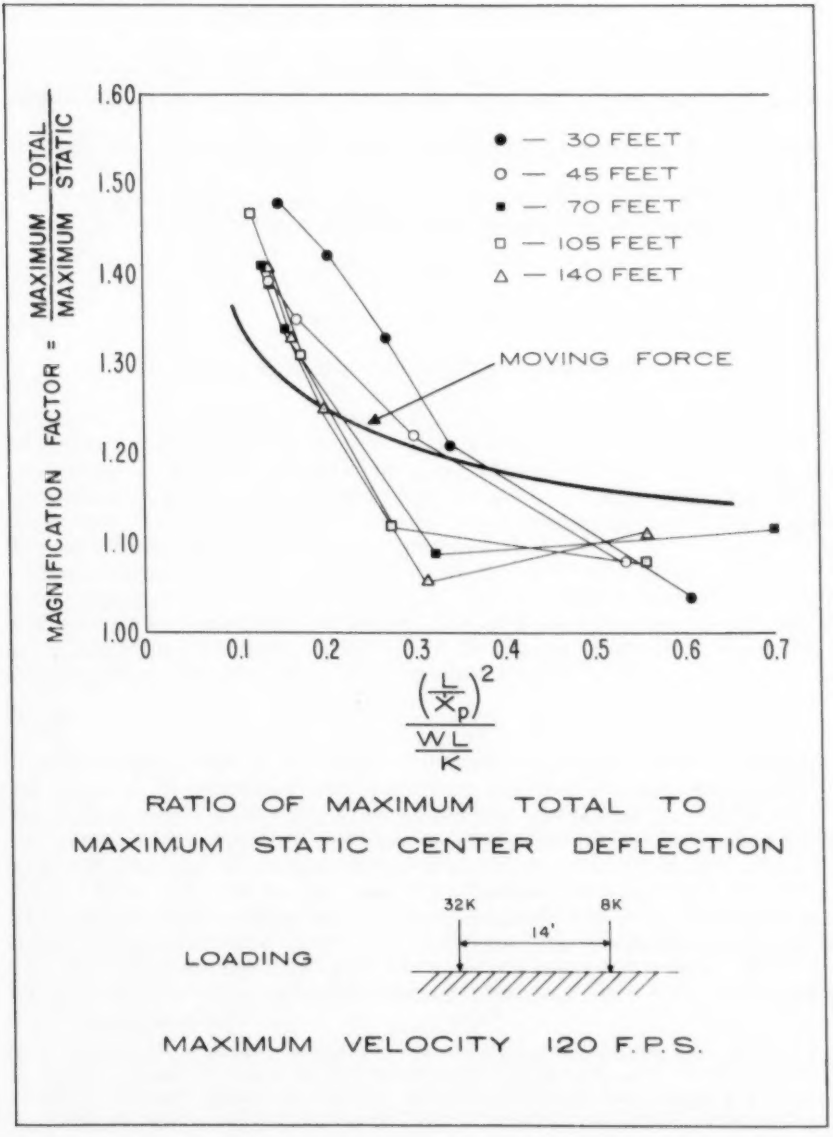

Figure 24. Relation Between Parameters : Magnification Factor VS Bridge and Truck Variables

Paper 1760 September, 1958 ST 5

Journal of the
STRUCTURAL DIVISION
Proceedings of the American Society of Civil Engineers

CAUSES OF DETERIORATION AND PROTECTIVE METHODS FOR TIMBER

PROGRESS REPORT OF A SUB-COMMITTEE OF THE COMMITTEE ON TIMBER STRUCTURES OF THE STRUCTURAL DIVISION[a]

(Proc. Paper 1760)

III Causes of Deterioration and Protection Methods

Wood in timber structures frequently gives long service life in its natural state, without any special protection. Under many service conditions, however, wood is attacked by deteriorating agencies that limit its useful life. A thorough understanding of the deteriorating agencies and the conditions that favor their development makes it possible to protect wood so that it will give long service life even under severe exposures.

The principal causes of deterioration of wood in timber structures are fungi, insects, marine borers, fire and high temperatures, abrasion, and weathering. For an adequate understanding of these agencies and methods of protecting wood from their depradations, the engineer may consult more comprehensive treatises than can be presented here.(5,24)

Fungi

Wood decay or rot is caused by wood-destroying fungi.(3,8,24) These are low forms of plant life that, when conditions are favorable to their development, grow within the wood and use it for food. Two broad types of decay, generally termed white rots and brown rots, are recognized, depending on the nature of attack on the wood components and the resultant color effects produced. There are also intermediate types between the white and brown rots. The white rot fungi destroy both the lignin and cellulose of wood and give a light, bleached, streaked effect. The brown rot fungi destroy the cellulose in concentrated areas and leave a brownish, easily crumbled residue. Both forms weaken the wood progressively and ultimately destroy its usefulness as a structural material.

Note: Discussion open until February 1, 1959. To extend the closing date one month, a written request must be filed with the Executive Secretary, ASCE. Paper 1760 is part of the copyrighted Journal of the Structural Division, Proceedings of the American Society of Civil Engineers, Vol. 84, No. ST 5, September, 1958.

a. This paper will form the basis for a chapter in a proposed revision to ASCE Manual of Engineering Practice No. 17 entitled "Timber Piles and Construction Timbers."

All wood-destroying fungi require moisture, although a few can conduct the needed water to dry wood from considerable distances. These are often referred to as "dry rot" fungi. Wood that remains at a moisture content below 20 percent (based on ovendry weight) does not decay. Fungi also require limited amounts of air and, for this reason, do not grow appreciably in wood that is saturated with water, such as in piles or timbers continuously submerged in water or mud. A favorable temperature is also necessary to fungus growth, and temperatures that are comfortable to humans are favorable to fungi and their development. The growth of fungi is arrested or inhibited by low moisture contents and low temperatures, but it again progresses when moisture and temperature conditions are favorable. However, decay-producing fungi are killed by sufficiently high temperatures or contact with toxic materials.

Woods differ greatly in their resistance to decay. The sapwood of all species of wood and the heartwood of many have low resistance. A few domestic structural species, however, such as California redwood, cypress, and the cedars, contain natural protective chemicals in their heartwood that make it highly resistant to decay. In general, however, the most practical and economical method of preventing decay in wood, used under conditions favorable to fungi, is to impregnate the wood with a suitable wood preservative. In this way, sapwood and low durability species can be made highly decay resistant and even the naturally durable woods may be benefited.

In addition to the wood-destroying fungi, there are certain woodstaining fungi and molds that can grow on the surfaces or in the sapwood of green or damp untreated timbers without serious harm to the strength of the wood.(19) Fungi that cause blue stain and mold on wood do not necessarily weaken it, but the conditions that favor their growth are also favorable to the growth of wood-destroying fungi. Heavily stained or molded wood, therefore, should be inspected with care to make sure that the discoloration has not been accompanied by incipient decay.

Wood-Boring Insects(3,5,8,16,24)

Termites are the principal insects that damage timber structures in the United States.(10,27,28) There are more than 40 species in this country. They are found in all states, but they are most plentiful and active in the warmer parts of the country.

Subterranean termites (Reticulitermes sp.) cause about 95 percent of the termite damage to timber structures. They have their nests in the soil and require moisture. They invade timber structures by building tunnels through the soil and over or through voids in obstacles until they reach the wood, which contains cellulose, their food. Their tunnels and excavations within the timbers of a structure seldom cause its collapse, but they may weaken individual members to the point of failure. No domestic wood species are immune to termite attack, but the close-grained heartwood of redwood and of tidewater red cypress, is somewhat resistant.(35) The best protection against subterranean termites is to build foundations so as to prevent access by termites to untreated wood or to use wood suitably treated with an effective preservative. Removal of all waste wood from near structures, avoidance of contact of untreated wood with the soil, and poisoning the earth adjacent to foundation walls and piers are also important protective measures.

The nonsubterranean termites do not require soil contact.(10,22) These so-called dry-wood termites can live without any other moisture than is found

in the normally dry wood of furniture, flooring, the tops of poles, and dry structural timbers. Fortunately, these termites confine their activities mostly to a narrow belt extending from Virginia to California along the southern border of the United States. They cause only about 5 percent of the total damage done by termites to wood products in the United States. They are a serious problem in the tropics and also locally in parts of Florida and California. A mating pair starts in a crack in a board or in a joint, and soon imbed themselves beneath the surface. The colony thus started builds up slowly but eventually it can do considerable damage. The elimination of crevices in wood, the painting of surfaces and the use of screens help to keep these termites out. In localized areas where damage is severe, it may be necessary to use wood that is properly impregnated with preservatives, as they will not attack it. When found in a structure the colony can be killed by skillfull application of poison dusts, by heat, or by fumigation.

The common Lyctus powder-post beetles are small elongate, brownish-black insects that work mainly in the sapwood of seasoning and seasoned hardwoods, particularly the large open-pored ones like ash, hickory and oak.[9,20,21,25] Other kinds of powder-post beetles cause damage to the sapwood and heartwood of softwoods in buildings. They seldom cause much structural damage in the United States, but they have been known to cause severe damage occasionally to portions of structures and frequently to susceptible wood products in long storage. The principal percaution to take to prevent damage to structures is to build with wood that is free from infestation and to avoid storage of infested wood products in the structure. When a powder-post beetle infestation is found in a building, it can be eradicated by suitable chemical spray or brush treatments, by fumigation, or by other control measures. Surfaces that have a finish coating and wood that has been treated resist attack.

Another insect that may cause structural damage to softwood timbers, is a large round-headed beetle commonly called the "old house borer" (Hylotrupes bajulus).[16] It bores holes about 1/4 inch in diameter usually in timbers such as floor joists of both new and old structures. There is some indication that wood exposed to high temperatures and humidities is most favorable for attack. Pine and spruce are their favorite hosts, although hemlock and fir are attacked on rare occasions. Damage is confined mainly to the sapwood. The use of suitably impregnated wood also will prevent attack. Saturating the surface of infested seasoned wood with an oil solution containing one of the chlorinated hydrocarbon insecticides mentioned for the powder-post beetles, will kill any of the borers that are located close to the surface of the wood.

The wharf borer, (Nacerda melanura), in contrast to the powder-post beetles, prefers very moist wood and is commonly associated with decay in piles, the under surfaces of wharves, and similar locations.[16] The damage is done by the larvae of a beetle that lays its eggs in the cracks and crevices of the timber. They do not work below water level, but they prefer timber that is just above the high water line or that which is kept in a wet condition. Piles beneath buildings near the water and screeds under floors that remain quite moist are also subject to attack. Precautions that prevent decay will protect wood from these borers.

Marine Borers (2,5,6,8,15,24)

Unprotected wood in salt or brackish water may be destroyed in a year or less by the attack of marine borers, which vary widely in size, form, and life habits. Some attack occurs in the brackish water of rivers emptying into salt water. The many individual species fall into two main classes; the molluscan borers, which are related to oysters and clams; and the crustacean borers, which are related to the lobsters and crabs.

The most important borers of the molluscan class are the shipworm, which include numerous species of Teredo and Bankia. Their grayish, wormlike bodies are equipped on the head end with a pair of shells with which they do their boring. They enter the wood when microscopic in size and increase in diameter and length as they extend their burrows. They fill the burrows and retain connection with the outside water by means of tubelike siphons to obtain food and oxygen. The sizes of mature shipworms vary with the species and the density of the population in the wood. Some may be 3/8 inch in diameter and 5 or 6 inches long while others may grow as large as an inch in diameter and 5 feet long. Since the entrance holes always remain very small, however, a pile may be riddled within but show practically no exterior evidence of its condition.

The pholads and martesia groups are also mollusks, but they are clamlike instead of wormlike in shape. They always remain completely enclosed in their shells but, like the shipwors, they enter the wood when very small and increase in size within the wood without greatly enlarging the entrance hole. They are more plentiful in tropical than in temperate waters. In the coastal waters of the United States, pile structures are seriously damaged by them.

The crustacean borers, in contrast to the mollusks, are free swimming and not necessarily confined within their burrows. They attack the surface of timbers and the damage they do is readily visible. Their burrows are not deep. When present in large numbers, however, the walls between the burrows are very thin and easily eroded away by waves and drift, thus inducing the borers to go deeper.

The most important group of crustacean borers are the Limnoria, of which there are several species. They are usually 1/8 to 1/4 inch long with a width of about 1/3 their length. Limnoria are very abundant and destructive. Under favorable conditions, they may destroy an untreated pile in less than a year in some harbors. Their attack may extend widely from the mud line to the water surface. It is likely to be most easily observed between tide levels where the erosion of their burrows reduces the pile to a typical hourglass shape. They are found from the Arctic to the Tropics and in both salt and fresh waters.

Sphaeroma, also of the crustacean clan, are very much like Limnoria, except that they are larger. They are not so widely distributed or found in as great number as Limnoria, but they are capable of causing considerable damage. Sphaeroma are generally found in tropical waters, either salt or fresh, and they are sometimes found in the temperate zone.

Chelura are crustaceans that resemble the ordinary sand hopper. They are slightly larger than Limnoria and are found in the same localities. The joints in the body, the antennae, and the legs are heavily feathered with long hairs and a spike projects from the back. When present in great numbers Chelura seem to drive out Limnoria, but they have not caused much damage to timbers in the coastal waters of the United States.

A few tropical timber species have shown fair natural resistance to some types of marine borers, but no domestic species of timber suitable for piles and timbers in marine structures have significant natural resistance. All native commercial timbers, when used without protection, may be destroyed within a year in waters where the borers are very active and numerous. The most effective preservative treatment is impregnation of the wood to saturation with coal-tar creosote or coal-tar creosote solution. Under moderate attack, such treatment may protect for 20 to 30 years. Under severe exposure, however, such as occurs in tropical waters, the life of well-treated piles may be only 1/3 as long. For maximum life, additional mechanical protection may have to be provided in the form of metal or concrete jackets or casings.(2,6)

It is especially important to avoid cutting into treated piles or timbers below water level for the attachment of braces or other reinforcing timbers.

Fire and High Temperatures (14,17,23,24,31)

The danger of destruction or serious damage by fire exists in all structures. Those built of incombustible materials do not burn, but they are often ruined by the burning of their contents. Heavy timber construction is rated fire resistant because of the slow rate of burning of wood in massive form. Other good construction details improve the fire performance of wood structures. Wood can also be impregnated with fire-retardant chemicals so that it is resistant to ignition and flaming. However, long exposure of wood to temperatures of 250°F. and above reduces its strength, even though no burning takes place. Consequently, wood should not be placed in contact with hot steam pipes or in other places where it will be exposed continuously to high temperatures.

Protection of wood structures from fire is accomplished by the use of heavy timbers, safety precautions against the start of fires, sprinkler systems, and impregnation of the wood with fire-retarding chemicals or application of fire-retardant coatings, where their use is practical.(12,32,33)

Abrasion

Abrasion can cause serious damage to wood surfaces exposed to the mechanical wear of traffic or to the impact of boats in ferry slips and similar situations. The obvious remedy in ferry slips is to use fender piles or timbers to take the wear and protect the timbers of the main structure. Traffic abrasion depends greatly on the nature and amount of traffic and remedies vary accordingly. Some species, such as black gum (Nyssa sylvatica), red gum (Liquidambar styraciflua), and hard maple (Acer, sp.) have high resistance to wear. Laying boards lengthwise in the direction of the traffic reduces the rate of wear. Pine and Douglas-fir boards laid with heart side down will resist splintering and mechanical wear longer than those laid the opposite way. Edgegrain board of these species will wear longer than flat grain boards. Wood blocks laid so as to expose end grain will resist wear and abrasion better than boards in which side grain is exposed. Abrasion is accelerated under conditions that favor decay. Hence good preservative treatment is important for all lumber and timber exposed to traffic under moist conditions.

Weathering[4]

Wood exposed directly to the weather undergoes both physical and chemical changes. The repeated wetting and drying of exposed wood surfaces results in checking, splitting, warping, and grain raising. Frost is a contributing factor to checking and splitting. The actions of sunlight, water, and air also cause chemical changes. The surface of the wood changes color and the cellulose and lignin become solubilized and leached out of the partly decomposed fibers. Thereafter, the loosely matted fibers are eroded at an approximate rate of 0.25 inch per hundred years.

Under many conditions, the effect of weathering goes unnoticed because the wood becomes decayed before weathering becomes serious. Severe weathering may sometimes be found, however, in wood shingles, unpainted wood siding, handrails of wood bridges, signboards, and other wood similarly exposed. In general, weathering (as distinguished from decay) is not a serious destroyer of structural wood.

Protection against weathering is provided by keeping the exposed surfaces adequately painted. Its progress is retarded by preservative treatment with preservatives of the oil type.

General Protection Methods

There are two general methods of protecting the wood of timber structures from deterioration in service. The first method is to design, build, and maintain the structures so as to avoid the conditions that favor deterioration. The second method of protection is to treat the wood with preservatives, insecticides, fire retardants, and water repellents to guard against deterioration from decay organisms, marine borers, insects, and weathering or a combination of them. The various methods are frequently combined for the protection of wood structures.

Design, Construction, and Maintenance

Much of the damage that occurs to wood structures from decay, insects, fire and weathering can be avoided by good design, construction and maintenance.(7,10,11,24,26,28) A most important consideration in eliminating decay from wood structures is to prevent the accumulation of moisture. Wood does not decay at a moisture content of 20 percent or less. Neither does it decay when continuously submerged in water. A second important consideration is to build so as to prevent the access of termites and other insect destroyers of wood. Poisoning of the earth adjacent to foundation walls and piers, design and construction of foundations free of cracks and crevices, and removal of all wood residues beneath and adjacent to structures are important protective measures against subterranean termites. Design and construction details, such as use of heavy timber construction, fire stops and sprinkler systems, have much to do with the fire performance of wood structures. These may be supplemented by fire-retardant treatments and special types of coatings to provide improved fire performance. Surface checking of timbers and lumber, a result of alternate wetting and drying usually associated with weathering, is largely prevented by the application and maintenance of coatings and the use of water-repellent materials. Detailed methods and recommendations for design, construction, and maintenance for protection of wood structures will be found in references cited and other publications.

Treating Methods

Treating wood with preservatives is in common use for the protection of lumber, timbers, and other wood products that are used in contact with the ground, in water, or otherwise under conditions that favor decay or attack by marine borers and some of the insects.(1,8,13) Likewise, impregnation with fire retardants is used to give wood improved fire performance.(1,24,32) Treatment with water-repellent preservatives is common for millwork and other above-ground uses to reduce moisture absorption by the wood and to protect it from decay.(18,32) Special treatments are used to give wood dimensional stability and other improved properties.(24) Dipping or spraying of wood and wood products with special insecticides and the use of paint and other special coatings give protection against some of the insects during seasoning, storage, and use.(9,16,20,25,26,28,34)

The effectiveness of any preservative treatment depends upon the inherent value of the preservative, the amount injected into the wood, and the depth and uniformity of penetration.

In general, standard wood preservatives used in wood-treating plants, are classified as oil borne or as water borne. Preservative oils include principally coal-tar creosote, creosote-coal-tar solution, creosote-petroleum solutions of pentachlorophenol or copper naphthenate in petroleum oil fractions. The water-borne preservatives include numerous combinations of salts of zinc, copper, arsenic, chromium, and others. They are sold under a variety of trade names (see Section VII).

Coal-tar creosote, creosote-coal-tar solution, and creosote-petroleum solution are usually preferred for outdoor uses where maximum service is desired and where color, odor, and cleanliness are of secondary importance. For protection against marine borers, however, only the creosote and the creosote-tar solutions are used.

Solutions containing pentachlorophenol or copper naphthenate in heavy petroleum oils may be used for decay and termite prevention for approximately the same purposes as creosote and its solutions, but they do not protect against marine borers. Lighter petroleum oils may be used as solvents, either with or without water-repellents, when clean, paintable surfaces are required.

Water-borne preservatives are mostly used where the wood is not in contact with the gound or water, although some of them are resistant to loss of preservative by leaching and give good protection even in ground contact. The water- borne preservatives leave the wood clean and paintable.

Other water- and oil-borne preservatives and insecticides are used to treat wood for specific uses or to protect it during drying and storage. Standard water-repellent preservatives are essentially anoil-borne preservative and a wax-type material that leave the wood clean and paintable. Insecticides recommended for treatment of wood by dip and spray methods are usually an oil solution or emulsion of a chlorinated hydrocarbon, such as DDT or benzene hexachloride. Dip treatments of logs and lumber to control blue stain and incipient decay normally involve water solutions of toxic chemicals.

Water-soluble chemical solutions, used to impregnate wood to improve its performance under fire conditions, are usually combinations of two or more materials. Four such fire-retardant chemicals or combinations with recommended retentions are given in Chapter VII. Fire retardant coatings for wood are usually sold under trade names that do not reveal their contents.

Preservatives seldom penetrate throughout the wood and are usually confined to an outer zone surrounding an unpenetrated interior. The depth of this zone and the concentration of preservative in it are highly important for many uses. Penetrations of 1 to 3 inches are common in round timbers that have comparable depths of sapwood. The penetration in the heartwood is often very limited.

The methods of applying wood preservatives vary widely. Brushing, spraying, or brief immersion give only limited absorption and penetration of preservative. Prolonged submersion, hot- and cold-bath, and vacuum processes give better retentions and penetrations. Pressure methods afford the best means of providing necessary retention and distribution of preservative for important structures and severe service conditions.

Detailed specifications covering treating conditions, preservatives, retentions, and penetrations for different wood species and wood requirements have been prepared by the Federal Government, the American Wood Preservers' Association, the American Railway Engineering Association, and by some public utilities and other large users of treated wood.[1,29] Specifications for preservative treatment by pressure processes are given in Section VII. Similar specifications for non-pressure processes are not available.

ACKNOWLEDGMENT

The Sub-Committee wishes to acknowledge the helpful comments and suggestions of the following: James A. Beal, Chief of the Division of Forest Insect Control, U. S. Forest Service; Albert P. Richards of the William F. Clapp Laboratories, Inc.; George M. Hunt, former Director of the Forest Products Laboratory; and Ralph M. Lindgren, Chief of the Division of Wood Preservation, Forest Products Laboratory, U. S. Forest Service.

Respectfully submitted,
R. P. A. Johnson
T. R. Truax, Chairman
Sub-Committee of the Committee
on Timber Structures

LITERATURE CITED

1. American Wood-Preservers' Association 1952. Manual of Recommended Practice. Standard Specifications (A looseleaf handbook, revised annually).
2. Atwood, W. G. and Johnson, A. A. 1924. Marine Structures, Their Deterioration and Preservation. Natl. Res. Council Rpt. Com. on Marine Piling Invest., 532 pp., illus.
3. Craighead, F. G. 1950. Insect Enemies of Eastern Forests. U. S. Dept. Agr. Misc. Pub. No. 657. 679 pp., illus.
4. Forest Products Laboratory 1956. Weathering and Decay. U. S. Forest Products Laboratory, Technical Note No. 221, 2 pp.
5. Greathouse, G. A. and Wessel, C. J. and others. 1954. Deterioration of Materials, Causes and Prevention Techniques, 835 pp., illus., New York.

6. Hill, C. L., and Kofoid, C. A. 1927. Marine Borers and Their Relations to Marine Construction on the Pacific Coast. San Francisco Bay Marine Piling Com. Final Rpt., 357 pp., illus.

7. Hoxie, F. J. 1935. Decay of Wood in Industrial Buildings. Associated Factory Mutual Fire Insurance Co., Inspection Dept., 79 pp., illus. Boston.

8. Hunt, G. M., and Garratt, G. A. 1953. Wood Preservation. 402 pp., illus., New York.

9. Johnston, H. R., Smith, R. H., and St. George, R. A. 1955. Prevention and Control of Lyctus Powder-Post Beetles. Southern Lumberman. 290 (2375) :72,74. March 1955.

10. Kofoid, C. A. and others. 1934. Termites and Termite Control: A Report ot the Termite Investigations Committee. Berkely, California, Univ. of Calif. Press. 734 pp., illus.

11. Laughnan, Don F. 1954. Natural Wood Finishes for Exteriors of Houses. Jour. Forest Prod. Res. Soc., 4(5) :343-345.

12. Lawson, D. I., Webster, C. T., and Ashton, L. A. 1952. Fire Endurance of Timber Beams and Floors. Struct. Engin. (England) 30(2): 7 pp., illus.

13. MacLean, J. D. 1952. Preservative Treatments of Wood by Pressure Methods. U. S. Dept. Agr. Handb. 40,160 pp. illus.

14. _____
1951. Rate of Disintegration of Wood Under Different Heating Conditions. Amer. Wood-Preservers' Assoc. Proc. 47: 155-168, illus.

15. _____
1954. Results of Experiments on the Effectiveness of Various Preservatives in Protecting Wood Against Marine-Borer Attack. U. S. Forest Prod. Lab. Rpt. D1773, 19 pp., illus.

16. Mallis, A. 1954. Handbook of Pest Control. 2d ed., 1068 pp., New York.

17. National Fire Protection Assocation 1948. Handbook of Fire Protection. 10th ed., 1544 pp., illus. Boston.

18. National Woodwork Manufactures Association. 1951. Minimum Standards for Water-Repellent Preservatives for Millwork. 2 pp., illus. Chicago.

19. Scheffer, T. C., and Lindgren, R. M. 1940. Stains of Sapwood and Sapwood Products and Their Control. U. S. Dept. Agr. Tech. Bul. 714, 123 pp., illus.

20. Smith, R. H. 1956. Lyctus Powder-Post Beetle Control by Surface Applications of Oil Preparations and Solvents. Pest Control 24(4): 42, 45. April 1956.

21. Snyder, T. E. 1926. Preventing Damage by Lyctus Powder Post Beetles, U. S. Dept. Agr. Farmers' Bul. 1477, 12 pp., illus.

22. _____ 1950. Control of Nonsubterranean Termites. U. S. Dept. Agr. Farmers' Bul. 2018, 16 pp., illus.

23. Underwriters Laboratories, Inc. 1939. Fire Exposure Tests of Loaded Timber Columns. Underwriters Labs. Bul. Res. 13, 23 pp., illus.

24. U. S. Dept. of Agr., Forest Service, Forest Products Laboratory 1955. Wood Handbook. Agricultural Handbook No. 72, 528 pp., illus.

25. _____ 1954. Division of Forest Insect Research, Wash. D. C. Powder-Post Beetles in Buildings, what to do about them. Leaflet 358, 8 pp., illus.

26. _____ 1956. U. S. Dept. Agr., Forest Service, Division of Forest Insect Research. Recommendations for Protecting Wood in New Construction from Attack by Subterranean Termites.

27. _____ 1949. Damage to Buildings by Subterranean Termites and Their Control. U. S. Dept. Agr. Farmers' Bul. 1911, 38 pp., illus. (Rev.)

28. _____ 1951. Decay and Termite Damage in Houses. U. S. Dept. Agr. Farmers' Bulletin 1993, 26 pp., illus. (Rev.)

29. U. S. Federal Supply Service 1950. Wood Preservative, Recommended Treating Practices. Fed. Specif. TT-W-571^{c}, 11 p. (See yearly index for specifications on individual preservatives).

30. _____ 1952. Wood Preservative; Water-repellant. Fed. Specif. TT-W-572.

31. U. S. National Bureau of Standards 1942. Fire Resistance Classification of Building Constructions. Bldg. Mater. and Struct. Rpt. 92, 70 pp.

32. U. S. Navy 1944. Chemicals, Fire-retardant, for Lumber and Timber (Recommended Treating Practice). Navy Dept. Specif. 51 C 40, i pp., illus.

33. Van Kleeck, A. 1953. Fire-retarding Coatings. U. S. Forest Prod. Lab. Rpt. R 1280, 11 pp. (Processed).

34. Verrall, A. F. and Scheffer, T. C. 1949. Control of Stain, Mold and Decay in Green Lumber and Other Wood Products. Forest Prod. Res. Soc. Proc. 3:9 pp., Illus.

35. Wolcott, George N. 1950. An Index to the Termite-resistance of Woods. Univ. of Puerto Rico, Agr. Exp. Sta. Bul 85.

Paper 1761 September, 1958 ST 5

Journal of the
STRUCTURAL DIVISION
Proceedings of the American Society of Civil Engineers

ANALYSIS OF RIGID FRAMES BY SUCCESSIVE REPLACEMENT

Chen Loh-Kwan,[1] M. ASCE and Li Seung Ping,[2] J. M. ASCE
(Proc. Paper 1761)

SYNOPSIS

An analytical method is developed for the calculation of moments at the supports or joints of rigid frames by replacing a portion of a structure with a member of its equivalent in stiffness or in rigidity. The derivation of formulas in this paper is based on the concept that when a member continuous over several supports or rigid joints is cut at any of its supports or joints the equilibrium of the two portions of the member is unaltered if the slope at the section is preserved. Thus either its left or its right portion can be replaced by any such torsion or flexure member that fulfills this requirement. This facilitates the transformation of a complicated plane or space frame into a much simpler type of plane structures for analysis.

INTRODUCTION

In the analysis of many structures the usual method of Moment Distribution has the following disadvantages. First, if it is desired to investigate the possible maximum moments induced in a continuous beam of many loaded spans, moment distribution has to be carried out for the loading in each span. Second, in space frames with both bending and torsion members meeting at joints, the usual way of distribution becomes very complicated. The aim of this paper is to present a method of 'Successive Replacement' to simplify the analysis of the following three types of structures.

(1) Continuous beams.
(2) Space frames with mutually perpendicular members.
(3) Space frames with inclined members.

Note: Discussion open until February 1, 1959. To extend the closing date one month, a written request must be filed with the Executive Secretary, ASCE. Paper 1761 is part of the copyrighted Journal of the Structural Division, Proceedings of the American Society of Civil Engineers, Vol. 84, No. ST 5, September, 1958.

1. Lecturer, Civ. Eng. Dept., Univ. of Hong Kong, Hong Kong, China.
2. Demonstrator, Civ. Eng. Dept., Univ. of Hong Kong, Hong Kong, China.

NOTATIONS

The notations used in this paper are the following:

L - Length of a member.
I - Moment of inertia of the cross-sectional area of a member about its centroidal axis.
K - Stiffness in bending (= I/L)
J - Torsional parameter.
Q - Torsional rigidity of a member (= J/L).
E - Modulus of elasticity.
G - Modulus of rigidity.
N - The ratio G/E.

Convention of Signs

Moment: Clockwise, positive; anticlockwise, negative.

Torque: A torque as shown in Fig. 1, applying at A tending to roll the member away from the observer is taken as positive. That applying at B tending to roll it towards the observer is taken as negative.

Continuous Beams

Suppose a continuous beam of two spans is acted upon by a moment at its end support, the magnitude of rotation at this end would depend on the stiffness of the two spans. If these two spans are the two end spans of a continuous beam and are unloaded they may be replaced by a single span of such stiffness that would preserve the original slope of the beam at the section over the support where the two parts are connected. Such replacement does not alter the equilibrium of the continuous beam. This process can be repeated successively for every two end spans up to an appropriate stage when the structure is ready for a quick and simple solution. Fig. 1a and 1b show respectively a continuous beam of two spans ABC and its equivalent beam AB', both acted upon at A by a unit moment.

The rotation at A for the equivalent beam AB' is given by

$$\theta_{AB'} = \frac{1}{3EK_1'} \tag{1}$$

where K_1' is the stiffness of the equivalent beam. Referring to Fig. 1a, the support moment at B is equal to $\frac{1}{2}\frac{K_2}{K_1 + K_2}$ and the resultant rotation at A is therefore given by

$$\theta_{ABC} = \frac{1}{3EK_1} - \frac{1}{2}\cdot\frac{1}{3EK_1}\cdot\frac{1}{2}\cdot\frac{K_2}{K_1+K_2} \tag{2}$$

Where K_1 and K_2 are respectively the stiffness of span AB and BC. Equating the rotation (1) and (2) and solving for K_1'

$$K_1' = \left(\frac{K_1 + K_2}{K_1 + 0.75K_2}\right)K_1 = C_1K_1 \tag{3}$$

Fig. 1.

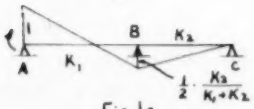

Fig. 1a

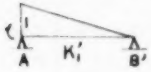

Fig. 1b.

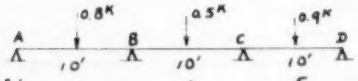

Fig. 1c.

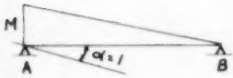

Fig. 2a.

Fig 2b

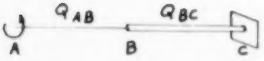

Fig. 3

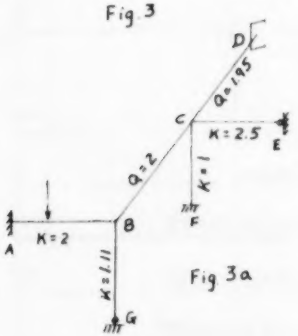

Fig. 3a

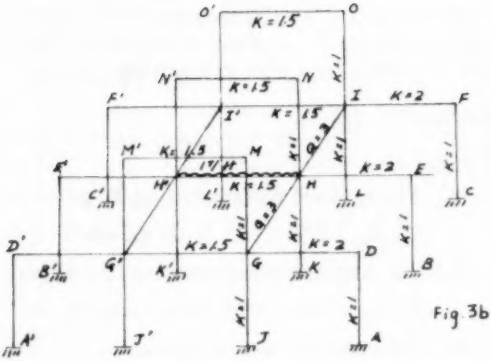

Fig. 3b

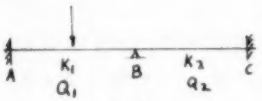

Fig. 4a
Front View

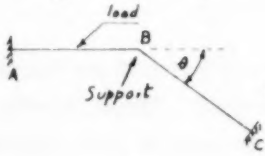

Fig 4b
Plan View

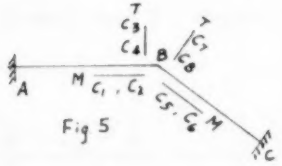

Fig 5

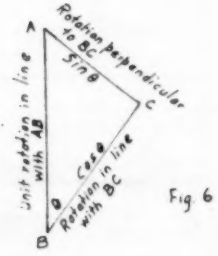

Fig 6

The factor C_1, called the 'coefficient of equivalent stiffness,' is given in Graph 1 for different values of K_1/K_2.

The ratio M_B/M_A ($= \frac{1}{2} \cdot \frac{K_2}{K_1 + K_2}$), called 'carry-over factor' and designated by C_2, can be obtained from Graph 2 as a function of K_1/K_2.

To illustrate the application of the method, two problems are worked out below in detail, and with explanation.

Problem (1) Fig. 1c

1st step

(i) For moment distribution at B, combine spans BCD into BC'.

$K_1/K_2 = 6/5 = 1.2$; from Graph 1, $C_1 = 1.128$. $K'_1 = 1.128 \times 6 = 6.77$

(ii) For moment distribution at C, combine spans ABC into B'C.

$K_1/K_2 = 6/4 = 1.5$; from Graph 1, $C_1 = 1.111$. $K'_1 = 1.111 \times 6 = 6.67$

(iii) Distribution factors at B are

$K_{AB} : K'_{BC} = 4 : 6.77 = 0.371 : 0.629$

Distribution factors at C are

$K_{B'C} : K_{CD} = 6.67 : 5 = 0.572 : 0.428$.

2nd step

(i) For carry-over from support B ⟶ C,

$C_2 = 0.227$ (From Graph 2, for $K_1/K_2 = 1.2$)

(ii) For carry-over from support C ⟶ B,

$C_2 = 0.200$ (From Graph 2, for $K_1/K_2 = 1.5$)

3rd step

K	A	4	B	6	C	5	D
K'D→A		4		6.77			
K'A→D				6.67		5	
C.O.F A→D / D→A				0.227 → ← 0.200			
Dist. Fact.		0.371		0.629	0.572	0.428	
F.E.M. ft-Kip	0	+1.500		-0.625	+0.625	-1.690	0
Dist. MB		-0.325		-0.550 →	-0.125	+0.125	
Dist. Mc		-0.122		+0.122 ←	+0.609	+0.456	
Sum	0	+1.05		-1.05	+1.11	-1.11	0

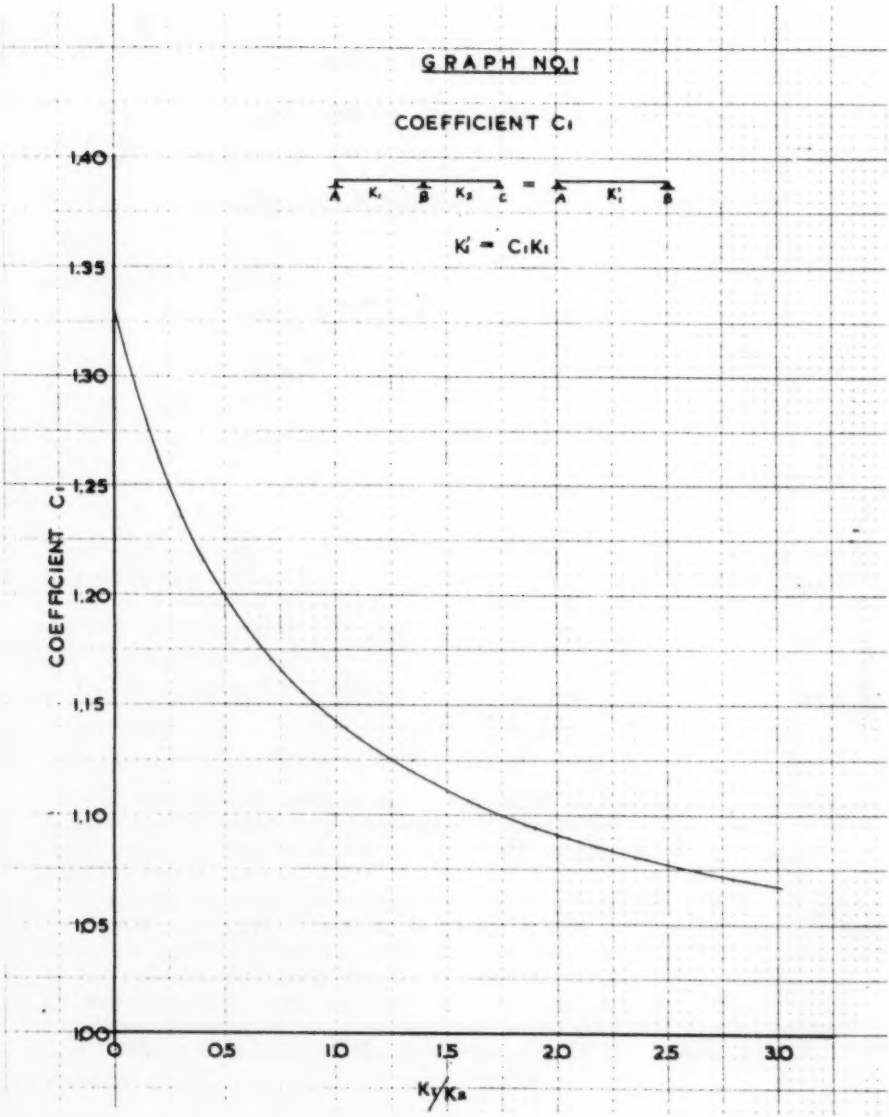
GRAPH NO.1
COEFFICIENT C1
A K1 B K2 C = A K'1 B
K'1 = C1K1
1.40
1.35
1.30
1.25
1.20
1.15
1.10
1.05
1.00
COEFFICIENT C1
0
0.5
1.0
1.5
2.0
2.5
3.0
K1/K2

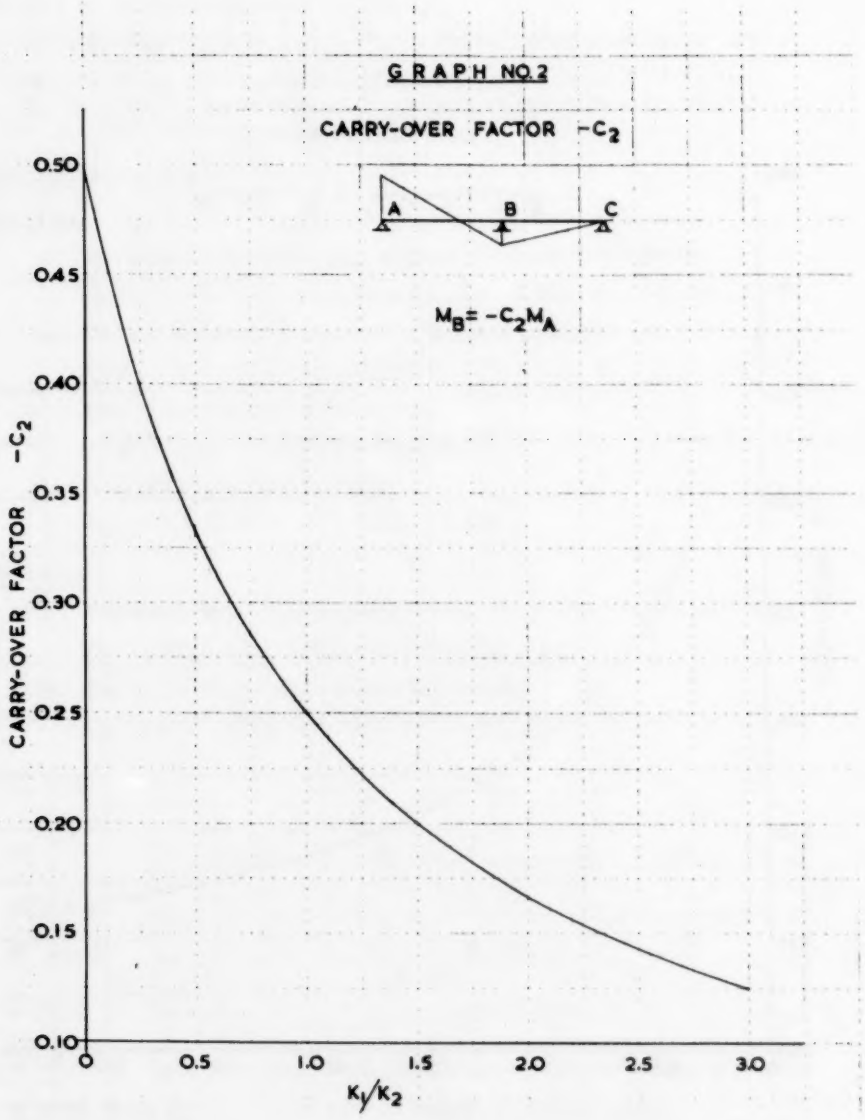
GRAPH NO.2
CARRY-OVER FACTOR $-C_2$
A
B
C
$M_B = -C_2 M_A$
CARRY-OVER FACTOR $-C_2$
0.50
0.45
0.40
0.35
0.30
0.25
0.20
0.15
0.10
0
0.5
1.0
1.5
2.0
2.5
3.0
K_1/K_2

Problem (2)

	A		B		C		D		E		F
K	1.0		1.0		1.2		1.5		1.5		
K' A→F	1.33		1.166		1.370		1.710				
K' F→A			1.170		1.400		1.710		1.5		
C.O.F A→F			0.295 →		0.293 →		0.250 →		0 →		
C.O.F F→A	← 0.50		← 0.285		← 0.246		← 0.236				
Dist. Fact.		0.534	0.466	0.455	0.545	0.445	0.555	0.534	0.466		
F. E. M.	-7	+3.2	-590	+396	-10	+10			-6		0
Dist. M_B	+156.4	+312.8	+27.4	+80.8	-80.8	-23.7	+23.7	+5.9	-5.9		0
" M_C	+24.6	+49.2	-49.2	-175.5	-210.5	-61.6	+61.6	+15.4	-15.4		0
" M_D	-0.15	-0.31	+0.31	+1.10	-1.10	-4.45	-5.45	-1.39	+1.39		0
" M_E	-0.03	-0.05	+0.05	+0.19	-0.19	-0.76	+0.76	+3.2	+2.8		0
Sum.	+173.8	+364.8	-364.8	+302.6	-302.6	+80.5	-80.5	+23.1	-23.1		0

B

(Note: When 'replacement' is repeated, the new 'equivalent stiffness' should be used to calculate another new equivalent stiffness and the carry-over factor.

e.g. in Problem (2) spans DEF are replaced by span DE' with equivalent stiffness 1.71 and carry-over factor 0.25. In replacing CDE' by CD', their values are obtained as follows:

$K_1/K_2 = 1.20/1.71 = 0.702$

From Graph 1, $C_1 = 1.171$; equivalent stiffness = 1.171 x 1.2 = 1.4

From Graph 2, $C_2 = 0.293$ = C.O.F.

It is seen that the fundamental of this method is moment distribution at one support for two spans simply supported at the two ends. Once distribution is done, the balancing moments are carried over to adjacent supports as indicated by the arrows.

Engineers versed in moment distribution will find this method very simple and handy after a little practice. If it is desired to find the maximum moment at any support due to any arrangement of loading, each fixed end moment has to be dealt with separately, e.g. in Problem (2), for support C we have first to distribute + 396 in one line and then - 10 in the next line. The maximum negative moment at one support, for example, is obtained by adding all the negative moments under that support; similarly for the maximum positive moment.

Space Frames with Mutually Perpendicular Members

Fig. 2a shows a beam simply supported at A and B. The end moment required to produce unit rotation at A is aEK in which the constant 'a' is 3 in this case. ('a' = 4 if B is fixed) Similarly, for the torsion member, CD,

Fig. 2b, the end torque required to produce unit angular detrusion at C is GQ. Equating the two expressions we obtain the relationship between bending and torsion members which would offer the same resistance to an applied load.

$$aEK = GQ \tag{4}$$

$$K = QN/a \tag{4a}$$

$$Q = Ka/N \qquad (G/E = N) \tag{4b}$$

Therefore a bending member can be 'replaced' by a fictitious torsion member when the Q-value of the latter is equal to a/N times the K-value of the former. Similarly, a torsion member can be replaced by a fictitious bending member when the K-value of the latter is equal to N/a times the Q-value of the former.

When a torsion member is composed of two or more sections of different Q-values about a common axis, as shown in Fig. 3, it can be replaced by a factitious member whose Q-value is found by equating the total effect of the angular detrusion of the member to that of the fictitious one under the same load.

Let Q'_{AC} be the equivalent Q-value of the fictitious member. Then,

$$\frac{T}{GQ_{AB}} + \frac{T}{GQ_{BC}} = \frac{T}{GQ'_{AC}} \tag{5}$$

Solving,

$$Q'_{AC} = \frac{Q_{AB}\ Q_{BC}}{Q_{AB} + Q_{BC}} \tag{5a}$$

Problem (3) Fig. 3a

Given: $N = G/E = 0.4$

F.E.M.: $M_{BA} = +96$ ft-lb.
$M_{AB} = -144$ ft-lb.

All values of stiffnesses are relative.

1st step Replacement

(i) CF + CE = CE';
$K'_{CE'} = 1.00 \times 1.33 + 2.50 = 3.83$

(ii) CE' + CD = CD';
$Q'_{CD'} = 1.95 + 7.5 \times 3.83 = 30.68$
(From equation 4b; $a/N = 3/0.4 = 7.5$)

(iii) BC + CD' = BC'
$Q'_{BC'} = \frac{30.68 \times 2}{(30.68 + 2)} = 1.88$
(From equation 5a)

(iv) $K'_{BC'} = 0.133 \times 1.88 = 0.25$ (equation 4a)

Total K-value meeting at joint B $= 1.33 \times 2 + 1.11 + 0.25 = 4.02$

2nd step Solution

$$M_{BA} = +96 - 96 \times \frac{2.66}{4.02} = +32.4$$

$$M_{BG} = -96 \times \frac{1.11}{4.02} = -26.5$$

$$T_{BC} = +96 \times \frac{0.25}{4.02} = +6.0$$

$$T_{CD} = +6.0 \times \frac{1.95}{30.68} = +0.4$$

$$M_{CF} = -(6.0 - 0.4) \times \frac{1.33}{3.83} = -2.0$$

$$M_{FC} = -2.0 \times 1/2 = -1.0$$

$$M_{CE} = -(6.0 - 0.4 - 2.0) = -3.6$$

$$M_{AB} = -144 - 1/2 \times 96 \times \frac{2.66}{4.02} = -175.8$$

Problem (4) Fig. 3b

Given: K-values of all central beams = 1.5
K- value of all side beams = 2
K - values of all columns = 1
Q - value of GH, HI, G'H', H'I' = 3
G/N = 0.4

Required: To find M_{AD}, M_{BE}, M_{HE}, and T_{HG} when beam HH' is loaded with a uniform load of 1 ton per ft.

Replacements

(i) GD and DA into GD'. $K_1/K_2 = 2/1.33 = 1.5$; $C_1 = 1.11$

$$K'_{GD} = K'_{HE'} = K'_{IF'} = 2 \times 1.11 = 2.22$$

(ii) Similarly,

GM and MM' into GM'. $K_1/K_2 = \frac{1}{2/3 \times 1.5} = 1$

$C_1 = 1.14$, $K'_{GM'} = K'_{HN'} = K'_{IO'} = 1.14 \times 1 = 1.14$

(iii) $K'_{GD'} + K'_{GM'} + K'_{GG'} + K'_{GJ} = 2.22 + 1.14 + 1.5 \times 2/3 + 1.33 = K'_{D'M'G'J'} = 5.69$

(iv) $Q = 3K/N = 3K/0.4 = 7.5K$. (equation 4b),

$$Q_{D'M'G'J'} = 7.5 \times 5.69 = 42.70$$

Combining with Q_{GH},

(equation 5a) $$Q'_{G'H} = \frac{42.7 \times 3}{42.7 + 3} = 2.80$$

(v) $K = NQ/3 = 0.4Q/3 = 0.133Q$; $K'_{G'H} = 0.133 \times 2.80 = 0.372$

Total K at H $= K_{HK} + K_{HH'} + K_{HN'} = K_{HE'} + 2K'_{HG'}$
$= 1.33 + 1.5 \times 2/3 + 1.14 + 2.22 + 2 \times 0.372 = 6.44$

Solution for moments

$$\text{F.E.M.} \quad M_{HH'} = \frac{1 \times 20 \times 20}{12} = 33.33 \text{ ft tons.}$$

$M_{HE} = 33.33 \times 2.22/6.44 = -11.5$ ft-tons

$M_{EH} = -11.5 \times 1.33/2(1.33 + 2) = -2.3$

$M_{BE} = 1/2 \times 2.3 = +1.15$ ft-tons

$T_{HG} = 33.33 \times 0.372/6.44 = 1.93$ ft-tons

$M_{GD} = 1.93 \times 2.22/5.69 = -0.75$

$M_{DG} = -0.75 \times 1.33/2(1.33 + 2) = -0.15$

$M_{AD} = 1/2 \times 0.15 = 0.075$ ft-tons

In solving the above space structure, the bending members AD, GD, GM, MM', GG', and GJ are successively grouped together and replaced by one bending member, which is then transformed into a torsion member to combine with GH to form a fictitious member HG'. The latter is then expressed in terms of K for ease of distribution. (The same holds for HI'.) We are then left with a few members all meeting at joint H for distribution. Graphs 1 and 2 may be used to advantage in getting equivalent coefficients and carry-over factors.

Space Frams with Inclined Members

In above sections, the method of 'Successive Replacements' has been shown to consist in reducing all members of a structure to two or more meeting at one support or joint. This principle can be applied to space frames with inclined members which take bending and torsion at the same time. Let us first deal with a simple case shown in Fig. 4, which shows two continuous members AB and BC in the same horizontal plane, BC being inclined to AB at an angle θ. It can be easily seen that either a moment or a torque applied to span BA at B will produce both bending and torsion in span BC, and vice versa. So a complete distribution at B, requires eight distribution factors, $C_1, C_2, C_3, \ldots\ldots C_8$ as shown in Fig. 5. The meaning of these factors is as follows.

Suppose a F.E.M. M_{BA} acts at B. When it is released in its bending plane only, the induced moment and torque M_{BC} and T_{BC}, acting along and perpendicular to BC, are given respectively by $M_{BA}C_1$ and $M_{BA}C_2$. (disregarding the sign for the time being). Similarly a F.E.T. T_{BA}, on being released in its torsion plane only, will give rise to a moment and a torque along and perpendicular to BC and equal to $T_{BA}C_3$ and $T_{BA}C_4$ respectively. The rest of the factors $C_5, C_6, \ldots\ldots C_8$ have similar meaning for a F.E.M. and a F.E.T. in BC at B.

Derivation of $C_1, C_2, \ldots\ldots C_8$

Referring to Fig. 4b, apply unit rotation at B in line with AB, while movement in AB perpendicular to itself is locked. The effect of this rotation on span BC is equivalent to two components of rotation, one parallel (bending), and the other perpendicular to it (torsion), as shown in Fig. 6. The moments and torque set up are as follows.

$$M_{BA} = 1 \times aEK_1$$

$$M_{BC} = \cos\theta \times aEK_2 \qquad a = 4 \text{ for fixed ends}$$

$$T_{BC} = \sin\theta \times GQ_2 \qquad = 3 \text{ for pinned ends.}$$

$$C_1 = \frac{M_{BC}}{M_{BA} + M_{BC}} = \frac{K_2 \cos\theta}{K_1 + K_2 \cos\theta} \tag{6}$$

$$C_2 = \frac{T_{BC}}{M_{BA} + T_{BC}} = \frac{NQ_1 \sin\theta}{aK_1 + NQ_2 \sin\theta} \tag{7}$$

On similar lines, the following expressions can be arrived at: –

$$C_3 = \frac{aK_2 \sin\theta}{NQ_1 + aK_2 \sin\theta} \tag{8}$$

$$C_4 = \frac{Q_2 \cos\theta}{Q_1 + Q_2 \cos\theta} \tag{9}$$

$$C_5 = \frac{K_1 \cos\theta}{K_2 + K_1 \cos\theta} \tag{10}$$

$$C_6 = \frac{NQ_1 \sin\theta}{aK_2 + NQ_1 \sin\theta} \tag{11}$$

$$C_7 = \frac{aK_1 \sin\theta}{NQ_2 + aK_1 \sin\theta} \tag{12}$$

$$C_8 = \frac{Q_1 \cos\theta}{Q_2 + Q_1 \cos\theta} \tag{13}$$

In the use of the above eight factors in distribution, as can be shown in the following illustrative problems, it is convenient to adhere to the convention of signs at the beginning of this paper. The signs of these factors will then be as follows: – $-C_1$, $-C_2$, $+C_3$, $-C_4$, $-C_5$, $+C_6$, $-C_7$, $-C_8$.

Problem (5) (Fig. 4a, 4b). Given: $N = 0.4$; $M^F_{AB} = -100$; $M^F_{BA} = +100$; $K_1 = K_2 = 1$; $Q_1 = Q_2 = 2$; $\theta = 40°$.

From equation (b), (7), (8), & (9), $C_1 = 0.433$; $C_2 = 0.116$; $C_3 = 0.762$; $C_4 = 0.433$.

Distribution

The distribution consists in alternate releasing of moment and torque. In the first line after the F.E.M. is distributed and balanced the locking torque is then released in the second line. It is to be noticed that 'balancing' and the evaluation of 'locking' torque or moment are achieved by resolving the distributed torque and moment on the right side into components along and perpendicular to member BA, e.g. in the first line, $-59.4 = -(100 - 43.3 \cos 40° - 11.6 \sin 40°)$ and in the second line, the 'locking' torque $-19.0 =$ accuracy is reached. In the above example, the answer for M_{BA} and T_{BA} are obtained by algebraic summation in the appropriate columns, while M_{BC}

A				B		C	
T	M	T_{BA}	M_{BA}	M	T	M	T
	-100		+100 →				
	- 29.7		← -59.4	- 43.3	- 11.6		
		- 19.0 →					
		+ 3.4		- 14.4	+ 8.2		
			+ 5.7 →				
	- 1.7		← -3.3	- 2.5	- 0.7		
		- 1.1 →					
		+ 0.3	+ 0.3	- 0.8	+ 0.5		
+ 16.4	- 131.4	- 16.4	+ 43.3	- 43.7 →	- 15.3 →	- 21.8	+ 15.3
				($-M_{BA}\cos\theta + T_{BA}\sin\theta$)	($-M_{BA}\sin\theta + T_{BA}\cos\theta$)		

C

and T_{BC} are found by resolution of M_{BA} and T_{BA} into components along and perpendicular to BC.

For convenience in design work, the following four Tables have been worked out mathematically to give a general solution of all cases. Let

$$C_1\cos\theta + C_2\sin\theta = P \quad (14) \qquad C_5\cos\theta + C_6\sin\theta = U \quad (18)$$

$$C_1\sin\theta - C_2\cos\theta = Q \quad (15) \qquad C_5\sin\theta - C_6\cos\theta = W \quad (19)$$

$$C_3\cos\theta - C_4\sin\theta = R \quad (16) \qquad C_7\cos\theta - C_8\sin\theta = X \quad (20)$$

$$C_3\sin\theta + C_4\cos\theta = S \quad (17) \qquad C_7\sin\theta + C_8\cos\theta = Y \quad (21)$$

Note: - In the use of the above Tables M^F & T^F should bear their correct signs.

Problem (6) Fig. 7

Given: (i) Assume for simplicity that Q = 2K for all members. (In design, the actual torsional parameter has to be used.)

(ii) N = 0.4

(iii) F.E.M. $M^F_{CD} = -50$; $M^F_{DC} = +50$.

(Note: Due to bending and torsion at C, Fig. 7c, member BE, which is assumed to be propped against sway, is subject to bending in two directions, one in line with AB and the other at 90° to it. The column CF acts in unison with beams CB and CD and is subject to bending in four directions, parallel and perpendicular to both CB and CD. These four bending moments, however, can be combined as shown later. In the analysis, therefore, CF has to be combined with both CB and CD in order to arrive at a simple structure as shown in Fig. 8. It is assumed for simplicity that the values of K and Q for such position of CF are the same for all axes.)

The first step in the solution of this problem is to replace the structure as shown in Fig. 7 by one as shown in Fig. 8.

Replacement

(i) For $K'_{C'B'}$

AB + BE = BA', $K'_{BA'} = 1 \times 1.333 + 0.8 \times 1.333 = 2.399$

Table 1

A		B			C		
T	M	T	M	M	T	M	T
	M^F_{AB}		M^F_{BA}				
$-T_{BA}$	$M^F_{AB}+\frac{1}{2}\left(\frac{P-1}{1-QR}\right)$	$M^F_{BA}\left(-\frac{QS}{1-QR}\right)$ $=T_{BA}$	$M^F_{BA}\left(\frac{P}{1-QR}\right)$ $=M_{BA}$	$(-M_{BA}\cos\theta+T_{BA}\sin\theta)$ $=M_{BC}$	$-(M_{BA}\sin\theta-T_{BA}\cos\theta)$ $=T_{BC}$	$+\frac{1}{2}M_{BC}$	$-T_{BC}$

Table 2

A		B			C		
T	M	T	M	M	T	M	T
T^F_{AB}		T^F_{BA}					
$T^F_{AB}+(T_{BA}-T^F_{BA})$	$\frac{1}{2}M_{BA}$	$T^F_{BA}\left(\frac{S}{1-QR}\right)$ $=T_{BA}$	$T^F_{BA}\left(-\frac{PR}{1-QR}\right)$ $=M_{BA}$	$(M_{BA}\cos\theta+T_{BA}\sin\theta)$ $=M_{BC}$	$(M_{BA}\sin\theta-T_{BA}\cos\theta)$ $=T_{BC}$	$+\frac{1}{2}M_{BC}$	$-T_{BC}$

Table 3

A		B			C		
T	M	T	M	M	T	M	T
				M^F_{BC}		M^F_{CB}	
$-T_{BA}$	$+\frac{1}{2}M_{BA}$	$(M_{BC}\sin\theta-T_{BC}\cos\theta)$ $=T_{BA}$	$-(M_{BC}\cos\theta+T_{BC}\sin\theta)$ $=M_{BA}$	$M^F_{BC}\left(\frac{U}{1-WX}\right)$ $=M_{BC}$	$M^F_{BC}\left(\frac{WY}{1-WX}\right)$ $=T_{BC}$	$M^F_{CB}+\frac{1}{2}\left(\frac{U-1}{1-WX}\right)$	$-T_{BC}$

Table 4

A		B			C		
T	M	T	M	M	T	M	T
					T^F_{BC}		T^F_{CB}
$-T_{BA}$	$+\frac{1}{2}M_{BA}$	$(M_{BC}\sin\theta-T_{BC}\cos\theta)$ $=T_{BA}$	$(M_{BC}\cos\theta+T_{BC}\sin\theta)$ $=M_{BA}$	$T^F_{BC}\left(\frac{UX}{1-WX}\right)$ $=M_{BC}$	$T^F_{BC}\left(\frac{Y}{1-WX}\right)$ $=T_{BC}$	$+\frac{1}{2}M_{BC}$	$T^F_{CB}+(T_{BC}-T^F_{BC})$

Note: - In the use of the above Tables M^F & T^F should bear their correct signs.

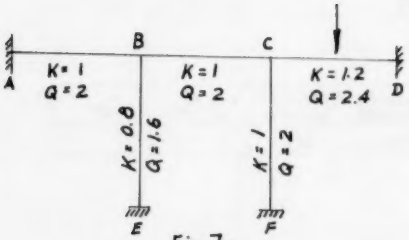

Fig. 7a
Front View

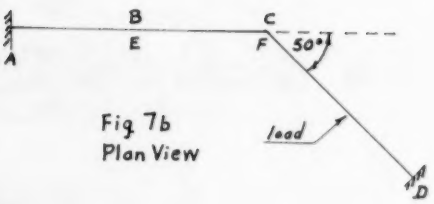

Fig. 7b
Plan View

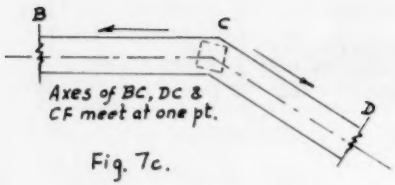

Fig. 7c.

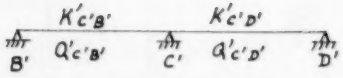

Fig. 8a
Front View

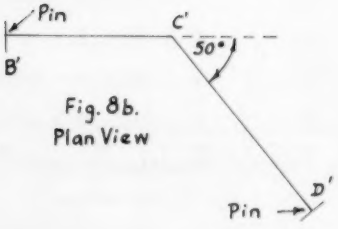

Fig. 8b.
Plan View

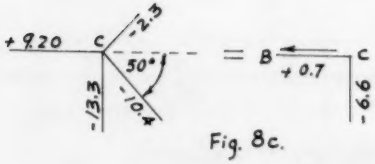

Fig. 8c.

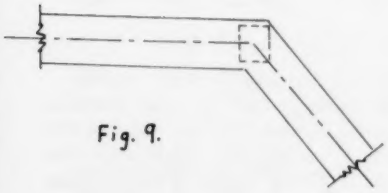

Fig. 9.

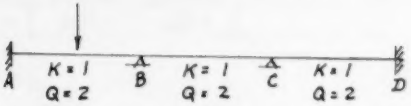

Fig. 10a
Front View

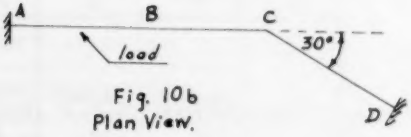

Fig. 10b
Plan View.

$BA' + BC = CB'$,

$K'_{CB'} = 1.214$ (from Graph I for $\frac{K_1}{K_2} = \frac{1}{2.39}$)

$CB' + CF + C'B'$,

$K'_{C'B'} = 1.214 + 1 \times 1.333 = 2.547$

(ii) For $K'_{C'D'}$

$CD + CF = C'D'$,

$K'_{C'D'} = 1.2 \times 1.333 + 1 \times 1.333$

$= 2.933.$

(iii) For $Q'_{C'B'}$

$AB + BE = BA'$,

$Q'_{BA'} = 2 + 7.5 \times 1.35 \times 0.8$

$= 10.$

$BA' + BC = CB'$; $Q'_{CB'} = 2 \times 10 / (2 + 10)$

$= 1.667$

$CB' + CF = C'B'$; $Q'_{C'B'} = 1.667 + 7.5 \times 1.33$

$= 11.667.$

(iv) For $Q'_{C'D'}$

$CD + CF = C'D'$; $Q'_{C'D'} = 2.4 + 7.5 \times 1.333$

$= 12.400$

From equation (10), $C_5 = 0.358$ From equation (18), $U = 0.451$

" " (11), $C_6 = 0.289$ " " (19), $W = 0.088$

" " (12), $C_7 = 0.541$ " " (20), $X = 0.060$

" " (13), $C_8 = 0.376$ " " (21), $Y = 0.657.$

Solution for Moments. (By Table 3)

$$M_{C'D'} = -50 \times \frac{U}{1 - WX} = -50 \times \frac{0.451}{1 - 0.088 \times 0.06} = -50 \times \frac{0.451}{0.995} = -22.7$$

$$M_{CD} = -22.7 \times \frac{1.2 \times 1.333}{2.933} = -12.3; \quad M_{DC} = +50 + 1/2(50 - 12.3) = +68.8$$

$$^1M_{CF} = -(22.7 - 12.3) = -10.4$$

$$T_{C'D'} = -50 \times \frac{WY}{1 - WX} = -50 \times \frac{0.088 \times 0.657}{0.995} = -2.9$$

$$T_{CD} = -2.9 \times \frac{2.4}{12.4} = -0.6; \quad T_{DC} = +0.6$$

$$^2M_{CF} = -(2.9 - 0.6) = -2.3$$

$$M_{C^{\perp}B'} = -(-22.7 \cos\theta - 2.9 \sin\theta) = 14.6 + 2.2 = +16.8$$

$$M_{CB} = +16.8 \times \frac{1.214}{2.544} = +7.6$$

$$^3M_{CF} = +16.8 - 7.6 = +9.2$$

$$T_{C^{\perp}B'} = -22.7 \sin\theta + 2.9 \cos\theta = -17.4 + 1.9 = -15.5$$

$T_{CB} = -15.5 \times \frac{1.667}{11.667} = -2.2$; $T_{BC} = +2.2$

$^4M_{CF} = -15.5 + 2.2 = -13.3$

$M_{BA'} = -7.6 \times 1/2 \times \frac{2.399}{1 + 2.399} = -2.7$

$M_{BA} = -2.7 \times \frac{1.333}{2.399} = -1.5$; $M_{AB} = -1/2 \times 1.5 = -0.8$

$^1M_{BE} = -2.7 + 1.5 = -1.2$; $^1M_{EB} = -1/2 \times 1.2 = -0.6$

$T_{BA} = -2.2 \times 2/10 = -0.4$; $T_{AB} = +0.4$

$^2M_{BE} = -2.2 + 0.4 = -1.8$; $^2M_{EB} = -1/2 \times 1.8 = -0.9$

Resultant Moments for CF. Fig. 8c

Resultant moment along CB $= +9.2 - 10.4 \cos 50^\circ - 2.3 \sin 50^\circ$
$= +9.2 - 6.7 - 1.8 = +0.7.$

Resultant moment perpendicular to CB,
$= -13.3 + 10.4 \sin 50^\circ - 2.3 \cos 50^\circ$
$= -13.3 + 8.0 - 1.5 = -6.6.$

Discussion

The values of K of CF in the above problem for bending along different axes depend on its own sectional shape and position. To simplify the calculation of stresses, the arrangement shown in Fig. 9 should be adopted where circumstance permits, since it is much easier to calculate stresses from the known resultant moments.

In this problem we have again replaced a complicated structure by a simple one. If there were another load in span BC, the analysis as outlined can still be applied, the moment and torque $M_{C'D'}$ and $T_{C'D'}$ (Fig. 8b) being just the algebraic sum of those due to the two separate loads. (Table 1 & 3 are used in calculation.)

Suppose that span AB is also loaded. Our previous practice requires that the loaded span be reserved and all others are replaced by one fictitious member. Such procedure in this case of combined bending and torque will be difficult, though not impossible. The following simple problem will illustrate the expedient to be employed in such cases.

Problem (8) Fig. 10

Given: (i) $N = 0.4$

(ii) F.E.M. $M^F_{AB} = -10$; $M^F_{BA} = +10.$

1st step Fix A and C. By moment distribution find F.E.M. at C.

2nd step Replace AB and BC by B'C.

$K_{B'C} = 1 \times \frac{1 + 1 \times 1.333}{1 + 0.75 \times 1.333} = 1.166$

$Q_{B'C} = 2 \times 2/(2 + 2) = 1.00$

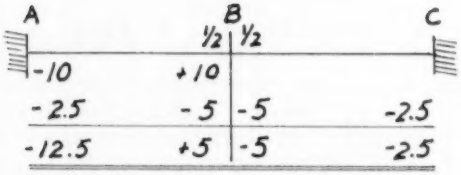

D

3rd step For spans B'C and CD, calculate the necessary factors

C_1, C_2, C_3, & C_4, For $K_1 = 1.166$; $Q_1 = 1$

$K_2 = 1.333$; $Q_2 = 2$

From equation (6), $C_1 = 0.497$. From equation (14), $P = 0.482$.
" " (7), $C_2 = 0.103$. " " (15), $Q = 0.160$.
" " (8), $C_3 = 0.833$. " " (16), $R = 0.404$.
" " (9), $C_4 = 0.634$. " " (17), $S = 0.966$.

4th step When F.E.M. at C (obtained in the 1st step) is released, moments and torque in B'CD will be due. $M^F_{CB'} = -2.5$

$$M_{CB} = -2.5 \times \frac{P}{1 - QR} = -2.5 \times 0.516 = -1.29 \text{ (From Table 1)}$$

$$T_{CB} = -2.5 \times \left(\frac{-QS}{1 - QR}\right) = +2.5 \times 0.166 = +0.42$$

$$M_{CD} = 1.29 \cos\theta + 0.42 \sin\theta = 1.12 + 0.21 = +1.33$$

$$M_{DC} = 1/2 \times 1.33 = +0.66$$

$$T_{CD} = 1.29 \sin\theta - 0.42 \cos\theta = 0.64 - 0.36 = +0.28$$

$$T_{DC} = -0.28$$

$$T_{AC} = -0.42$$

The carry-over of moment from C to B and then to A is carried out not for the full value of $M_{CB} = -2.5$, but for $M_{CB} = -2.5 + 1.29 = -1.21$.

$$M_{BC} = +1.21 \times 1/2 \times \frac{1.333}{1 + 1.333} = +0.35$$

$$M_{BA} = -0.35$$

$$M_{AB} = -1/2 \times 0.35 = -0.18$$

5th step Add results obtained in 1st and 4th steps as follows.

	A		B			C			D			E
	T	M	T	M	M	T	T	M	M	T	M	T
1st Step	0	-12.50	0	+5.00	-5.00	0	0	-2.50	0	0	0	0
Release Mc												
4th Step	-0.42	-0.18		-0.35	+0.35		+0.42	-1.29	+1.33	+0.28	+0.66	-0.28
Sum	-0.42	-12.68		+4.65	-4.65		+0.42	-1.29	+1.33	+0.28	+0.66	-0.28

CONCLUSION

The method presented in this paper serves to reduce the difficulty encountered in analysing complicated plane and space frames by Moment Distribution. It is to balance the unbalanced moment at each joint and to get the moments induced at all other joints by use of carry-over factors. By the Principle of Superposition the final results are obtained by summing the moments at each joint. When a space frame is loaded at several members it is still found easier to distribute joint moments each at a time using this method of replacements and carry-over factors than the usual Moment Distribution. In any case when the method is applicable it simplifies the structure to such a stage that it can be interpreted in terms of a simple plane structure whereby direct distribution can be carried out without difficulty.

A method is also developed at the last part to take care of such members that are called upon to resist both bending and torsion at the same time. The coefficients derived are found to be useful in the analysis of concrete frames with inclined members.

However it is to be noted that replacements cannot be made for such members whose relative values of stiffness for Moment Distribution are not known as the case of a box frame, unless the structure is symmetrical both in loading and in shape. Therefore this paper does not claim to give a general method of structural analysis. It presents a method of Direct Distribution, and also a method to simplify the analysis of many complicated Space Structures.

Paper 1762 September, 1958 ST 5

Journal of the
STRUCTURAL DIVISION
Proceedings of the American Society of Civil Engineers

ANALYSIS OF CONTINUOUS BEAMS BY CARRY-OVER MOMENTS

Jan J. Tuma,[1] M. ASCE
(Proc. Paper 1762)

SYNOPSIS

A general procedure for the analysis of continuous beams subjected to transverse loads, applied couples, displacement of supports, and change in volume is presented. The depth of the beam may be constant or variable and the continuity may be interrupted by a mechanical hinge. The recommended procedure is a successive approximation which may be carried out to a desired degree of accuracy. The possibility of computing the moments at supports by means of infinite series is demonstrated. One starting value is computed at each support, and the continuity of the elastic curve is established by means of carry-over factors only. Tables especially suitable for the analysis of continuous welded, reinforced, or prestressed concrete girders of constant or variable depth are enclosed. Numerical examples are also included.

INTRODUCTION

The general three-moment equation is introduced as a mathematical model from which a simple and workable procedure of analysis of continuous beams is derived. Mathematically this procedure is a numerical, successive approximation (iteration), which may be carried out to a desired degree of accuracy. Physically it has a deeper meaning, which depends upon three concepts:

a) Fictitious hinges are placed at all supports and the continuous beam is considered as a series of simple beams.

Note: Discussion open until February 1, 1959. To extend the closing date one month, a written request must be filed with the Executive Secretary, ASCE. Paper 1762 is part of the copyrighted Journal of the Structural Division, Proceedings of the American Society of Civil Engineers, Vol. 84, No. ST 5, September, 1958.

1. Prof. of Civ. Eng., Oklahoma State Univ., Stillwater, Okla.

b) Then from the end slopes of these simple structures starting moments are computed. (The starting moment is the bending moment required at a support to produce the continuity at that point when the far ends of the adjacent spans are still hinged.)

c) Finally by means of a direct carry-over procedure, the full continuity of the elastic curve is established.

The beam may be of constant or variable depth and the continuity may be interrupted by an intermediate, mechanical hinge. The deformation of the structure may be caused by transverse loads, applied couples, nonuniform change in volume, or displacement of supports.

The numerical procedure is similar in form to the moment distribution method(1) and to the balancing angle change method,(2,3,4) but it differs in the relaxation technique as well in the concept of approach in that:

a) One assumed starting moment is computed at each support.

b) One final moment is obtained at each support.

c) No distribution of unbalances is required during the relaxation procedure.

d) The relaxation procedure is carried out by means of carry-over factors only.

e) The procedure is self checking.

This study is restricted to coplanar systems and the customary assumptions of beam analysis are introduced. Since deformation because of shear is assumed to be small, it is neglected. The sign convention of the three-moment equation is adopted.

The subsequent discussion is divided into ten parts, with the derivation of the angular and moment functions given in the first two parts. Influence of special conditions, change in volume and displacement of supports is discussed in Parts 3, 4, and 5. The numerical procedure in two different forms is demonstrated in Parts 6 and 7, and the derivation of the moment coefficients by means of infinite, convergent geometric series is shown in Part 8. In Part 9 the computation of influence lines for the moments at supports by means of numerical and algebraic carry-over moment procedure is presented.

References to the existing tables of numerical constants and the meaning of enclosed tables are discussed in the last part of the paper.

1. Angular Functions

A continuous beam of variable cross-section acted on by a general system of transverse loads is considered. The unyielding supports are denoted by 0, 1, 2, 3, . . . , i, j, k, . . ., n and the lengths of spans by L_1, L_2, L_3, . . . , L_j, L_k, . . . , L_n. The ends are simply supported and the bending moments at intermediate supports M_1, M_2, M_3, . . . , M_i, M_j, M_k, . . . , M_{n-1} are selected as unknowns. The location of a cross-section of the beam is given by the ordinates x and x', measured from the respective end of the span. The general three-moment equation written for the intermediate joint j (any joint) in terms of angular flexibilities (F's), angular carry-over values (G's), angular load functions (τ's), and redundant moments, is (Fig. 1):

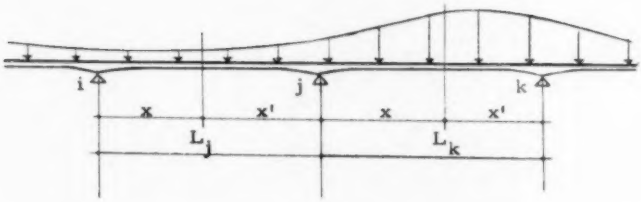

Isolated Portion of a Continuous Beam on
Fig. 1

$$G_{ij}M_i + (F_{ji} + F_{jk})M_j + G_{kj}M_k = -\tau_{ji} - \tau_{jk} . \qquad (1)$$

a) The angular flexibility F_{ji} (or F_{jk}) is the end slope of the simple beam ij (or jk) at j, due to a unit moment applied at that end (Fig. 2).

$$F_{ji} = \int_0^{L_j} \frac{x^2 dx}{L_j^2 E I_x} \qquad F_{jk} = \int_0^{L_k} \frac{x'^2 dx}{L_k^2 E I_x} . \qquad (2)$$

If the cross-section is constant

$$F_{ji} = \frac{L_j}{3 E I_j} \qquad F_{jk} = \frac{L_k}{3 E I_k} . \qquad (3)$$

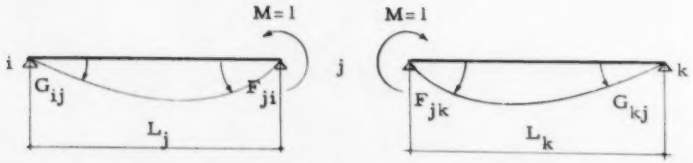

Angular Flexibilities and Carry-Over Values
Fig. 2

b) The carry-over value G_{ij} (or G_{kj}) is the end slope of the simple beam ij (or jk) at i (or k), due to a unit moment applied at the far end j (Fig. 2).

$$G_{ij} = \int_0^{L_j} \frac{x\,x'dx}{L_j^2 E I_x} \qquad G_{kj} = \int_0^{L_k} \frac{x\,x'dx}{L_k^2 E I_x} . \qquad (4)$$

If the cross-section is constant

$$G_{ij} = \frac{L_j}{6\,E\,I_j} \qquad G_{kj} = \frac{L_k}{6\,E\,I_k} \tag{5}$$

c) The angular load function τ_{ji} (or τ_{jk}) is the end slope of the simple beam ij (or jk) at j, due to loads (Fig. 3).

$$\tau_{ji} = \int_0^{L_j} \frac{\overline{BM}_x\, x\, dx}{L_j\, E\, I_x} \qquad \tau_{jk} = \int_0^{L_k} \frac{\overline{BM}_x\, x'\, dx}{L_k\, E\, I_x} \tag{6}$$

$\overline{BM}_x$ is the bending moment of the simple beam due to loads.

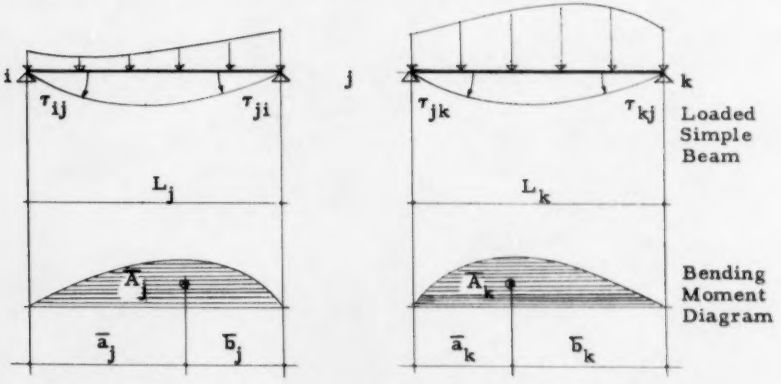

Angular Load Functions
Fig. 3

In the case of constant cross-section

$$\tau_{ji} = \frac{\bar{A}_j\,\bar{a}_j}{L_j\,E\,I_j} \qquad \tau_{jk} = \frac{\bar{A}_k\,\bar{b}_k}{L_k\,E\,I_k} \tag{7}$$

The symbols in Eq. (7) are:

$\bar{A}_j$, $\bar{A}_k$ . . . Area of the bending moment diagram of the respective simple beam

$\bar{a}_j$, $\bar{b}_k$ . . . Lever arm, measured from the support to the centroid of A_j or A_k, respectively.

2. Moment Functions

Both sides of Eq. (1) are divided by

$$\Sigma F_j = F_{ji} + F_{jk} \tag{8}$$

and new symbols

$$-\frac{G_{ij}}{\Sigma F_j} = r_{ij} \qquad -\frac{G_{kj}}{\Sigma F_j} = r_{kj} \tag{9}$$

$$-\frac{\tau_{ji} + \tau_{jk}}{\Sigma F_j} = -\frac{\Sigma \tau_j}{\Sigma F_j} = m_j \tag{10}$$

are introduced.

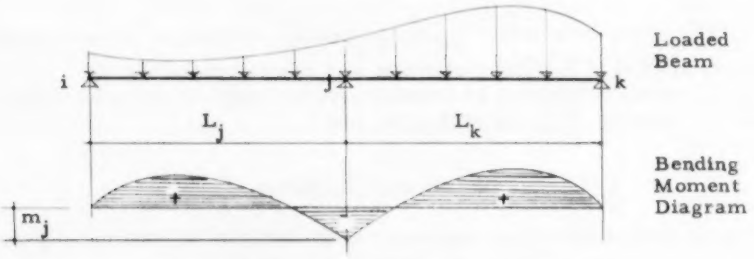

Two Span Continuous Beam $\overline{ijk}$
Fig. 4

With notation (9, 10) the three-moment Eq. (1) becomes:

$$M_j = r_{ij}M_i + m_j + r_{kj}M_k \ . \tag{11}$$

This new form of Eq. (1) consists of the starting moment m_j, the carry-over factor r_{ij} and r_{kj}, and redundant moments. The starting moment and the carry-over factors are parameters of the two span beam $\overline{ijk}$ of which ends are simply supported (Fig. 4, 5, 6).

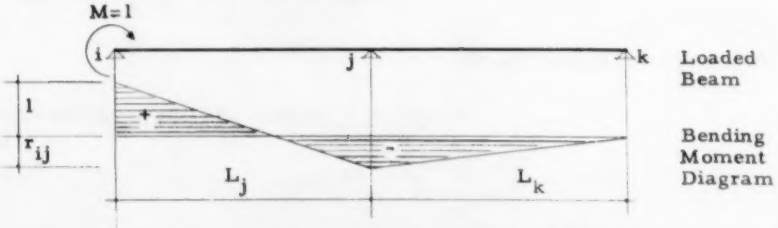

Two Span Continuous Beam $\overline{ijk}$
With Applied Couple M = 1 at i
Fig. 5

a) The starting moment m_j is the bending moment at j, due to loads if the moments M_i and M_k are equal to zero (Fig. 4).

b) The carry-over factor r_{ij} is the bending moment at j, due to a unit moment applied at i, if the moment at k is equal to zero (Fig. 5).

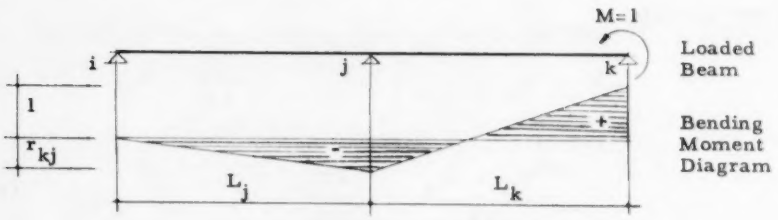

Two Span Continuous Beam $\overline{ijk}$
With Applied Couple M = 1 at k
Fig. 6

c) The carry-over factor r_{kj} is the bending moment at j, due to a unit moment applied at k if the moment at i is equal to zero (Fig. 6).

If the moment of inertia is constant over the length of any given span, the relative values of F, G and τ may be used.

3. Special Conditions

Three special conditions may occur in the analysis of continuous beams:

a) Fixed end
b) Overhanging end
c) Intermediate hinge.

If the end 0 of a continuous beam is fixed, the three-moment equation (11) reduces to:

$$M_0 = m_0 + r_{10} M_1 \tag{12}$$

where the starting moment (Eq. 10)

$$m_0 = -\frac{\tau_{01}}{F_{01}} \tag{13}$$

and the carry-over factor (Eq. 9)

$$r_{10} = -\frac{G_{10}}{F_{01}} \; . \tag{14}$$

If the end 0 is free and the span L_1 overhangs the support 1, the starting moment at 1 is computed from statics and the carry-over factor

$$r_{21} = 0 \quad . \tag{15}$$

Finally if the continuity of the elastic curve is interrupted by an intermediate, mechanical hinge in span $\overline{ij}$ (Fig. 7), the starting moment at j is computed from statics, and the carry-over factors are:

$$r_{ij} = -\frac{d_j'}{d_j} \qquad r_{kj} = 0 \quad . \tag{16}$$

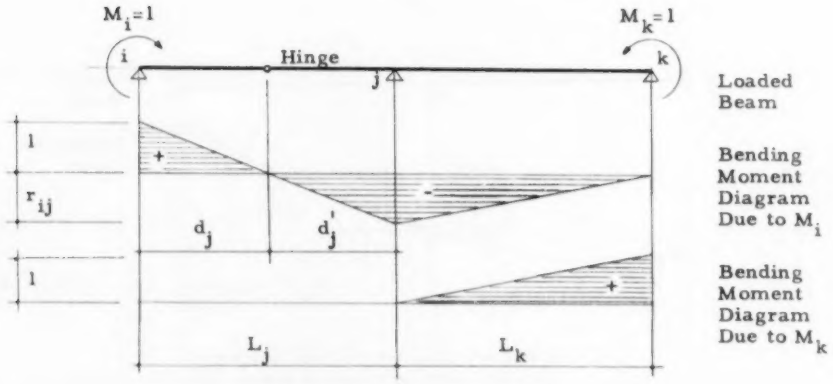

Two Span Continuous Beam $\overline{ijk}$
With Applied Couples M = 1 at i and k
Fig. 7

4. Change in Volume

The nonuniform change in temperature or in moisture content introduces moments which in some cases must be considered. The variation is assumed to be linear and ϵ_T , ϵ_B is the strain due to this change at the top and at the bottom, respectively. The variable depth of the section is h_x. The end slopes (if $\epsilon_T < \epsilon_B$) are:

$$\tau_{ji}^{(V)} = \int_0^{L_j} \frac{(\epsilon_B - \epsilon_T)x\,dx}{L_j\,h_x} \qquad \tau_{jk}^{(V)} = \int_0^{L_k} \frac{(\epsilon_B - \epsilon_T)x'\,dx}{L_k\,h_x}$$

from which the starting moment at j (Eq. 10)

$$m_j^{(V)} = -\frac{\tau_{ji}^{(V)} + \tau_{jk}^{(V)}}{\Sigma F_j} \quad . \tag{17}$$

5. Displacements of Supports

In some cases the effect of displacements of supports must be known. If the relative displacements (Fig. 8) are denoted by

$$\Delta_{ijy} \ , \ \Delta_{jky} \ ,$$

the end slopes become:

$$\tau_{ji}^{(Y)} = \frac{\Delta_{ijy}}{L_j} \qquad \tau_{jk}^{(Y)} = - \frac{\Delta_{jky}}{L_k}$$

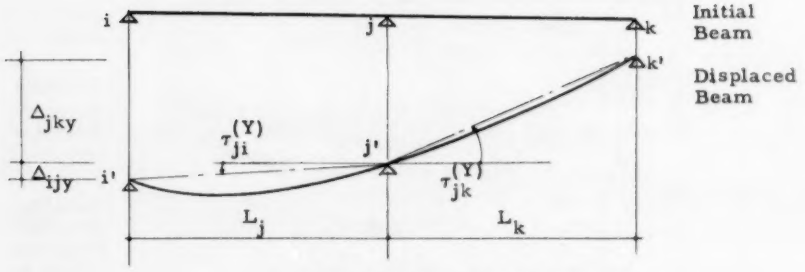

General Displacement of Supports of Two Span Continuous Beam $\overline{ijk}$
Fig. 8

The starting moment at j (Eq. 10) in terms of $\tau_{ji}^{(Y)}$, $\tau_{jk}^{(Y)}$ is:

$$m_j^{(Y)} = - \frac{\tau_{ji}^{(Y)} + \tau_{jk}^{(Y)}}{\Sigma F_j} \ . \qquad (18)$$

6. Numerical Procedure

Once the basic functions are defined, their application to the analysis of continuous beams subjected to stationary loads may be easily shown. Two examples are introduced to illustrate the numerical procedure. Because the flexural rigidity is constant in a given span, relative values of F, G, and τ are used in both problems. All values are given in feet, kips, or kip-feet.

Example 1. A three span beam of constant cross-section, loaded as shown (Fig. 9) is analyzed.

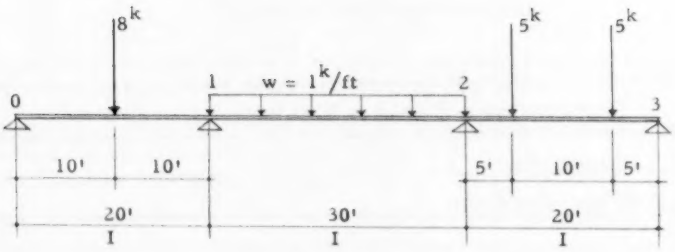

Three Span Beam
Fig. 9

a) Angular Flexibilities (Eqs. 3, 8):

$$F_{10} = F_{23} = 20 \qquad F_{12} = F_{21} = 30 \qquad \Sigma F_1 = \Sigma F_2 = 50$$

b) Carry-Over Factors (Eq. 9):

$$r_{12} = r_{21} = -\frac{1}{2}\frac{30}{50} = -.3$$

c) Starting Moments (Eq. 10):

$$m_1 = -\frac{\tau_{10} + \tau_{12}}{\Sigma F_1} = -3\,\frac{\frac{(8)(20)^2}{16} + \frac{(1)(30)^3}{24}}{50} = -79.50$$

$$m_2 = -\frac{\tau_{21} + \tau_{23}}{\Sigma F_2} = -3\,\frac{\frac{(1)(30)^3}{24} + \frac{(5)(5)(15)}{2}}{50} = -78.75$$

The values of τ for various load conditions are given in Table A of the Appendix.

d) Carry-Over Procedure (Table 1): The final moments are shown in the same table. Each final moment is equal to the sum of all values in the respective column.

e) Numerical Control (Eq. 11):

$$M_1 = m_1 + r_{21}M_2 = -61.40$$

$$M_2 = m_2 + r_{12}M_1 = -60.32$$

f) Physical Interpretation:

Carry-Over Table - Example 1 - Table 1		
Supports	1 →	← 2
Carry-Over Factors	- .3	- .3
Starting Moments	- 79.50	- 78.75
1.C.O.M.	+ 23.63	+ 23.85
2.C.O.M.	- 7.16	- 7.09
3.C.O.M.	+ 2.13	+ 2.15
4.C.O.M.	- 0.65	- 0.64
5.C.O.M.	+ 0.19	+ 0.20
6.C.O.M.	- 0.06	- 0.06
Final Moments	- 61.42	- 60.34

1) Fictitious hinges are placed at 1 and 2. Thus the continuous beam is transformed into a series of simple beams ($\overline{01}$, $\overline{12}$, $\overline{23}$).

2) The end slopes of these beams at 1 and 2 are τ_{10}, τ_{12} and τ_{21}, τ_{23}, respectively.

3) The hinge at 1 is removed and the bending moment required to produce the continuity at that point is the starting moment m_1. Independently, the hinge at 2 is removed, but the hinge at 1 is assumed to be preserved. Then the bending moment required to produce the continuity at 2 is the starting moment m_2.

4) Simultaneously, the starting moment m_1, now acting at the hinge 1, carries-over to 2 a carry-over moment $r_{12}m_1$; and the starting moment m_2, acting at the hinge 2, develops a carry-over moment $r_{21}m_2$ at 1. Because of the nature of the carry-over factors, the carry-over moment becomes at the same time a new starting moment.

5) The step (4) is repeated in a number of cycles till the continuity of the elastic curve is established.

The physical interpretation leads to an alternate procedure. After the starting moments have been determined, the larger m_1 is carried-over to 2 and added algebraically to m_2.

$$m_2^* = - 78.75 + 23.85 = - 54.90.$$

When the carry-over procedure is started with this modified moment, the convergency improves considerably.

7. Alternate Numerical Procedure

The application of the alternate numerical procedure and the influence of special end conditions is presented in the following example.

Example 2. A five span beam loaded as shown (Fig. 10) is analyzed. The intensity of the uniformly distributed load is $1^k/ft$.

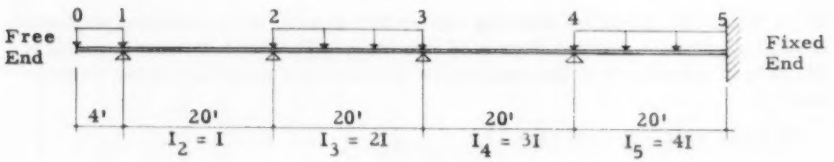

Five Span Beam
Fig. 10

a) Angular Flexibilities (Eqs. 3, 8):

$$F_{12} = F_{21} = \frac{20}{1} = 20 \qquad \Sigma F_2 = 30$$

$$F_{23} = F_{32} = \frac{20}{2} = 10 \qquad \Sigma F_3 = 16.67$$

$$F_{34} = F_{43} = \frac{20}{3} = 6.67 \qquad \Sigma F_4 = 11.67$$

$$F_{45} = F_{54} = \frac{20}{4} = 5 \qquad \Sigma F_5 = 5$$

b) Carry-Over Factors (Eqs. 9, 14, 15):

$$r_{12} = -\frac{1}{2}\frac{20}{30} = -.33 \qquad r_{21} = 0$$

$$r_{23} = -\frac{1}{2}\frac{10}{16.67} = -.30 \qquad r_{32} = -\frac{1}{2}\frac{10}{30} = -.17$$

$$r_{34} = -\frac{1}{2}\frac{6.67}{11.67} = -.29 \qquad r_{43} = -\frac{1}{2}\frac{6.67}{16.67} = -.20$$

$$r_{45} = -\frac{1}{2}\frac{5}{5} = -.50 \qquad r_{54} = -\frac{1}{2}\frac{5}{11.67} = -.21$$

c) Starting Moments (Eq. 10, 13):

$$m_1 = -(1)(4)(2) = -8.0 \qquad m_2 = -3\frac{\frac{(1)(20)^3}{(24)(2)}}{30} = -16.67$$

$$m_3 = -3\frac{\frac{(1)(20)^3}{(24)(2)}}{16.7} = -30.0 \qquad m_4 = -3\frac{\frac{(1)(20)^3}{(24)(4)}}{11.7} = -21.43$$

$$m_5 = -3\frac{\frac{(1)(20)^3}{(24)(4)}}{5} = -50.0$$

d) Carry-Over Procedure in Modified Form (Table 2): The starting moment at 1 and at 3 is carried-over to 2 and added algebraically to m_2. Thus the modified starting moment at 2,

$$m_4^* = -21.40 + 8.70 + 10.50 = -2.20 .$$

Similarly,

$$m_2^* = -16.70 + 2.64 + 5.10 = -8.96 .$$

When these two modified starting values are known, the relaxation procedure is carried on to a desired degree of accuracy. The final moments, equal to the sum of all values in the respective column, are recorded in the same table.

e) Numerical Control (Eq. 11):

$$M_2 = m_2 + r_{12}M_1 + r_{32}M_3 = -9.57$$

$$M_3 = m_3 + r_{23}M_2 + r_{43}M_4 = -26.42$$

$$M_4 = m_4 + r_{34}M_3 + r_{54}M_5 = -3.63$$

$$M_5 = m_5 + r_{45}M_4 = -48.22$$

8. Moment Coefficients

It is quite easy to determine the bending moments over each support in a continuous beam by the numerical carry-over moment procedure when only one system of stationary loads is involved. If various load conditions or moving loads must be considered, the numerical labor can be reduced by using the method of moment coefficients in numerical or algebraic form. The derivation of the algebraic coefficients follows.

a) Basic Series. If the carry-over moment procedure is used to compute the moments in three and four span beams and the relaxation is expanded algebraically, each moment consists of a series that is infinite, convergent, and geometric (hereafter denoted as a basic series).

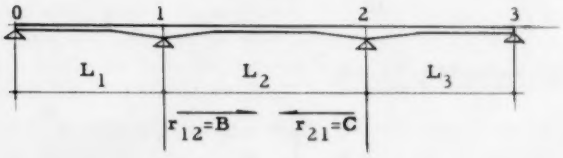

Three Span Beam
Fig. 11

To illustrate the computation of final moments by means of basic series, a three span bridge girder (Fig. 11) of variable cross-section is considered. The carry-over factors are denoted by B and C and the starting moment by $m_1 = 1$. The algebraic carry-over procedure follows in Table 3. The series

Carry-Over Table - Example 2 - Table 2

Supports	1	2	3	4	5
Carry-Over Factors	- .33	.0 - .30	- .17 .29	- .20 - .50	- .21
Starting Moments	- 8.00	- 16.70	- 30.00	- 21.40	- 50.00
Modified		+ 2.64		+ 8.70	
Starting Moments		+ 5.10		+ 10.50	
1. C.O.M.			+ 2.69		+ 1.10
			+ 0.44		
2. C.O.M.				- 0.91	
		- 0.53		- 0.23	
3. C.O.M.			+ 0.16		+ 0.58
			+ 0.23		
4. C.O.M.				- 0.11	
		- .08		- 0.12	
5. C.O.M.			+ .02		+ 0.12
			+ .05		
Final Moments	- 8.00	- 9.57	- 26.41	- 3.57	- 48.20

formed by carry-over moments in each column is a basic series. When all terms in the first column of Table 3 are summed, the final moment due to m_1 becomes:

$$M_1 = 1 + (BC)^1 + (BC)^2 + (BC)^3 \ldots = \frac{1}{X_{12}}$$

where

$$X_{12} = 1 - BC .$$

Similarly $$M_2 = \frac{B}{X_{12}} .$$

Final moments due to m_1 and m_2 are tabulated in the Appendix, Table C.

Algebraic Carry-Over Table - Table 3

Supports	1	2
Carry-Over Factors	B →	← C
Starting Moment	1	0
1. C.O.M.		B
2. C.O.M.	B C	
3. C.O.M.		B^2C
4. C.O.M.	B^2C^2	
5. C.O.M.		B^3C^2
⋮	⋮	⋮
Final Moments	Σ	Σ

In the case of a four span beam (Fig. 12), the final moments are formed by basic series of which denominator

$$Y_{13} = 1 - BC - DE .$$

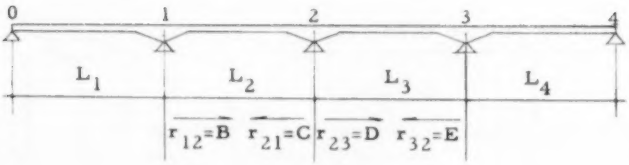

Four Span Beam
Fig. 12

All final moments are recorded in the Appendix, Table D.

b) Series of Series. The basic series has proved itself to be a useful tool in the two preceding cases. If beams have more than four spans, it would be difficult to derive the moment coefficients by the previous procedure.

The series forming these coefficients are geometric and convergent, but not simple geometric ones. The final moment is a combination of an infinite number of infinite series. In order to be able to separate the particular series and to find the sum as well as the sum of the sums, new tools have to be developed. They are denoted as the carry-over series α and β, and their usefulness is now demonstrated.

A five span beam (Fig. 13) of variable cross-section is considered. The carry-over factors are denoted by B, C, D, E, F, G and the starting moment $m_1 = 1$ is assumed.

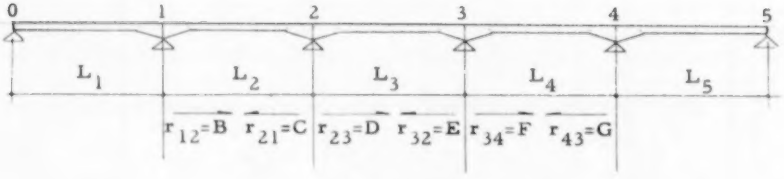

Five Span Beam
Fig. 13

A permanent, fictitious hinge is placed at 3 and a three span beam $\overline{03}$ (Beam I) is isolated. The algebraic relaxation follows in Table 3 and gives:

$$M_1^{(0)} = \frac{1}{X_{12}} \qquad M_2^{(0)} = \frac{B}{X_{12}} .$$

Then the hinge at 3 is removed and a new, permanent hinge is placed at 2. Thus a new three span beam $\overline{25}$ (Beam II) is obtained. The algebraic relaxation of the carried-over value, from Beam I to Beam II,

$$\frac{BD}{X_{12}} = \alpha_0$$

follows in Table 5 and gives:

Beam $\overline{03}$ Table 4

Algebraic Carry-Over Procedure

Supports	1	2
Carry-Over Factors	B	C
Starting Moment		β_0
1. C.O.M.	β_0 C	
2. C.O.M.		β_0 CB
3. C.O.M.	β_0 C^2B	
4. C.O.M.		β_0 C^2B^2
5. C.O.M.	β_0 C^3B^2	
6. C.O.M.		β_0 C^3B^3
7. C.O.M.	β_0 C^4B^3	
⋮	⋮	⋮
⋮	⋮	⋮
Final Moments	$\sum$	$\sum$

Beam $\overline{25}$ Table 5

Algebraic Carry-Over Procedure

Supports	3	4
Carry-Over Factors	F	G
Starting Moment	α_0	
1. C.O.M.		α_0 F
2. C.O.M.	α_0 FG	
3. C.O.M.		α_0 F^2G
4. C.O.M.	α_0 F^2G^2	
5. C.O.M.		α_0 F^3G^2
6. C.O.M.	α_0 F^3G^3	
7. C.O.M.		α_0 F^4G^3
⋮	⋮	⋮
⋮	⋮	⋮
Final Moments	$\sum$	$\sum$

$$M_3^{(1)} = \frac{1}{X_{34}}\,\alpha_0 \qquad M_4^{(1)} = \frac{F}{X_{34}}\,\alpha_0 .$$

Now the hinge at 2 is removed and the permanent hinge at 3 is restored again. The algebraic relaxation of the returned moment

$$\frac{E}{X_{34}}\,\alpha_0 = \beta_0$$

shown in Table 4 gives:

$$M_1^{(2)} = \frac{C}{X_{12}}\,\beta_0 \qquad M_2^{(2)} = \frac{1}{X_{12}}\,\beta_0 .$$

The functions

$$X_{12} = 1 - BC \qquad X_{34} = 1 - FG$$

are denominators of the respective basic series, and they are specific parameters of the isolated beams.

This procedure of placing hinges at 2 and 3, alternately, is repeated infinite times. Thus the continuity between the isolated beams is gradually established. The carry-over moments from Beam I to Beam II and from Beam II to Beam I are denoted as functions α and β, respectively. Tables 6 and 7 demonstrate that these moments form an infinite, convergent geometric series. When the basic series and the carry-over series recently derived are superimposed, the final moment at 1 due to $m_1 = 1$, becomes:

$$M_1 = M_1^{(0)} + M_1^{(2)} + M_1^{(4)} + M_1^{(6)} + \cdots$$

$$= \frac{1}{X_{12}} + \frac{C}{X_{12}}\,(\beta_0 + \beta_1 + \beta_2 + \cdots) .$$

From Table 6 (series β in terms of α)

$$\sum_0^\infty \beta_n = \frac{E\alpha}{X_{34}Z_{14}}$$

where $\alpha = \dfrac{BD}{X_{12}}$. With this substitution, the final moment simplifies to:

$$M_1 = \frac{1}{X_{12}} + \frac{BCDE}{X_{12}^2 X_{34} Z_{14}} = 1 + \frac{BC}{X_{12}Z_{14}} .$$

Table 6
Series α and β in Terms of Function α

Series α	Series β
$a_0 = \left[\frac{DE}{X_{12}X_{34}}\right]^0 \alpha$	$\beta_0 = \left[\frac{DE}{X_{12}X_{34}}\right]^0 \frac{E\alpha}{X_{34}}$
$a_1 = \left[\frac{DE}{X_{12}X_{34}}\right]^1 \alpha$	$\beta_1 = \left[\frac{DE}{X_{12}X_{34}}\right]^1 \frac{E\alpha}{X_{34}}$
$a_2 = \left[\frac{DE}{X_{12}X_{34}}\right]^2 \alpha$	$\beta_2 = \left[\frac{DE}{X_{12}X_{34}}\right]^2 \frac{E\alpha}{X_{34}}$
$a_n = \left[\frac{DE}{X_{12}X_{34}}\right]^n \alpha$	$\beta_n = \left[\frac{DE}{X_{12}X_{34}}\right]^n \frac{E\alpha}{X_{34}}$
$\sum_0^\infty a_n = \frac{\alpha}{1 - \frac{DE}{X_{12}X_{34}}} = \frac{\alpha}{Z_{14}}$	$\sum_0^\infty \beta_n = \frac{\frac{E\alpha}{X_{34}}}{1 - \frac{DE}{X_{12}X_{34}}} = \frac{E\alpha}{X_{34}Z_{14}}$

Table 7
Series α and β in Terms of Function β

Series α	Series β
$a_0 = \left[\frac{DE}{X_{12}X_{34}}\right]^0 \frac{D\beta}{X_{12}}$	$\beta_0 = \left[\frac{DE}{X_{12}X_{34}}\right]^0 \beta$
$a_1 = \left[\frac{DE}{X_{12}X_{34}}\right]^1 \frac{D\beta}{X_{12}}$	$\beta_1 = \left[\frac{DE}{X_{12}X_{34}}\right]^1 \beta$
$a_2 = \left[\frac{DE}{X_{12}X_{34}}\right]^2 \frac{D\beta}{X_{12}}$	$\beta_2 = \left[\frac{DE}{X_{12}X_{34}}\right]^2 \beta$
$a_n = \left[\frac{DE}{X_{12}X_{34}}\right]^n \frac{D\beta}{X_{12}}$	$\beta_n = \left[\frac{DE}{X_{12}X_{34}}\right]^n \beta$
$\sum_0^\infty a_n = \frac{\frac{D\beta}{X_{12}}}{1 - \frac{DE}{X_{12}X_{34}}} = \frac{D\beta}{X_{12}Z_{14}}$	$\sum_0^\infty \beta_n = \frac{\beta}{1 - \frac{DE}{X_{12}X_{34}}} = \frac{\beta}{Z_{14}}$

Similarly

$$M_2 = \frac{B}{X_{12}} + \frac{1}{X_{12}} \sum_0^\infty \beta_n = \frac{B}{X_{12} Z_{14}}$$

$$M_3 = \frac{1}{X_{34}} \sum_0^\infty a_n = \frac{B}{E}\left(\frac{1}{Z_{14}} - 1\right)$$

$$M_4 = \frac{F}{X_{34}} \sum_0^\infty a_n = \frac{BF}{E}\left(\frac{1}{Z_{14}} - 1\right).$$

Final moments due to m_1, m_2, m_3, m_4 are recorded in the Appendix, Table E.

In the case of a six span beam, three isolated beams $\overline{03}$, $\overline{24}$, $\overline{36}$ may be used. In the analysis of a seven span beam, two isolated beams $\overline{04}$ and $\overline{37}$ are suggested. Finally in the case of an eight span beam, three isolated beams $\overline{04}$, $\overline{35}$, $\overline{48}$ may be selected. A detailed investigation of continuous beams by the algebraic moment distribution and the existence of basic series and carry-over series was reported in this writer's earlier works.(5,6) References to some other investigations of moment distribution by series may be found in his recent paper.(7)

The investigations in this paper are limited to three, four, and five span bridge girders. Beams with more spans are rather exceptions. The extension of the philosophy of algebraic carry-over procedure to a larger number of spans is, however, possible. In many cases it becomes necessary to decide which division is the most appropriate. The results will always be the same although the algebraic form may differ.

c) Algebraic Control. The results may be checked by means of Eq. (11), and in the case of the five span beam, (Fig. 13), the following conditions must be satisfied: ($m_1 = 1$, $m_2 = 0$, $m_3 = 0$, $m_4 = 0$)

$$M_1 = 1 + C(M_2)$$

$$M_2 = B(M_1) + E(M_3)$$

$$M_3 = D(M_2) + G(M_4)$$

$$M_4 = F(M_3) .$$

9. Influence Lines

The application of the numerical and algebraic carry-over moment coefficients to the computation of the bending moment influence values in continuous girders is presented as the last example.

Example 3. The influence lines for the bending moments M_1, M_2, M_3 in a symmetrical four span beam (Fig. 14) are required. The real structure $\overline{04}$ is resolved into four basic structures ($\overline{01}$, $\overline{12}$, $\overline{23}$, $\overline{34}$). Because of symmetry, only the elastic constants of two basic beams ($\overline{01}$, $\overline{12}$) are computed.

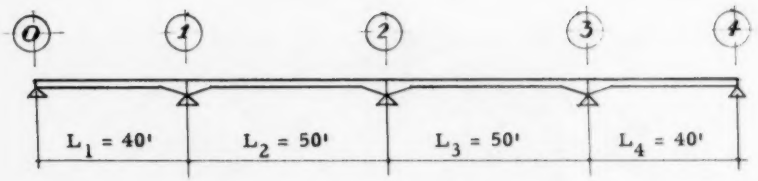

Four Span Beam
Fig. 14

The method of finite strips ($\Delta x = 5'$) is introduced as a fair approximation for the computation of F's, G's, and τ's, defined by Eqs. (2, 4, 6). The computation of these values is facilitated by means of the conjugated beam (Table 8, 9). Because the length of finite strips is the same in all spans, only relative values in terms of λ_x, $\frac{x}{L}$, and $\frac{x'}{L}$ are considered.

a) Relative Angular Flexibilities:

$$F_{10} = F_{34} = 1.435 \qquad \text{(Table 8)}$$

$$F_{12} = F_{21} = F_{23} = F_{32} = 2.007 \qquad \text{(Table 9)}$$

b) Carry-Over Factors: From symmetry of Member $\overline{12}$ and $\overline{23}$

$$G_{12} = G_{21} = G_{23} = G_{32} = 1.379 \qquad \text{(Table 9)}$$

$$r_{12} = r_{32} = -\frac{G_{12}}{\Sigma F_2} = -\frac{1.379}{4.014} = -.344$$

$$r_{21} = r_{23} = -\frac{G_{12}}{\Sigma F_1} = -\frac{1.379}{3.442} = -.400 \qquad \text{(Eq. 9)}$$

c) Numerical Coefficients: The moment coefficients due to $m_1 = 1$ and $m_2 = 1$ are computed by the numerical carry-over procedure in Tables 10 and 11. The moment coefficients due to $m_3 = 1$ are obtained from symmetry.

d) Algebraic Coefficients: The same but somewhat more precise results are obtained by means of algebraic coefficients (Appendix, Table D).

The denominator of the basic series is:

$$Y_{13} = 1 - r_{12}r_{21} - r_{23}r_{32} = .725$$

Example 3 First Span Table 8

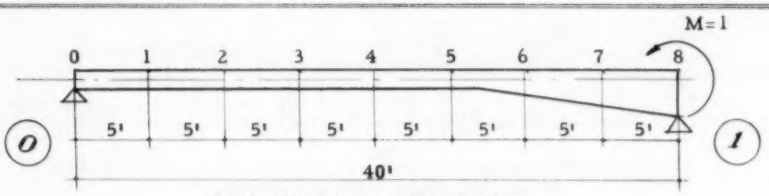

Basic Structure - Simple Beam

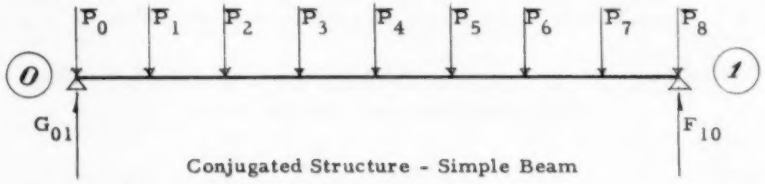

Conjugated Structure - Simple Beam

$$\lambda_x = \frac{I_0}{I_x} \qquad \overline{P}_x = \frac{x}{L}\lambda_x$$

$$G_{01} = \sum_0^L \overline{P}_x \frac{x'}{L} = \underline{1.151} \qquad F_{10} = \sum_0^L \overline{P}_x \frac{x}{L} = \underline{1.435}$$

$$\overline{V}_x = G_{01} - \sum_0^x \overline{P}_x \qquad \overline{M}_x = \overline{M}_{(x-\Delta x)} + \overline{V}_x \Delta_x$$

Relative Functions of Conjugated Structure

m	λ_x	$\frac{x}{L}$	$\overline{P}_x$	$\overline{V}_x$	$\overline{M}_x/\Delta x$	$\overline{M}_x = \tau_{10}$
0	1.000	.000	.000	1.151	.000	.000
1	1.000	.125	.125	1.026	1.151	5.755
2	1.000	.250	.250	.776	2.177	10.885
3	1.000	.375	.375	.401	2.953	14.765
4	1.000	.500	.500	- .099	3.354	16.770
5	1.000	.625	.625	- .724	3.256	16.275
6	.579	.750	.434	- 1.158	2.531	12.655
7	.244	.875	.214	- 1.372	1.373	6.865
8	.125	1.000	.063		.000	.000
$\sum$			2.586	.000	16.794	83.970

Example 3 — Second Span — Table 9

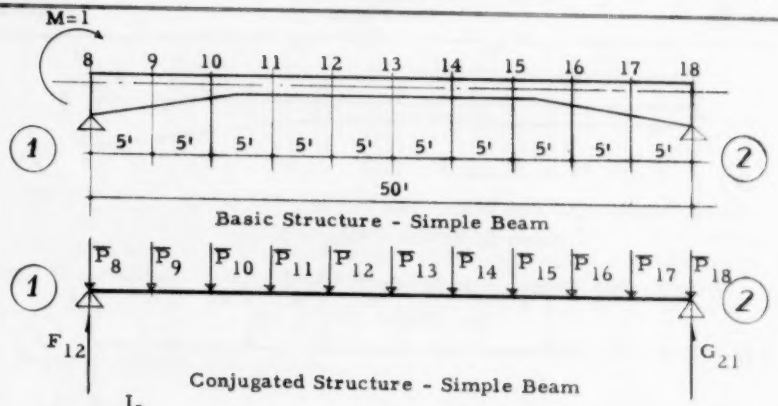

Basic Structure - Simple Beam

Conjugated Structure - Simple Beam

$$\lambda_x = \frac{I_0}{I_x} \qquad \overline{P}_x = \frac{x'}{L}\lambda_x$$

$$F_{12} = \sum_0^L \overline{P}_x \frac{x'}{L} = \underline{2.007} \qquad G_{21} = \sum_0^L \overline{P}_x \frac{x}{L} = \underline{1.379}$$

$$\overline{V}_x = F_{12} - \sum_0^x \overline{P}_x \qquad \overline{M}_x = \overline{M}_{(x-\Delta x)} + \overline{V}_x \Delta x$$

Relative Functions of Conjugated Structure

m	λ_x	$\frac{x'}{L}$	$\overline{P}_x$	$\overline{V}_x$	$\overline{M}_x/\Delta x$	$\overline{M}_x = \tau_{12}$
8	.125	1.000	.063	1.944	.000	.000
9	.244	.900	.220	1.724	1.944	9.720
10	.579	.800	.463	1.261	3.668	18.340
11	1.000	.700	.700	.561	4.929	24.645
12	1.000	.600	.600	- .039	5.490	27.450
13	1.000	.500	.500	- .539	5.451	27.255
14	1.000	.400	.400	- .939	4.912	24.560
15	1.000	.300	.300	- 1.239	3.973	19.865
16	.579	.200	.116	- 1.355	2.734	13.670
17	.244	.100	.024	- 1.379	1.379	6.895
18	.125	.000	.000		.000	.000
$\sum$			3.386	.000	34.480	172.400

Example 3 — Moments Due to $m_1 = +1$ — Table 10

Supports	1	2	3
Carry-Over Factors	→ - .344	← - .400 → - .400	← - .344
Starting Moment	+ 1.000		
1. C.O.M.		- .344	
2. C.O.M.	+ .138		+ .138
3. C.O.M.		- .047 - .047	
4. C.O.M.	+ .038		+ .038
5. C.O.M.		- .013 - .013	
6. C.O.M.	+ .010		+ .010
7. C.O.M.		- .003 - .003	
Final Moments	+ 1.186	- .470	+ .186

Example 3 — Moments Due to $m_2 = +1$ — Table 11

Supports	1	2	3
Carry-Over Factors	→ - .344	← - .400 → - .400	← - .344
Starting Moment		+ 1.000	
1. C.O.M.	- .400		- .400
2. C.O.M.		+ .138 + .138	
3. C.O.M.	- .110		- .110
4. C.O.M.		+ .038 + .038	
5. C.O.M.	- .030		- .030
6. C.O.M.		+ .010 + .010	
7. C.O.M.	- .008		- .008
Final Moments	- .548	+ 1.372	- .548

The influence value equations (Table D) are:

$$M_1 = + 1.190m_1 - .552m_2 + .190m_3$$

$$M_2 = - .475m_1 + 1.380m_2 - .475m_3$$

$$M_3 = + .190m_1 - .552m_2 + 1.190m_3$$

The final and more suitable of the influence value equations in terms of

$$m_j = - \frac{\Sigma \tau_j}{\Sigma F_j}$$

is:

$$M_1 = - .346\ \Sigma\tau_1 + .138\ \Sigma\tau_2 - .055\ \Sigma\tau_3$$

$$M_2 = + .138\ \Sigma\tau_1 - .344\ \Sigma\tau_2 + .138\ \Sigma\tau_3$$

$$M_3 = - .055\ \Sigma\tau_1 + .138\ \Sigma\tau_2 - .346\ \Sigma\tau_3 .$$

e) End Slope Influence Values: The end slope influence line of a simple beam is represented by the elastic curve of that beam, due to a unit moment applied at the respective end (Maxwell's Theorem) or the bending moment curve of the simple beam, conjugated to the first one (Mohr's Theorem). Thus $\bar{M}_x$'s in Tables 8 and 9 are the relative influence values of the respective slopes.

f) Moment Influence Values: The influence values for M_1, M_2, and M_3 may now be easily obtained by substituting the values of τ's from Tables 8 and 9 into the final form of moment equations (Step d), as shown in Tables 12 and 13.

ACKNOWLEDGMENT

In checking the numerical examples and proofreading the typed manuscript, the writer was assisted by Mr. Therman Lassley, Graduate Assistant in the School of Civil Engineering, and by Mr. Sien Y. Li, Graduate Student in Civil Engineering. He expresses sincere thanks to both of them.

APPENDIX

The derivation of the general three moment equation (Eq. 1) is not shown in this paper, but references are given to works of Nishkian and Steinman,(8) Bažant,(10,11,12) Biezeno and Grammel.(13)

Example 3 — Load in First and Fourth Span - Influence Values M_1, M_2, M_3 — Table 12

m	τ_{10}	M_1 $-.346\tau_{10}$	M_2 $+.138\tau_{10}$	M_3 $-.055\tau_{10}$	
0	.000	.000	.000	.000	36
1	+ 5.755	- 1.991	+ .794	- .316	35
2	+ 10.885	- 3.766	+ 1.502	- .599	34
3	+ 14.765	- 5.109	+ 2.038	- .812	33
4	+ 16.770	- 5.803	+ 2.314	- .922	32
5	+ 16.275	- 5.631	+ 2.246	- .895	31
6	+ 12.655	- 4.377	+ 1.746	- .696	30
7	+ 6.865	- 2.375	+ .946	- .378	29
8	.000	.000	+ .000	.000	28
		M_3	M_2	M_1	m

Example 3 — Load in Second and Third Span - Influence Values M_1, M_2, M_3 — Table 13

m	τ_{12}	τ_{21}	M_1 $-.346\tau_{12}$	$+.138\tau_{21}$	Σ	M_2 $+.138\tau_{12}$	$-.344\tau_{21}$	Σ	M_3 $-.055\tau_{12}$	$+.138\tau_{21}$	Σ	
8	.000	.000	.000	.000	.000	.000	.000	.000	.000	.000	.000	28
9	+ 9.720	+ 6.895	- 3.363	+ .952	- 2.411	+ 1.341	- 2.372	- 1.031	- .535	+ .952	+ .417	27
10	+ 18.340	+ 13.670	- 6.346	+ 1.886	- 4.460	+ 2.531	- 4.702	- 2.171	- 1.009	+ 1.886	+ .877	26
11	+ 24.645	+ 19.865	- 8.527	+ 2.741	- 5.786	+ 3.401	- 6.833	- 3.432	- 1.355	+ 2.741	+ 1.386	25
12	+ 27.450	+ 24.560	- 9.498	+ 3.389	- 6.109	+ 3.788	- 8.449	- 4.661	- 1.510	+ 3.389	+ 1.879	24
13	+ 27.255	+ 27.255	- 9.430	+ 3.761	- 5.669	+ 3.761	- 9.376	- 5.615	- 1.499	+ 3.761	+ 2.262	23
14	+ 24.560	+ 27.450	- 8.498	+ 3.788	- 4.710	+ 3.389	- 9.443	- 6.054	- 1.351	+ 3.788	+ 2.437	22
15	+ 19.865	+ 24.645	- 6.873	+ 3.401	- 3.472	+ 2.741	- 8.478	- 5.737	- 1.093	+ 3.401	+ 2.308	21
16	+ 13.670	+ 18.340	- 4.730	+ 2.531	- 2.199	+ 1.886	- 6.309	- 4.423	- .752	+ 2.531	+ 1.779	20
17	+ 6.895	+ 9.720	- 2.386	+ 1.341	- 1.045	+ .952	- 3.344	- 2.392	- .379	+ 1.343	+ .962	19
18	.000	.000	.000	.000	.000	.000	.000	.000	.000	.000	.000	18
			M_3			M_2			M_1			m

The constants F's, G's, and τ's in the case of constant moment of inertia may be easily computed by means of Eq's. (3, 5, 7). The amplification of Eq's. (7) for particular load conditions may be found in various books on strength of materials. For the convenience of the reader, a table of end slope formulas (Table A) and a 100 point influence value table (Table B) are included in this part of the paper.

Tables and charts of F's, G's, and τ's for members of variable moment of inertia were prepared by Strassner,(14) Guldan,(15,16) Ruppel,(19) and Timoshenko.(17) The modification of the moment distribution constants(18) was discussed by Michalos and Wilson.(4) A new book of constants and influence values is being prepared by Lassley and the writer.(19) Moment tables for three, four, and five span continuous girders of constant or variable cross-section computed by means of infinite, geometric series are included in this part of the paper (Tables C, D, E). All expressions in these tables are algebraic and their numerical equivalents must be substituted with their proper signs (carry-over factors and starting moments). A more elaborate set of moment tables is being prepared by Havner and the writer.(20) The application of the carry-over moment procedure to the analysis of continuous trusses and prestressed concrete beams was developed and is being prepared for publication in the near future.

REFERENCES

1. "Analysis of Continuous Frames by Distributing Fixed End Moments," by Hardy Cross, Transactions, A.S.C.E., Vol. 97, 1932, pp. 1-10.
2. "Analysis of Continuous Frames by Balancing Angle Changes," by L. E. Grinter, Transactions, A.S.C.E., Vol. 102, 1937, p. 1020.
3. "Determining Influence Lines by Balancing Angle Changes," by L. E. Grinter, Engineering News Record, Vol. 121, 1938, p. 443.
4. "Influence Lines by Corrections to an Assumed Shape," by J. P. Michalos and E. N. Wilson, Proceedings, A.S.C.E., Vol. 78, April, 1952, No. 124.
5. "Analysis of Continuous Beams by Infinite Series," by J. J. Tuma and M. T. Anderson, Oklahoma Engineering Experiment Station Publication, Oklahoma State University, Stillwater, No. 91, 1954.
6. "Analysis of Continuous Beams of Variable Section," by J. J. Tuma, Oklahoma Engineering Experiment Station Publication, Oklahoma State University, Stillwater, No. 96, 1956.
7. "Analysis of Frames with Curved and Bent Members," by J. J. Tuma, K. S. Havner, and F. Hedges, Proceedings, A.S.C.E., Vol. 82, 1958.
8. "Moments in Restrained and Continuous Beams by the Method of Conjugated Points," by L. H. Nishkian and D. B. Steinman, Transactions, A.S.C.E., Vol. 90, p. 1-206, 1927.
9. Ibid, Discussion, W. Ruppel, P. 152.
10. "Theorie Čar Příčinkových," by Z. Bažant, Vol. III, Praha, 1912, p. 124.
11. "Stavebná Mechanika," by Z. Bažant, Vol. IV, 2nd Ed., Praha, 1955, pp. 7-24.

End Slopes τ_{ij} and τ_{ji} - Table A

(1)

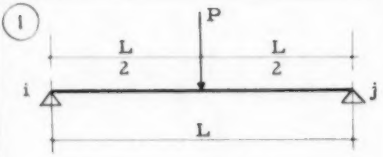

$$\tau_{ij} = \frac{PL^2}{16EI}$$

$$\tau_{ji} = \frac{PL^2}{16EI}$$

(2)

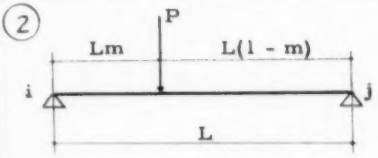

$$\tau_{ij} = \frac{PL^2m(1 - m)(2 - m)}{6EI}$$

$$\tau_{ji} = \frac{PL^2m(1 - m^2)}{6EI}$$

(3)

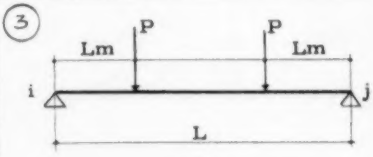

$$\tau_{ij} = \frac{PL^2m(1 - m)}{2EI}$$

$$\tau_{ji} = \frac{PL^2m(1 - m)}{2EI}$$

(4)

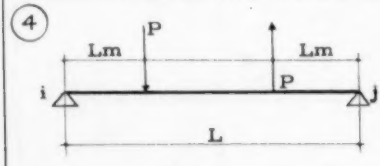

$$\tau_{ij} = \frac{PL^2m(1 - m)(1 - 2m)}{6EI}$$

$$\tau_{ji} = -\frac{PL^2m(1 - m)(1 - 2m)}{6EI}$$

(5)

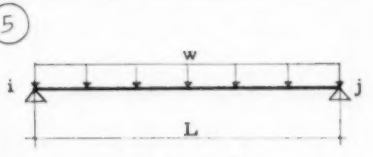

$$\tau_{ij} = \frac{wL^3}{24EI}$$

$$\tau_{ji} = \frac{wL^3}{24EI}$$

(6)

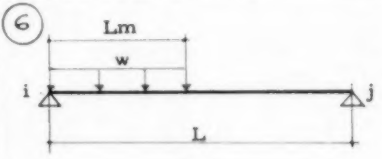

$$\tau_{ij} = \frac{wL^3m^2(2 - m)^2}{24EI}$$

$$\tau_{ji} = \frac{wL^3m^2(2 - m^2)}{24EI}$$

(7)

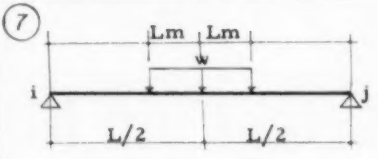

$$\tau_{ij} = \frac{wL^3m(3 - 4m^2)}{24EI}$$

$$\tau_{ji} = \frac{wL^3m(3 - 4m^2)}{24EI}$$

(8)

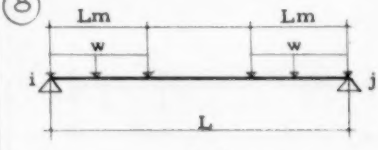

$$\tau_{ij} = \frac{wL^3m^2(3 - 2m)}{12EI}$$

$$\tau_{ji} = \frac{wL^3m^2(3 - 2m)}{12EI}$$

End Slopes τ_{ij} and τ_{ji} - Table A (Con't.)

9

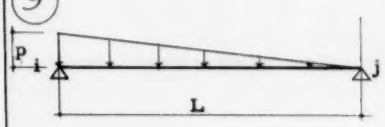

$$\tau_{ij} = \frac{pL^3}{45EI}$$

$$\tau_{ji} = \frac{7\ L^3}{360EI}$$

10

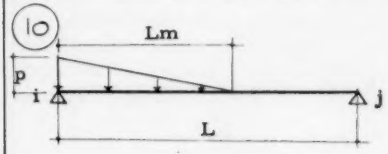

$$\tau_{ij} = \frac{pL^3m^2(20 - 15m + 3m^2)}{360EI}$$

$$\tau_{ji} = \frac{pL^3m^2(10 - 3m^2)}{360EI}$$

11

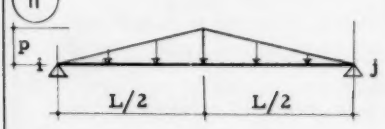

$$\tau_{ij} = \frac{5pL^3}{192EI}$$

$$\tau_{ji} = \frac{5pL^3}{192EI}$$

12

$$\tau_{ij} = \frac{pL^3}{64EI}$$

$$\tau_{ji} = \frac{pL^3}{64EI}$$

13

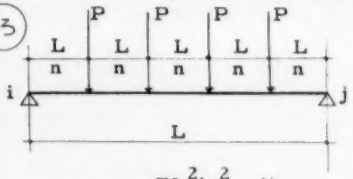

$$\tau_{ij} = \frac{PL^2(n^2 - 1)}{24\ n\ EI}$$

$$\tau_{ji} = \frac{PL^2(n^2 - 1)}{24\ n\ EI}$$

14

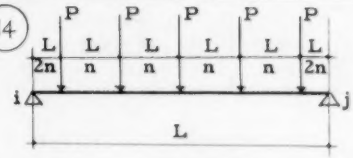

$$\tau_{ij} = \frac{PL^2(2n^2 + 1)}{48\ n\ EI}$$

$$\tau_{ji} = \frac{PL^2(2n^2 + 1)}{48\ n\ EI}$$

15

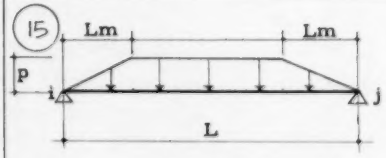

$$\tau_{ij} = \frac{pL^3(1 - 2m^2 + m^3)}{24EI}$$

$$\tau_{ji} = \frac{pL^3(1 - 2m^2 + m^3)}{24EI}$$

16

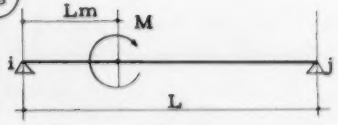

$$\tau_{ij} = \frac{ML(3m^2 - 6m + 2)}{6EI}$$

$$\tau_{ji} = \frac{ML(1 - 3m^2)}{6EI}$$

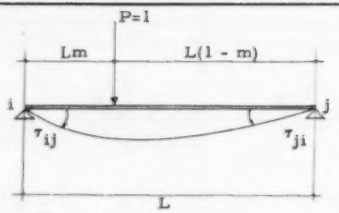

Influence Values τ_{ij} and τ_{ji} - Table B

$$\tau_{ij} = \frac{L^2\eta}{EI}$$

$$\tau_{ji} = \frac{L^2\eta'}{EI}$$

$\eta_{max} = \eta_{m=.4226} = .06415$

$\eta'_{max} = \eta'_{m=.5774} = .06415$

100 Point Table of Influence Values η and η'

m	0	1	2	3	4	5	6	7	8	9	m
0.0	.00000 .00000	.00328 .00166	.00647 .00333	.00955 .00499	.01254 .00666	.01544 .00831	.01824 .00996	.02094 .01161	.02355 .01325	.02607 .01488	0.0
0.1	.02850 .01650	.03084 .01811	.03309 .01971	.03525 .02130	.03732 .02288	.03931 .02444	.04122 .02598	.04304 .02751	.04477 .02903	.04643 .03052	0.1
0.2	.04800 .03200	.04949 .03346	.05091 .03489	.05224 .03631	.05350 .03770	.05469 .03906	.05580 .04040	.05683 .04172	.05779 .04301	.05868 .04427	0.2
0.3	.05950 .04550	.06025 .04670	.06093 .04787	.06154 .04901	.06208 .05012	.06256 .05119	.06298 .05222	.06333 .05322	.06361 .05419	.06384 .05511	0.3
0.4	.06400 .05600	.06410 .05685	.06415 .05765	.06413 .05842	.06406 .05914	.06394 .05981	.06376 .06044	.06352 .06103	.06232 .06157	.06289 .06206	0.4
0.5	.06250 .06250	.06206 .06289	.06157 .06232	.06103 .06352	.06044 .06376	.05981 .06394	.05914 .06406	.05842 .06413	.05765 .06415	.05685 .06410	0.5
0.6	.05600 .06400	.05511 .06384	.05419 .06361	.05322 .06333	.05222 .06298	.05119 .06256	.05012 .06208	.04901 .06154	.04787 .06093	.04670 .06025	0.6
0.7	.04550 .05950	.04427 .05868	.04301 .05779	.04172 .05683	.04040 .05580	.03906 .05469	.03770 .05350	.03631 .05224	.03489 .05091	.03346 .04949	0.7
0.8	.03200 .04800	.03052 .04643	.02903 .04477	.02751 .04304	.02598 .04122	.02444 .03931	.02288 .03732	.02130 .03525	.01971 .03309	.01811 .03084	0.8
0.9	.01650 .02850	.01488 .02607	.01325 .02355	.01161 .02094	.00996 .01824	.00831 .01544	.00666 .01254	.00499 .00955	.00333 .00647	.00166 .00328	0.9

Three Span Beam - Table C

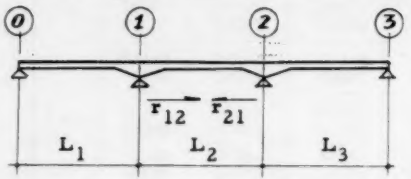

$$X_{12} = 1 - r_{12}r_{21}$$

Final Moments

Moment	m_1	m_2
M_1	$\frac{1}{X_{12}}$	$\frac{r_{21}}{X_{12}}$
M_2	$\frac{r_{12}}{X_{12}}$	$\frac{1}{X_{12}}$

Four Span Beam - Table D

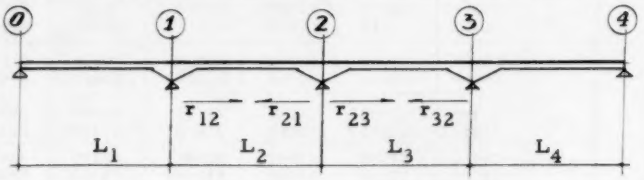

$$Y_{13} = 1 - r_{12}r_{23} - r_{23}r_{32}$$

Final Moments

Moment	m_1	m_2	m_3
M_1	$1 + \frac{r_{12}r_{21}}{Y_{13}}$	$\frac{r_{21}}{Y_{13}}$	$\frac{r_{21}r_{32}}{Y_{13}}$
M_2	$\frac{r_{12}}{Y_{13}}$	$\frac{1}{Y_{13}}$	$\frac{r_{32}}{Y_{13}}$
M_3	$\frac{r_{12}r_{23}}{Y_{13}}$	$\frac{r_{23}}{Y_{13}}$	$1 + \frac{r_{23}r_{32}}{Y_{13}}$

Five Span Beam - Table E

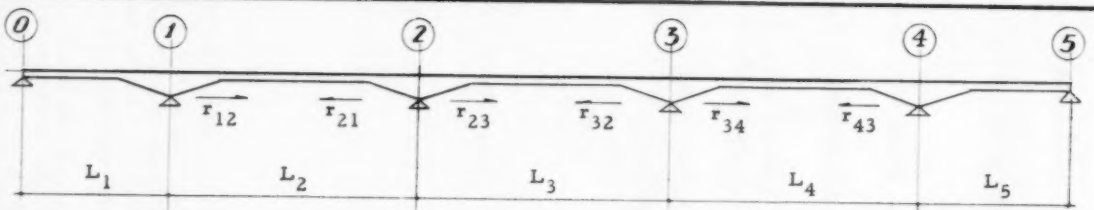

$$X_{12} = 1 - r_{12}r_{21} \qquad Z_{14} = 1 - \frac{r_{23}r_{32}}{X_{12}X_{34}} \qquad X_{34} = 1 - r_{34}r_{43}$$

Final Moments

Moment	m_1	m_2	m_3	m_4
M_1	$1 + \frac{r_{12}r_{21}}{X_{12}Z_{14}}$	$\frac{r_{21}}{X_{12}Z_{14}}$	$\frac{r_{21}}{r_{23}}\left(\frac{1}{Z_{14}} - 1\right)$	$\frac{r_{21}r_{43}}{r_{23}}\left(\frac{1}{Z_{14}} - 1\right)$
M_2	$\frac{r_{12}}{X_{12}Z_{14}}$	$\frac{1}{X_{12}Z_{14}}$	$\frac{1}{r_{23}}\left(\frac{1}{Z_{14}} - 1\right)$	$\frac{r_{43}}{r_{23}}\left(\frac{1}{Z_{14}} - 1\right)$
M_3	$\frac{r_{12}}{r_{32}}\left(\frac{1}{Z_{14}} - 1\right)$	$\frac{1}{r_{32}}\left(\frac{1}{Z_{14}} - 1\right)$	$\frac{1}{X_{34}Z_{14}}$	$\frac{r_{43}}{X_{34}Z_{14}}$
M_4	$\frac{r_{12}r_{34}}{r_{32}}\left(\frac{1}{Z_{14}} - 1\right)$	$\frac{r_{34}}{r_{32}}\left(\frac{1}{Z_{14}} - 1\right)$	$\frac{r_{34}}{X_{34}Z_{14}}$	$1 + \frac{r_{34}r_{43}}{X_{34}Z_{14}}$

12. "Nauka o Pružnosti a Pevnosti," by Z. Bažant, A. Nedoma, K. Spála, 5th Ed., Praha, 1955, pp. 100-105.

13. "Technische Dynamik," by C. B. Bienzeno and R. G. Grammel, Vol. 1, 2nd Ed., Berlin, 1953, pp. IV, 2-5.

14. "Neure Methoden zur Statik der Rahmentragwerke," by A. Strassner, 4th Ed., Vol. I, Berlin, 1937.

15. "Rahmentragwerke and Durchlaufträger," by R. Guldan, 5th Ed., Wien, 1952.

16. "Die Cross-Methode," by R. Guldan, Wien, 1955.

17. "Theory of Structures," by S. Timoshenko and D. H. Young, New York, 1945, pp. 406-411.

18. "Handbook of Frame Constants," Portland Cement Association, Chicago, Ill., 1947.

19. "Beam Constants by High Speed Computers," by T. Lassley and J. J. Tuma, Oklahoma Engineering Experiment Station Publication, Oklahoma State University, Stillwater, (in preparation).

20. "Influence Lines for Continuous Beams," by K. S. Havner and J. J. Tuma, Oklahoma Engineering Experiment Station Publication, Oklahoma State University, Stillwater, (in preparation).

Paper 1763 September, 1958 ST 5

Journal of the
STRUCTURAL DIVISION
Proceedings of the American Society of Civil Engineers

GENERAL CONSIDERATIONS FOR REACTORS AND RELATED PLANT TYPES[a]

John F. Stolz,[1] A.M. ASCE
(Proc. Paper 1763)

INTRODUCTION

In discussing the general subject of reactor plant considerations, it would seem appropriate to:

1. Examine the basic reasons we are interested in nuclear power at all;
2. Review the basic parts of a reactor system, outlining the functions of each part;
3. Describe the major factors involved in assembling a reactor plant;
4. Outline relative costs of nuclear power plants.

Reactors may be typed or classified according to their purpose — research and testing, production of fissionable material, power production, propulsion, industrial processing, and dual purpose type where both power and production of fissionable material is desired.

Most of our comments will be pointed to those reactor plants designed for power generation since that field holds somewhat more appeal for engineers than other reactor types.

Energy Sources

From a practical engineering standpoint, our interest in nuclear reactors lies chiefly in their ability to provide energy to supplement, and probably eventually, replace chemical energy sources for the earth's increasing electrical power demands. It has been estimated for example that our consumption of energy by the year 2000 will be from four to ten times as great as at

Note: Discussion open until February 1, 1959. To extend the closing date one month, a written request must be filed with the Executive Secretary, ASCE. Paper 1763 is part of the copyrighted Journal of the Structural Division, Proceedings of the American Society of Civil Engineers, Vol. 84, No. ST 5, September, 1958.

a. Presented at Convention Structural Div., Committee on Nuclear Structures and Materials, Chicago, Ill. February 25, 1958.

1. Project Engr., Design Eng. Group, Atomics International, North American Aviation, Inc., Canoga Park, Calif.

present.[1] Under these conditions, the world's economically useful reserves of fossil fuels could be exhausted within a 100 years.

An important, though not a complete answer to this dilemma is nuclear power. As we know it today, part of the economic success of nuclear power depends on the cost and availability of the two potential fuels uranium and thorium. Fig. 1 shows the relative availability of these fuels together with convention types.[2] Comparing energy contents and allowing for practical considerations of energy conversion of nuclear fuels, we see that our energy potential has been increased by at least a factor of fifteen.

Reactor Core

The reactor core assembly provides the plant energy source. It typically is made up of fuel, moderator, coolant, structural materials, reflector, and a means of control. (Fig. 2). It is the suitable combination of active core and reflector that maintains the fission chain reaction at the proper power level. A shield usually surrounds the core assembly to provide protection to equipment and personnel from radiation.

Fuel

The fuel contained in a nuclear reactor must be capable of capturing a neutron to cause a subsequent fission or splitting of its nucleus and release of energy. There are three practical fissionable species which can be considered as fuels — Uranium-235, Uranium-233, and Plutonium-239. Both Uranium-233 and Plutonium-239 are artificially produced in nuclear reactors by a "conversion" or "breeding" process. Here the natural fuels previously mentioned, Thorium and Uranium, serve as the fertile materials which absorb neutrons and convert respectively to Uranium-233 and Plutonium-239. Uranium-235 is found in nature as a small fraction of natural uranium.

Reactor fuels may be in liquid or solid form, although most power reactors use solid fuel elements. The solid element consist of fissionable material clad with a thin appropriate material, such as stainless steel, zirconium alloy, aluminum, or ceramics. The cladding prevents fission fragments from entering the coolant surrounding the element, and also protects the fuel from corrosion by the coolant.

Moderator

A moderator is used in the thermal reactors to slow down the fast fission neutrons to thermal energies where the probability of capture and subsequent fission by the reactor fuel is greatest. This material must be able to elastically scatter neutrons without tending to absorb them. Substances commonly used here are water, heavy water, and graphite. Note that these are among the lighter elements.

Coolant

If the power of a reactor is appreciable, some form of cooling must be provided. Actually, aside from structural limitations, there is no upper limit to power density (kw per kg of fuel) and, therefore, the power of a chain reaction at appreciable power levels is dependent on how rapidly heat is removed from the system. Coolants should primarily have good heat transfer characteristics

and must not absorb neutrons to any extent. They should also be non-corrosive to reactor materials and be stable to reactor radiations and temperatures.

These are rather rigid requirements. Examples of coolants considered for use include air, CO_2, helium, water, heavy water, organics (Biphenyl and terphenyl), and liquid metals (sodium, mercury, and sodium-potassium alloy).

Structural Materials

Structural materials appear in the reactor core as cladding around fuel elements, as structural supports for moderator and fuel, as a containment vessel, pipes and other applications. In addition to normal requirements known to structural engineers, structural core materials must have a low capture cross-section (probability for capture) for neutrons, must be able to resist radiation damage effects and must be corrosion-resistant at operating temperatures. Lead, bismuth, tin, beryllium, aluminum, magnesium, zinc and zirconium have sufficiently low cross-sections from a nuclear standpoint. Of these, aluminum and magnesium have been used where corrosion has not been severe. Zirconium is suitable for higher temperature operation and more severe corrosion conditions. The other elements have drawbacks from structural or a corrosion-resistant standpoint. Stainless steel has a higher absorption cross-section than the previous elements mentioned, but is, nevertheless, a common reactor core material because of its other excellent properties.

Reflector

A reflector is used to blanket the core and scatter neutrons back into the reactor. By reducing this neutron "leakage," the reflector can effectively reduce the size of the critical core over one that does not have a reflector. Thermal reactors, (i.e., those employing slow neutrons for fission) would use materials similar to the moderator such as heavy water, beryllium, and graphite. Again, these materials have good neutron-scattering characteristics with relatively low absorption. Fast reactors (using fast neutrons for fission) on the other hand would use heavier elements such as uranium, thorium, or bismuth to scatter neutrons back into the core without excessive loss of neutron energy.

Control

Control of the reactor may be achieved by regulating the neutron flux (intensity of neutron radiation). This, in turn, can be done with control rods containing a strong neutron absorber or by moving parts of the core reflector to regulate the escape of neutrons. Neutron absorbers in control rods may be boron, cadmium, or hafnium. Both boron and hafnium are capable of operating at higher temperatures normally found in power reactors. Cadmium, because of its low melting point, is restricted to reactors whose temperatures are relatively low.

Shielding

A "biological shield" placed around the core structure must reduce the leaking neutrons and gamma rays to a safe tolerance level outside this shield in operating areas.

FIG. 1 (1) ESTIMATED WORLD RESERVES OF FUEL

TYPE	WORLD RESERVES	ENERGY CONTENT (Btu)
COAL	3.5×10^{12} TONS	72.2×10^{18}
OIL	1.2×10^{12} BARRELS	7.6×10^{18}
GAS	5.6×10^{14} FEET^3	0.6×10^{18}
TOTAL CONVENTIONAL		$80. \times 10^{18}$
URANIUM	$25. \times 10^{6}$ TONS	$1700. \times 10^{18}$
THORIUM	$1. \times 10^{6}$ TONS	$71. \times 10^{18}$
		$1771. \times 10^{18}$

1763-4 ST 5 September, 1958

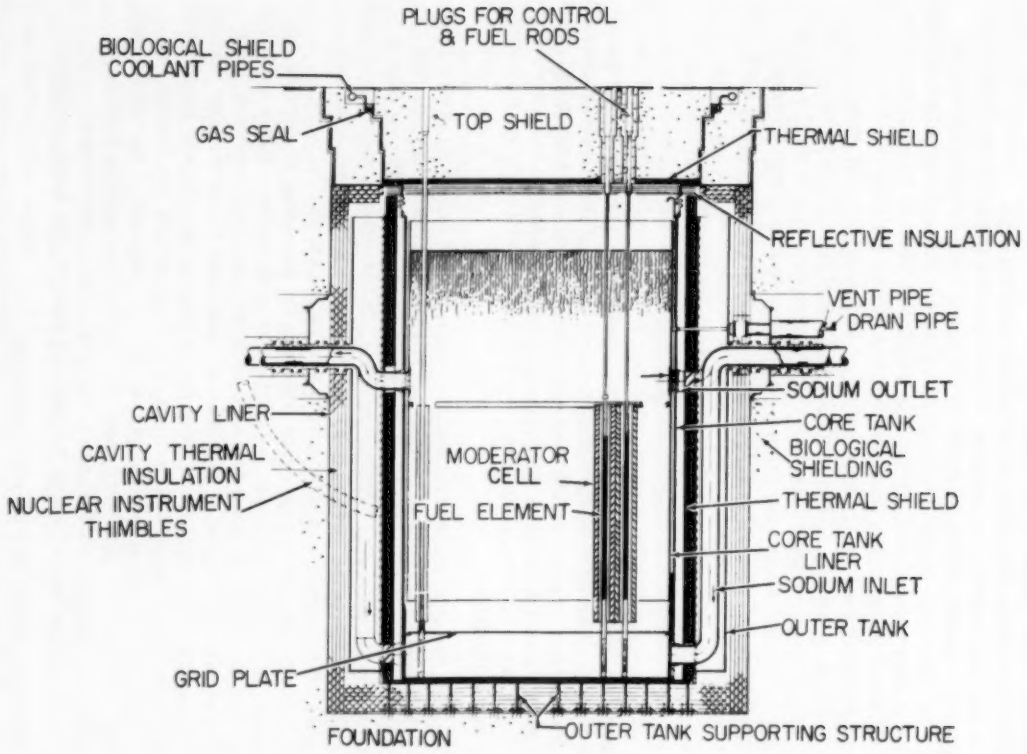

FIG. 2-REACTOR CORE

Concrete can be made to serve both as a gamma and neutron shield and thus has been a useful biological shield. It contains large amounts of hydrogen which can effectively slow down and absorb neutrons. Also, when we use iron-ore aggregates, barytes, or steel punches in the mix, these heavier elements can

(1) inelastically scatter fast neutrons to lower energies (<0.5 mev) where the hydrogen will be effective for further slowing to thermal energies and final absorption of the neutrons; and
(2) provide high density required to absorb gamma rays.

When a thermal neutron is captured in the shield, especially by iron, another energetic gamma ray is given off which itself may require additional shielding. An alternate solution to increasing shield thickness would be to add colemanite, a boron compound, to the mix which will absorb thermal neutrons and give off short range alpha particles instead of gamma rays.

The energy dissipated during attenuation of fast neutrons and gamma rays is converted to heat energy. This could be sufficient flux to cause excessive temperatures and temperature gradients in the concrete shield on the inside faces causing thermal stress cracking. For this reason a dense "thermal" shield, with a high melting point, such as iron, is placed between the core and the biological shield to remove a major portion of this energy.

Plant Arrangement

The major factors in setting plant configuration for a nuclear power reactor are: the reactor core installation; process cooling systems and power generation systems; reactor safety considerations; reactor fuel handling and storage system; reactor control, operation and maintenance.

Reactor Core Installation

Depending on the type of reactor decided upon, actual practical power reactor core sizes can vary approximately from cylinders less than two feet high x two feet diameter for a fast reactor up to greater than 25 feet high x 25 feet diameter for a natural uranium reactor. It has usually been found economical to place the reactor core underground to reduce concrete shielding requirements on the sides and bottom with equivalent earth.

The decision to use heavy aggregate concrete for shielding or regular concrete is based on the economics of the particular installation. While installed heavy concrete costs run at least twice those of conventional concrete, excavation, plant space and lengths of mechanical equipment to service the reactor can provide savings sufficient to warrant heavy aggregate. Access to the core for reactor control may be at the top face or bottom face of the reactor. A physical advantage of bottom control is that you can maintain a top shield face free of drive mechanism. However, bottom control does usually introduce mechanical seal problems with common types of control mechanisms used today and requires additional space beneath the reactor for drive equipment.

Process Cooling Systems and Power Generation

All reactor core coolants due to neutron bombardment become more or less radioactive. These so-called primary coolant systems must then also be shielded against the induced gamma activity.

The Sodium-Graphite Reactor Experiment, designed, built and operated for the AEC by Atomics International, (Fig. 3) typifies the layout points under consideration. Primary coolant piping was arranged in shielded, gas-tight

galleries to accomodate pumps, heat exchangers, valves, plus other equipment. The piping arrangement was also checked to maintain thermal stresses within safe limits under allowable design temperatures in this case of (1200° F).

The desirability of providing plant flexibility and continuous operation on a full scale power plant calls for multiple independent primary loops with a corresponding increase in numbers of pumps, heat exchangers, valves, and space. (Fig. 4).

A secondary coolant system transfers heat from the primary system to the steam generator. This secondary system is non-radioactive and, therefore, need not be shielded nor contained.

The provisions for the remainder of the power generation systems are similar to conventional plants.

Reactor Safety

Overall reactor safety is of prime concern since any conceivable accident that might release radioactive material could be a source of public hazard. It should first be emphasized that thermal power reactors are inherently safe and that many of the postulated hazards pessimistically assume simultaneous failure of several safety devices normally designed to cut back and/or shut down the reactor.

The problem then is to examine conceivable failures, or combinations of failures, involving mechanical equipment, electrical equipment, electrical power, instrumentation, loss of coolants, reactor systems materials, plant operators and acts of God. From these hypothetical conditions, the subsequent effects are analyzed for (1) nuclear excursions, (2) chemical reactions within the reactor system, (3) stored thermal energy releases and (4) damage by internal missiles and external forces. Containment required as a result of these unlikely conditions is for the sole purpose of confining radioactive material.

Nuclear incidents in power reactors are not in the same category damage-wise as the reaction from a nuclear weapon. Power reactors relatively speaking do not provide the fuel concentrations and the triggering mechanism that characterize the weapon counterpart. We have previously noted that structural limitations placed ceilings on reactor temperatures. If, therefore, it was somehow possible to make a reactor supercritical, the power increase might cause fuel elements and the structural materials to melt, which in the case of most reactors would result in a sub-critical configuration and subsequent shutdown. The nuclear energy release here is of a relative low order of magnitude, something like that released in buring several gallons of gasoline.(3,5)

An example of a chemical reaction within a reactor system would be a zirconium and water reaction or a molten fuel and water reaction. This might occur if the reactor core approached melting temperatures from other causes such as loss of coolant accidents etc. The energy releases here could be much higher than the nuclear release obtainable in a thermal reactor. Another example of a chemical reaction would be a sodium and water reaction. If the sodium that might react is radioactive, as it is in a primary coolant system, then it would constitute a hazard. The containment sphere for the SIR reactor built by General Electric at West Milton, New York was an example of a containment vessel built under the latter criteria.

FIG. 3 SRE GENERAL ARRANGEMENT

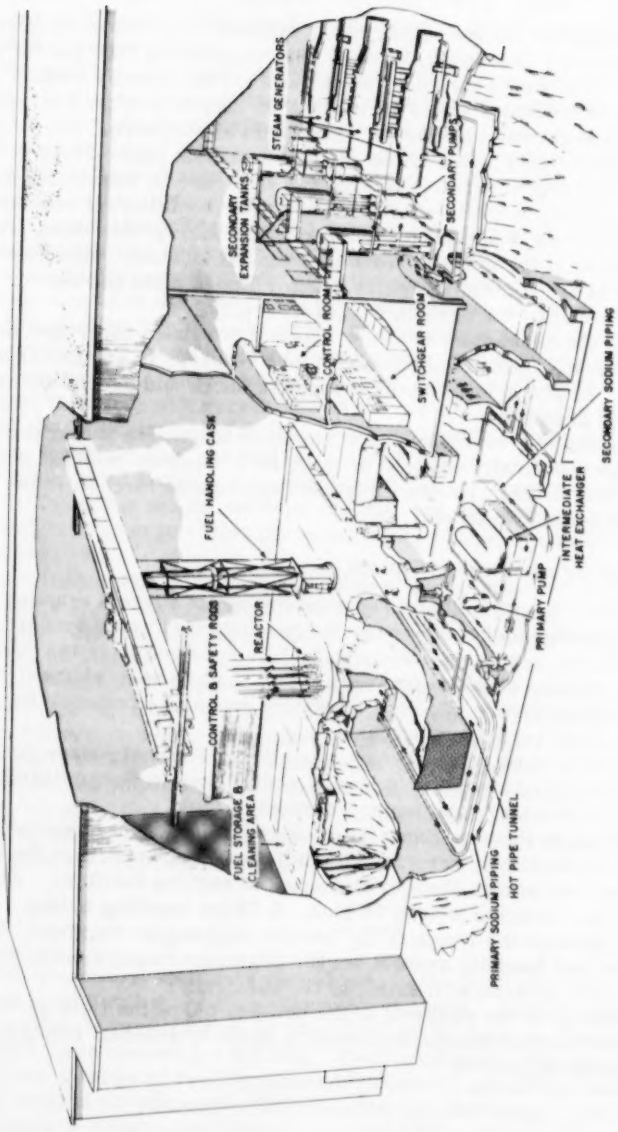

FIG. 4—SGR PERSPECTIVE

Stored thermal energy releases are important considerations in high pressure primary coolant systems. The assumption of a complete rupture here would result in a large release of the internal energy of the coolant, requiring secondary containment. The Pressurized Water Reactor at Shippingport, Pa., had its containment vessel designed for this condition. These energies can be in the same order of magnitude as the chemical releases previously described.

The problem of stored thermal energy is minimized in a sodium system because of low operating pressures, 25 to 50 psi compared to 2000 psi for a pressurized water reactor. Therefore, if the radioactive primary sodium systems cannot have a sodium-water accident, they may be enclosed in sealed concrete galleries containing nitrogen or other inert atmosphere. The inert atmosphere will not support a fire in the event of a sodium leak. The conventional reactor building superstructure may in this case be considered to act as a possible tertiary enclosure with no particular containment requirements save that all doors, ventilation openings, etc. would be shut down prior to building evacuation in the event of some unimagined incident. This system is essentially that of the Sodium-Graphite Reactor Experiment and its full scale power plant version, the Shelden Nuclear Facility.

The potential of the explosive reactions of radiolytic gases (hydrogen and oxygen) released during operation of homogeneous reactors is another chemical reaction type. Analysis here involves study of shock and detonation as well as equilibrium pressures.

Design of a containment vessel to resist assumed fragments and missiles can follow principles generally outlined in classified "weapons effects" publications used by our military people. Wind and earthquake forces can be handled in the conventional manner.

Reactor Fuel Handling and Storage System

Nuclear fuels must be periodically replaced for one of several reasons, such as radiation damage and build-up fission products that would tend to poison or shut down the reactor. The spent fuel is removed from the core and discharged by remote shielded means to a fuel storage area where it is allowed to decay radioactively. Cooling is usually provided to remove the heat generated by decaying fission products.

Some reactor plants such as the Pressurized Water Plant at Shippingport and the Argonne National Laboratory's Experimental Boiling Water Reactor have provided for underwater handling and storage of fuel.

The Sodium-Graphite Reactor Experiment uses a shielded fuel handling coffin (Fig. 3) which physically removes complete fuel elements from the top face of the reactor and carries them to cleaning and storage facilities. The coffin is about 35 feet long and weighs 50 tons. A 75 ton handling bridge carries the coffin through the length of the reactor building as required. In this plant then, the fuel handling system set the headroom requirements and the major criteria for structural framing of the building.

A hot cell is located in the west end of the building below the floor level to permit fuel examination and partial disassembly prior to eventual shipment to a chemical processing facility.

Control, Operation, and Maintenance

Control of the reactor and power plant is physically done in a control room where most of the instruments are located that tell the reactor operator essential information about the reactor at any time.

The operator, together with automatic controls, interprets this information and effects the desired control action either on the reactor control rods and/or process equipment. The layout of this area is similar to those employed for electrical power plants.

The reactor instrumentation and control engineer requires, among other things, that essential services, normally electrical, should be duplicated. To the structural engineer or architect concerned with plant layout, this means providing facilities for secondary or emergeny electrical power, such as batteries or battery-driven motor-alternators. Thus, essential equipment such as control room instruments and coolant pumps will still be able to perform after a normal power failure and subsequent reactor shutdown. Normally, from an economic and operational standpoint, electrical switchgear and emergency equipment are arranged near the control room (Fig. 5).

The content of the rest of the plant depends on the prime purpose of the facility, chiefly involving the extent of experimental and research facilities. Experience has shown need for maintenance space for electrical and mechanical components. Decontamination areas, provisional radioactive storage, and laundry facilities will greatly assist maintenance after the reactor starts up. Plant should be arranged so that areas that might accidentally become radioactive, (possible "hot" areas) be isolated from clean areas and administrative space (cold areas). Personnel traffic to and from possible "hot" areas and "cold" areas can be better controlled through change rooms, or their equivalent, where facilities for monitoring, changing clothes and showering are provided.

Ventilation systems are designed to achieve flows and air pressures so that air will not spread the effects of a radioactive spill. If necessary, discharge filters and dispersal stacks can be provided for ventilation exhaust that might possible become radioactively contaminated.

The problem of maintenance, including possible replacement of reactor and process components, requires detailed study. Things that are usually affected here, in addition to space requirements are (1) crane loadings, (2) removable shielding, (3) increased floor loads possibly up to 2000 psf in certain areas where shielding and/or heavy equipment may have to be laid down, (4) provision for large access doors or removable wall panels in the building proper, (5) special impervious finished to facilitate clean-up in cases of accidental radioactive spills.

Costs

Our discussion up to now should lead to the obvious conclusion that nuclear power plants cost more than conventional plants. This is illustrated on a curve (Fig. 6) presented in October 1957 by W. Kenneth Davis, Director of Reactor Development for the AEC, which plotted estimated and actual capital costs for a range of reactor plants.(6) Several qualifying notes on Fig. 6 have been omitted for purposes of simplifying our discussion. Nuclear power capital costs in dollars per kilowatt averaged from several thousand dollars for small pilot plants to several hundred dollars for full-scale power plants.

FIG. 6 (6)

NUCLEAR POWER CAPITAL COSTS SEPTEMBER 1957

NO.	GOVERNMENT	MWE	MILLIONS OF $ CONSTRUCTION	NUCLEAR $/Kw
1	NRE-2	(5) MWT	3.3	3400
2	APPR	1.8	4.3	2400
3	LMPR	(20) MWT	17.5	3020
4	EBWR	5	4.9	900
5	SRE	6	9.3	1550
6	EBR-2	15	29.1	1940
7	PWR 1st CORE	60	77.5	1290
8	PWR-2nd CORE	100		

NO.	PDRP & PRIVATE	MWE	MILLIONS OF $ CONSTRUCTION	NUCLEAR $/Kw
9	WOLVERINE	10	14.7	1710
10	CHUGACH	10	8.6	860
11	PIQUA	12.5	8.0	640
12	RCPA	22	11.5	700
13	CPPD	75	42.5	560
14	PRDC	100	45.2	450
15	YANKEE	134	37.0	280
16	CON. ED.	275	70	320
17	PPL	150	42	280
18	COM. ED.	180	45	250
19	FLA. N.P. GROUP	136	40.2	300

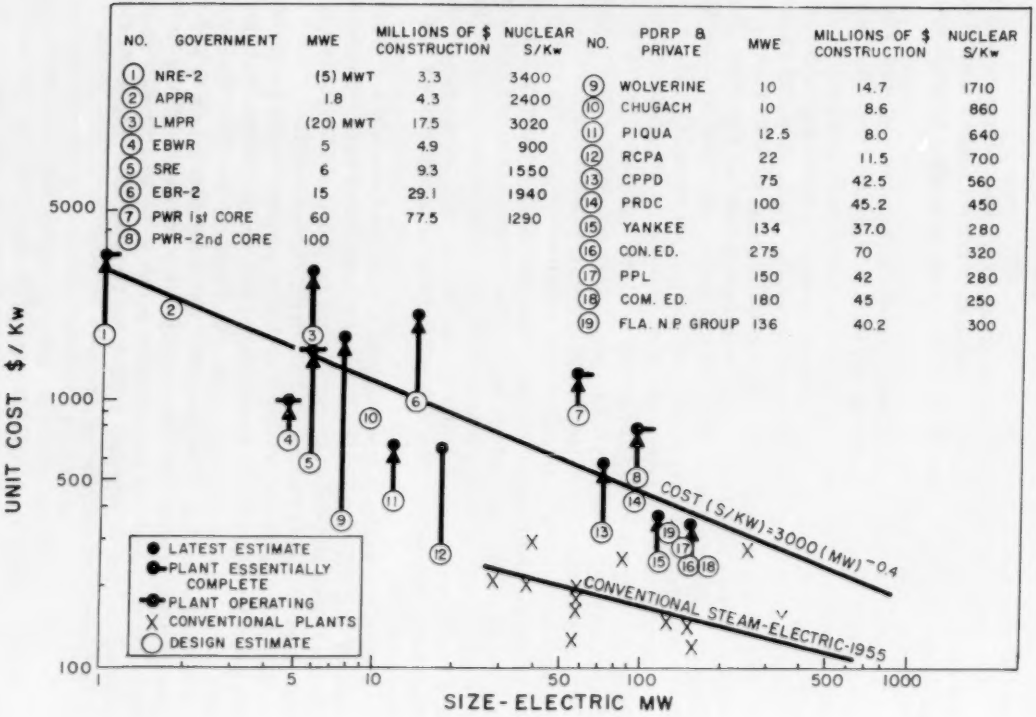

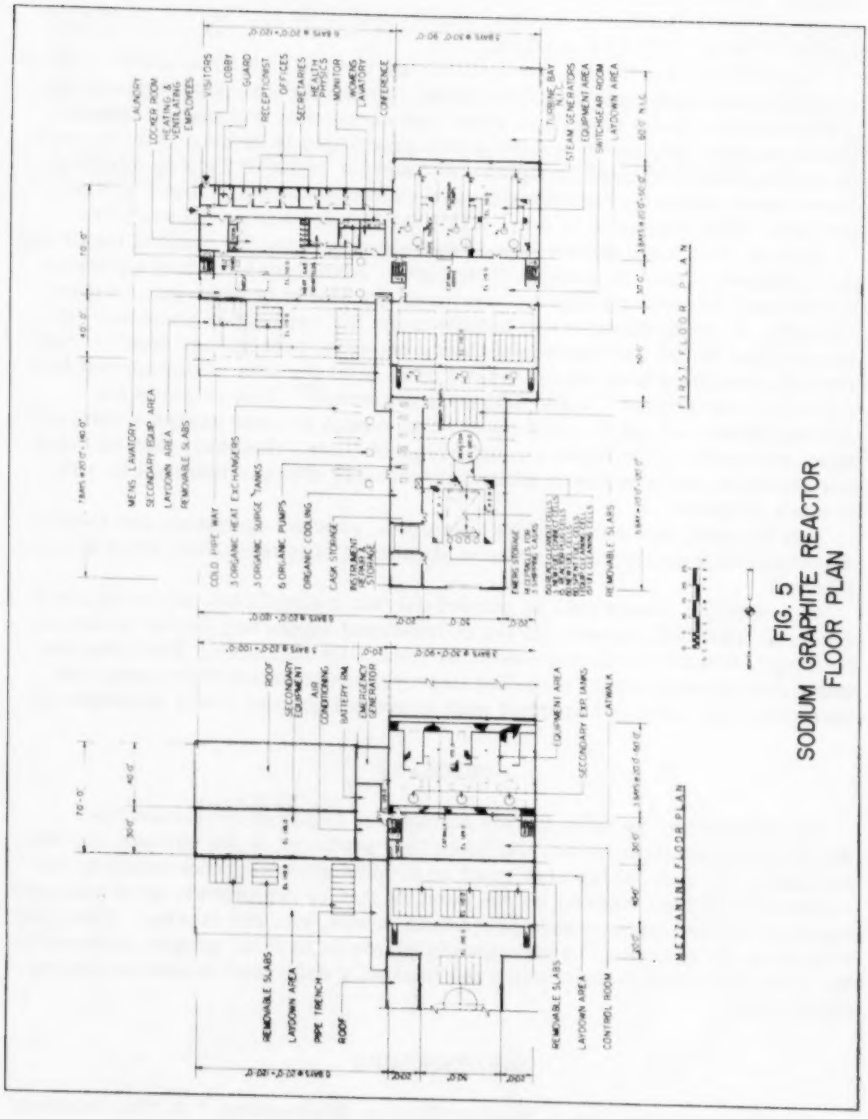

FIG. 5
SODIUM GRAPHITE REACTOR
FLOOR PLAN

These costs in general are two to three times those of conventional steam-electric plants. Expressed in terms of mils or tenths of a cent per kwh of electrical power produced, nuclear capital cost estimates vary from approximately 6 mils to 73 mils per kwh.

Capitalized costs shown here are only part of the picture however. Operating and maintenance costs and fuel costs in mils per kwh should be included. These last two items contribute more cost uncertainty for nuclear power plants because they cover factors where experience is lacking. Maintenance on radioactive components coupled with need for highly skilled operating personnel runs estimates for operating and maintenance costs from 2 to 8 mils per kwh. This compares to 0.5-1.0 mil per kwh for a conventional plant.

Nuclear fuel costs should include considerations for the costs of fabricated fuel elements, costs of fissionable material "burned up," costs of chemical processing, interest charges on fuel inventory stored in plant, and shipping charges. A credit allowance is usually made for fissionable plutonium converted from U-238 and recovered during chemical processing. Nuclear fuel costs so computed have varied from 3 to 22 mils per kwh. Conventional fuel costs can run between 1.5 and 4.25 mils per kwh.(7) These figures for nuclear plants are not in most cases solid enough to make accurate comparisons, but merely to indicate a rough range of costs. However, they do focus our attention to areas where additional technical effort is required to make it more competitive.

Containment, fuel handling, fuel elements, process equipment and reactor materials all represent areas where significant cost reductions could achieve this end.

In passing, it should also be pointed out that a significant portion of plant costs, at least 50%, represents the conventional supporting facilities such as buildings, site services, and electrical generation facilities. Technical contributions to these areas, including improved construction techniques, can, therefore, also play an important role in overall nuclear power development.

SUMMARY

To summarize, we have merely touched the highlight of reactor plant design considerations here. The feasibility problems of the nuclear, mechanical and metallurgical features must be at least generally understood by the structural engineer working on the plant so that he can provide extra judgment required in those areas where precedents, codes, etc. are lacking. Thus, consideration of the overall aspects should enable us to focus proper attention on the more important factors which are presently deterrents to economical nuclear power.

BIBLIOGRAPHY

1. Glasstone, "Principles of Nuclear Reactor Engineering, " D. Van Nostrand Co. Inc., (1956).

2. W. L. Cisler, "Atomic Opportunities in New England," Atomic Industrial Forum (1955).

3. Siler and Zick, "Design Considerations in an Atomic Power Reactor Containment Structure," ASCE Paper (October 15, 1956).

4. "Experimental Boiling Water Reactor," ANL-5609.

5. J. R. Dietrich, "Experimental Determinations of the Self-Regulation and Safety of Operating Water-Moderated Reactors," International Conference on Peaceful Uses of Atomic Energy Held in Geneva, Vol. 13 (August 1955).

6. W. Kenneth Davis talk at Atomic Industrial Forum, New York City, N. Y. (October 30, 1957).

7. P. Sporn, "Power Reactors — Outlooks for Utilities," Nucleonics, 15, p. 105 (Sept. 1957).

Paper 1764 September, 1958 ST 5

Journal of the
STRUCTURAL DIVISION
Proceedings of the American Society of Civil Engineers

ANALYSIS OF FRAMES WITH CURVED AND BENT MEMBERS

Jan J. Tuma,[1] M. ASCE, Kerry S. Havner[2]
and Frank Hedges,[3] J.M. ASCE
(Proc. Paper 1764)

SYNOPSIS

The application of a modified moment distribution method to the analysis of continuous and complex frames with curved and bent members is presented. The moment distribution and shear equilibrium constants are derived in general form. A new structural parameter, the moment-thrust factor, is introduced. The possibility of computing the moments due to rotation by the sum of infinite series is demonstrated. Numerical studies are included.

INTRODUCTION

The analysis of continuous and complex frames with symmetrical or unsymmetrical curved or bent members (Figures 1a, b, c, d) by means of energy or deformation methods is a laborious and cumbersome procedure. The main difficulty lies in the preparation and solution of a system of simultaneous equations, which only in special cases can be readily solved by numerical iteration.

The modern philosophy of structural analysis introduced by Cross(1) was modified to the analysis of continuous arches on elastic piers by Larson.(2) The convergency of Larson's approach was improved by Cross.(3)

Variations of the general method offering the improvement of convergency or a more direct approach were developed by Hrennikoff,(4) Francis,(5) Morgan,(6) Griffiths,(7) and Diwan.(8) The common characteristic of all these attempts is the effort to eliminate the labor connected with the solution of simultaneous equations.

Note: Discussion open until February 1, 1959. To extend the closing date one month, a written request must be filed with the Executive Secretary, ASCE. Paper 1764 is part of the copyrighted Journal of the Structural Division, Proceedings of the American Society of Civil Engineers, Vol. 84, No. ST 5, September, 1958.

1. Prof. of Civ. Eng., Oklahoma State Univ., Stillwater, Okla.
2. Instr. of Civ. Eng., Oklahoma State Univ., Stillwater, Okla.
3. Graduate Student, Stanford Univ., Palo Alto, Calif.

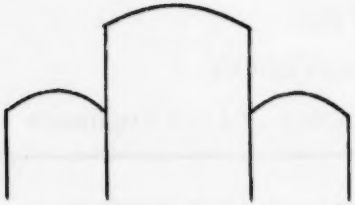

Figure 1c
Complex Frame
With Curved Members

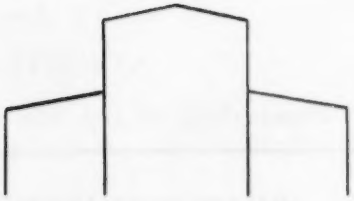

Figure 1d
Complex Frame
With Bent Members

Figure 1a
Continuous Frame
With Curved Members

Figure 1b
Continuous Frame
With Bent Members

The application of the principles of moment distribution and shear equilibrium to the analysis of continuous arches on flexible piers was introduced by Maugh,(9) Bebr,(10) Lindner,(11) Michalos and Girton,(12) and Riley.(13) An interesting analysis of continuous arches on flexible piers by means of the Ellipse of Elasticity was devised by Polivka.(14)

A general analytical study of frames shown in Figures (1a, b, c, d) based on the principles of moment distribution and shear equilibrium is presented in this paper. The well-known two step procedure of analysis of frames with straight members:

1. Distribution of assumed fixed end moments
2. Shear equilibrium of joints

is supplemented by an intermediate step: computation of shears due to rotation of joints by means of the moment-thrust factor. The study is restricted to coplanar systems only. The customary assumptions of the rigid frame analysis are taken for granted. The deformations due to normal forces and shearing forces are assumed to be small and are neglected. The sign convention of the slope deflection method is adopted. The positive reactive moments and angular rotations are clockwise. The positive reactive forces and linear displacements are to the right and upward. It is assumed that the reader is familiar with the Cross method.(1)

In the case of continuous elastic arches on flexible piers, formed by symmetrical members, the general procedure reduces to the approach suggested by Michalos and Girton.(12)

In the case of continuous frames with straight members, the general procedure reduces to the approach recommended by Ferguson.(15)

The general procedure, in a somewhat different form, was applied by Havner(16) to the analysis of frames with curved members and by Hedges(17) to the analysis of gable frames.

An additional tool of analysis, the distribution of fixed end moments by means of infinite convergent, geometric series is applied.(18,19,20,21,22,23, 24,25)

The subsequent discussion is divided into six parts. The derivation of the general deformation equations by means of minimum energy is given in a very short form in the first part of this paper. The writers are aware of some other possibilities as given in the works of Melan,(26) Beyer,(27) Fowler,(28) and Parcel and Moorman.(29)

The deformation equations are presented only to provide a logical and direct basis for the derivation of the moment distribution and shear equilibrium constants as shown in Parts II and III.

The numerical procedure and the algebraic abbreviation are discussed in Parts IV and V. Two numerical examples are presented in the last part of the paper.

The standard nomenclature is used throughout the paper. The meaning of special symbols is explained wherever they occur.

Part I. Deformation Equations

A fixed end, unsymmetrical curved bar of variable cross-section acted upon by a general system of vertical loads is considered (Fig. 2).

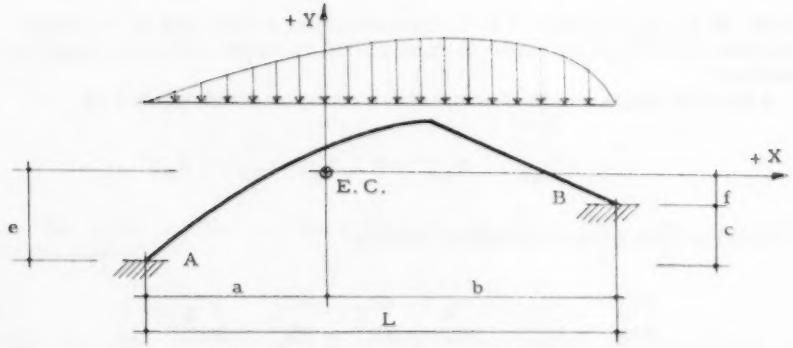

Fig. 2
Loaded Structure

The redundants at an arbitrary cross-section are transferred to the elastic center and denoted as X_1, X_2, and X_3 (Fig. 3).

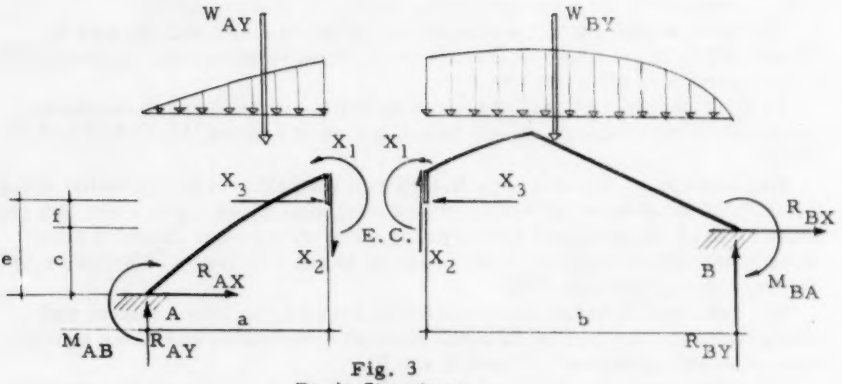

Fig. 3
Basic Structure

The reactions in terms of loads and redundants are:

$$R_{AX} = -X_3 \qquad R_{BX} = X_3$$

$$R_{AY} = W_{AY} + X_2 \qquad R_{BY} = W_{BY} - X_2 \tag{1}$$

$$M_{AB} = -\overline{SM}_{AC} + X_1 - X_2 a - X_3 e \qquad M_{BA} = \overline{SM}_{BC} - X_1 - X_2 b + X_3 f$$

where W is the resultant of loads corresponding to one part of the basic structure and $\overline{SM}$ is the static moment of that resultant about the respective fixed end.

A general displacement of supports is introduced and denoted as:

$$\circlearrowright \theta_A \,,\ \overrightarrow{\Delta_{AX}} \,,\ \uparrow \Delta_{AY} \quad \text{and} \quad \circlearrowright \theta_B \,,\ \overrightarrow{\Delta_{BX}} \,,\ \uparrow \Delta_{BY} \,.$$

From the principle of minimum energy:

$$\frac{\partial U_R}{\partial X_1} = \frac{\partial U_S}{\partial X_1} \,,\ \frac{\partial U_R}{\partial X_2} = \frac{\partial U_S}{\partial X_2} \,,\ \frac{\partial U_R}{\partial X_3} = \frac{\partial U_S}{\partial X_3} \tag{2}$$

in which

$$U_R = \begin{bmatrix} \theta_A M_{AB} + \Delta_{AX} R_{AX} + \Delta_{AY} R_{AY} \\ \theta_B M_{BA} + \Delta_{BX} R_{BX} + \Delta_{BY} R_{BY} \end{bmatrix} \tag{3}$$

and

$$U_S = \int_A^B \frac{M^2 ds}{2EI} \tag{4}$$

Expressing Equation (2) by means of Equations (1), (3), and (4):

$$\begin{aligned} \theta_A - \theta_B &= a_{10} + a_{11}X_1 + a_{12}X_2 + a_{13}X_3 \\ -a\theta_A - b\theta_B + \Delta_y &= a_{20} + a_{21}X_1 + a_{22}X_2 + a_{23}X_3 \\ -e\theta_A + f\theta_B - \Delta_x &= a_{30} + a_{31}X_1 + a_{32}X_2 + a_{33}X_3 . \end{aligned} \tag{5}$$

The equivalents used in Equations (5) are:

$$a_{10} = \int_A^B \frac{\overline{BM}\, ds}{EI} \qquad a_{20} = \int_A^B \frac{\overline{BM}\, x\, ds}{EI} \qquad a_{30} = \int_A^B \frac{\overline{BM}\, y\, ds}{EI}$$

$$a_{11} = \int_A^B \frac{ds}{EI} \qquad a_{22} = \int_A^B \frac{x^2\, ds}{EI} \qquad a_{33} = \int_A^B \frac{y^2\, ds}{EI}$$

$$a_{12} = a_{21} = \int_A^B \frac{x\, ds}{EI} \qquad a_{13} = a_{31} = \int_A^B \frac{y\, ds}{EI}$$

$$a_{23} = a_{32} = \int_A^B \frac{xy\, ds}{EI}$$

$$\Delta_X = \Delta_{AX} - \Delta_{BX} \qquad \Delta_Y = \Delta_{AY} - \Delta_{BY}$$

where $\overline{BM}$ is the bending moment of the basic structure. From the definition of elastic center,

$$a_{12} = a_{21} = 0 \text{ and } a_{13} = a_{31} = 0 .$$

Substituting these conditions into Equations (5) and solving for the redundants:

$$\begin{aligned} X_1 &= \frac{\theta_A}{a_{11}} - \frac{\theta_B}{a_{11}} - \frac{a_{10}}{a_{11}} \\ X_2 &= \frac{a_{33}}{N}(-a\theta_A - b\theta_B + \Delta_Y - a_{20}) \\ &\quad + \frac{a_{23}}{N}(e\theta_A - f\theta_B + \Delta_X + a_{30}) \end{aligned} \tag{6}$$

$$X_3 = \frac{a_{22}}{N}(-e\theta_A + f\theta_B - \Delta_X - a_{30}) + \frac{a_{23}}{N}(a\theta_A + b\theta_B - \Delta_Y + a_{20})$$

where $N = a_{22}a_{33} - a_{23}a_{23}$.

From Equations (1) and (6) the horizontal thrust is

$$H = R_{AX} = -R_{BX} = \frac{a_{22}e - a_{23}a}{N}\theta_A - \frac{a_{22}f + a_{23}b}{N}\theta_B + \frac{a_{22}}{N}\Delta_X + \frac{a_{23}}{N}\Delta_Y + \frac{a_{22}a_{30} - a_{23}a_{20}}{N} \quad (7)$$

and the end moments are

$$M_{AB} = (\frac{1}{a_{11}} + \frac{a_{33}}{N}a^2 - 2\frac{a_{23}}{N}ae + \frac{a_{22}}{N}e^2)\theta_A + (-\frac{1}{a_{11}} + \frac{a_{33}}{N}ab + \frac{a_{23}}{N}(af - be) - \frac{a_{22}}{N}ef)\theta_B + \frac{a_{22}e - a_{23}a}{N}\Delta_X + \frac{a_{23}e - a_{33}a}{N}\Delta_Y - \frac{a_{10}}{a_{11}} + \frac{a_{33}a_{20} - a_{23}a_{30}}{N}a + \frac{a_{22}a_{30} - a_{23}a_{20}}{N}e - \overline{SM}_{AC} \quad (8)$$

$$M_{BA} = (\frac{1}{a_{11}} + \frac{a_{33}}{N}b^2 + 2\frac{a_{23}}{N}bf + \frac{a_{22}}{N}f^2)\theta_B + (-\frac{1}{a_{11}} + \frac{a_{33}}{N}ab + \frac{a_{23}}{N}(af - be) - \frac{a_{22}}{N}ef)\theta_A - \frac{a_{22}f + a_{23}b}{N}\Delta_X - \frac{a_{23}f + a_{33}b}{N}\Delta_Y + \frac{a_{10}}{a_{11}} + \frac{a_{33}a_{20} - a_{23}a_{30}}{N}b - \frac{a_{22}a_{30} - a_{23}a_{20}}{N}f + \overline{SM}_{BC}.$$

If a general system of horizontal loads is applied, the modification of Equations (7) and (8) is made from the conditions of static equilibrium.

In the case of a symmetrical bar, in Equations (7) and (8)

$$a = b = \frac{L}{2}, \quad e = f, \quad c = 0$$

and

$$a_{23} = 0 .$$

The matrix notation may be easily replaced by the column analogy notation,[28] if desired. The selection of the basic structure is a matter of convenience. Two cantilever bars as introduced here are only one of many possibilities.

Part II. Moment Distribution Constants

In applying the moment distribution method to the analysis of a given structure, several constants must be determined before the distribution process can be carried out. These constants are:

a) fixed end moments due to loads

b) fixed end moments due to Δ_X

c) fixed end moments due to Δ_Y

d) angular stiffness factors

e) carry-over factors

The analytical expressions for these constants are developed from their definitions by means of Equations (8).

a) Fixed end moments due to loads:

$$FM_{AB}^{(L)} = -\frac{a_{10}}{a_{11}} + \left(\frac{a_{33}}{N}a - \frac{a_{23}}{N}e\right)a_{20} + \left(\frac{a_{22}}{N}e - \frac{a_{23}}{N}a\right)a_{30} - \overline{SM}_{AC} .$$

$$FM_{BA}^{(L)} = \frac{a_{10}}{a_{11}} + \left(\frac{a_{33}}{N}b + \frac{a_{23}}{N}f\right)a_{20} - \left(\frac{a_{22}}{N}f + \frac{a_{23}}{N}b\right)a_{30} + \overline{SM}_{BC} . \qquad (9)$$

b) Fixed end moments due to relative horizontal displacement Δ_X:

$$FM_{AB}^{(X)} = \left(\frac{a_{22}}{N}e - \frac{a_{23}}{N}a\right)\Delta_X$$

$$FM_{BA}^{(X)} = -\left(\frac{a_{22}}{N}f + \frac{a_{23}}{N}b\right)\Delta_X . \qquad (10)$$

c) Fixed end moments due to relative vertical displacement Δ_Y:

$$FM_{AB}^{(Y)} = -\left(\frac{a_{33}}{N}a - \frac{a_{23}}{N}e\right)\Delta_Y \qquad (11)$$

$$FM_{BA}^{(Y)} = -\left(\frac{a_{33}}{N}b + \frac{a_{23}}{N}f\right)\Delta_Y \ . \tag{11}$$

d) Angular stiffness factors:

$$\begin{aligned} K_{AB} &= \frac{1}{a_{11}} + \left(\frac{a_{22}}{N}e - \frac{a_{23}}{N}a\right)e + \left(\frac{a_{33}}{N}a - \frac{a_{23}}{N}e\right)a \\ K_{BA} &= \frac{1}{a_{11}} + \left(\frac{a_{22}}{N}f + \frac{a_{23}}{N}b\right)f + \left(\frac{a_{33}}{N}b + \frac{a_{23}}{N}f\right)b \ . \end{aligned} \tag{12}$$

e) Carry-over factors:

$$C_{AB} = \frac{C_{AB}K_{AB}}{K_{AB}} \qquad C_{BA} = \frac{C_{BA}K_{BA}}{K_{BA}} \tag{13}$$

where

$$C_{AB}K_{AB} = C_{BA}K_{BA} = -\frac{1}{a_{11}} - \left(\frac{a_{22}}{N}f + \frac{a_{23}}{N}b\right)e + \left(\frac{a_{33}}{N}b + \frac{a_{23}}{N}f\right)a \ .$$

In terms of these constants, Equations (8) are:

$$\begin{aligned} M_{AB} &= \underbrace{K_{AB}\theta_A + C_{BA}K_{BA}\theta_B}_{RM_{AB}} + \underbrace{FM_{AB}^{(X)} + FM_{AB}^{(Y)} + FM_{AB}^{(L)}}_{FM_{AB}} \\ M_{BA} &= \underbrace{K_{BA}\theta_B + C_{AB}K_{AB}\theta_A}_{RM_{BA}} + \underbrace{FM_{BA}^{(X)} + FM_{BA}^{(Y)} + FM_{BA}^{(L)}}_{FM_{BA}} \end{aligned} \tag{14}$$

where

RM = moment due to rotation

FM = fixed end moment.

The fixed end moment may be distributed by the regular moment distribution procedure to obtain the final moments in terms of loads and displacements of joints.

Part III. Shear Equilibrium Constants

Once the equilibrium of moments is established at all joints of the structure, the equilibrium of horizontal and vertical shears must be secured.

The equilibrium of horizontal forces at Joint B (Fig. 4) is:

$$\Sigma F_{BX} = -H_{BA} + H_{BC} - V_{BO} = 0 \ . \tag{15}$$

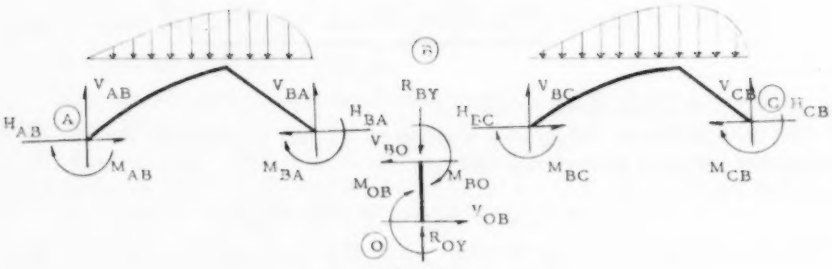

Fig. 4
Cross-Sectional Elements
At a Typical Joint

The equilibrium of vertical forces is:

$$\Sigma F_{BY} = V_{BA} + V_{BC} - R_{BY} = 0 . \tag{16}$$

Each of the horizontal thrusts in Equation (15) consists of the following functions:

a) fixed end thrust due to loads

b) fixed end thrust due to Δ_X

c) fixed end thrust due to Δ_Y

d) induced thrust due to rotation.

The analytical expressions for these functions are developed from their definitions by means of Equation (7).

a) Fixed end thrust due to loads:

$$\overrightarrow{FH}_{AB}^{(L)} = \overleftarrow{FH}_{BA}^{(L)} = \frac{a_{22}}{N} a_{30} - \frac{a_{23}}{N} a_{20} . \tag{17}$$

b) Fixed end thrust due to relative horizontal displacement Δ_X:

$$\overrightarrow{FH}_{AB}^{(X)} = \overleftarrow{FH}_{BA}^{(X)} = \frac{a_{22}}{N} \Delta_X . \tag{18}$$

c) Fixed end thrust due to relative vertical displacement Δ_Y:

$$\overrightarrow{FH}_{AB}^{(Y)} = \overleftarrow{FH}_{BA}^{(Y)} = \frac{a_{23}}{N} \Delta_Y . \tag{19}$$

d) Thrust due to rotation:

$$\overrightarrow{RH}_{AB} = \overleftarrow{RH}_{BA} = (\frac{a_{22}}{N} e - \frac{a_{23}}{N} a) \theta_A - (\frac{a_{22}}{N} f + \frac{a_{23}}{N} b) \theta_B . \tag{20}$$

In terms of these functions, Equation (7) is:

$$H = RH_{AB} + \underbrace{FH_{AB}^{(X)} + FH_{AB}^{(Y)} + FH_{AB}^{(L)}}_{FH_{AB}} \tag{21}$$

where FH = total fixed end thrust.

The induced thrust RH_{AB} is a function of θ_A and θ_B but may be expressed in terms of RM_{AB} and RM_{BA}.

From Equation (14)

$$\begin{aligned} RM_{AB} &= K_{AB}\theta_A + C_{BA}K_{BA}\theta_B \\ RM_{BA} &= K_{BA}\theta_B + C_{AB}K_{AB}\theta_A . \end{aligned} \tag{22}$$

Solving Equations (22) simultaneously for θ_A and θ_B and substituting into Equation (20):

$$\overrightarrow{RH_{AB}} = \overleftarrow{RH_{BA}} = S_{AB}RM_{AB} + S_{BA}RM_{BA} \tag{23}$$

where

$$S_{AB} = \frac{1}{1 - C_{AB}C_{BA}}\left[\left(\frac{a_{22}}{N}e - \frac{a_{23}}{N}a\right)\frac{1}{K_{AB}} + \left(\frac{a_{22}}{N}f + \frac{a_{23}}{N}b\right)\frac{C_{AB}}{K_{BA}}\right]$$

$$S_{BA} = -\frac{1}{1 - C_{AB}C_{BA}}\left[\left(\frac{a_{22}}{N}f + \frac{a_{23}}{N}b\right)\frac{1}{K_{BA}} + \left(\frac{a_{22}}{N}e - \frac{a_{23}}{N}a\right)\frac{C_{BA}}{K_{AB}}\right] . \tag{24}$$

These constants are hereafter called the moment-thrust factors. The moment-thrust factor for one end of a member is the thrust developed in the member by a unit moment applied at that end with the opposite end free to rotate.

The horizontal shear V_{BO} in Equation (15) and the vertical shears in Equation (16) are computed from equations of static equilibrium. The axial force R_{BY} in the column is computed from Equation (16).

Part IV. Numerical Moment Distribution Method

The application of the numerical moment distribution method to the analysis of frames with straight members is well known. The modification of this method to the analysis of frames with curved members consists of the following steps:

1. Determine stiffness, carry-over, distribution, and moment-thrust factors.

2. Compute the fixed end moments and thrusts in terms of loads and arbitrary (unknown) displacements of joints.

3. Using the moment distribution procedure, calculate the resulting moments due to each unbalance of fixed end moments.

4. Write as many independent shear equations as there are unknown displacements and solve the equations simultaneously for Δ's or their equivalents.

5. Compute the final end moments and thrusts.

It is important to observe that:

1. One moment distribution solution is required for each independently translating joint.

2. The horizontal thrusts in curved members are redundants and cannot be computed directly from the end moments by means of static equilibrium but must be computed from Equation (21) in terms of Equation (23).

3. Each moment due to rotation (RM) is the difference between the corresponding fixed end and final moments.

4. The vertical end shears in curved members can be computed directly from the end moments and horizontal thrusts by means of static equilibrium.

Part V. Algebraic Moment Distribution Method

If the method of numerical moment distribution is applied to the computation of end moments due to rotation of joints, the process must be repeated in as many separate tables as there are load conditions and independent joint displacements. The numerical labor may be reduced by using the method of coefficients in numerical[31] or algebraic form.[20]

The algebraic moment distribution when applied to the analysis of continuous beams or one story frames can be performed in terms of two types of infinite series:

1. Basic series

2. Carry-over series.

The basic series is an infinite, convergent, geometric series, each term of which is a finite number.

$$\text{Basic Series} = Qq^0 + Qq^1 + Qq^2 + \ldots + 0.$$

The carry-over series is an infinite, convergent, geometric series, each term of which is another infinite, convergent, geometric series.

$$\text{Carry-Over Series} = \begin{bmatrix} Qq^0s^0 + Qq^1s^0 + Qq^2s^0 + \cdots + 0 \\ Qq^0s^1 + Qq^1s^1 + Qq^2s^1 + \cdots + 0 \\ Qq^0s^2 + Qq^1s^2 + Qq^2s^2 + \cdots + 0 \\ \cdot \quad \cdot \quad \cdot \quad \cdots \quad \cdot \\ \cdot \quad \cdot \quad \cdot \quad \cdots \quad \cdot \\ 0 \quad 0 \quad 0 \quad \cdots \quad 0 \end{bmatrix}$$

The sum of the basic series $= \frac{Q}{1 - q}$ and the sum of the carry-over series $= \frac{Q}{(1 - q)(1 - s)}$. The existence of these series is shown elsewhere.(22)

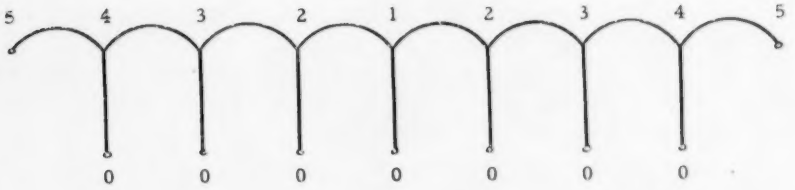

Fig. 5
Eight Span Continuous Frame

The application of these series to the analysis of continuous and complex frames is demonstrated in the following example:

An eight span continuous, unsymmetrical frame is considered (Fig. 5). The distribution factors are denoted as A_{ij} and B_{ij} and the carry-over factors as a_{ij} and b_{ij}. The symbols A, a correspond to the left portion of the frame and the symbols B, b to the right portion. The product of the distribution factor and the corresponding carry-over factor is

$$a_{ij}A_{ij} = E_{ij} \text{ and } b_{ij}B_{ij} = F_{ij} .$$

The denominators of basic series are:

$$X_{ij} = 1 - E_{ij}E_{ji} \qquad Y_{ij} = 1 - F_{ij}F_{ji}$$

$$X_{ik} = 1 - E_{ij}E_{ji} - E_{jk}E_{kj} \qquad Y_{ik} = 1 - F_{ij}F_{ji} - F_{jk}F_{kj}$$

and

$$X_{22} = Y_{22} = Z_{22} = 1 - E_{12}E_{21} - F_{12}F_{21} .$$

The denominators of carry-over series are:

$$Z_{33} = 1 - \frac{E_{12}E_{21}}{X_{23}} - \frac{F_{12}F_{21}}{Y_{23}}$$

$$Z_{44} = 1 - \frac{E_{12}E_{21}X_{34}}{X_{24}} - \frac{F_{12}F_{21}Y_{34}}{Y_{24}} .$$

The denominator Z_{22} forms a link between the basic and the carry-over series.

a) Four span system:

The unbalance of M = 1 is introduced at Joint 1 and the Joints 3 are temporarily fixed. The moment distribution procedure is carried out algebraically. When all terms in Column $\overline{10}$ are summed, the final moment

$$M_{10} = - A_{10}\left(\frac{1}{Z_{22}}\right)$$

in which

$$\frac{1}{Z_{22}} = 1 + (E_{12}E_{21} + F_{12}F_{21}) + (E_{12}E_{21} + F_{12}F_{21})^2 + \cdots$$

All final moments similarly derived are recorded in Table 1.

b) Six span system:

The same unbalance is introduced at Joint 1 and the Joints 4 are temporarily fixed. The moment distribution procedure is carried out algebraically. When all terms in Column $\overline{10}$ are summed, the final moment

$$M_{10} = - A_{10}\left(\frac{1}{Z_{33}}\right)$$

in which

$$\frac{1}{Z_{33}} = 1 + \left(\frac{E_{12}E_{21}}{X_{23}} + \frac{F_{12}F_{21}}{Y_{23}}\right) + \left(\frac{E_{12}E_{21}}{X_{23}} + \frac{F_{12}F_{21}}{Y_{23}}\right)^2 + \cdots$$

All final moments similarly derived are recorded in Table 2.

In preparing the final values, three isolated parts of the frame were used (Fig. 6). This separation makes the study of basic and carry-over series possible. For details compare with (22).

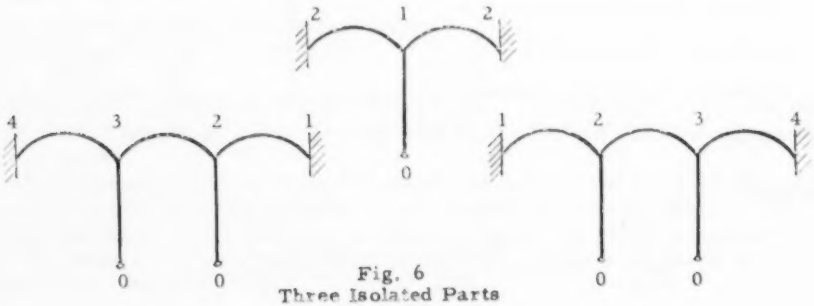

Fig. 6
Three Isolated Parts

c) Eight span system:

The same unbalance is introduced at Joint 1 and all joints are free to rotate. The final moment

$$M_{10} = - A_{10}\left(\frac{1}{Z_{44}}\right)$$

Four Span System End Moment Coefficients Due to Unbalanced Unit-Moment at 1*.	
M_{10}	$(-A_{10})\frac{1}{Z_{22}}$
M_{12}	$(E_{12}E_{21} - A_{12})\frac{1}{Z_{22}}$
M_{21}	$(E_{12}A_{21} - E_{12})\frac{1}{Z_{22}}$
M_{20}	$(E_{12}A_{20})\frac{1}{Z_{22}}$
M_{23}	$(E_{12}A_{23})\frac{1}{Z_{22}}$
M_{32}	$(E_{12}E_{23})\frac{1}{Z_{22}}$

Table 1

* End moment coefficients for the left side of the system are tabulated. The right side coefficients are cyclosymmetrical.

Six Span System End Moment Coefficients Due to Unbalanced Unit-Moment at 1*.	
M_{10}	$(-A_{10})\frac{1}{Z_{33}}$
M_{12}	$(\frac{E_{12}E_{21}}{X_{23}} - A_{12})\frac{1}{Z_{33}}$
M_{21}	$(\frac{E_{12}A_{21}}{X_{23}} - E_{12})\frac{1}{Z_{33}}$
M_{20}	$(\frac{E_{12}A_{20}}{X_{23}})\frac{1}{Z_{33}}$
M_{23}	$\frac{E_{12}}{X_{23}}(A_{23} - E_{23}E_{32})\frac{1}{Z_{33}}$
M_{32}	$\frac{E_{12}}{X_{23}}(E_{23} - E_{23}A_{32})\frac{1}{Z_{33}}$
M_{30}	$(-\frac{E_{12}E_{23}A_{30}}{X_{23}})\frac{1}{Z_{33}}$
M_{34}	$(-\frac{E_{12}E_{23}A_{34}}{X_{23}})\frac{1}{Z_{33}}$
M_{43}	$(-\frac{E_{12}E_{23}E_{34}}{X_{23}})\frac{1}{Z_{33}}$

Table 2

in which

$$\frac{1}{Z_{44}} = 1 + (\frac{E_{12}E_{21}X_{34}}{X_{24}} + \frac{F_{12}F_{21}Y_{34}}{Y_{24}}) + (\frac{E_{12}E_{21}X_{34}}{X_{24}} + \frac{F_{12}F_{21}Y_{34}}{Y_{24}})^2 + \ldots .$$

All final moments similarly derived are recorded in Table 3.

In preparing the final values, three isolated parts of the frame were again used (Parts $\overline{51}$, $\overline{22}$, and $\overline{15}$).

Eight Span System
End Moment Coefficients Due to
Unbalanced Unit-Moment at 1*.

M_{10}	$(-A_{10})\frac{1}{Z_{44}}$	M_{32}	$\frac{E_{12}}{X_{24}}(E_{23}X_{34} - E_{23}A_{32})\frac{1}{Z_{44}}$
M_{12}	$(\frac{E_{12}E_{21}X_{34}}{X_{24}} - A_{12})\frac{1}{Z_{44}}$	M_{30}	$(-\frac{E_{12}E_{23}A_{30}}{X_{24}})\frac{1}{Z_{44}}$
M_{21}	$(\frac{E_{12}A_{21}X_{34}}{X_{24}} - E_{12})\frac{1}{Z_{44}}$	M_{34}	$-\frac{E_{12}E_{23}}{X_{24}}(A_{34} - E_{34}E_{43})\frac{1}{Z_{44}}$
M_{20}	$(\frac{E_{12}A_{20}X_{34}}{X_{24}})\frac{1}{Z_{44}}$	M_{43}	$-\frac{E_{12}E_{23}}{X_{24}}(E_{34} - E_{34}A_{43})\frac{1}{Z_{44}}$
M_{23}	$\frac{E_{12}}{X_{24}}(A_{23}X_{34} - E_{23}E_{32})\frac{1}{Z_{44}}$	M_{40}	$(\frac{E_{12}E_{23}E_{34}A_{40}}{X_{24}})\frac{1}{Z_{44}}$
		M_{45}	$(\frac{E_{12}E_{23}E_{34}A_{45}}{X_{24}})\frac{1}{Z_{44}}$

Table 3

* End moment coefficients for the left side of the system are tabulated. The right side coefficients are cyclosymmetrical.

Although the investigation was limited to four, six, and eight span systems, it is evident that the philosophy of approach is general and valid for any number of spans.

The investigation of the spread of an unbalanced moment at a joint through a larger number of joints is, however, of theoretical interest only. In most cases it is sufficient to consider the adjacent one or two joints on each side. From Tables 1, 2, and 3 a numerical procedure is possible as shown in Tables 4, 5, and 6.

Part VI. Numerical Examples

Two numerical examples are introduced to illustrate the application of the general procedure. The first example is an actual structure. The second is an artificial problem representing three types of unsymmetrical members. The flexural rigidity EI of all members is assumed to be constant. All values are given in feet, kips or kip-feet.

Four Span System - Numerical Procedure								
23	20	21	12	10	12	21	20	23
			$-\frac{A_{12}}{Z_{22}}$	$-\frac{A_{10}}{Z_{22}}$	$-\frac{B_{12}}{Z_{22}}$			
$\frac{A_{23}E_{12}}{Z_{22}}$	$\frac{A_{20}E_{12}}{Z_{22}}$	$-\frac{E_{12}}{Z_{22}}$ $\frac{A_{21}E_{12}}{Z_{22}}$				$-\frac{F_{12}}{Z_{22}}$ $\frac{B_{21}F_{12}}{Z_{22}}$	$\frac{B_{20}F_{12}}{Z_{22}}$	$\frac{B_{23}F_{12}}{Z_{22}}$
			$\frac{E_{12}E_{21}}{Z_{22}}$		$\frac{F_{12}F_{21}}{Z_{22}}$			
Σ	Σ	Σ	Σ	Σ	Σ	Σ	Σ	Σ^*

* Final moment is equal to the sum of all numbers in the respective column.

Table 4

Six Span System - Numerical Procedure							
34	30	32	23	20	21	12	10
						$-\frac{A_{12}}{Z_{33}}$	$-\frac{A_{10}}{Z_{33}}$
			$\frac{A_{23}E_{12}}{X_{23}Z_{33}}$	$\frac{A_{20}E_{12}}{X_{23}Z_{33}}$	$-\frac{E_{12}}{Z_{33}}$ $\frac{A_{21}E_{12}}{X_{23}Z_{33}}$		
$-\frac{A_{34}E_{12}E_{23}}{X_{23}Z_{33}}$	$-\frac{A_{30}E_{12}E_{23}}{X_{23}Z_{33}}$	$\frac{E_{12}E_{23}}{X_{23}Z_{33}}$ $-\frac{A_{32}E_{12}E_{23}}{X_{23}Z_{33}}$				$\frac{E_{12}E_{21}}{X_{23}Z_{33}}$	
			$-\frac{E_{12}E_{23}E_{32}}{X_{23}Z_{33}}$				
Σ	Σ	Σ	Σ	Σ	Σ	Σ	Σ*

*Final moment is equal to the sum of all numbers in the respective column. The cyclosymmetrical right side of this table is not shown.

Table 5

Eight Span System - Numerical Procedure						
45	43	34	32	23	21	12
						$-\frac{A_{12}}{Z_{44}}$
				$\frac{A_{23}E_{12}X_{34}}{X_{24}Z_{44}}$	$-\frac{E_{12}}{Z_{44}}$ $\frac{A_{21}E_{12}X_{34}}{X_{24}Z_{44}}$	
		$-\frac{A_{34}E_{12}E_{23}}{X_{24}Z_{44}}$	$\frac{E_{12}E_{23}X_{34}}{X_{24}Z_{44}}$ $-\frac{A_{32}E_{12}E_{23}}{X_{24}Z_{44}}$			$\frac{E_{12}E_{21}X_{34}}{X_{24}Z_{44}}$
$\frac{A_{45}E_{12}E_{23}E_{34}}{X_{24}Z_{44}}$	$-\frac{E_{12}E_{23}E_{34}}{X_{24}Z_{44}}$ $\frac{A_{43}E_{12}E_{23}E_{34}}{X_{24}Z_{44}}$			$-\frac{E_{12}E_{23}E_{32}}{X_{24}Z_{44}}$		
		$\frac{E_{12}E_{23}E_{34}E_{43}}{X_{24}Z_{44}}$				
Σ	Σ	Σ	Σ	Σ	Σ	Σ^*

* Final moment is equal to the sum of all numbers in the respective column. The cyclosymmetrical right side of this table and the column moments are not shown.

Table 6

Example 1. A four-span gabled frame with dimensions and loads as shown (Fig. 7) is analysed.(32)

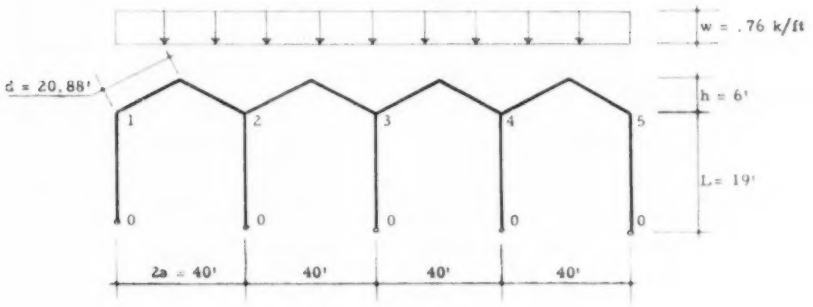

Four Span Gabled Frame
Fig. 7

From the symmetry:

$$\theta_1 = -\theta_5 \quad \theta_2 = -\theta_4 \quad \theta_3 = 0$$

$$\Delta_{1X} = -\Delta_{5X} \quad \Delta_{2X} = -\Delta_{4X} \quad \Delta_{3X} = 0 .$$

Moment Distribution Constants

Bent member ij:

$$FM_{ij}^{(L)} = -FM_{ji}^{(L)} = -\frac{wa^2}{12} = -25.333 \qquad \text{(Eq. 9)}$$

$$FM_{ij}^{(X)} = -FM_{ji}^{(X)} = \frac{6EI}{2dh}\Delta_{ijX} = .023946EI\Delta_{ijX} \qquad \text{(Eq. 10)}$$

$$K_{ij} = K_{ji} = \frac{7EI}{2d} = .1676EI \qquad \text{(Eq. 12)}$$

$$C_{ij} = C_{ji} = -\frac{1}{7} = -.1429 \qquad \text{(Eq. 13)}$$

Column io:

$$FM_{io}^{(X)} = -\frac{3EI}{L^2}\overrightarrow{\Delta_{iX}} = -.008310EI\overrightarrow{\Delta_{iX}} \qquad K_{io} = \frac{3EI}{L} = .1579EI$$

All fixed end moments are recorded in Table 9.

Shear Equilibrium Constants

Bent member ij:

$$\overrightarrow{FH}_{ij}^{(L)} = \overleftarrow{FH}_{ji}^{(L)} = \frac{wa^2}{2h} = 25.333 \qquad \text{(Eq. 17)}$$

$$\overrightarrow{FH}_{ij}^{(X)} = \overleftarrow{FH}_{ji}^{(X)} = \frac{12EI}{2dh^2}\Delta_{ijX} = .007982EI\Delta_{ijX} \quad \text{(Eq. 18)}$$

$$S_{ij} = -S_{ji} = \frac{3}{4h} = .125 \quad \text{(Eq. 23)}$$

All fixed end thrusts and shears are recorded in Table 9.

Distribution Factors

$D_{10} = .4851$ $D_{21} = .3399$

$D_{12} = .5149$ $D_{20} = .3202$

$D_{23} = .3399$

Distribution of Unbalanced Unit-Moment At Joint 1 is shown in Table 7.

From Table 4

$$\frac{M_1}{X_{12}} = \frac{1}{1 - C_{12}C_{21}D_{12}D_{21}} = 1.0036 .$$

The moment coefficients due to unbalanced unit-moment at Joint 1 are denoted as $RM_{ij}.^{(1)}$

10	12	21	20	23	32	
.4851	.5149	.3399	.3202	.3399	.3399	D
.0000	-.1429	-.1429	.0000	-.1429	-.1429	C
-.4868	-.5168					
		+.0738				
		-.0251	-.0236	-.0251		
	+.0036				+.0036	
-.4868	-.5132	+.0487	-.0236	-.0251	+.0036	$RM^{(1)}$

Distribution of Unbalanced Unit-Moment at Joint 1
Table 7

Distribution of Unbalanced Unit-Moment at Joint 2 is shown in Table 8.

From Table 4

$$\frac{M_2}{X_{12}} = \frac{1}{1 - C_{12}C_{21}D_{12}D_{21}} = 1.0036 .$$

The moment coefficients due to unbalanced unit-moment at Joint 2 are denoted as $RM_{ij}.^{(2)}$

10	12	21	20	23	32	
.4851	.5149	←.3399	.3202	→.3399	←.3399	D
.0000	-.1429	-.1429	.0000	-.1429	-.1429	C
		-.3411	-.3214	-.3411		
	+.0487				+.0487	
-.0236	-.0251				.0000	
		+.0036		.0000		
-.0236	+.0236	-.3375	-.3214	-.3411	+.0487	$RM^{(2)}$

Distribution of Unbalanced Unit-Moment at Joint 2
Table 8

Unbalance of Fixed End Moments

At Joint 1: (From Table 9.)

$$\Sigma FM_1 = -25.333 - .015636EI\overleftarrow{\Delta}_{1X} + .023946EI\overleftarrow{\Delta}_{2X}$$

At Joint 2: (From Table 9.)

$$\Sigma FM_2 = .023946EI\overleftarrow{\Delta}_{1X} - .039582EI\overleftarrow{\Delta}_{2X}$$

Moments Due to Rotation of Joints in terms of loads and unknown displacements and defined as

$$RM_{ij} = RM_{ij}^{(1)}\Sigma FM_1 + RM_{ij}^{(2)}\Sigma FM_2$$

are recorded in Table 9. $RM_{ij}^{(1)}$ and $RM_{ij}^{(2)}$ are the end moments due to the unbalance of unit-moment at 1 and 2 respectively.

Thrusts Due to Rotation of Joints in terms of loads and unknown displacements and given by Equation (23) as

$$\overrightarrow{RH}_{ij} = \overleftarrow{RH}_{ji} = .125(RM_{ij} - RM_{ji})$$

and end shears in columns are recorded in Table 9.

Equations of Shear Equilibrium

At Joint 1: (From Table 9.)

$$\Sigma F_{1X} = 0 = 26.463 - .006612EI\overleftarrow{\Delta}_{1X} + .005078EI\overleftarrow{\Delta}_{2X}$$

At Joint 2: (From Table 9.)

$$\Sigma F_{2X} = 0 = -1.719 + .005079EI\overleftarrow{\Delta}_{1X} - .011729EI\overleftarrow{\Delta}_{2X}$$

	END MOMENTS					END FORCES				
	⊕	LOAD	$EI\Delta_{1X}$	$EI\Delta_{2X}$	Σ	+	LOAD	$EI\Delta_{1X}$	$EI\Delta_{2X}$	Σ
10	FM	0	+ .008310	0		FV	0	- .000437	0	
	RM	+ 12.332	+ .007047	- .010723		RV	- .649	- .000371	+ .000565	
	M	+ 12.332	+ .015357	- .010723	+ 76.34	V	- .649	- .000808	+ .000565	- 4.02
12	FM	- 25.333	- .023946	+ .023946		FH	+ 25.333	- .007982	+ .007982	
	RM	+ 13.001	+ .008589	- .013223		RH	+ 1.779	+ .002178	- .003469	
	M	- 12.332	- .015357	+ .010723	- 76.34	H	+ 27.112	- .005804	+ .004513	+ 4.01
21	FM	+ 25.333	+ .023946	- .023946		FH	- 25.333	+ .007982	- .007982	
	RM	- 1.234	- .008843	+ .014525		RH	- 1.779	- .002178	+ .003469	
	M	+ 24.099	+ .015103	- .009421	+ 89.73	H	- 27.112	+ .005804	- .004513	- 4.01
20	FM	0	0	+ .008310		FV	0	0	- .000437	
	RM	+ .598	- .007327	+ .012157		RV	- .031	+ .000386	- .000640	
	M	+ .598	- .007327	+ .020467	+ 6.55	V	- .031	+ .000386	- .001077	- .34
23	FM	- 25.333	0	- .023946		FH	+ 25.333	0	- .007982	
	RM	+ .636	- .007776	+ .012900		RH	+ .091	- .001111	+ .001843	
	M	- 24.697	- .007776	- .011046	- 96.27	H	+ 25.424	- .001111	- .006139	+ 4.36
32	FM	+ 25.333	0	+ .023946		FH	- 25.333	0	+ .007982	
	RM	- .091	+ .001110	- .001842		RH	- .091	+ .001111	- .001843	
	M	+ 25.242	+ .001110	+ .022104	+ 84.25	H	- 25.424	+ .001111	+ .006139	- 4.36

Table 9

from which

$$EI\overleftarrow{\Delta_{1X}} = 5828 \text{ and } EI\overleftarrow{\Delta_{2X}} = 2377 .$$

Final Moments, Thrusts, and Shears are obtained by substituting the numerical values of $EI\Delta_{1X}$ and $EI\Delta_{2X}$ for the unknowns in Table 9 and are recorded in the columns denoted by Σ.

Example 2. A three span complex frame with dimensions and loads as shown (Fig. 8) is analyzed. The axis of the member $\overline{DE}$ is a parabola of 2^{o} and $EI_{\alpha} = EI \sec \alpha$.

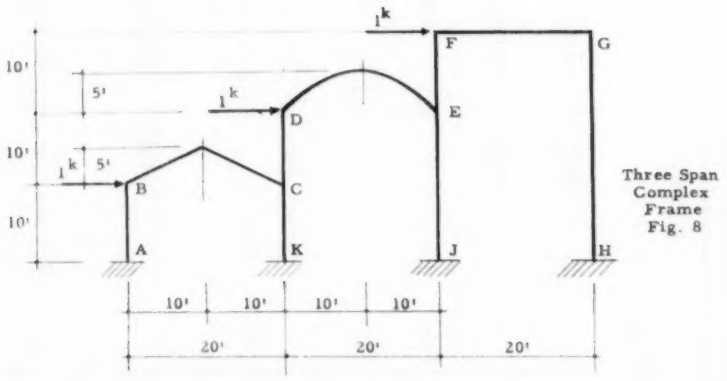

Three Span Complex Frame Fig. 8

The frame is resolved into five basic members: $\overline{ABC}$, $\overline{CDE}$, $\overline{EFGH}$, $\overline{EJ}$ and $\overline{CK}$. The moment distribution constants of members $\overline{ABC}$, $\overline{CDE}$ and $\overline{EFGH}$ are recorded in Tables 10, 11 and 12. The computation of column constants and distribution factors is not shown. Two independent horizontal displacements $\overleftarrow{\Delta_{CX}}$ and $\overleftarrow{\Delta_{EX}}$ are assumed. All fixed end moments, thrusts, and shears are listed in Table 14.

Distribution of Unbalanced Unit-Moment at Joints C and E is shown in Table 13. From Table 4

$$\frac{M_C}{X_{CE}} = \frac{M_E}{X_{CE}} = \frac{1}{1 - C_{CE}C_{EC}D_{CE}D_{EC}} = 1.021 .$$

The moment coefficients due to unbalanced unit-moment at C and E are denoted as $RM_{ij}^{(C)}$ and $RM_{ij}^{(E)}$, respectively.

Unbalance of Fixed End Moments

At Joint C: (From Table 14.)

$$\Sigma FM_C = -3.473 - .02361EI\overleftarrow{\Delta_{CX}} - .02163EI\overleftarrow{\Delta_{EX}}$$

Elastic Constants - Member $\overline{ABC}$ - Table 10

Member $\overline{ABC}$:

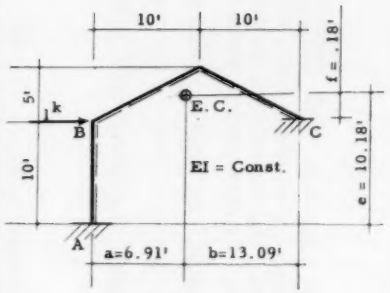

Basic Equivalents: (Eq. 5)

$a_{11} = \frac{32.36}{EI}$ $\quad a_{10} = -\frac{50}{EI}$

$a_{22} = \frac{1437}{EI}$ $\quad a_{20} = \frac{345.5}{EI}$

$a_{33} = \frac{520}{EI}$ $\quad a_{30} = \frac{342.5}{EI}$

$a_{23} = \frac{517.5}{EI}$ $\quad N = \frac{477000}{(EI)^2}$

Moment Distribution Constants:

$FM_{AC}^{(L)} = -1.750$ $\quad FM_{CA}^{(L)} = -1.611$ Eq. 9

$FM_{AC}^{(X)} = .02315EI\overset{\frown}{\Delta_{CX}}$

$FM_{CA}^{(X)} = -.01476EI\overset{\frown}{\Delta_{CX}}$ Eq. 10

$K_{AC} = .242EI$ $\quad K_{CA} = .223EI$ Eq. 12

$C_{AC} = -.335$ $\quad C_{CA} = -.364$ Eq. 13

Shear Equilibrium Constants:

$FH_{AC}^{(L)} = -.344$ $\quad FH_{CA}^{(L)} = .656$ Eq. 17

$\overleftarrow{FH}_{AC}^{(X)} = \overrightarrow{FH}_{CA}^{(X)} = .003011EI\overset{\frown}{\Delta_{CX}}$ Eq. 18

$S_{AC} = .08359$ $\quad S_{CA} = -.03577$ Eq. 23

Elastic Constants - Member $\overline{CDE}$ - Table 11

Member $\overline{CDE}$:

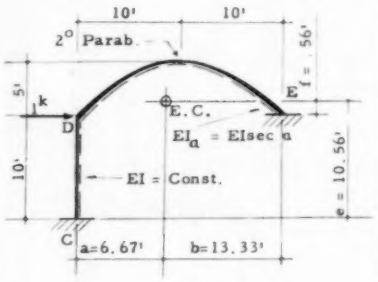

Basic Equivalents: (Eq. 5)

$a_{11} = \frac{30}{EI}$ $\quad a_{10} = -\frac{50}{EI}$

$a_{22} = \frac{1333.3}{EI}$ $\quad a_{20} = \frac{333.3}{EI}$

$a_{33} = \frac{590.7}{EI}$ $\quad a_{30} = \frac{361.1}{EI}$

$a_{23} = \frac{555.5}{EI}$ $\quad N = \frac{478700}{(EI)^2}$

Moment Distribution Constants:

$FM_{CE}^{(L)} = -1.862$ $\quad FM_{EC}^{(L)} = -2.116$ Eq. 9

$FM_{CE}^{(X)} = .02163EI(\overrightarrow{\Delta_{CX}} - \overrightarrow{\Delta_{EX}})$

$FM_{EC}^{(X)} = -.01702EI(\overrightarrow{\Delta_{CX}} - \overrightarrow{\Delta_{EX}})$ Eq. 10

$K_{CE} = .235EI$ $\quad K_{EC} = .271EI$ Eq. 12

$C_{CE} = -.421$ $\quad C_{EC} = -.365$ Eq. 13

Shear Equilibrium Constants:

$FH_{CE}^{(L)} = -.381$ $\quad FH_{EC}^{(L)} = .619$ Eq. 17

$\overrightarrow{FH_{CE}^{(X)}} = \overleftarrow{FH_{CE}^{(X)}} = .002785EI(\overrightarrow{\Delta_{CX}} - \overrightarrow{\Delta_{EX}})$ Eq. 18

$S_{CE} = .07761$ $\quad S_{CE} = -.03454$ Eq. 23

Elastic Constants - Member $\overline{EFGH}$ - Table 12

Member $\overline{EFGH}$:

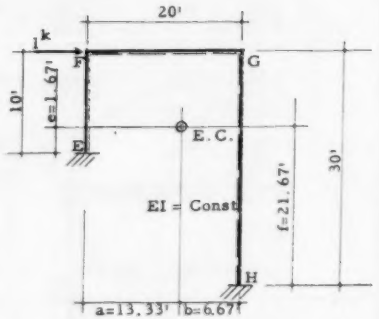

Basic Equivalents: (Eq. 5)

$a_{11} = \frac{60}{EI}$ $\quad a_{10} = -\frac{50}{EI}$

$a_{22} = \frac{4000}{EI}$ $\quad a_{20} = \frac{666.6}{EI}$

$a_{33} = \frac{5167}{EI}$ $\quad a_{30} = -\frac{83.3}{EI}$

$a_{23} = -\frac{2333}{EI}$ $\quad N = \frac{15225000}{(EI)^2}$

Moment Distribution Constants:

$FM_{EH}^{(L)} = -6.185$ $\quad FM_{HE}^{(L)} = -1.149$ Eq. 9

$FM_{EH}^{(X)} = .002481EI\overrightarrow{\Delta_{EX}}$

$FM_{HE}^{(X)} = .004671EI\overrightarrow{\Delta_{EX}}$ Eq. 10

$K_{EH} = .0845EI$ $\quad K_{HE} = .1108EI$ Eq. 12

$C_{EH} = -.456$ $\quad C_{HE} = -.348$ Eq. 13

Shear Equilibrium Constants:

$FH_{EH}^{(L)} = -.920$ $\quad FH_{HE}^{(L)} = .080$ Eq. 17

$\overrightarrow{FH_{EH}^{(X)}} = \overleftarrow{FH_{HE}^{(X)}} = .000263EI\overrightarrow{\Delta_{EX}}$ Eq. 18

$S_{EH} = .01204$ $\quad S_{HE} = -.03795$ Eq. 23

CA	CK	CE	EC	EJ	EH	
.260	.466	.274	.488	.360	.152	D
-.364	+.500	-.421	-.365	+.500	-.456	C
-.265	-.476	-.280				
			+.118			
			-.0576	-.0425	-.0179	
		+.0210				
-.265	-.476	-.259	+.0604	-.0425	-.0179	$RM^{(C)}$
			-.498	-.368	-.155	
		+.1818				
-.0473	-.0847	-.0498				
			+.0210			
-.0473	-.0847	+.1320	-.477	-.368	-.155	$RM^{(E)}$

AC	KC	
+.0965	-.238	$RM^{(C)}$
+.0172	-.0423	$RM^{(E)}$

JE	HE	
-.0212	+.0082	$RM^{(C)}$
-.184	+.0707	$RM^{(E)}$

Distribution of Unbalanced Unit-Moment at Joints C and E
Table 13

At Joint E: (From Table 14.)

$$\Sigma FM_E = -8.301 - .01702EI\overrightarrow{\Delta_{CX}} + .00450EI\overrightarrow{\Delta_{EX}}$$

Moments Due to Rotation of Joints in terms of loads and unknown displacements and defined as

$$RM_{ij} = RM_{ij}^{(C)}\Sigma FM_C + RM_{ij}^{(E)}\Sigma FM_E$$

are recorded in Table 14. $RM_{ij}^{(C)}$ and $RM_{ij}^{(E)}$ are the end moments due to the unbalance of unit moment at C and E, respectively.

Thrusts Due to Rotation of Joints in terms of loads and unknown displacements as given by Equation 23 and end shears in columns are recorded in Table 14.

		End Moments				End Forces				
	⊕	LOAD	$EI\Delta_{CX}$	$EI\Delta_{EX}$	Σ	+	LOAD	$EI\Delta_{CX}$	$EI\Delta_{EX}$	Σ
EC	FM	- 2.116	- .01702	+ .01702		FH	- .619	- .00279	+ .00279	
	RM	+ 3.750	+ .00669	- .00345		RH	+ .145	- .00007	- .00060	
	M	+ 1.634	- .01033	+ .01357	+ 7.23	H	- .474	- .00286	+ .00219	+ .19
ET	FM	0	0	- .01500		FV	0	0	+ .00006	
	RM	+ 3.202	+ .00727	- .00074		RV	- .240	- .00055	+ .00150	
	M	+ 3.202	+ .00727	- .01574	- 4.25	V	- .240	- .00055	+ .00156	+ .53
EH	FM	- 6.185	0	+ .00248		FH	- .920	0	+ .00026	
	RM	+ 1.349	+ .00306	- .00031		RH	+ .040	+ .00009	- .00001	
	M	- 4.836	+ .00306	+ .00217	- 2.99	H	- .880	+ .00009	+ .00025	- .72
JE	FM	0	0	- .01500		FV	0	0	- .00006	
	RM	+ 1.601	+ .00363	- .00037		RV	+ .240	+ .00055	- .00150	
	M	+ 1.601	+ .00363	- .01537	- 6.38	V	+ .240	+ .00055	- .00156	- .53
ME	FM	- 1.149	0	- .00467		FH	- .080	0	- .00026	
	RM	- .615	- .00140	+ .00014		RH	- .040	- .00009	+ .00001	
	M	- 1.764	- .00140	- .00453	- 4.61	H	- .120	- .00009	- .00025	- .28

Table 14 (con'd.)

	End Moments					End Forces				
	↻+	LOAD	$EI\Delta_{CX}$	$EI\Delta_{EX}$	Σ	→ +	LOAD	$EI\Delta_{CX}$	$EI\Delta_{EX}$	Σ
AC	FM	- 1,750	- .02315	0		FH	- .344	- .003011	0	
	RM	- .478	- .00267	- .00201		RH	- .087	- .00047	- .00037	
	M	- 2.228	- .02572	- .00201	- 8.57	H	- .431	- .00348	- .00037	- 1.34
CA	FM	- 1.611	+ .01476	0		FH	- .656	+ .00301	0	
	RM	+ 1.313	+ .00706	+ .00552		RH	+ .087	+ .00047	+ .00037	
	M	- .298	+ .02182	+ .00552	+ 7.24	H	- .569	+ .00348	+ .00037	+ .34
CK	FM	0	- .06000	0		FV	0	+ .01200	0	
	RM	+ 2.356	+ .01268	+ .00992		RV	- .353	- .00190	- .00149	
	M	+ 2.356	- .04732	+ .00992	- 1.59	V	- .353	+ .01010	- .00149	+ .85
CE	FM	- 1.862	+ .02163	- .02163		FH	- .381	+ .00279	- .00279	
	RM	- .196	+ .00387	+ .00620		RH	- .145	+ .00007	+ .00060	
	M	- 2.058	+ .02550	- .01543	- 5.65	H	- .526	+ .00286	- .00219	- 1.19
KC	FM	0	- .06000	0		FV	0	- .01200	0	
	RM	+ 1.178	+ .00634	+ .00496		RV	+ .353	+ .00190	+ .00149	
	M	+ 1.178	- .05366	+ .00496	- 6.86	V	+ .353	- .01010	+ .00149	- .85

Table 14

Equations of Shear Equilibrium

At Joint C: (From Table 14.)

$$\Sigma F_{CX} = 0 = 1.4486 - .016432EI\widehat{\Delta_{CX}} + .003306EI\widehat{\Delta_{EX}}$$

At Joint E: (From Table 14.)

$$\Sigma F_{EX} = 0 = 1.5941 + .003310EI\widehat{\Delta_{CX}} - 003994EI\widehat{\Delta_{EX}}$$

from which

$$EI\widehat{\Delta_{CX}} = 202.2 \text{ and } EI\widehat{\Delta_{EX}} = 566.7 .$$

Final Moments, Thrusts, and Shears are obtained by substituting the numerical values of $EI\Delta_{CX}$ and EI_{EX} for the unknowns in Table 14. The final answers are shown in the same table in the columns denoted by Σ.

REFERENCES

1. "Analysis of Continuous Frames by Distributing Fixed-End Moments," by Hardy Cross, Transactions, ASCE, Vol. 97, 1932, pp. 1-10.
2. Ibid, Discussion, Donald E. Larson, pp. 127-133.
3. "Continuous Frames of Reinforced Concrete," by Hardy Cross and N. D. Morgan, John Wiley and Sons, Inc., New York, 1932, pp. 316-326.
4. "Analysis of Multiple Arches," by A. Hrennikoff, Transactions, ASCE, Vol. 101, 1936, pp. 221-223.
5. "The Analysis of Single-Story Multi-Bay Gabled Rigid Frames," by A. J. Francis, Structural Engineer, London, Vol. 29, No. 7, 1951, pp. 189-202.
6. "An Exact Method of Analysis of Continuing Parabolic Arches," by V. A. Morgan, Conc. and Const. Eng., London, Vol. 47, No. 11, 1952, p. 343.
7. "Multiple Span Gabled Frames," by J. D. Griffiths, Transactions, ASCE, Vol. 121, 1956, pp. 1288-1307.
8. Ibid, Discussion, A. F. Diwan, pp. 1308-1315.
9. "Statically Indeterminate Structures," by L. C. Maugh, John Wiley and Sons, Inc., New York, 1946, pp. 230-242.
10. "Řešení Spojitého Oblouku Na Pružných Pilířích Methodou, Rozdělování Momentu," by Antonín Bebr, Technický Obzor, Praha, 1949, p. 185.
11. "Berechnung Gekruemmter Rahmen Staebe nach dem Moment-ausgleichverfahren," by H. Lindner, Bautechnik, Vol. 31, No. 5, 1954, pp. 152-155.
12. "Continuous Arches on Elastic Piers," by James Michalos and D. D. Girton, Proceedings, ASCE, Vol. 81, 1956, Paper No. 827.
13. "Analysis of Continuous Arches on Flexible Piers," by W. E. Riley, Journal, ACI, Vol. 28, No. 10, 1957, pp. 999-1012.

14. "Continuous Arches on Elastic Supports (Elastic Foundations)," by J. J. Polivka, Der Brueckenbau, Heidelberg, 1920, Vols. 4, 5, and 6.

15. "Equilibrium Equations Without Restraining Forces for Moment Distribution - Sway Problems," by P. M. Ferguson, Bureau of Engineering Research, University of Texas, Austin, Circular No. 13, 1950.

16. "Analysis of Symmetrical and Unsymmetrical Curved Member Frames by Moment Distribution," by K. W. Havner, M. S. Report, Oklahoma State University Library, Stillwater, 1956.

17. "Moment Distribution in Frames With Bent Members," by Frank Hedges, M. S. Report, Oklahoma State University Library, Stillwater, 1956.

18. "Analysis of Continuous Frames by Distributing Fixed-End Moments," by Hardy Cross, Transactions, ASCE, Vol. 97, 1932, p. 150.

19. "Continuous Frames of Reinforced Concrete," by Hardy Cross and N. D. Morgan, John Wiley and Sons, Inc., New York, 1932, pp. 124-125.

20. "Influence Lines for Frames," by Jan Tuma, Oklahoma Engineering Experiment Station Publication, Oklahoma State University, Stillwater, No. 85, 1952.

21. "Numerical Moment Distribution by Infinite Series," by G. J. Johnson, M. S. Report, Oklahoma State University Library, Stillwater, 1953.

22. "Analysis of Continuous Beams by Infinite Series," by Jan Tuma and M. T. Anderson, Oklahoma Engineering Experiment Station Publication, Oklahoma State University, Stillwater, No. 91, 1954.

23. "Sequence Summation Factors," by Andrian Pauw, Proceedings, ASCE, Vol. 81, Paper No. 763, 1955 and discussion by Polivka, Weleef and Giangreco.

24. "Analysis of Rigid Frames by Balancing Members Series," by Torazo Yoshimura, Memoirs of the Faculty of Engineering, Kumamoto University, Kumamoto, Japan, 1955.

25. "Balancing Member Series by Parts," by T. Yochimura and T. Marakami, Memoirs of the Faculty of Engineering, Kumamoto University, Kumamoto, Japan, 1955.

26. "Plain and Reinforced Concrete Arches," by J. Melan, John Wiley and Sons, Inc., New York, 1917, pp. 71-78.

27. "Die Statik Im Stahlbetonbau," by Kurt Beyer, Springer Verlag, Berlin 1948, pp. 347-349.

28. "Slope Deflection Equations for Curved Members," by K. T. Fowler, Transactions, ASCE, Vol. 116, 1951, pp. 125-143.

29. "Analysis of Statically Indeterminate Structures," by J. I. Parcel and R. B. Moorman, John Wiley and Sons, Inc., New York, 1955, pp. 408-430.

30. "The Column Analogy," by Hardy Cross, Engineering Experiment Station Bulletin, University of Illinois, Urbana, No. 215, 1930.

31. "Elementary Structural Analysis," by J. B. Wilbur and C. H. Norris, McGraw-Hill, Inc., New York, 1948, p. 454.

32. "Examples of Plastic Design for Structural Steel," by E. R. Estes, University of Kansas Structural Conference, Lawrence, Kansas, 1956.

Paper 1787 September, 1958 ST 5

Journal of the
STRUCTURAL DIVISION
Proceedings of the American Society of Civil Engineers

CONTENTS

DISCUSSION
(Proc. Paper 1787)

Page

Distribution of Loads on Bridge Decks, by A. M. Lount. (Proc. Paper 1303, July, 1957. Prior discussions: 1442, 1522, 1576. Discussion closed.)
by A. M. Lount (closure) 1787-3

Vibration Susceptibilities of Various Highway Bridge Types, by Leroy T. Oehler. (Proc. Paper 1318, July, 1957. Prior discussions: 1442, 1522. Discussion closed.)
by Leroy T. Oehler (closure) 1787-7

University Research in Structural Engineering, by Frank Baron. (Proc. Paper 1357, September, 1957. Prior discussion: 1522, 1576. Discussion closed.)
by Frank Baron (closure). 1787-9

Torsion Anaylysis for Suspention Bridges, by Nan-Sze Sih. (Proc. Paper 1431, November, 1957. Prior discussion: 1576. Discussion closed.)
by Nan-Sze Sih (closure) 1787-13

The Design of Rigid Frame Bents, by Richard Z. Zimmermann, Jr. (Proc. Paper 1434, November, 1957. Prior discussion: 1576, 1656. Discussion closed.)
by Richard Z. Zimmermann, Jr. (closure) 1787-17

Ultimate Strength Analysis of Long Hinged Reinforced Concrete Columns by Bengt Broms and I. M. Viest. (Proc. Paper 1510, January, 1958. Prior discussion: 1576, 1721. Discussion closed.)
by T. Jumikis and A. S. Hall. 1787-19

(Over)

Note: Paper 1787 is part of the copyrighted Journal of the Structural Division, Proceedings of the American Society of Civil Engineers, Vol. 84, ST 5, September, 1958.

Page

Tentative Recommendations for Prestressed Concrete: Report of the Joint ACI-ASCE Committee of Prestressed Reinforced Concrete. (Proc. Paper 1519, January, 1958. Prior discussion: 1656, 1721. Discussion closed.)
by Charles D. Susman 1787-21

Lateral Bracing of Columns and Beams, by George Winter. (Proc. Paper 1561, March, 1958. Prior discussion: 1656. Discussion closed.)
by Marvin A. Larson 1787-25
by Giles G. Green 1787-35
by Bruce G. Johnston 1787-39
by A. Chibaro 1787-40

Numerical Solutions for Beams on Elastic Foundations, by Henry Malter. (Proc. Paper 1562, March, 1958. Prior discussions: none. Discussion closed.)
by Alexander Dodge 1787-41
by Lymon C. Reese 1787-57

Earthquake Response of Elevated Tanks and Vessels, by D. F. Moran and J. A. Cheney. (Proc. Paper 1563, March, 1958. Prior discussion: none. Discussion closed.)
by A. A. Eremin 1787-63

Moments in Beams by the Method of Partial Moment, by Harry Posner. (Proc. Paper 1567, March, 1958. Prior discussion: 1721. Discussion closed.)
by A. A. Eremin 1787-65

Deflection Limitations of Bridges: Progress Report of the Committee on Deflection Limitation of Bridges of the Structural Division. (Proc. Paper 1633, May, 1958. Prior discussion: none. Discussion open until November 1, 1958.)
by Fritz Leonhardt 1787-67

Specifications for Preservative Treatment of Timber: Progress Report of the Sub-Committee on Timber Structures of the Structural Division. (Proc. Paper 1637, May, 1958. Prior discussion: none. Discussion open until November 1, 1958.)
by W. H. O'Brien 1787-69

Wind Forces on Structures: Nature of the Wind, by Robert H. Sherlock. (Proc. Paper 1711, July, 1958. Prior discussion: none. Discussion open until January 1, 1959.)
Corrections 1787-71

DISTRIBUTION OF LOADS ON BRIDGE DECKS[a]

Closure by A. M. Lount

A. M. LOUNT,[1] A. M. ASCE.—The writer is much indebted to the interest taken in his outline of the potential application of the electronic computer to engineering problems.

With regard to Mr. Naruoka's comments on fatigue, the point which the writer was making was that, with transverse load distribution, the maximum stress in a given member on a bridge structure can only be reached when all the lanes producing that maximum stress are loaded. Single loading on the bridge with diaphragms will not create a stress as close to the allowable working stresses in the structure as in the case of a bridge without transverse distribution. Therefore, the stress level in the bridge with distribution under normal highway loading is bound to be maintained at a lower value.

We can therefore tolerate a greater cycle of loadings on bridge structures so designed.

Mr. Naruoka is correct in assuming that the writer referred to the diaphragm as the load distributing cross beam and not the lateral and sway bracing. It is agreed that maximum saving can be achieved in structures with high live load to dead load ratios. The writer has, in several instances, found that there is a considerable saving over the loading as specified by AASHO. The diagram in the original article showing the maximum design moments for the "Big East River" bridge shows the loads for which the girders would have to be designed under the AASHO specification, and the corresponding loads under the load distribution theory. As may be seen from this, there is a considerable reduction in the moment for which the beams must be designed. There has been recently a case where a four girder bridge with unequal spacing was approximately 20 per cent lighter than the corresponding structure designed under AASHO specifications. A contributing factor to this is the limitation of depth on the girders. None of the existing wide flange sections could be made to satisfy design stresses in a four girdered layout under AASHO empirical loadings. However, allowing for the distribution due to the diaphragms we were able to use four 36 inch deep beams instead of five.

The writer agrees with Mr. Naruoka's general observations on wider bridges when the spacing of the girders is maintained constant. It has been found, however, that diaphragm loading enables the designer to widen the spacing between the girders, thereby achieving considerable saving. There is often little advantage to going to a grid type of design if the spacing is maintained at 5 or 6 feet. However, using spacings of 8 to 9 feet between

---

a. Proc. Paper 1303, July, 1957, by A. M. Lount.

1. Partner, T. O. Lazarides, Lount and Partners, Cons. Engrs., Toronto, Canada.

girders does achieve substantial savings in the structure. This appears to be the key to success in using load distribution.

The elastic calculations on the Niagara Bridge did not include any allowance for torsion whatsoever. The Massonnet figures were shown as compared to the Guyon figures to obtain a relative idea of the amount of torsion. If to the difference between the Massonnet and Guyon lines you add the extra amount due to the effect Mr. Naruoka mentions and then to this is added the total torque allowance to the line for elastic non-torque distribution, it will be seen that the results are almost in complete correspondence.

The writer has recently completed a design for a skew bridge with diaphragms at right angles. In this case the effect of the diaphragm is most pronounced since not only does it contribute to lateral distribution between individual girders, but it also has an effect similar to that encountered in skew slabs, i.e. the effective span length is shortened.

Of course, it must be borne in mind that the development of this strict analytical theory has as its main purpose the incorporation of this design into electronic computer analysis. It is far easier in a computer to calculate something precisely than it is to select values from tables.

The writer is most gratified to see the valuable contribution to this discussion by Mr. Fok. He has covered several points which could be fully covered within the scope of the paper. Of particular interest are the comments on the number of required significant figures in the calculations.

There are many methods of utilizing the point interaction forces. The method outlined by Mr. Fok appears to be quite effective. The method now in use by the writer on grids with up to 12 grid points involves the following procedure: (1) Linear lateral and longitudinal interpolation of the load, assuming supports at each grid point. (2) Determination of "secondary" moments. (3) Release of assumed supports. (4) Calculation of moments due to release. (5) Summation.

A less tedious procedure at this stage, even with computer assistance, is most welcome.

Mr. Balog's ideas are of great interest since they represent a strong discussion in favour of the empirical approach. Mr. Balog has presented his case with clarity. However, the writer believes that the proponents of the empirical approach overlook a few very important factors:

(1) Electronic computation does not represent a complex approach. It is a popular misconception that a problem solved by computer must be complicated. In fact, the theory behind the whole computer approach is much simpler, is not open to the same question as the empirical methods mentioned, and is applicable to any case. In fact, it is a rational approach which could be readily used under the permissive paragraphs of AASHO.

(2) Measurements on existing bridges can only be used to evolve empirical formulae suitable for structures with exactly the same basic characteristics.

(3) Torsion was not considered as effective on the Niagara bridge as a matter of design policy, not because the computer approach could not be extended. It is interesting to note at this point an understandable reluctance on the part of public authorities to place too much reliance on torsion, when, in fact, we have little reliable information on the behaviour of prestressed concrete under prolonged application of this type of loading.

(4) Torsion is only a major factor in reducing costs where heavily eccentric loadings are applied to bridges with very stiff diaphragms.
(5) Neglecting torsion is inevitably on the side of safety.
(6) Rational approach when based on valid assumptions, i.e. stiffness of girders, modulus of elasticity of component materials, enables the computation of any grid situation: continuous, with variable moments of inertia or with right diaphragms on skew structures. The simple fundamental theory is applicable to any one of these cases. As an example we attach the load distribution chart for a skew bridge 1) with skew diaphragms and 2) with right diaphragms. This clearly shows the increased effectiveness of the right diaphragms. The writer knows of no existing method other than the rational approach to provide a satisfactory general solution to this problem. It can of course be readily extended to consider torsion.
(7) The cost of an exact computer solution is usually less than that required to apply (and justify to the proper authorities) an empirical approach.

Mr. Makowski has contributed a very useful bibliography on this subject.

With reference to the various methods developed in Europe for the computation of interconnected bridge systems, these are for the most part based on a symmetrical arrangement of square bridges consisting of simple span girders with constant moments of inertia. Both girders and diaphragms are at uniform spacing. In fact, some theories require all girders or diaphragms to have identical moments of inertia.

This happy state of affairs virtually never exists. The extension of most methods to even a few of the variations has not, in our experience, been either valid or very useful.

On structures with variable girder or diaphragm spacing and moment of inertia, we have found wide variation in the results obtained by means of Leonhardt's tables, by means of charts published by the Cement and Concrete Institute, and by what we now term rational analysis. A chart, however simple to use, is useless unless it gives correct results or results sufficiently correct so as to permit close design. As a result of many comparisons over a number of cases, the writer has come to the conclusion that, except in the case of structures reasonably close to those for which the theory assumptions were made, no great reliance can be placed on charts. Square bridges are the exception rather than the rule. Non-uniform girder spacing is more economical and logical than uniform spacing. We need a single theory to cover all cases with no exceptions.

The extension of the so-called rational approach to the problem of diaphragm-skew bridges is simple and straightforward. The additional savings resulting from the "reduced span" effect is appreciable.

The availability of computers is now quite different from the situation as it existed here a few years ago or as it may now still exist in Europe. Maybe there computers are beyond the reach of most engineers. This just is not so in Canada and the United States. There are at least twenty computers of various sizes and types available in Toronto alone. The basic program is simple. In case a specially written program is not available, a regular matrix inversion program may be used quite readily.

Twelve decimal or "double precision" accuracy is advisable for continuous structures or for systems with more than eight unknowns if it is desired to apply structural checks such as reciprocity.

The writer agrees that, insofar as the diaphragms are concerned, a single diaphragm at the centre of the bridge is the most efficient for moment distribution.

However, it must be remembered that shear must be distributed as well as moments. This was a major factor in the design of the Big East River Bridge. A different diaphragm arrangement would have required thicker web plates. Also there are considerations of maximum diaphragm spacing and shop practice.

In summary, the advent of the electronic computer enables us to review our approach to problems. The methods we would use manually are not necessarily the ones we would use on a computer.

VIBRATION SUSCEPTIBILITIES OF VARIOUS HIGHWAY BRIDGE TYPES[a]

Closure by LeRoy T. Oehler

LEROY T. OEHLER,[1] A. M. ASCE.—In reply to Mr. Etkin concerning the unusual agreement of the calculated and experimental values of fundamental natural frequency, the writer would like to point out that the per cent error did not average less than one per cent as Mr. Etkin stated, but was an average of 1.48 per cent for the eight simple spans, 1.53 per cent for the average of seven continuous spans, and 3.65 per cent for the two cantilever-type bridge spans. Thus the average error for the 17 spans was 1.75 per cent. The assumed modulus of elasticity of the concrete and the method of obtaining the effective moment of inertia of the cross section, for the case of composite and non-composite beam spans, was the same for all bridge spans tested, and was exactly the same as reported in the second reference to the paper. (This was reported previous to the start of the subject bridge test program.)

The modulus of elasticity of concrete for natural frequency computations was assumed to be 5×10^6 psi. (p. 40 of the report) regardless of the age of the concrete in the bridges, which varied from two to seven years. This value for the modulus was selected as being reasonably representative of the dynamic modulus of elasticity of concrete. Of the factors influencing the value of the theoretical fundamental natural frequency, only the modulus of elasticity, E, and the effective moment of inertia of the cross section, I, cannot be determined precisely. However, for the composite spans (9 of the 17) the moment of inertia can be considered as the full composite cross-section of steel and concrete, and since the E for steel is known rather precisely, the only pure assumption concerns the value of the modulus of elasticity of the concrete. In order to show that this assumption can be materially incorrect without greatly affecting the calculated theoretical fundamental natural frequency of vibration, calculations were made for spans 2, 4, and 5 of bridge B1 and B2 of 33-6-4 for an E of concrete of 3.75×10^6 psi., and 7.5×10^6 psi., in addition to 5×10^6 psi. Lowering the E of the concrete by 25 per cent results in an increase of only 5.1 per cent in the calculated fundamental natural frequency of vibration. Increasing the E of the concrete by 50 per cent lowered the calculated frequency of vibration by 3.4 per cent. Thus the assumed E of the concrete might be considerably in error without resulting in an error of more than 3 or 4 per cent in the calculated natural frequency of vibration. In line with this observation, an average error of 1.75 per cent does not appear to unreasonably precise. In accordance with the AASHO specifications for deflection calculations, the modulus of elasticity of the

a. Proc. Paper 1318, July, 1957, by Leroy T. Oehler.

1. Physical Research Engr., Office of Testing and Research, Michigan State Highway Dept., Lansing, Mich.

concrete was assumed to be 3×10^6 psi. (p. 40 of the report). Using two values for the modulus of elasticity of concrete for two different purposes, deflection and frequency of vibration is reasonable and consistent since in the first case the secant modulus is a reasonable selection and for vibration a tangent modulus at small loads, or initial tangent modulus, is reasonable.

In reply to Mr. Naruoka concerning the ratio of observed to theoretical deflection, it should be emphasized that the theoretical deflections were computed as prescribed by the AASHO specifications for Highway Bridges. It was realized at the outset that these theoretical deflections would not agree with the experimental values, but since deflections are computed for design purposes on the basis of this specification it appeared as a logical standard for comparison between theoretical and experimental deflections. The load distribution action of the bridge deck was also calculated on the basis of the AASHO Specifications.

In the calculation of the theoretical values of the fundamental natural frequency of vibration, the AASHO Specifications do not prescribe calculation methods, assumptions for the modulus of elasticity of the concrete, or the effective contribution of the bridge deck to the moment of inertia for non-composite spans; therefore any logical method which gives reasonable agreement between calculated and experimental values appeared practical. The method used, as previously stated, was developed prior to the bridge testing reported in this paper and was based on simple beam theory. Mr. Naruoka suggests that better agreement could have been obtained between calculated and observed values if the fundamental natural frequency of vibration had been calculated by the theory for the orthotropic plate, especially when the ratio of width to length of span approaches one. In this connection the ratio of width to span length ranged from 0.544 to 0.702 with an average of 0.625 for the eleven simple spans. This same ratio varied from 0.477 to 1.19 with an average of 0.88 for the seven continuous spans, and from 0.323 to 1.27 with an average of 0.619 for the 16 cantilever-type spans. Even though the ratio of width to span length did vary widely in the bridge spans tested, the difference between the theoretical fundamental natural frequency of vibration and the observed value was not appreciably affected. It appeared that the accuracy obtained on the basis of calculations based on simple beam theory was satisfactory for design purposes, and a more complicated method for calculating the fundamental frequency of vibration was not desirable or required.

UNIVERSITY RESEARCH IN STRUCTURAL ENGINEERING[a]

Closure by Frank Baron

FRANK BARON,[1] M. ASCE.—The writer is indebted to the various discussers for their views. Apparently, each discusser would welcome additional remarks regarding proper ethical standards of university research practice. The writer will restrict his remarks to matters of black and white and will not deal with matters of the different shades of gray. The latter shades however are much less confusing than some individuals, other than the discussers, would make of them.

At the outset, the moral code of the great teachers of mankind, the code of ethics of our parent society, and the rules and regulations of any university should serve as effective guides to ethical standards of university practice. These codes and regulations are available to any faculty and are written in understandable language. Only an unthinking or a misguided person would attempt to distort them.

Existing regulations of a university usually prohibit the use of university facilities for the personal gain of individuals. For example:

> "University participation in tests and investigations shall be limited to activities which lead to the extension of knowledge or to increased effectiveness in teaching. Routine tasks of a common-place type will not be undertaken.
>
> University laboratories, bureaus and facilities are not to be used for tests, studies, or investigations of a purely commercial character, . . . except when it is shown conclusively that satisfactory facilities for such services do not exist elsewhere. . . . All persons other than members of the faculty, to be engaged in such research must be approved by the University. All payments made to members of the faculty or to other persons for their services in connection with such research shall be made solely by the University, except in case of any full time, permanent employee of the sponsoring agency. Acceptance of responsibilities by members of the faculty with reference to such research must not interfere with regular University duties, or be of a routine character undertaken primarily to supplement personal income."

The preceding quotation is from a standing regulation of the President of the University of California. The statement is clear and needs no further interpretation.

Referring to the specific comments of Professor Johnston, it would be naive to take for granted that research at any great university would attain

---

a. Proc. Paper 1357, September, 1957, by Frank Baron.

1. Prof. of Civ. Eng., Univ. of California, Berkeley, Calif.

high standards that would warrant its definition as an "objective search for truth". Such standards need continuous definition. They can only be defined by a competent faculty having the support of an able administration. The writer is in full agreement with Professor Johnston that research in any field, to be worthy of the name should be uncompromisingly "an objective search for truth". Any compromise in standards or in intellectual honesty would defeat university research. The latter is said in recognition that intellectual honesty does not come naturally to some individuals; it takes lots of work and training.[2]

In regard to trade associations and their sponsorship of research projects, they can be and usually are as objective in defining research as any university community. This is particularly apparent in the participation of their representatives in various research councils and technical committees of our engineering societies. The differences in views that sometimes occur are usually the result of loss of communication or exchange of ideas. They are sometimes the result of conflicting responsibilities. Worthy research projects can and will be sponsored by trade associations that have the promotion of a certain product or class of products as a major aim. The latter aim however is the business of an association and not of a university. In America, the tradition of universities reserving the right to publish their findings needs to be preserved. It is only by this means that universities can protect their integrity. Incidentally, it is the integrity and technical competence of a university faculty that are in demand by the engineering profession. Technical competence without integrity would in time be unacceptable.

The prerequisites for the selection of sponsored research as stated by Professor Brennan are excellent. The writer would modify his item 5 by removing the word faculty and substituting research staff for it. Otherwise, academic freedom and university scholarship can be and often are sacrificed. If budgetary problems for faculty salaries should exist, and they do, they should be solved by other means than through sponsored research. They might even have to be lived with.

The comments by Professor Brennan concerning the consultation activities of engineering teachers are pertinent to the discussion. Such activities are usually permitted with restrictions by universities. In no case should such employment be solicited or interfere with regular University duties.

As Professor Brennan has said, the consulting activities of a university faculty are intended for public service. They are also intended for teachers of professional subjects to maintain and improve professional competency. Permission to engage in such activities should not be seized upon by faculty as a license to engage in private practice. The code of ethics of our Society is specific on this point. Reference is made to Section 8 of this code.

Referring to Mr. Lane's comments, the writer will deal only with those pertaining to credit. Such credit as suggested by Mr. Lane is always given. It is a rare instance when a paper or a book is published by an individual wherein the concepts and ideas were initiated and developed by others but are presented as his own. Unfortunately, such an instance can and has occurred. It is then a gross violation of elementary ethics.

The writer will close by referring to Thomas Hobbes who developed a complete set of mathematical equations to explain ethics. It has been said

2. "Engineers and Ivory Towers", by Hardy Cross, McGraw-Hill Book Co., Inc., 1952, p. 88.

that his equations "plussed or minussed you to heaven or hell . . . so that none but the expert mathematician would ever be able to settle his accounts with Saint Peter." The writer sincerely hopes that he has not played Hobbes.

TORSION ANALYSIS FOR SUSPENSION BRIDGES[a]

Closure by Nan-Sze Sih

NAN-SZE SIH,[1] A. M. ASCE.—The writer would like to thank Mr. Chu for his interest and comments on the paper. The notations defined by Mr. Chu will certainly help the reading of this paper. There are few notations the writer would like to clarify further;

S = Panel shear in one plane of the horizontal bracing or the vertical truss (components of the axial stresses of the diagonals in the plane).

$\oint$ = Length measured along the perimeter of the cross section.

$L_s = \sum \int_o^l \frac{ds^3}{dx^2}$ for the cable (where ds is the arc length of the cable).

m = Simple beam bending moment.

Corrections for Eq. (4) and all other comments made by Mr. Chu are all in agreement with the writer.

The writer would like to take this opportunity to make few corrections of the paper, which was the result of the careful checking by Mr. H. Weissman during some office design work. And also to include here the solution for the general loading case, which was derived after the publication of the paper.

In Eq. (14) there is an equal to zero left out on the right hand side of the equation.

In Eq. (19) and (20) there are an factor one half left out on the right hand side of the equation.

In the constants for the examples H' should be 23200.

As a result of the above corrections, example A should be corrected as follows, with the corrected answers underlined.

	ΔH	$E\omega^*$	$\theta \cdot 10^5$	q_o	q_c	q_ω	q_h	q_v	S_h	S_v
1	---	---	9.83	9.89	2.85	---	7.04	7.04	634	127
2	---	-.013	9.25	do	2.69	-0.65	6.55	7.85	590	141
3	15	- --	9.7	do	2.98	---	6.91	6.91	622	124
4	15	-.013	9.1	do	2.8	-.65	6.44	7.74	580	140

a. Proc. Paper 1431, November, 1957, by Nan-Sze Sih.

1. Structural Engr., Ammann & Whitney Consulting Engr., New York, N. Y.

In example B, under this loading the center section only remains fixed in rotation with respect to the longitudinal axis of the bridge, and it is not fixed in longitudinal displacement. The results of the example should be corrected as follows;

$$T = 16000 \quad \Delta H = 0 \quad q_o = 4.95 \quad q_c = 1.26 \quad q_\omega = -.65$$

$$q_h = 3.04 \quad q_v = 4.34 \quad S_h = 273 \quad S_v = 78 \quad \sigma = o$$

The solution for the general loading case shown in Fig. 6;

$$A_1 = \frac{l}{\lambda}\frac{1}{\lambda^2 EJ}\frac{t_2 - t_2\cosh\lambda l + (t_1 - t_2)\cosh(l-\varphi)}{\sinh\lambda l} \qquad B_1 = \frac{t_1}{\lambda}\frac{1}{\lambda^2 EJ}$$

$$A_2 = \frac{1}{\sinh\lambda l}\left(\frac{t_2}{\lambda}\frac{1}{\lambda^2 EJ} - B_2\cosh\lambda l\right) \qquad B_2 = \frac{1}{\lambda}\frac{1}{\lambda^2 EJ}\left[t_1 - (t_1 - t_2)\cosh\lambda\varphi\right]$$

$$T_1 = t_1\varphi\left(1 - \frac{\varphi}{2l}\right) + \frac{t_2}{2}\left(1 - \frac{\varphi}{l}\right)^2 l \quad , \quad T_2 = t_1\varphi + t_2(l-\varphi) - T_1 = \frac{t_1\varphi^2}{2l} + \frac{t_2 l}{2}\left(1 - \frac{\varphi^2}{l^2}\right)$$

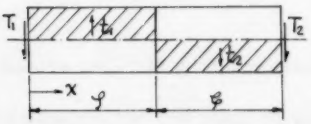

Fig. 6

In closing, to give a practical example, the writer would like to include here the results of the application of the analysis to the George Washington Bridge in connection with the addition of the lower deck.

The design live load for the bridge is 7200 pounds per foot of bridge, for torsional analysis, due to the unusual combination of the loading, specification calls use one half of the intensity of the live load to be placed in any position on the bridge.

The wind stresses was determined by the same principle that was first developed by Mr. Leon S. Moisseiff, which take into account the cable interaction.

Specification calls for the laterals to be designed either for 30 pound wind or L.L. + 15# W, with 25% increase in allowable stress.

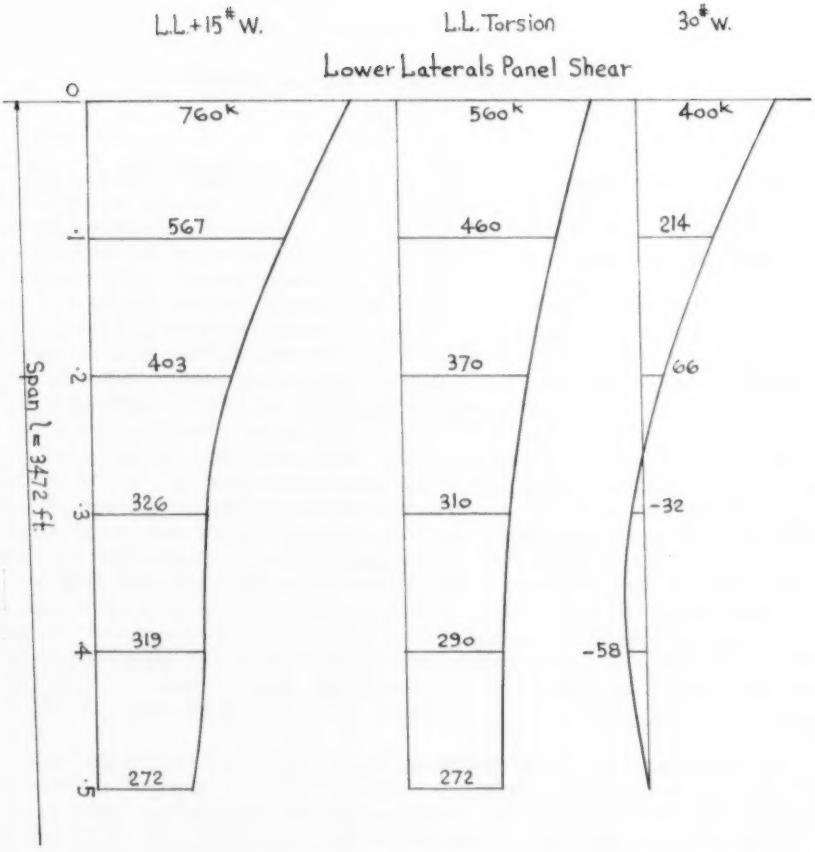
L.L.+15# W.
L.L. Torsion
30# W.
Lower Laterals Panel Shear
0
.1
.2
.3
.4
.5
Span l = 347.2 ft.
760k
567
403
326
319
272
560k
460
370
310
290
272
400k
214
66
-32
-58

Fig. 7

THE DESIGN OF RIGID FRAME BENTS[a]

Closure by Richard Z. Zimmermann, Jr.

RICHARD Z. ZIMMERMANN, JR.[1] A. M. ASCE.—The unexpected response to this paper was both gratifying and surprising. It was evident from the discussions that many people did not limit themselves to criticisms of the presentation or correction of arithmetical or typographical errors. On the contrary, most of the comments included a further amplification of the methods of analysis or supplemental information which represented the expenditure of a great deal of time and effort by the writers. This friendly exchange of ideas and voluntary labor on behalf of knowledge is in the highest tradition of a profession and the various discussions are eloquent testimony to the intellectual vigor of the civil engineering community.

The writer accepts, as semantically more proper, the comment by Mr. Gere that the title of the paper should have been "The Analysis of Rigid Frame Bents". In regard to original theoretical ideas, the short introduction, and the several references scattered throughout, testify to the modest scope of the paper. The writer is content to leave the development of entirely new analysis techniques to more brilliant and inventive minds.

In addition to the small errors of omissions pointed out by Mr. Gere, attention is directed to an incorrect algebraic sign in the distribution shown in Fig. 4. The second carry-over moment at the base of the lefthand column (designated point "A" on the bent) should read minus (-) 17.6 instead of plus. This will obviously increase the value of the fixed end moment there and alter slightly the value of the horizontal shear force computed on the previous page 1434-9.

The "principles of moment areas" presented by Mr. Hromadik for the analysis of the same bent are extremely intriguing. The method is a clear-cut application of fundamental theory and is quite consistent with the purpose of the paper. Mr. Hromadik's exposition also has the distinct advantage of being readily applicable to gabled bents composed of members having variable cross-sectional moments of inertia. The moment area principles should certainly have been included as a fourth method of analysis, since they are quite general in application and the computations may be systematically charted—as Mr. Hromadik has clearly shown.

The modification of the method of moment distribution presented by Mr. MacKenzie is an ingenious addition. However, such "short cuts" were considered as corollaries or supplemental information to the basic theory and consequently belong to the tool kit of the more advanced designer. Such useful adaptations or abbreviations are fairly numerous; but their inclusion in

a. Proc. Paper 1434, November, 1957, by Richard Z. Zimmermann, Jr.

1. Structural Engr., Day & Zimmermann, Inc., Philadelphia, Pa.

the paper seemed too much of a digression from the intended simple exposition of fundamental theory. This does not imply that special methods such as that presented by Messrs. MacKenzie and Bowles may not be very valuable knowledge for the practical design office.

The very gracious and indulgent comments of Mr. Eremin were also appreciated. As he points out, the method of graphical analysis offers several very real advantages. Perhaps the most conspicuous of these are speed, less vulnerability to accidental errors and a continuous picture of what is actually happening to the structural frame. This latter virtue helps the engineer to unconsciously develop a sympathetic "feel" for stresses in the structure as he proceeds with various load calculations.

The obvious objection to graphical solutions on 8-1/2 by 11-inch sheets that the results are not precise or "exact" is frequently not valid in practice. There are many situations where the live loads on the building frame are completely arbitrary assumptions based upon local building codes or the judgment of the individual engineer. Moreover, even the dead loads of a frame are seldom known with any accuracy until the individual members have been appropriately sized. On a concrete structure the dead loads are quite a significant factor. The results of a graphical analysis may always be checked by the classical computations, if desired.

Messrs. Tamanini and Mullins point out with complete justification that the "Method of Least Work" should logically have been included in the paper. The author quite agrees and wishes to thank those gentlemen for assiduously adding that presentation. The consideration of influence lines for moving loads is another subject in itself; but it is especially significant in a time when highway construction is being emphasized for the national economy.

Mr. Harris also discovered the erroneous algebraic sign in Fig. 4. The writer has no occasion to quarrel with most of Mr. Harris' comments, except to reiterate, somewhat defensively, that he had never intended to demonstrate the shortest possible analysis procedures. However, these special "Aspects" may be quite consistently included in the discussions.

It must be admitted that the writer has encountered few practicing engineers within his limited experience who scrupulously adhere to three significant figures in the moment distribution factors. The reason for this carelessness is not always mere indolence or intransigence; but often is produced by a healthy skepticism about the methods of American construction workers. The engineer who has seen steel plate stacked on precast roof plank decks or holes burned through the webs or flanges of steel beams for conduit or reinforcing steel bars placed upside down in the forms, is understandably unimpressed by a third decimal point. Sometimes he may be forgiven, but it must be conceded that accuracy is a virtue which is essential for some cases.

The point made by Mr. Lewis is well taken. Sign conventions and algebraic signs can be treacherous under any mathematical conditions. Perhaps because the writer is slightly more practiced with moment distribution methods, it always seemed easier to sense an error with that method that with Slope Deflection. Remembering Fig. 4 again, that may be a rash statement. At any rate, it is perfectly true that a check of the vertical shears in the bent does not imply that the moments need be correct for the frame analyzed.

All the contributors to the discussions should be sincerely complimented for their intellectual alertness and conscientious industry. Many of the discussions represented a great deal of time and tedious labor. This response speaks well for all engineers and seems to assure a healthy future for the profession.

ULTIMATE STRENGTH ANALYSIS OF LONG HINGED REINFORCED CONCRETE COLUMNS[a]

Discussion by T. Jumikis and A. S. Hall

T. JUMIKIS[1] and A. S. HALL,[2] A. M. ASCE.—The investigation of buckling in reinforced concrete lags far behind that of flexure, as regards both theory and experiment. The paper by the authors is therefore very welcome. Besides making a distinct contribution to the subject, it contains a most useful bibliography and will no doubt stimulate interest and discussion.

While agreeing with much of the theory put forward, there are one or two sections which the writers would like to discuss. First there is the question of the manner in which the columns fail. The authors divide these into buckling failures and material failures. As the definition of "buckling" they take the usual mathematical concept of instability. Presumably it is to be divorced from the idea of material failure. Now whether or not this idealized situation could occur in other media, it is certainly very difficult to imagine a true buckling failure in reinforced concrete. Furthermore the instability concept envisages a state of completely neutral equilibrium, whereas Bleich(1) suggests that this is, strictly speaking, the result of approximation. If in the basic differential equation the exact term is used for curvature instead of the approximate term $\frac{d^2y}{dx^2}$, the sharp discontinuity at the Euler load changes to a transition zone. In effect there is really no load for which the deflection is indeterminate. Every load is associated with a distinct deflection shape and consequently with specific strains and stresses in the material. Thus for any practical column the final collapse is still due to a material failure.

Incidentally, it would seem that the mathematical definition of buckling has very little application in the field of reinforced concrete, and indeed in many other fields of structural engineering. Most engineers would prefer to use the term buckling for cases where the applied bending moment is a function of the deflection. This definition has its pitfalls, and the writers would be interested to know if any satisfactory definition along these lines has been evolved.

In the work on eccentrically loaded columns the authors neglect the tensile strength of the concrete between cracks, admitting that this will lead to the predicted ultimate loads being somewhat lower than the actual. Coupled with this is the assumption of a cosine curve of deflection as a basis for the mathematical theory. This surely implies that the effective moment of inertia is

---

a. Proc. Paper 1510, January, 1958, by Bengt Broms and I. M. Viest.

1. Asst. Designing Engr., Julius Poole & Gibson, Cons. Engrs., Sydney, Australia.
2. Associate Prof. of Civ. Eng., N. S. W. University of Technology, Sydney, Australia.

constant throughout the length of the column, and hence that cracking takes place at close spacing over the full length. It is more likely that cracking will occur over a limited length near the mid-section, gradually extending as the load increases. This expectation is supported by photographs of tests such as those reported by Hognestad.* Work carried out at the New South Wales University of Technology by Brettle[2] suggests that the difference between the actual case and the assumption of uniformity is considerable. The effective moment of inertia of a cross-section immediately after cracking is very much smaller than its value before cracking, the reduction depending upon the steel percentage and upon the axial compression. Even after some simplification, the writers conceive the column as one which has a reduced section over the middle part of its length.

On this view the major part of the curvature will take place in this portion, and the deflected shape will not resemble a cosine wave, but may approximate more to a triangle with a rounded apex. Again, photographs of test specimens support this contention. It is possible that a number of test results discarded by investigators as being caused by local material faults have really been examples of the suggested behaviour. Such deviations from the cosine wave would involve more discrepancy in some ranges of slenderness than in others.

Any attempt to take account of discontinuity due to cracking leads to the necessity for some form of numerical analysis which, as the authors remark, is very laborious.

REFERENCES

1. Bleich, F., Buckling Strength of Metal Structures, McGraw-Hill, 1952.
2. Brettle, H. J., Flexural Strength and Elastic Properties of Pretensioned Beams, Ph.D. Thesis (unpublished).

*See Authors' reference No. 1.

TENTATIVE RECOMMENDATIONS FOR PRESTRESSED CONCRETE: REPORT OF THE JOINT ACI-ASCE COMMITTEE OF PRESTRESSED REINFORCED CONCRETE[a]

Discussion by Charles D. Susman

CHARLES D. SUSMAN,[1] J. M. ASCE.—Valuable as the recommendations of the Committee are to the engineering profession, a discussion of the background of the clauses would have enhanced even further the usefulness of the report. It was primarily the discussion features that made the Bureau of Public Roads Criteria,(1) and the article, "Application of AASHO Specifications to Bridge Design",(2) so valuable to the design engineer. It is highly unlikely that the Committee was unanimous on all points; and, since the report is meant as a recommendation rather than a specification, it would be a great help to the designer to know the varied opinions of some of the foremost authorities in the field.

Many of the Committee's recommendations are based on experimental results. It is difficult for anyone not engaged in research to keep up with the constant world-wide flow of new facts about prestressed concrete. The conscientious design engineer, therefore, would welcome a bibliography of all the experimental data that guided the Committee in the preparation of its report, so that he could make his own investigations in connection with his work.

It is laudable that the Committee did not wish the report to be used as a specification, and thereby perhaps retard the progress of prestressed concrete design. However, one must not overlook the fact that prestressed concrete is no longer being designed by specialists, but has become a common construction material together with conventional reinforced concrete, timber and structural steel. More and more engineers are designing in prestressed concrete, who have had no previous experience in this medium. More often than not, they are working under severe time and budgetary limitations that preclude adequate study of the subject. They need a Code to guide them, and they are using the Committee's report as a Code—the Committee's recommendations notwithstanding.

The writer knows of several instances in the Miami area where the report has been used as a Code, and its inclusion verbatim into the South Florida Building Code has been recommended by leading structural engineers in the area. With this in mind, the report ought to be written in such a way that its use as a Code, while not giving necessarily the best or most economical design, will give invariably a safe and adequate design. Otherwise, dangerous practices could result. It is not clear whether the report, in its present form, fulfills this function.

---

a. Proc. Paper 1519, January, 1958, by ASCE-ACI Joint Committee.

1. Structural Engr., Miami, Florida.

The Committee should be commended for the excellent discussion of fatigue in Article 206. This writer, however, feels that a concrete stress of 0.45 f'c should be allowed in the compressive zone of long span composite bridge beams, where the live load stress variation is small and the bulk of the stress is due to dead load.

The writer also questions the high tensile stresses allowed in the precompressed tensile zone of building members. Rapid obsolescence of buildings is quite common, and frequently, because of conversion, a building may have to sustain over a long period of time loads far greater than the ones it originally was designed for. The allowable tensile stress is approximately 80% of the modulus of rupture. Frequently the loads, dead or live, cannot be determined accurately with this margin. Any cracks in a member, designed for tensile stresses under working loads, will not close at the allowable stress value but only at zero tension. Even if the cracks themselves are not objectionable, they will reduce the moment of inertia, and thereby increase the deflection of the member. Furthermore, if the regions of high moment and shear coincide, (e.g. over supports of continuous beams and at points of concentrated loads), flexural tension, combined with the shear stress will cause high principal tensile stresses and early formation of cracks whose direction is close to normal to the horizontal axis.

Article 207.3.1b.2 allows high temporary tensile stresses provided non-prestressed reinforcement is furnished to resist the tensile forces. This Article further provides that the tensile stresses are to be computed on the basis of an uncracked homogeneous section. This seems to be in conflict with Article 207.2, which provides that non-prestressed reinforcement used in conformance with Article 207.3.1b.2 may be assumed stressed to 20,000 p.s.i. If the section is homogeneous and uncracked, as it will be at the concrete stresses that are recommended, then the maximum stress that can occur in the non-prestressed reinforcement equals "n" times the stress in surrounding concrete. This stress will be very low. Furthermore, creep and shrinkage will induce compressive stresses in the reinforcement that exceed the tensile stresses. Non-prestressed reinforcement will therefore not be effective as long as the section is uncracked. Hence, the contradiction between Articles 207.2 and 207.3.1b.2. A more thorough discussion of the subject can be found in Professor Lin's book, "Design of Prestressed Concrete Structures".(3)

Article 210.1.1 will be welcomed by all designers, who ever have had occasion to compute principal stresses, and confirms the writer's own experience. A designer, however, would feel more at ease if the formula in Article 210.2.1 were to be expressed in terms of shear and normal stress rather than ratios. More background discussion of the factor "1/2" in Article 210.2.2 also would be welcomed.

Article 212.3 provides that shear connections in composite construction be designed for ultimate load. This raises the question of the values of I and Q to be used at ultimate load when the section already may have cracked. The writer presumes that the bond values in Article 212.3.3 are based on the load being transmitted through the composite element and thereby include the benefit of increased friction due to compression normal to the shear surface. If the load is not applied in this manner, e.g., a hanging load, shear keys should be mandatory. In the absence of any recommendation by the Committee, shear keys can be designed by the elastic method. Full scale tests of composite sections on the Lower Tampa Bay Bridge several years ago failed to disclose any shear key distress even at ultimate load.

In conclusion, a word about load factors. The Committee quite properly emphasizes safety at ultimate loads and gives a set of load factors for the guidance of the designer. But if ultimate strength were the only consideration, one would not go to the trouble and expense of prestressing concrete. Ultimate strength is only half the story. The prestressed member should be homogeneous and within the elastic range under the entire gamut of loads, including wind and earthquake that it may conceivably expect to receive during its lifetime. What increases therefore, should be allowed for infrequent loads? How much, for instance, should the tensile stress be under combination of DL + LL + W, when it is zero under DL + LL alone? What should be the allowable stress in a bridge stringer when the design load is lighter than H-20, and the member has to resist a 100% overload required by the AASHO Specifications?(4) What should be the method of design in the elastic range of a member subject to both flexure and axial load? At the moment, each designer has his own ideas, and probably no two of them are alike. Some authoritative guidance on the subject would be welcome.

In closing, the writer would like to commend the Committee for the tremendous job it has accomplished and trusts that his few remarks will help contribute to further clarification of the subject.

REFERENCES

1. "Criteria for Prestressed Concrete Bridges", Dept. of Commerce, Bureau of Public Roads, 1954.
2. Eric L. Ericson and Neil Van Eenan, "Application and Development of AASHO Specifications to Bridge Design", ASCE Proceedings Paper 1320, July 1957.
3. T. Y. Lin, "Design of Prestressed Concrete Structures", Chapter 9, John M. Wiley, 1955.
4. The American Association of State Highway Officials, "Standard Specifications for Highway Bridges", Seventh Edition, 1957, Article 1.2.4.

LATERAL BRACING OF COLUMNS AND BEAMS[a]

Discussions by Marvin A. Larson, Giles G. Green, Bruce G. Johnston and A. Chibaro

MARVIN A. LARSON,[1] A. M. ASCE.—This excellent paper treats a subject on which but meager information is available in a form to be of aid to the practical designer. Our present design specifications give empirical rules for the design of members which are either laterally braced or unbraced, but are of little assistance in prescribing just what constitutes adequate lateral bracing. Professor Winter has explored this matter with regard to several problems involving the lateral buckling of compression members and compression elements of flexural members, and has illustrated rather simple procedures for determining whether the lateral support requirements, both as to strength and stiffness are met.

The principal deficiency of the paper is the implicit assumption that the relationships derived are directly applicable to problems commonly encountered in the design of practical structures. Actually, such is not the case, and some modifications of the procedure must be made, else erroneous results will be obtained. It will be shown that even with the specific examples used in the paper, the true condition is at considerable variance with that stated, and in some instances even in direct opposition.

As developed in the paper, the member under consideration is considered to be laterally supported at one or more points along its length through elastic members connected at the far end to a point considered fixed in space relative to the two ends of the primary member under consideration. This situation is, for practical purposes, achieved under the conditions of the laboratory test described in which the flexible sheet steel column was braced to the massive, rigid frame of the testing machine. In an actual structure, this situation might occur occasionally, as where a flexible beam or column may run parallel and adjacent to a relatively stiff and massive masonry wall to which it is attached at intervals. However, in the majority of cases, such as the columns of a long mill-type building, parallel beams of a floor system above the first floor of a building, and the upper chords of roof trusses, such a fixed point is not conveniently available for the attachment of bracing. In actual practice, bracing is most commonly effected by interconnecting various members of the structure (each of which may have little lateral stiffness by itself) in such a manner as to provide by combined action greater resistance to buckling than is provided by the sum of the individual members acting independently.

---

a. Proc. Paper 1561, March, 1958, by George Winter.

1. Civ. and Structural Engr., Hall, Pregnoff & Mather, San Francisco, Calif.

The floor system described in the paper, composed of two 18WF50 beams of 30 ft. span and 12 ft. spacing supporting a 16 ga. cellular steel deck will illustrate the significance of the support conditions. Using all dimensions and physical properties as in the original, this assembly is loaded as shown in Fig. 1a. From the original load-deflection curve, to produce deflections of 0.01" at points E and F, with both points moving in the same direction, jack loads of 1.0 kips each will be required at points B and C. Assigning this entire force to shear deformation stresses induced in the steel deck, we perceive that a total shear force of 1.0 kip is induced in the deck between points A and B, and likewise a shear force of equal magnitude but opposite sense between points C and D. The steel deck between points B and C is undeformed, hence develops no shear stresses.

Now let us load the same structural system as in Fig. 1b, this time applying loads so as to produce deflections of 0.01" at both points E and F, but in opposite directions. Again, total shear forces of 1.0 kips will be developed in the end panels AB and CD, but this time of like sense. In addition, the center panel of steel deck from B to C will be subjected to a shear deformation twice as great as the end panels, hence will develop a shear force of 2.0 kips of a sense opposite to that of the end panels. The jacking loads required to produce the deformation shown in Fig. 1b are 3.0 kips each at points B and C.

The implications of the above are immediately apparent. In all the relationships developed in the original paper, the lateral restraining force on a member at a point of lateral support was assumed to be a function of the lateral displacement of that point only, and independent of the lateral displacement of any other point on the member. In the present instance, such is not the case. The author, proceeding from a loading condition as shown in Fig. 1a derived an equivalent support rigidity of 100,000 lbs./inch, and then assumed that this applied also to conditions as shown in Fig. 1b. Actually, for Fig. 1b the support rigidity is 300,000 lbs./inch.

Since the action of a diaphragm in restraining lateral buckling is not properly represented by the equivalent elastic supports used by the author in deriving buckling equations, it will be necessary to start anew to develop relationships expressing the criteria for stability against lateral buckling. We must first recognize that the stabilizing force developed at a point is a function of the deflection not only of the point of attachment being considered, but of the deflection of adjacent points of lateral bracing as well. It will be convenient to express the resistance of the diaphragm to shear deformation as a function γ which is the total shear force required to produce a shear deformation of one radian. Thus, continuing with the same structure as before, a shear force of 1.0 kips produced a deformation of 0.01" in a length of 120", and γ is equal to 12,000 kips per radian.

Let us consider the beams and deck of Fig. 1a to be a part of a continuous floor system such that each beam receives the benefit of the bracing effect of a full 12 ft. width of steel deck. Considering only the compression elements of the beam, assuming that this compression is introduced by means of concentrated compressive forces on the ends of the beam, assuming an ideal member (no end eccentricity or initial crookedness) and assuming that loading has reached the critical buckling stage, the condition of the member can be represented by Fig. 2, in which all properties are expressed in general terms. Deflections at points B and C have purposely been shown as unequal.

The shear forces developed in the several panels of the diaphragm are as follows:

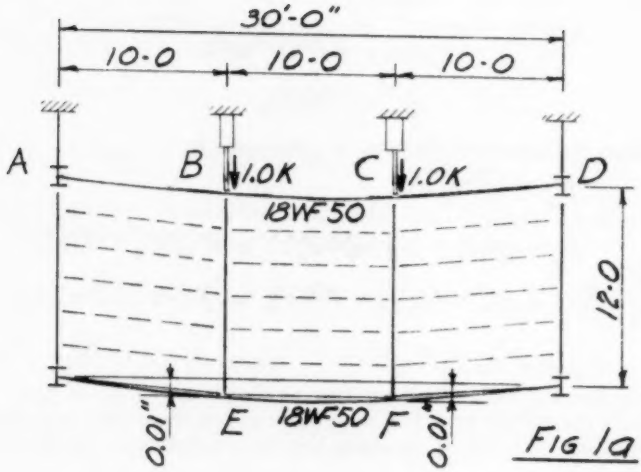

FIG 1a

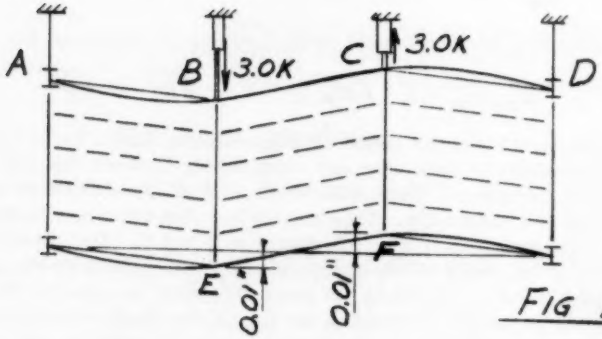

FIG 1b

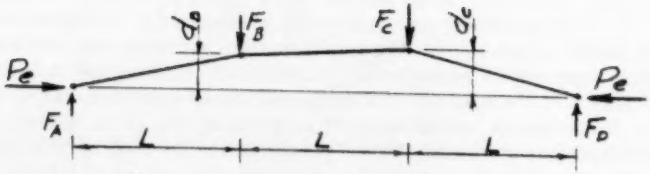

FIG 2

$$V_{AB} = \gamma d_b / L$$

$$V_{BC} = \gamma (d_c - d_b)/L$$

$$V_{CD} = -\gamma d_c / L$$

From which the lateral forces can be obtained:

$$F_A = \gamma d_b / L$$

$$F_B = \gamma d_b / L - \gamma (d_c - d_b)/L = \gamma (2d_b - d_c)/L$$

$$F_C = \gamma (d_c - d_b)/L + \gamma d_c / L = \gamma (-d_b + 2d_c)/L$$

$$F_D = \gamma d_c / L$$

with all forces and deflections positive as shown in Fig. 2.

The relationship between the buckling load and the diaphragm stiffness can be immediately obtained by summing the moments about point B of forces applied at A, as

$$d_b \cdot P_e - L \cdot \gamma d_b / L = 0 \; ; \quad \gamma_{id} = P_e \tag{1}$$

Likewise, summing moments about point C of forces applied at D,

$$d_c \cdot P_e - L \cdot \gamma d_c / L = 0 ; \; \gamma_{id} = P_e \tag{1}$$

It should be noted that the required diaphragm stiffness has been obtained without the necessity of assuming any relationship between the deflections at points B and C. A careful check will reveal that all forces are in balance, both internally and externally. This means that there are no compatibility conditions to be satisfied by the deflections at B and C. The condition shown in Fig. 2 is a stable stage of buckling, and the buckling load is the same whether points B and C deflect in the same direction, in opposite directions, equal distances or unequal distances, or one or the other remains at the neutral position. In addition, if the member were extended by the addition of successive increments of length L to four, five, or more spans, the required shear stiffness would retain the same value of

$$\gamma_{id} = P_e$$

and the deflection of each of the three, four or more points of support would remain independent of the others.

For an ideal column or beam and for equal spacing of points of support we are freed from the necessity of considering symmetrical, antisymmetrical or zig-zag modes of buckling. The total length of member and number of intermediate supports is immaterial. A series of coefficients such as the author's Table 2 is not needed. The required diaphragm stiffness to prevent buckling at the points of lateral support as given by Eq. (1) is independent of the mode of buckling or the number of panels in the bracing system but is uniquely determined by the length of a panel between points of lateral support and the critical buckling load of the column associated with this length.

Let us now turn to consideration of an imperfect (i.e., initially bowed) compression member, as represented by Fig. 3a. The required strength and stiffness of the diaphragm can be obtained as follows:

$$F = \gamma d/L = P(d+d_o)/L = S_{req} \tag{2}$$

$$\gamma_{req} = S_{req}/d = P\left(\frac{d+d_o}{d}\right) \tag{3}$$

Again, let us consider a member with initial imperfections as shown in Fig. 3b. For this case, the required strength and stiffness are

$$F = \gamma d/L = P(d+d_o)/L = S_{req} \tag{2}$$

$$\gamma_{req} = S_{req}/d = P\left(\frac{d+d_o}{d}\right) \tag{3}$$

We now see that the mode of buckling is influenced by the nature of the initial imperfections, but that the required strength or stiffness of the diaphragm is not, so long as the initial deflections d_o are the same in either case. If we add the practical consideration that the magnitude of the initial deflection will in all probability be less for 3b than for 3a, then buckling as shown in Fig. 3a is the more likely.

Armed with Eqs. (2) and (3) above, let us re-evaluate the adequacy of the diaphragm to furnish lateral bracing for the 18WF50 beam as in the original article. For loads, properties of members, and the like, refer to the original article.

$\gamma_{id} = P = 191$ kips/radian

Assuming $d_o = d = 3L/500 = 360"/500 = 0.72"$

$$\gamma_{req} = 191 \times \left(\frac{0.72+0.72}{0.72}\right) = 382 \text{ kips/radian}$$

and, if $\gamma_{act} = \gamma_{req}$, then

$$S_{req} = 191 \times (0.72+0.72)/120 = 2.3 \text{ kips}$$

If the actual stiffness furnished by the diaphragm is greater than required to restrain the lateral deflection to the specified maximum value, then the actual deflection and the required strength will be given by the equations

$$d = \frac{P}{\gamma_{act} - P} d_o \tag{4}$$

$$S_{req} = \gamma_{act}\, d/L = \frac{\gamma_{act}\, P}{\gamma_{act} - P} \cdot \frac{d_o}{L} \tag{5}$$

In the present case, γ has the value of 12,000 kips per radian, from which:

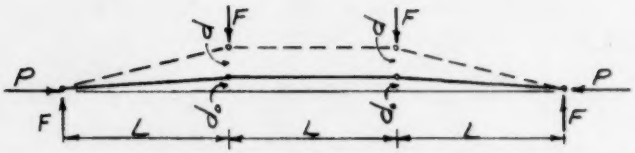

FIG 3a

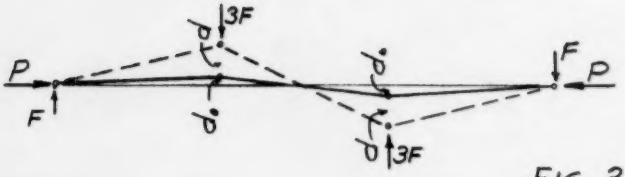

FIG 3b

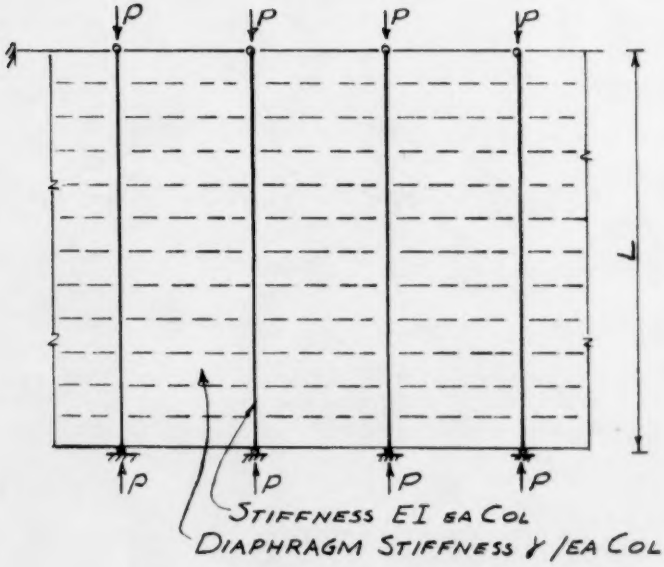

FIG 4

$$d = \frac{191}{12{,}000 - 191} \times 0.72'' = 0.0117''$$

$$S_{req} = 1.17 \text{ kips}$$

The steel deck actually furnishes a stiffness of 12,000 kips per radian and a strength at the elastic limit of about 12.5 kips. These values are about 30 times and 11 times as great as required, rather than 10 times and 3.5 times as given in the original paper.

Let us now turn to the case of a continuously braced member. The author treats this as a column on an elastic foundation. While the relationships developed are rigorously correct for a structure which can properly be so represented, such cases will rarely be found in actual practice, and are not necessary for an adequate bracing system. Instead, bracing is usually provided by a system of internal ties, or by the roof diaphragm, and these are not analogous to the elastic foundation.

Before passing on, it might be noted that the author's Eq. (19b) is not stated in its simplest and most useful form, either in the paper under discussion or in the source reference from which it is drawn. Let L be the length between nodes of the buckled compression member, rather than the overall length. The buckling load then is given by the author's Eq. (19), which is rewritten here as

$$P_{cr} = \frac{\pi^2 EI}{L^2} + \frac{\beta L^2}{\pi^2} \tag{6}$$

Now if we omit consideration of end conditions, we may find a buckling length L', for which the buckling load given by Eq. (6) is a minimum. This is:

$$L' = \pi \sqrt[4]{EI/\beta} \tag{7}$$

And for this buckling length L', the minimum critical buckling load is

$$P' = 2\sqrt{EI\beta} \tag{8}$$

The general procedure then for computing the critical buckling load is:

(1) Compute L' from Eq. (7).
(2) Compare L' with the overall length of the member. Determine closest lengths L_1 and L_2, larger and smaller than L' into which the overall length is evenly divisible.
(3) Evaluate Eq. (6) for both lengths L_1 and L_2. The lesser of these is the critical buckling load.
(4) If L' is small compared with the overall length, or if it differs by but a small amount from L_1 or L_2, the critical buckling load will be given with little error by Eq. (8).

As an illustration of the use of the above procedure, the following example is given. A column on an elastic foundation has an overall length between pin-connected ends of 100". EI is 2500 # in^2, and β is 1#/in/in. What is the buckling load for the column?

(7) $L' = 22.2"$

(8) $P' = 100\#$

(6) $L_1 = 20"$, $P_1 = 61.7 + 40.6 = 102.3\#$

(6) $L_2 = 25"$, $P_2 = 39.4 + 63.2 = 102.6\#$

The above were obtained by the use of a 6" slide rule and direct substitution in Eqs. (6), (7), and (8). Certainly there is nothing tedious about the computations. Moreover, the value from Eq. (8) is acceptably close to the true value, and on the conservative side.

Consider a series of columns of length L, bending stiffness EI, braced against buckling in their weak direction by a continuous diaphragm (such as a steel roof deck) with a shearing stiffness γ, all as shown in Fig. 4. Isolate one column and its associated width of diaphragm as in Fig. 5a. Assume an initial crookedness which for mathematical convenience is expressed as

$$y_o = d_o \sin \frac{\pi x}{L}$$

Apply end loads P to the column such that the column buckles laterally a slight distance from its initial position. Use coordinate axes as shown, except that y distances are measured from the initial centerline of the column before application of loads.

If an elemental segment of the column and attached diaphragm is isolated, forces as in Fig. 5b will be found to be acting. These can be evaluated in terms of the geometry and physical properties as follows:

$$M = -EI\, d^2y/dx^2$$

$$dM = -EI\, d^3y/dx^3\, dx$$

$$V = \gamma\, dy/dx$$

Applying the principles of statics to the forces on the element,

$$dM = P\left(dy + \frac{\pi}{L} d_o \cos \frac{\pi x}{L} dx\right) - V dx$$

which leads to the differential equation

$$-EI\, d^3y/dx^3 = P\, dy/dx + P\frac{\pi}{L}\cos\frac{\pi x}{L} - \gamma\, dy/dx$$

This is easily solved to yield the particular solution

$$y = \frac{P d_o}{\pi^2 EI/L^2 - (P-\gamma)} \sin \frac{\pi x}{L} \qquad (9)$$

$$dy/dx = \frac{P d_o}{\pi^2 EI/L^2 - (P-\gamma)} \frac{\pi}{L} \cos \frac{\pi x}{L} \qquad (10)$$

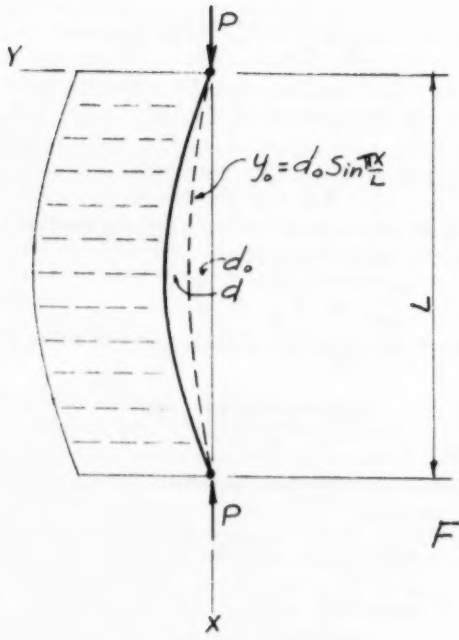
P
Y
$y_o = d_o \sin\frac{\pi x}{L}$
d_o
d
L
P
X

FIG 5a

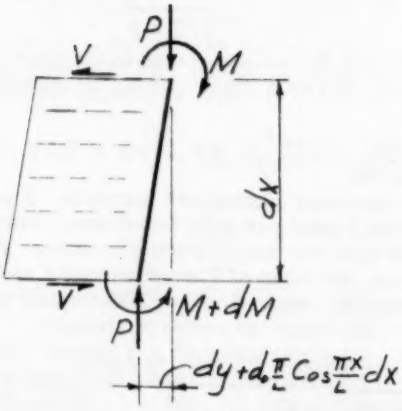
P
V
M
dx
V
M+dM
P
$dy + d_o \frac{\pi}{L} \cos\frac{\pi x}{L} dx$

FIG 5b

Substituting d for y and L/2 for x, we get

$$d = \frac{P d_o}{\pi^2 EI/L^2 - (P-\gamma)} \qquad (11)$$

Noting that $\pi^2 EI/L^2$ is the Euler buckling load, for which we make the substitution P_e, the equation can be re-arranged in the form

$$P = (P_e + \gamma)\frac{d}{d+d_o} \qquad (12)$$

From Eq. (12) we can obtain the equation for the buckling load on an ideal column by setting d_o equal to zero, which gives

$$P_{cr} = P_e + \gamma$$

For the practical case of the imperfect column, we can solve Eq. (12) for the required value of γ:

$$\gamma_{req} = P\left(\frac{d+d_o}{d}\right) - P_e$$

The maximum shear stress occurs at the supports. Setting x = 0 in (10), and substituting d from (11), we get

$$dy/dx = \pi d/L$$

If γ_{act} is exactly equal to γ_{reg}, then

$$S_{req} = P\frac{\pi}{L}(d+d_o) - P_e\frac{\pi}{L}d \qquad (15)$$

And, if $\gamma_{act} \neq \gamma_{reg}$, then

$$S_{req} = \pi d\gamma/L = \frac{\pi P\gamma d_o/L}{(P_e+\gamma) - P} \qquad (16)$$

Armed with Eqs. (14), (15) and (16) we can return to the upper chord of the roof truss treated in Professor Winter's paper. Using the same physical properties as before we find

$$\gamma_{req} = 53.1 \text{ kips}\left(\frac{0.48" + 0.48"}{0.48"}\right) - 9.6 \text{ kips} = 96.6 \text{ kips/radian}$$

The type of roof deck and the truss spacing are not given. A particular name brand of roof deck having a single 18 gage fluted sheet showed a stiffness when tested of about 300 kips per foot of width per radian. Assuming a truss spacing of 8-foot centers, the value of γ supplied would be 2400 kips/radian. This is about 25 times the required value of 96.6 kips/radian.

Using the actual value of γ we obtain the required strength

$$S_{req} = \frac{\pi \times 53.1 \times 2400 \times 0.48"/240"}{(9.6 + 2400) - 53.1} = 0.34 \text{ kips}$$

The same roof deck had a strength at yield of about 800 pounds per foot, or 6.4 kips for an eight-foot width. This is about 20 times the required value. From this it appears that the bracing requirements are easily met.

It is hoped that the foregoing will cast some additional light on the principles of action of bracing systems, and, in conjunction with the excellent presentation by Professor Winter, help point the way toward a method of determining bracing requirements for structures.

GILES G. GREEN,[1] A. M. ASCE.—The author has presented a clear step-by-step derivation of the required stiffness and strength of the bracing for compression members with elastic lateral supports. The required stiffness and strength of the lateral bracing is a function of the critical column load, the column length, the assumed initial bow of the column, d_o, and the additional deflection under load, d. The latter two quantities are related for unsupported columns and for point braced columns with elastic lateral supports by the expression:

$$d = \frac{Pd_o}{P_{cr}-P}$$

where P is any load less than the critical value, P_{cr}, allowance being made for the effect of the lateral bracing in increasing the critical column load. The initial shape of the column causes the greatest load on the lateral bracing when it is similar to the characteristic mode of distortion equal in number to the number of equally spaced concentrated supports. The strength and rigidity of the lateral supports for optimum efficiency should be sufficient to cause the column to buckle in a characteristic mode of distortion one greater than the number of such supports, that is, with a node at each support as illustrated by Fig. 4. The writer's Fig. 1 shows the change in the mode of distortion with increase in the stiffness of the lateral support. Thus, the break in the curve labeled "1 support" represents the change from the first characteristic mode of distortion indicated by the sloping portion and the dotted curve of Fig. 4 to the second mode indicated by the horizontal portion and the solid curve of Fig. 4. It is informative to replot Fig. 1 in terms of P_e, the Euler load of a column whose free length is the distance between supports. This is shown below where only the two highest modes of distortion for each number of lateral supports is drawn. The sloping portion of each curve may be approximated by a straight line with an equation as shown in the table below, where n is both the number of supports and the characteristic mode of distortion.

Values of P_{cr}

n =	1	2	3	4
P_{cr} =	$\frac{P_e}{4} + \frac{3}{8}kL$	$\frac{P_e}{2.14} + 0.178kL$	$\frac{P_e}{1.555} + 0.1044kL$	$\frac{P_e}{1.308} + 0.0649kL$

The limiting value of P_{cr} in each case is P_e. These values may be used to compute d at the point of lateral support from the above expression for d in terms of P, d_0 and P_{cr}, but only for values of k such that $P_{cr} < P_e$, that is, for values of k less than k_{id}. As P approaches P_{cr}, d becomes infinite, indicating failure of the bracing simultaneously with failure of the column.

1. Hardesty and Hanover, New York, N. Y.

Critical Load for Elastically Supported Columns with Number of Supports and Characteristic Mode of Distortion Shown

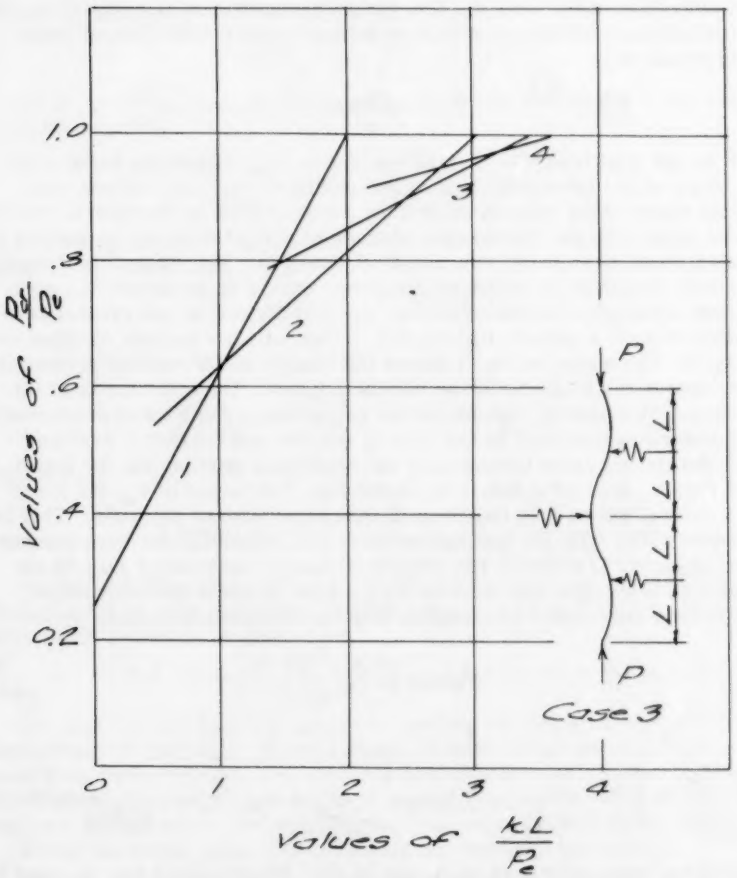

Fig. 1

However, as k exceeds k_{id} and the column buckles in the next higher mode of distortion, at a load $P_{cr} = P_e$, d refers to the amplitude of the bowing curve of that higher mode which then occurs midway between the points of lateral support. Practically in the design of the lateral bracing the suggestion that d be made equal to the assumed value of d_o seems conservative when the lateral bracing is stiff enough to cause a node. If the lateral bracing is more flexible than this requirement, the deflection under load should be computed as previously indicated.

As an example of the use of the above relationships, the column shown in Fig. 2 will be investigated. This column consists of a 12" - 30# channel 30 feet long braced against buckling about its minor axis by the beam action of two pairs of 3-1/2" x 3-1/2" x 3/8" angles 9 ft. long, bracing the column at its third points.

$L/R_{1-1} = 120/0.77 = 155.5$ - controls

$L/R_{2-2} = 360/4.28 = 84$

for $L/R = 155.5$, F_c allow. = 6310 p.s.i. (AISC Mbk., p.210)

$P_{des} = 6300 \times 8.79$ sq.in. = 55,500 lbs.

$P_{ult} = 1.9 \times 55{,}500 = 105{,}500$ lbs.

$$P_e = \frac{\pi^2 \times 3 \times 10^7 \times 5.2}{120^2} = 106{,}700 \text{ lbs.}$$

$$k_{id} = \frac{3P_e}{L} = \frac{3 \times 106{,}700}{120} = 2670 \text{ lbs/in.}$$

$$d_o = 1/1000 \times \text{length} = \frac{360}{1000} = 0.36$$

k furnished by 2/S 3½" x 3½" x 3/8" x 9' long

$$\text{is } \frac{48\,EI}{L^3} = \frac{48 \times 3 \times 10^7 \times 2 \times 2.9}{(9 \times 12)^3} = 6620 \text{ lbs/in} = k_{act}$$

$$k_{req} = k_{id}\left(\frac{d_o}{d} + 1\right)$$

$$k_{req} = 2670\left(\frac{0.36}{0.36} + 1\right) = 5340 \text{ lbs./in.}$$

thus $k_{act} > k_{req}$

$S_{req} = k_{act}\, d = 6620 \times 0.36 = 2390$ lbs.

$$f_t)_{act} = \frac{M}{S} = \frac{2390 \times 9' \times 12"}{4 \times (2 \times 1.2)} = 26{,}900 \text{ p.s.i.} < 33{,}000 \text{ p.s.i.}$$

It is seen from the above computations that in order for the column to be adequately braced about its minor axis at the third points, a certain spring constant of the supports, k_{req} is needed. This quantity is computed and compared with that actually supplied to see that the bracing is stiff enough. With

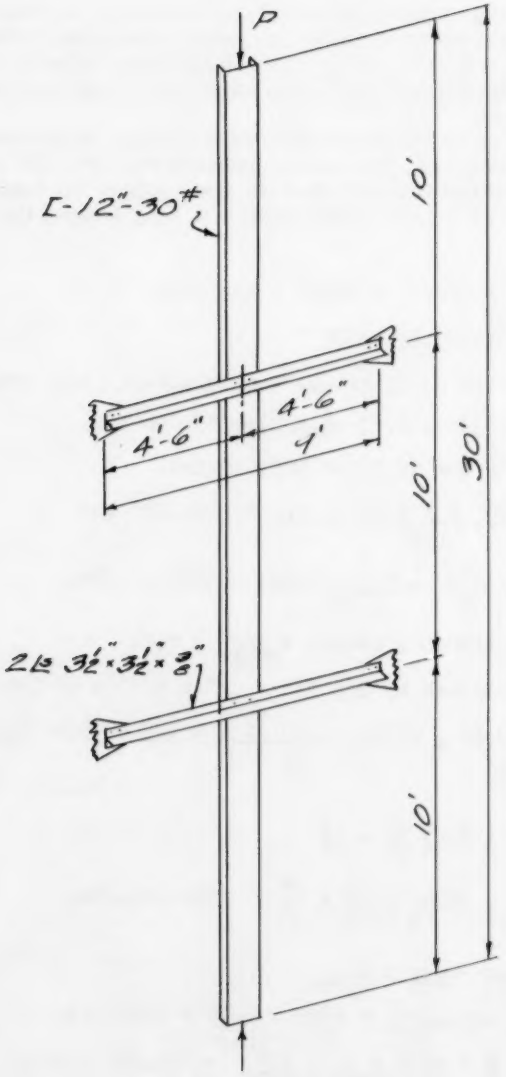

Column with Two Braces

Fig. 2

the effective length of the column about its minor axis now 1/3 the total length, the ultimate load is then computed from the AISC column formula times the approximate factor of safety, 1.9. Taking the initial crookedness of the column as 1/1000 of its length, the required strength of the bracing, S_{req} is then computed. Since this force is found to cause a stress in the bracing less than its yield point stress, the bracing is strong enough to withstand the forces induced in it by the action of the ultimate column load.

In the event that the lateral bracing is not stiff enough to cause a node at the point of support, it can still be utilized to increase the strength of the column. Thus, in the above example, if the bracing angles were 14 feet long:

$$k_{act} = \frac{48 \times 3 \times 10^7 \times 2 \times 2.9}{(14 \times 12)^3} = 1760 \text{ lbs./in}$$

this is less than k_{id}, so

$$P_{cr} < P_e$$

$$P_{cr} = P_e/2.14 + 0.178\,kL$$

$$= 106{,}700/2.14 + 0.178 \times 1760 \times 120$$

$$P_{cr} = 87{,}500 \text{ lbs.}$$

At the yield point, the bracing can withstand a force computed from:

$$33{,}000 = \frac{S \times 14 \times 12}{4\,(2 \times 1.2)}$$

whence: S = 1880 lbs.

and: $d = \frac{1880}{1760} = 1.07''$

In order to obtain the load on the column causing this lateral deflection, solve:

$$d = \frac{Pd_o}{P_{cr} - P}$$

$$1.07 = \frac{P \times 0.36}{87{,}500 - P}$$

$$P = 65{,}500 \text{ lbs.}$$

thus, $P_{allow} = P/1.9 = 65{,}500/1.9 = 34{,}500$ lbs.

Although this column load is less than that permitted if the bracing were sufficiently rigid, it is considerably greater than that of the unbraced column.

BRUCE G. JOHNSTON.[1]—This paper is an important contribution to a subject about which little has been written in spite of the fact that it has been an area in which information has been needed by engineers for many years. The author is to be congratulated on the well balanced combination of tests, intuitive judgment, and analysis that are combined with a practical approach to the design problem.

The writer was particularly interested in the statement in the last paragraph of the section on "Lateral Bracing of Beams and Girders: which reads:

1. Prof. of Structural Engr., Univ. of Michigan, Ann Arbor, Michigan.

'Hence, mere friction between the top of beam and the floor which rests on it would suffice to develop the force required for lateral bracing.' This statement is apt to be taken out of context by engineers who, perhaps quite rightly, would like to rely solely on friction for lateral support. However, the author qualifies this statement in the following setence so as not to commit himself definitely to the implied conclusion. It would be desirable to pin this matter down more definitely. The matter of what does constitute minimum requirement for lateral support seems still to be left open. Is it, in fact, permissible to rely only on friction? Does the type of floor have anything to do with the problem? For example, some beams may support timber planking or lightweight open metal grid. Is the friction in this case sufficient? Does the matter of dynamic or vibratory loads affect the problem? In the latter case it might well be argued that when, due to vibration, the friction is absent the load also is simultaneously absent. The writer does not contest the correctness of the author's conclusion but in view of the fact that engineering teachers have been recommending flange embedment in concrete as a minimum for top flange lateral support of beams this question needs a little further elaboration.

The writer wishes to emphasize the importance of this matter in relation to current engineering practice and the recommendations that are given in most texts on design.

A. CHIBARO,[1] M. ASCE.—The author deserves praise for clearly presenting, in simple terms, solutions of a number of problems encountered in the proportioning of lateral bracing. Although the approach is not new, he has skillfully extended its application considerably, and presented the profession with a much needed design method.

Much to his surprise, the writer found it relatively simple to calculate the value of

$$k_{id} = \frac{3.63\ P_e}{L}$$

for the case n = 4, given in table 2, by using the author's method.

1. Structural Engr., Jackson & Moreland, Inc., Boston, Mass.

NUMERICAL SOLUTIONS FOR BEAMS ON ELASTIC FOUNDATIONS[a]

Discussions by Alexander Dodge and Lymon C. Reese

ALEXANDER DODGE,[1] M. ASCE.—The author gives numerical solutions for beams on elastic foundations by two approximate methods and compares the results with those obtained by the "rigorous method." His work is in the field of engineering which is avoided in practice, no doubt, for the reason of the erroneous impression that the subject is deeply involved in mathematics and that solution of a problem is a cumbersome and time-consuming analysis. Therefore, some other reasonable solution is sought, or the problem is entirely neglected. The author should be commended for demonstrating the ease with which an approximate solution of a problem can be obtained by the finite difference method.

In his introduction the author states that "a 'rigorous' method should at all times be sought after" and, later, that "Recognizing the nature of the entire problem, it is often preferable to use an approximate method, and to quickly obtain a solution—one that may in actuality be no farther removed from a 'true and exact' solution than that derived by a 'rigorous' method." From past experience in this field the writer believes that an approximate solution is more than ample in all but a few cases. Precision in computations is justified when a purely academical approach to a problem is desired, when the establishment of certain assumptions must be verified, when an independent check or comparison with some other exact method is sought, or when thorough working knowledge of the subject is required. In practice one is guided by design codes, manuals, specifications, also formulas and tables of moments, deflection, and a multitude of other coefficients. The problem of beams on elastic foundation is no different, and the writer will try to illustrate how solutions of such problems can be quickly made by charts. The discussion will be divided into three steps:

(1) Exact solution.
(2) Approximate solution.
(3) Simple solution.

Exact Solution

The oldest theory of bending a beam on elastic foundation was developed by E. Winkler and applies to "Winkler" foundation as described by the author.

a. Proc. Paper 1562, March, 1958, by Henry Malter.
1. Consultant, Design Branch, U. S. Army Engr. District, Portland, Ore.

Application of the theory was demonstrated by S. Timoshenko* in whose nomenclature the deflection equation of a bar of infinite length on an elastic foundation can be represented by the equation:

$$y = e^{\beta x}(A \cos \beta x + B \sin \beta x) + e^{-\beta x}(C \cos \beta x + D \sin \beta x) \quad (1)$$

Where $\beta = \sqrt[4]{\frac{k}{4EI}}$, k is the modulus of foundation and A, B, C, and D are the constants of integration.

This method of solution has been available to the engineering profession for at least 30 years, but to the writer's knowledge its use has been neglected, probably because its universality was not readily recognized and properly appreciated. Applying this method to a bar of finite length (the writer's Fig. 1) and integrating within definite limits, the following equations will result:

Fig. 1. Bar of Finite Length Loaded at End.

$M_{\beta x=0} = 0$ ---------- $B = D$ ---------- (2)

$M_{\beta x} = 2EI\beta^2[A\mu + B(\theta - \eta) - C\omega]$ ---------- (2')

$M_{\beta \ell} = M = 2EI\beta^2[A\mu + B(\theta - \tau) - C\omega]$ ---------- (2")

$S_{\beta x} = 2EI\beta^3[A\varepsilon - B(\tau + \varphi) - C\psi]$ ---------- (3)

$S_{\beta x=0} = 0$ ---------- $-A + 2B + C = 0$ ---------- (3')

$S_{\beta \ell} = P = 2EI\beta^3[A\varepsilon - B(\tau + \varphi) - C\psi]$ ---------- (3")

$y = A\eta + B(\mu + \omega) + C\theta$ ---------- (4)

$\frac{dy}{dx} = Ay + B(\varepsilon + \psi) - C\varphi$ ---------- (5)

Where,

$$\mu = e^{\beta x} \sin \beta x,\ \eta = e^{\beta x} \cos \beta x,\ \theta = e^{-\beta x} \cos \beta x,\ \omega = e^{-\beta x} \sin \beta x,$$
$$\varphi = \theta + \omega,\ \psi = \theta - \omega,\ \tau = \eta - \mu,\ \varepsilon = \eta + \mu$$

positive moment indicates tension on bottom, positive shear - left part tends to go up, positive deflection down and positive slope clockwise. Exponential and circular function being available in many engineering handbooks, the constants of integration A, B, and C can be readily determined from the writer's Eqs. 2", 3', and 3". Applying the above notations to the author's Example 1, using stepped foundation modulus, the following beam constants will be obtained:

Item	k = 650	500	300	150
β	.0259	.0243	.0214	.01797
ℓ	20	40	40	20
$\beta\ell$	.518	.972	.856	.03594

Table 1. Beam Constants

*"Strength of Materials" by S. Timoshenko, Part II, D. Van Nostrand Co., Inc. 1930, p. 402.

Then considering the end load P = 100# and the end moment M = 1000"# as separate problems and solving equations 2", 3', and 3" for each segment of the beam, the resulting values of end deflections and slopes will be as shown in the writer's Table 2.

		Due to Unit Loading			
		P = 100 #		M = 1000" #	
Segment	Point	y	$\frac{dy}{dx}$	y	$\frac{dy}{dx}$
A–B	A	– .015 417	.002 511 4	.025 114	– .002 307 7
	B	.030 886	.002 520 7	– .025 207	– .002 335 5
C–D	C	– .009 852 2	.000 755 22	.007 552 2	– .000 559 28
	D	.020 085	.000 770 05	– .007 700 5	– .000 414 56
E–F	E	– .016 429	.001 228 0	.012 280	– .000 606 64
	F	.033 280	.001 264 9	– .012 649	– .000 662 05
G–H	G	– .066 578	.009 985 7	.099 857	– .009 982 0
	H	.133 210	.009 994 9	– .099 949	– .010 009 7

Table 2. End Deflections and Slopes of Beam Segments.

Knowing the end slopes and deflections of the beam segments due to unit loads, continuity of the beam is restored in the usual manner by introducing unknown (interacting) shears and moments, as shown in the writer's Fig. 2 and Table 3, and by equating the final slopes and deflection at common points BC, DE, and FG.

Therefore there will be six equations:

$$\Delta_B - \Delta_C = 0 = +.0509713_1 + .01550678_1 + .0098322S_2 + .0075322M_2 - .15417 \quad \ldots\ldots\ldots\ldots (6)$$

$$\Delta_D - \Delta_E = 0 = +.0098322S_1 - .0075322M_1 + .0553655_2 - .0049487M_2 + .0164293_3 + .012280M_3 \quad \ldots\ldots (7)$$

$$\Delta_F - \Delta_G = 0 = \quad + .0164293_2 - .012280M_2 + .166490S_3 - .097500M_3 \quad \ldots\ldots (8)$$

$$\phi_B - \phi_C = 0 = +.001550678_1 + .00275006M_1 - .000755225_2 - .0005592SM_2 - .0025114 \quad \ldots\ldots\ldots\ldots (9)$$

$$\phi_D - \phi_E = 0 = +.000755225_1 - .0005592SM_1 - .000494878_2 + .00107659M_2 - .001228S_3 - .000606644_3 \quad \ldots\ldots (10)$$

$$\phi_F - \phi_G = 0 = \quad + .001228S_2 - .000606644_2 - .008730S_3 + .01067175M_3 \quad \ldots\ldots (11)$$

Where Δ and ϕ are final deflections and slopes at the point indicated by a subscript.

Fig. 2. Interacting Shears and Moments.

Solution of these equations, as well as similar equations due to load P_H = 100#, yields the values given in the writer's Table 4. Values for intermediate points of a segment may be found, if necessary, by substitution of the proper βx values in equations 2' and 3. Solution of equations for both loads or for any number of loads at different point of the beam can be made at once, but in studies as well as in practical designs, solution for a unit load or moment is more valuable.

Unless one is interested in the mechanics of all operations performed in solution of this problem, there is no justification for going through the maze of such computations. The validity of the solution can be verified simply by

POINTS							
A	B	C	D	E	F	G	H
End Slopes, , Radians							
$-.0023207$	$-.0023114$						
$+.0023114S_1$	$+.0023207S_1$	$+.00077003S_1$	$+.00077003S_2$	$+.0012649S_2$	$+.0012649S_3$	$+.0099949S_3$	$+.0099857S_3$
$+.0023077M_1$	$+.0023355M_1$	$-.00041456M_1$	$+.00041456M_2$	$-.00066203M_2$	$+.00066203M_3$	$-.0100097M_3$	$-.0099820M_3$
		$+.00073522S_2$	$+.00073522S_1$	$+.0012280S_3$	$+.0012280S_2$		
		$+.00055928M_2$	$-.00055928M_1$	$+.00060664M_3$	$-.00060664M_2$		
End Deflections, , Inches							
$+.050886$	$-.015417$						
$-.015417S_1$	$+.050886S_1$	$-.020085S_1$	$+.020085S_2$	$-.053280S_2$	$+.053280S_3$	$-.133210S_3$	$+.066578S_3$
$-.023114M_1$	$+.023207M_1$	$+.0077003M_1$	$+.0077003M_2$	$+.012649M_2$	$+.012649M_3$	$+.099949M_3$	$-.099857M_3$
		$-.0098522S_2$	$+.0098522S_1$	$-.016429S_3$	$+.016429S_2$		
		$-.0073522M_2$	$-.0073522M_1$	$-.012280M_3$	$-.012280M_2$		
Final Deflections Due to P_A = 100							
.00855	.004538	.004539	-.000164	-.000165	-.00188	-.0018	-.00249
Final Deflections Due to P_H = 100							
-.002482	-.001518	-.001518	.002120	.002116	.01227	.01231	.019873
Final Deflections Due to P_A = 100 and P_H = 100							
By Exact Solution							
.006068	.003020	.003021	.001956	.001951	.010389	.010432	.017383
By Approximate Solution							
.005	.00346		.00260			.01026	.0149
Foundation Pressure by Exact Solution, pounds per square inch							
3.94	1.96	1.51	.98	.59	3.1	1.55	2.61

Table 3. Beam Deflections and Slopes

	Exact Solution			Approximate Solution		
	Due to Load			Due to Load		
Item	P_A = 100 #	P_H = 100 #	$P_A + P_H$	P_A = 100 #	P_H + 100 #	$P_A + P_H$
S_1 lbs	- 16.0	- 26.0	- 42	- 18.6	- 27.9	- 46.5
M_1 in-lbs	1073	281	1354	1111	308	1419
S_2	20.4	- 26.8	- 6.4	21.2	- 26.2	- 4
M_2	675	1574	2249	750	1679	2409
S_3	6.6	51.9	58.5	7.4	55	62.4
M_3	69	1481	1550	78	1515	1593

Table 4. Beam Shears and Moments.

computing the moment of the $\frac{M}{EI}$ diagram for the loads equal to the foundation pressures shown in the writer's Table 3. When a plot of such values (deflections from the end tangent) coincides with deflections shown in the same table, also if the area of the foundation pressures is equal to the superimposed loads, and moment equilibrium is satisfied, veracity of the solution is established. It was found that these conditions are entirely satisfied. In this respect problems on elastic supports are easier and faster to verify than solution of other indeterminate structures. It should be noted that when deflections are computed on the assumption of a stepped modulus of foundation, the latter must be also used to evaluate foundation pressures, and the foundation pressures so determined must be used to establish validity of the solution. Failure to observe this procedure will lead to inequalities in equations of statics $\Sigma V = 0$ and $\Sigma M = 0$, and also may give quite a large disparity in elastic curves. Therefore, from a theoretical standpoint, deflections at points A and D by finite difference method in the author's Table 4 should be 3.11 and 2.62 instead of 3.35 and 1.74 as shown, respectively. From a practical standpoint such a refinement may be immaterial.

In the progress of work, it is well to remember and observe that such other controlling conditions, as slope due to unit load equals deflection due to unit moment, or the Maxwell's law of reciprocal deflections, are satisfied. (Observe values in the writer's Tables 2 and 3 in this respect.) Moreover, a sufficiently close check of values in the writer's Table 2 can be made by statics, assuming that a segment of the beam has infinite stiffness. For example, in this problem the segment EF = Bb = .856 and the foundation modulus k = 300. Therefore, due to the end load,

$$P = 100 \text{ lbs} \quad . \quad . \quad . \quad \frac{4}{5} P = \frac{k y_E \times 40 \times 2}{2 \times 5}$$

Deflection, $y_E = .0333"$, $\qquad y_F = \frac{1}{2} y_E = .01667"$

Slope $= -\frac{1.5}{40} y_E = -.00125$ radians

Similarly, due to the end moment,

$$M = 1000 \text{ in-lbs} \quad \ldots \quad \frac{M \times 5}{40 \times 2} = \frac{k y_E \times 40}{2 \times 2}$$

Deflection, $y_E = y_F = .0125"$

Slope $= \frac{2\, y_E}{40} = .000625$ radians

There is no question that once the method is understood, it will be realized how much tedious, subprofessional work is involved in performing a series of similar computations. The description of such a method is given here as a reminiscence of analysis developed for the design of the Lake Washington Floating Bridge in Seattle, Washington. A general description of the bridge may be found in Western Construction News of September 1939, although information therein regarding live load distribution requiring "no longitudinal span" was incorrectly stated and should be superceded by material presented in this discussion. To begin with, determination of the maximum length of an individual unit and the maximum number of units which could be rigidly connected in a continuous structure were sought. Without precedent in design of such bridges, pioneering in analysis started by the method recommended above for checking validity of solutions; namely, realizing that water was a perfect "Winkler's" foundation, deflections of the unit were assumed and corrected until the assumed deflections came into close agreement with computed deflections after conditions of static equilibrium by equations $\Sigma V = 0$ and $\Sigma M = 0$ were satisfied. When a continuous bridge of approximately 1000 feet in length was analyzed, it was evident that for such length the maximum live load and temperature stresses were practically the same as for a bridge of infinite length. For these reasons all units were rigidly connected by prestressing and grouting into one continuous structure approximately 6500 feet long. Continuity has been interrupted only by the movable, telescoping span required by navigation. This 378-foot span was connected to the east part of the bridge by a hinged joint, and to the west part by two sets of vertical rollers. To determine statically indeterminate reactions at the rollers and the hinge by the "hit and miss" method, as well as to derive the load distribution on the transition span of variable moment of inertia, was beyond engineering patience. For these reasons the exact method presented here was developed; thereafter, influence lines for the above reactions were easily determined. The magnificent performance of the bridge after two decades of service speaks for itself as testimony to the validity of the analysis.

Later, as more applications of the method were made to various structures, the data on deflections, slopes and moments of beams of finite length were accumulated and compared with the respective values computed for a unit load or moment acting at the end of an (infinitely) long bar. Equations for beams of infinite length are as follows:*

$$y_o = \frac{P_i}{2EI\beta^3}, \quad \frac{dy_o}{dx} = -\frac{P_o}{2EI\beta^2} \quad \text{and} \quad M_{max} = -\frac{.32235\, P_o}{\beta} \quad \ldots \text{(12a, b \& c)}$$

or

$$y_o = \frac{-M_o}{2EI\beta^2}, \quad \frac{dy_o}{dx} = \frac{M_o}{EI\beta} \quad \text{and} \quad M_{max} = M_o \quad \ldots\ldots \text{(13a, b \& c)}$$

*"Strength of Materials" by S. Timoshenko, Part II, D. Van Nostrand Co., Inc. 1930, p. 408.

The ratios of $\frac{(y)}{(y_o)}$ = $\frac{\text{Deflection of a beam of a finite length at any point,}}{\text{Deflection of a beam of infinite length at the end}}$ similarly, $\frac{(dy/dy_o)}{(dy/dx)}$ and $\frac{(M)}{(M_o)}$ were found and plotted with respect to βb values. Plots of such ratios provide the means for approximate solutions.

Approximate Solution

In most solutions of beams on elastic foundations, only end deflections and slopes are of useful values. Therefore, deflection and slope ratios were plotted and curves developed for both ends of the beams as shown on the writer's charts, Fig. 3, 4, 6, and 7. Knowledge of deflection ratios for intermediate points is hardly needed but for refinement in an analysis. For example, in the above problem, knowledge of such ratio at the center line of the segment C-D defines the shape of the elastic curve more precisely and gives more accurate data, verification of which establishes validity of the analysis. The purpose of this discussion being to show a quick, approximate method of an analysis, intermediate values of deflection ratios could be omitted. Nevertheless, they are plotted in the writer's Fig. 3 and 6 for two segments of the beam, also for a beam of infinite length, because such curves show that beams of length βb equal 0.5, or even 1.0, can be designed on an assumption of infinite stiffness. Moment values are, generally, needed in design for all points of a beam; for this reason, all moment ratios are plotted in the writer's charts, Fig. 5 and 8.

To get an approximate solution of the author's Problem 1, the values of deflection and slope ratios are taken from charts; then, by reversing the process of their preparation, the true values of deflections and slopes, in terms of unknown shears and moments, are computed. A sample of computations is shown in Table 5 below for the segment AB, βb = .518.

	Deflection Ratios			End Deflections	
Due To	Point A	B	y_o *	A	B
P_A = 100 lb	3.9	- 1.95	.008	.0312	-.0154
S_1	$-1.95S_1$	$3.9S_1$	.008	$-.0154S_1$	$.0312S_1$
M_1	$-11.3M_1$	$-11.3M_1$	.00207	$-.0235M_1$	$.0235M_1$
	Slope Ratios			End Slopes	
Due To	A	B	$\frac{dy_o}{dx}$ *	A	B
P_A = 100 lb	-11.3	-11.3	.000207	-.00235	-.00235
S_1	$11.3S_1$	$11.3S_1$	.000207	$.00235S_1$	$.00235S_1$
M_1	$22M_1$	$22M$	.0001075	$.00235M_1$	$.00235M_1$

* By equations (12's) and (13's)

Table 5. Sample of Computations of Deflections and Slopes by Charts, Fig. 3, 4, 6 and 7

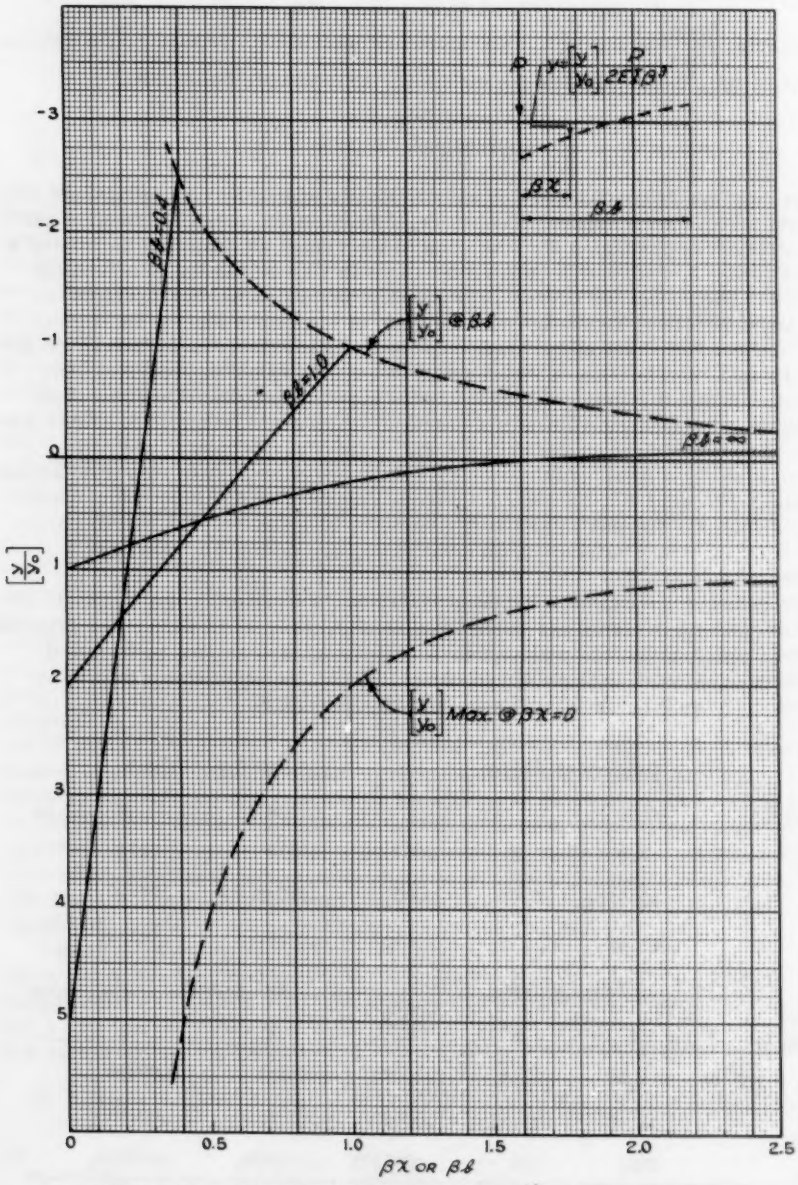

FIG. 3 - Deflection Ratio, $\frac{y}{y_o}$, for Various Lengths of Beams, $\beta \ell$

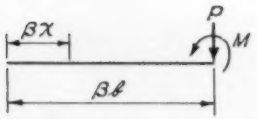

FIG. 1 - Bar of Finite Length Loaded at End

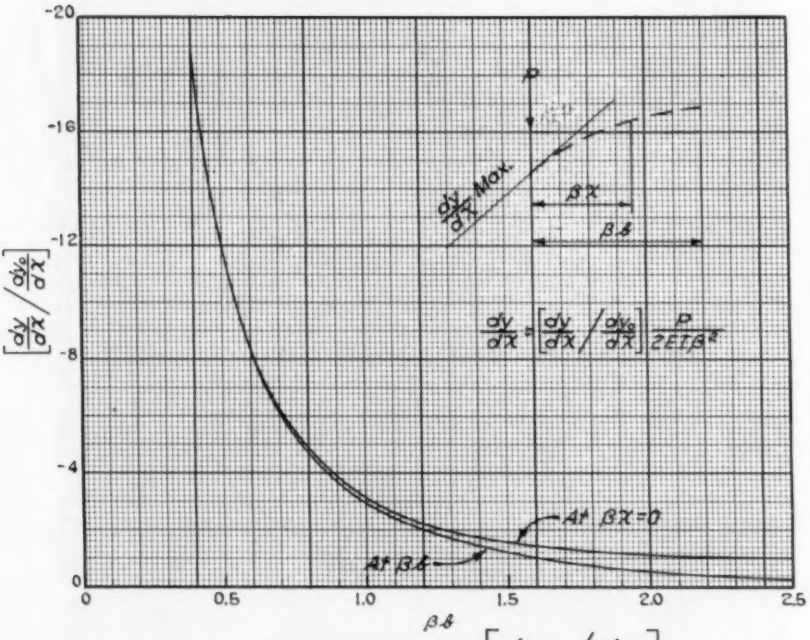

FIG. 4 - Slope Ratio, $\left[\frac{dy}{dx}\Big/\frac{dy_o}{dx}\right]$, for Various Lengths of Beams, $\beta\ell$

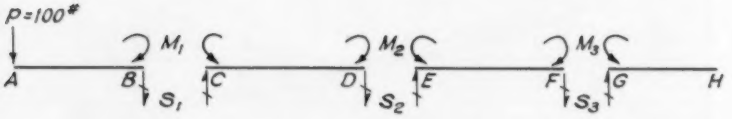

FIG. 2 - Interacting Shears and Moments

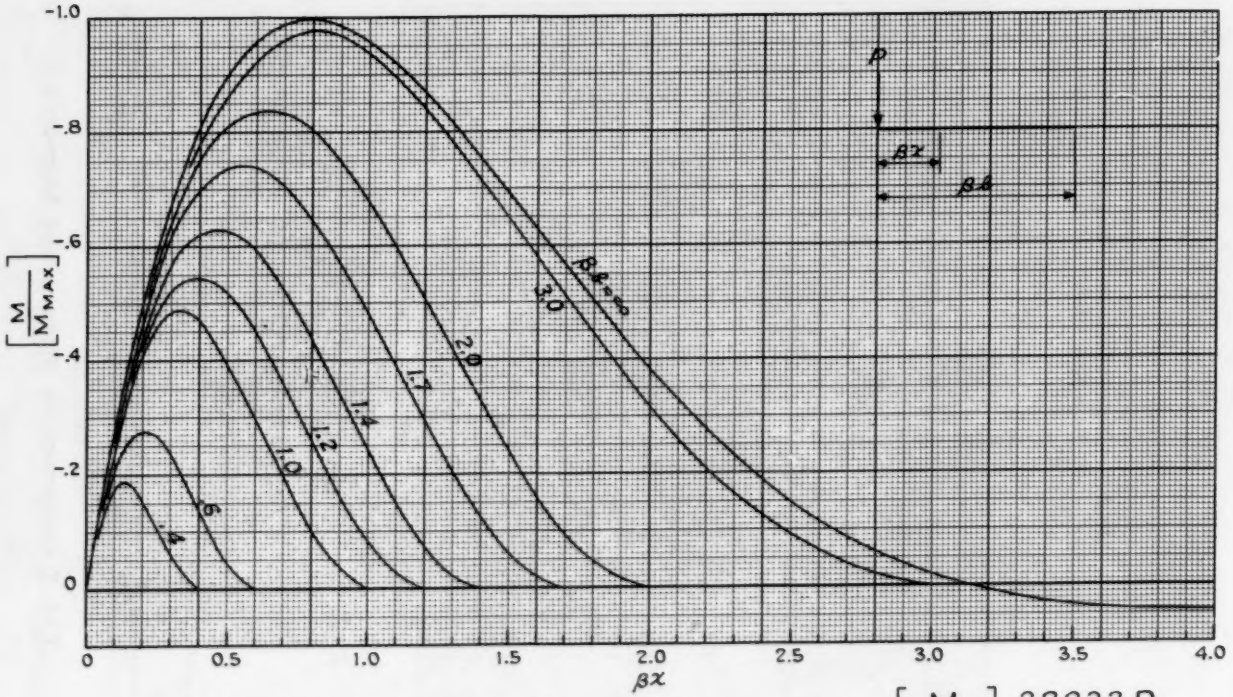

FIG. 5 - Moment at βX, Due to Load P, $M_{\beta x} = \left[\frac{M}{M_{Max.}}\right] \frac{.32233\,P}{\beta}$

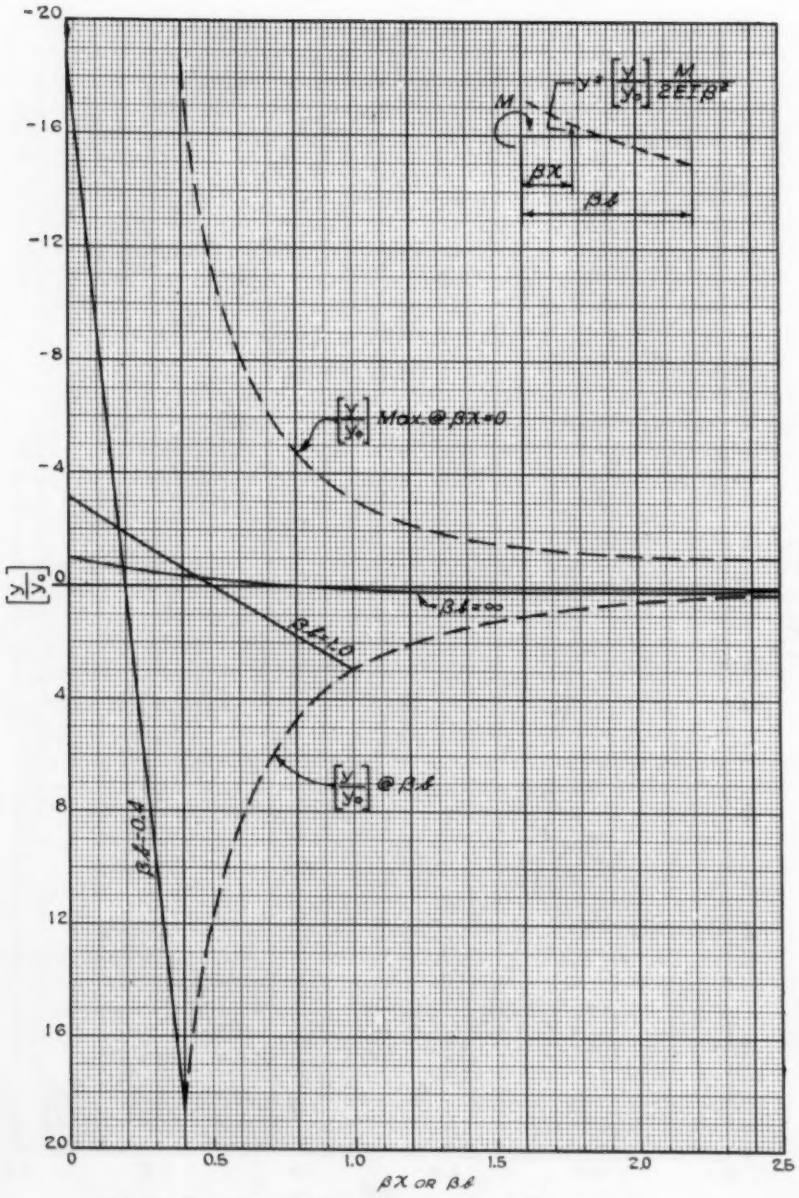

FIG. 6 -Deflection Ratio, $\frac{y}{y_0}$, for Various Lengths of Beams, $\beta\ell$

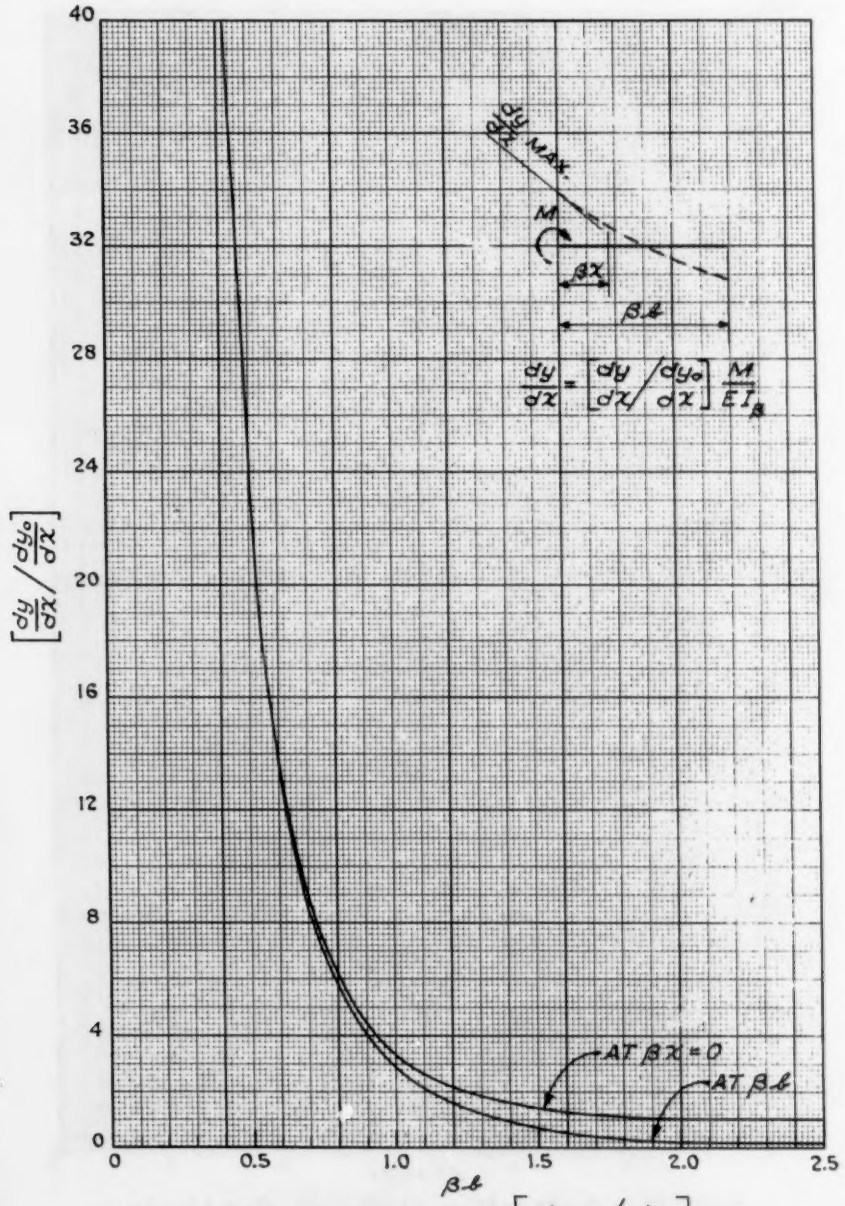

FIG. 7 - Slope Ratio, $\left[\frac{dy}{dx}/\frac{dy_o}{dx}\right]$, for Various Lengths of Beams, $\beta\ell$

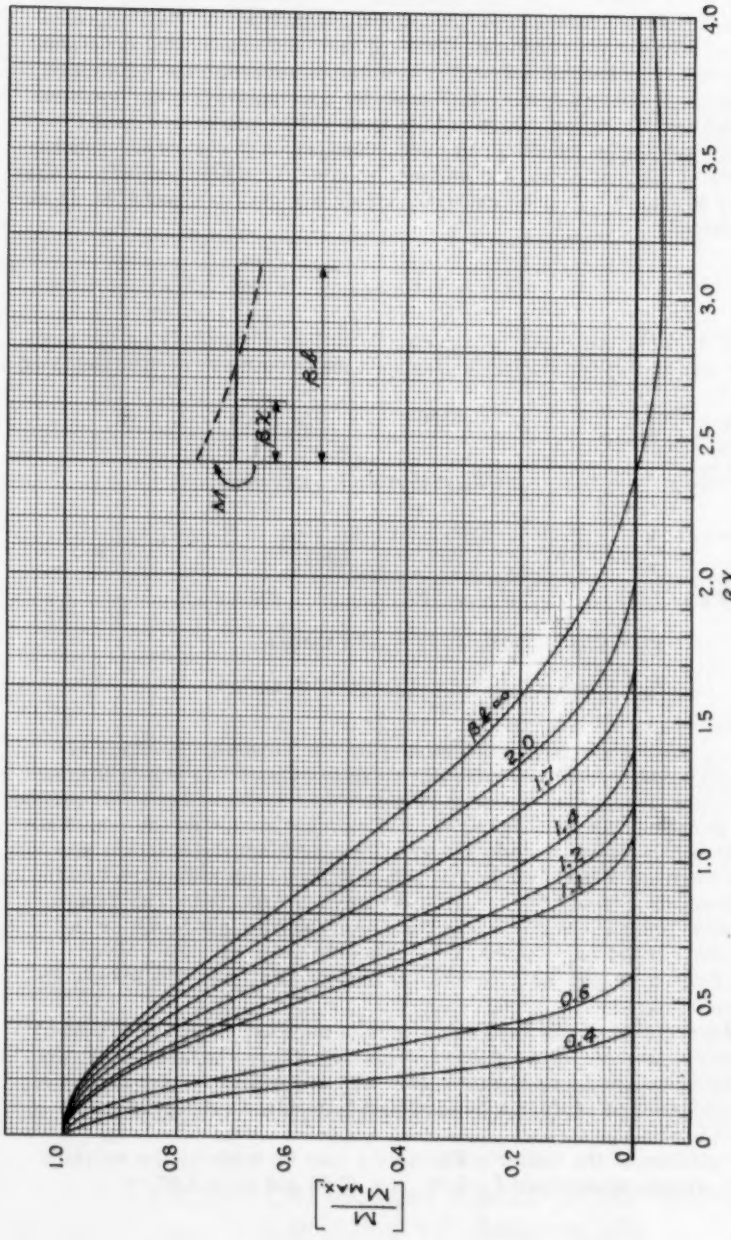

FIG. 8 - Moment at $\beta\chi$, Due to End Moment M, $M_{\beta\chi} = \left[\frac{M}{M_{Max.}}\right] M$

Proceeding in the same manner for other segments, composing and solving six equations, the resulting values of shears and moments were obtained as shown in the writer's Table 4, and the deflections in Table 3. The approximate solution actually preceded the exact solution and shows what precision can be expected from the analysis. The precision, unquestionably, is more than adequate in problems dealing with doubtful constants—variable modulus of foundations and EI values. Fortunately, wide variations in k, E, and I values result, relatively speaking, in minor changes of β and, correspondingly, in deflection, slopes, shear and moment values. This fact permits another more speedy approach to a problem which, from a practical standpoint, is entirely satisfactory.

Simple Solution

Referring again to the author's Example 1, with two end loads on the beam and stepped modulus of foundation, deflections and moments can be calculated as follows:

Assuming k = 650, $\beta = .0259$, $\beta b = 3.11$.

By Eqs. (12a) and (12c),

$$y_A = \left(\sum \frac{Y}{Y_o}\right) \frac{P}{2EI\beta^3} = (1.04 - .25)(.008) = .0063 \text{ inches}$$

$$M_{C_L} = -\left(\sum \frac{M}{M_{max}}\right) \frac{.322P}{\beta} = -(2 \times .67) \frac{.322 \times 100}{.0259} = -1670 \text{ in-lbs.}$$

Assuming k = 150, $\beta = .01797$, $\beta b = 2.16$

$$y_H = (1.1 - .54)(.0239) = .018 \text{ inches}$$

$$M_C = -(2 \times .71) \frac{.322 \times 100}{.01797} = -2540 \text{ in-lbs.}$$

Deflections y_A and y_H are influenced mostly by the foundation modulus at their respective ends and are sufficiently close to be used, as found, without corrections. The average of moments at center line (2105 in-lbs.) will suffice for a quick, practical design. Deflection and moment values for intermediate points can be similarly estimated. It should be noted that the author's Example 1 is a theoretical problem and in actual design such wide variation in modulus of foundation would be objectionable and not expected. The design, no doubt, would consist of some means for improving the foundation or incorporating devices for adjustments in a structure for a possible uneven settlement. Even with such unfavorable foundation conditions, the simple solution is satisfactory.

Clear understanding of physical behavior of a structure must be gained by experience and is prerequisite for good judgment. Thereafter, the developed charts and formulas can be used with confidence and will eliminate almost all subprofessional work in problems dealing with variable elastic properties and modulus of foundation.

A simple solution of the author's Example 2 may be made by the writer's chart, Fig. 9, assuming constant I = 5.33, $\beta = .0755$ and $\beta b = 2.27$.

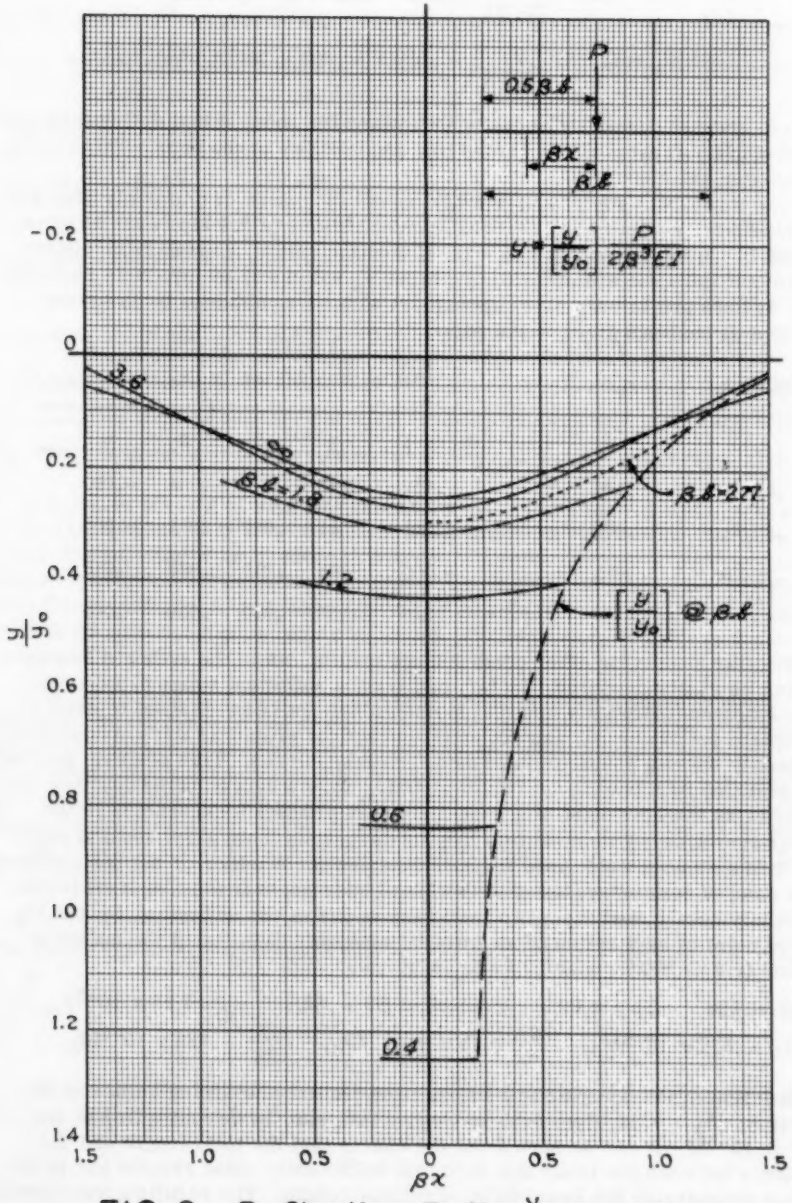

FIG. 9 - Deflection Ratio, $\frac{y}{y_o}$, for Various Lengths of Beams, $\beta\ell$

$$y_{0_L} = (.293)\frac{P}{2EI\beta^3} = .0221 = .148 \times 10^{-3}P, \text{ feet.}$$

$$y_A = (.113)\left(\frac{P}{2EI\beta^3}\right) = .00855 = .057 \times 10^{-3}P, \text{ feet.}$$

Due to greater flexibility of the beam toward the ends, actual deflections are only slightly greater at the center line and smaller at the ends. This can be seen from the chart.

The third example may be readily solved by charts, if uniformly distributed load were replaced by two equal concentrations of 2.4 kips each at points C and D. In the tabulation below the deflection ratios, as read from charts, were multiplied on a slide rule by proper y_o value and the products recorded. The results are in very close agreement with those obtained by the exact method of analysis given in the paper.

Load at	y_o	Deflection Ratios x y_o, inches				
		Point A	B	C	D	E
$.25\beta b$	.148	.037	.043	.021	.003	-.010
$.50\beta b$	.071	-.003	.011	.019	.011	-.003
$.75\beta b$	.071	-.005	.001	.010	.020	.018
	Σ =	.029	.055	.050	.034	.005

Similar charts for other conditions of loading, as in the author's Example 4, can be easily prepared. So far, however, a sufficient range of ratios for concentrated (externally applied) moments has not been obtained to draw a complete set of curves, and not enough practical problems were encountered to justify special preparation of data for these curves. This problem may be exemplified by a cantilever retaining wall where a concentrated moment, applied at an interior point of a base slab, may produce local tension in the foundation area. This condition may be dangerous from a percolation standpoint in retaining walls used for dam abutments. Whether or not the problem is a case of symmetry, the distribution of base pressures in such walls can be easily determined from two linear equations in two unknowns, S_1 and M_1, at the point of application of an external moment. Solution of the author's Example 4 by charts may proceed as follows:

$\beta = .126$, $\beta b = 4.02$, Moment at $\beta x = .50$, $y_o = 4.16 \times 10^{-5}P_o$,
$y_o = .525 \times 10^{-5}M_o$, $\frac{dy_o}{dx} = .525 \times 10^{-5}P_o$, $\frac{dy_o}{dx} = .132 \times 10^{-5}M_o$

Solution of the equation and substitution yield the following values of deflection: $\Delta_A = -.44$, $\Delta_B = -.15$ and $\Delta_E = .198$, each to be multiplied by the factor $10^{-5}M$. It can be seen from the charts that the total length and the distance between the loads are such that sufficiently close results can be obtained considering the beam to be of infinite length. The resulting values will be $\Delta_A = -.81 \times .525 = -.428$, $\Delta_B = -.28 \times .525 = -.147$ and $\Delta_E = 2 \times .185 \times .525 = .194$.

POINTS				
A	B	(B)	B	(B)
Deflection Ratios			Slope Ratios	
		- .97		.95
$-2.0S_1$	$4.02S_1$	$.90S_1$	$11.9S_1$	$.97S$
$-11.8M_1$	$11.9M_1$	$.97M_1$	$23.5M_1$	$-.95M_1$
Deflections			Slopes	
		- .51		.125
$-8.32S_1$	$16.7S_1$	$-3.74S_1$	$6.23S_1$	$.510S_1$
$-6.20M_1$	$6.23M_1$	$.51M_1$	$3.09M_1$	$-.125M_1$

$\Delta_B - \Delta_{(B)} = 20.44S_1 + 5.72M_1 + .51 = 0$, $\phi_B - \phi_{(B)} = 5.72S_1 + 3.214M_1 - .125 = 0$

The charts presented with this discussion give the simplest and quickest method of solution of beams on elastic foundations and will suffice for practical problems. There is no doubt that a set of similar charts to cover a range of beams with variable elastic properties and modulus of foundation will be available to designers, and that solutions of beams on elastic foundation will become as common a problem as solutions of other indeterminate structures.

LYMON C. REESE,[1] A. M. ASCE.—The problem discussed by Professor Malter is encountered in the design of laterally loaded piles. Gleser[(1)] has proposed a numerical method for calculating stresses in soil-supported structures based on the fourth difference equation. The following paragraphs show the application of the Gleser Method to solve Example 1 of the author's paper. A representation of the problem posed in Example 1 is shown in Fig. 1.

The beam is divided into a number of increments of equal length such that

$$h = \frac{L}{n} \tag{1}$$

The fourth difference equation, where y_m is the deflection of the beam at point m, is

$$y_{m-2} - 4y_{m-1} + 6y_m - 4y_{m+1} + y_{m+2} = \frac{k_m}{EI}\left(\frac{L}{n}\right)^4 y_m \tag{2}$$

Considering the laterally loaded pile for the moment, both the shear and moment at the pile tip (at Point O) are equal to zero, or

$$-y_2 + 2y_1 - 2y_{-1} + y_{-2} = 0 \tag{3}$$

1. Associate Prof. of Civ. Eng., Univ. of Texas, Austin, Tex., and Engr., Shell Development Co., Houston, Tex.

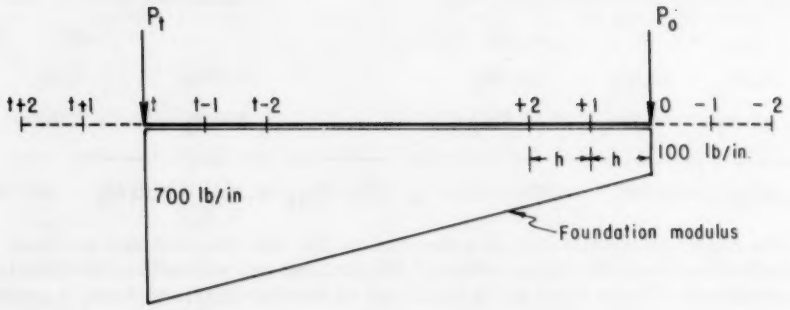

FIGURE 1.
SUBDIVISION OF BEAM FOR DIFFERENCE
EQUATION SOLUTION

and

$$y_1 - 2y_0 + y_{-1} = 0 \tag{4}$$

Using Eqs. (2), (3), and (4), one may start at the pile tip and eliminate the y_{-1} and y_{-2} terms. Successive points up the pile are considered and an expression is derived, as follows:

$$y_m = -B_{2m}\, y_{m+2} + B_{2m+1}\, y_{m+1} \tag{5}$$

where

$$B_{2m} = \frac{1}{6 + A_m - B_{2m-4} - B_{2m-1}\,(4 - B_{2m-3})} \tag{6}$$

$$B_{2m+1} = B_{2m}\,(4 - B_{2m-1}) \tag{7}$$

$$A_m = \frac{k_m}{EI}\left(\frac{L}{n}\right)^4 \tag{8}$$

Eqs. (6) and (7) hold for all the B-values with three exceptions. These exceptions are:

$$B_0 = \frac{2}{A_0 + 2} \tag{9}$$

$$B_1 = 2B_0 \tag{10}$$

$$B_2 = \frac{1}{5 + A_1 - 2B_1} \tag{11}$$

Now in the case of the beam, Example 1 in Professor Malter's paper, shown in Fig. 1, the boundary conditions at Point O are given by Eq. (4) and a new expression, as follows

$$-y_2 + 2y_1 - 2y_{-1} + y_{-2} = -\frac{2P_0\left(\frac{L}{n}\right)^3}{EI} \tag{12}$$

Using Eq. (12) instead of Eq. (3) and proceeding as before, a general expression for y_m is determined, as follows:

$$y_m = -B_{2m}\, y_{m+2} + B_{2m+1}\, y_{m+1} - D_m \tag{13}$$

where

$$D_m = (4 - B_{2m-3})\, D_{m-1} - D_{m-2}\, B_{2m} \tag{14}$$

and all other terms are defined as before. Eq. (14) holds for all D-values with two exceptions. These exceptions are

$$D_0 = -\frac{2P_0\left(\frac{L}{n}\right)^3}{EI\,(A_0 + 2)} \tag{15}$$

$$D_1 = 2D_0B_2 \tag{16}$$

Using Eq. (14) and the boundary conditions at the other end of the beam, Point t, one may calculate expressions for the deflections, as follows

$$y_{t+2} = C_1 B_{2t+1} y_{t+1} - C_1 y_t - C_1 D_t \tag{17}$$

$$y_{t+1} = \frac{(2-B_{2t-1}) y_t + D_{t-1}}{1 - B_{2t-2}} \tag{18}$$

$$y_t = \frac{[E_1 - C_1 D_t - (2-B_{2t-3}) D_{t-1} + D_{t-2}][1-B_{2t-2}] + C_2 D_{t-1}}{C_3(1-B_{2t-2}) - C_2 (2-B_{2t-1})} \tag{19}$$

where

$$C_1 = \frac{1}{B_{2t}} \tag{20}$$

$$C_2 = C_1 B_{2t+1} - 2 - B_{2t-2} (2-B_{2t-3}) \tag{21}$$

$$C_3 = C_1 - B_{2t-4} - B_{2t-1} (2-B_{2t-3}) \tag{22}$$

$$E_1 = \frac{2P_t}{EI} \left(\frac{L}{n}\right)^3 \tag{23}$$

This completes the derivation of the necessary equations. One makes a solution by first calculating A, B, D, C, and E-values; then the y-values at one end of the beam may be calculated by using Eqs. (17) through (19). Finally, Eq. (13) can be used to calculate other y-values.

The Gleser Method was used to solve the problem posed in Example 1, with h taken as 10 inches or n taken as 12. The results are as follows.

Point	y, in.	q, lb/in.
0	0.01918	1.92
1	.01525	2.29
2	.01158	2.32
3	.00834	2.09
4	.00567	1.70
5	.00362	1.27
6	.00222	0.89
7	.00145	0.65
8	.00126	0.63
9	.00160	0.88
10	.00239	1.43
11	.00353	2.29
12	.00487	3.41

Points 0. 4, 8, and 12 correspond to Professor Malter's points D, C, B, and A, respectively.

The author is correct when he states that a method using the fourth difference equation cannot be applied readily to problems involving variable moments of inertia, but the writer and a colleague have formulated the necessary compatibility equations for the Gleser Method for solving the problem of the laterally loaded pile where there is an abrupt change in moment of inertia of the pile.

The Gleser Method is particularly adaptable for use on a high-speed digital computer. For a laterally loaded pile made of three sections, each with a different moment of inertia, a difference equation solution where 50 points are used along the pile can be obtained on the IBM-650 Digital Computer in about three minutes.

It is true that more accurate solutions than those indicated by the author are seldom needed, since the foundation modulus ordinarily cannot be obtained very accurately. However, with regard to the laterally loaded pile, research has been done [2] and is continuing [3] which should allow the soil modulus to be obtained with reasonable accuracy.

It is believed that the Gleser Method can be applied to all of the examples shown in Professor Malter's paper. This method should prove advantageous in certain instances.

REFERENCES

1. Gleser, Sol M. (1953), "Lateral Load Tests on Vertical Fixed-Head and Free-Head Piles." Symposium on Lateral Load Tests on Piles, ASTM Special Technical Publication No. 154.
2. McClelland, Bramlette, and Focht, John A., Jr. (October 1956). "Soil Modulus of Laterally Loaded Piles." Proceedings, American Society of Civil Engineers, Vol. 82, Paper 1081.
3. Matlock, Hudson, and Ripperger, E. A. (1956). "Procedures and Instrumentation for Tests on a Laterally Loaded Pile." Proceedings, Eighth Texas Conference on Soil Mechanics and Foundation Engineering, The University of Texas, Austin.

EARTHQUAKE RESPONSE OF ELEVATED TANKS AND VESSELS[a]

Discussion by A. A. Eremin

A. A. EREMIN,[1] A. M. ASCE.—The authors of this paper have made a valuable contribution by analysing the stresses and damages in water tank towers and refining vessels caused by the recent earthquake shocks in California. The stresses and strains computed with the assumed dynamic forces, according to the spectrum in Figs. A and B are in close agreement with those which have caused damages in these structures. However, in the paper it was stated that "over simplification of dynamic analysis . . . may result in dangerous errors". The purpose of research has always been to find more exact interpretations and to reduce over-simplifications.

In California all structures located in the vicinity of the fault lines are analysed for the effect of earthquake shocks.

Seismic stresses in bridges are computed with the assumed horizontal force V, which is

$$V = CW$$

where W is dead load weight of structure and C is coefficient equal to 0.02, 0.04, and 0.06 for the rock foundation, spread footing and pile foundation respectively.(2) Force V acts in any direction and is applied at the centroid of the dead load weights.

Only minor damage to the anchor bolts in bridges have been reported during the recent earthquake shocks in California. However, it may also be stated that improvement in analysis of the seismic forces in bridges may result in a more economic use of materials.

In a more exact analysis of seismic forces it may be considered that the spectrum shown by the authors in Figs. A and B should include the effect of various foundation soil conditions. Furthermore, the dynamic stresses in water tank towers should consider impact forces caused by the mass of water in the tanks.

In refiner vessels considerable effect on the stresses in the anchor bolts may be produced by transverse vibration of the circular section of the vessels.

Regarding increased horizontal load coefficients in the lower water tank towers, the authors refer to the higher acceleration stresses at the 2% of damping. Similar effect on the stresses in water tank towers may also be explained by the higher vibration frequency in the lower towers.

Discussion of dynamic forces in structures is quite timely. Therefore, the authors deserve high praise for their paper.

---

a. Proc. Paper 1563, March, 1958, by D. F. Moran and J. A. Cheney.

1. Assoc. Bridge Engr., Bridge Dept. Div. of Highways, State Dept. of Public Works, Sacramento, Calif.

REFERENCES

1. Associate Bridge Engineer, Bridge Department, California, State Highways, Sacramento, California.

2. "Highway and Railroad Bridges" by A. A. Eremin, 1956.

MOMENTS IN BEAMS BY THE METHOD OF PARTIAL MOMENTS[a]

Discussion by A. A. Eremin

A. A. EREMIN,[1] A. M. ASCE.—Mr. Posner has shown the simplified method of moment distribution with summation of the partial moments in the continuous beam. Two methods of computing the partial moments have been shown; that is, by algebraic formulas and by the graphical method with the graphs for bending moments, computed for uniformly distributed loading and concentrated unit forces.

The moment distribution method presented by the author has two advantages: It is simple for visual control and it can be checked in the separate steps of computation.

The graphical construction of the partial moments can also be performed directly with the simple bending moment diagram on the loaded span as shown in Fig. 2. The characteristic points on the beam in Fig. 2 are determined by the graphical construction termed "three-line polygon".(1,2) Lines MB and MC drawn through the central moments and points of supports intersect the inflection point verticals at points on the bending moment closing line, Fig. 2.

For the loading given in Fig. 2 the partial moments can be performed by summation in the same manner as shown by the author.

The bending-moment graphs shown by the authors will not be required with the graphical construction in Fig. 2.

The method of moment distribution, using partial moments, should result in savings of time and effort. The author is to be complimented for his valuable paper.

REFERENCES

1. "Simplified Graphical Distribution of Bending Moments", by A. A. Eremin, 1948.
2. Transaction ASCE, 1950, p. 630, discussion of "Arches and Bents".

a. Proc. Paper 1567, March, 1958, by Harry Posner.
1. Assoc. Bridge Engr., Bridge Dept. Div. of Highways, State Dept. of Public Works, Sacramento, Calif.

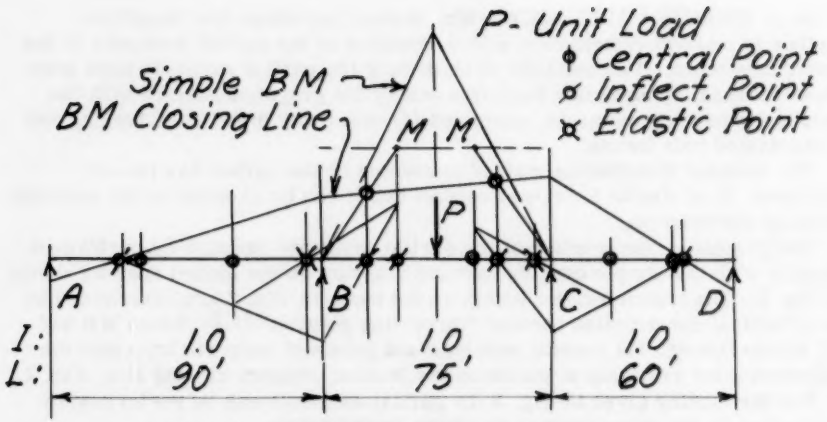

Fig. 2. Partial Moments

DEFLECTION LIMITATIONS OF BRIDGES: PROGRESS REPORT OF THE COMMITTEE ON DEFLECTION LIMITATION OF BRIDGES OF THE STRUCTURAL DIVISION[a]

Discussion by Fritz Leonhardt

FRITZ LEONHARDT,[1] M. ASCE.—In 1946, the writer designed the first extremely slender steel girder bridge across the Rhine from Cologne to Deutz with a depth of only 3.3 m over a large part of the main span of 184 m i.e. a depth-span ratio of 1/56. The writer made this design with the clear knowledge that neither a limitation of the depth-span ratio nor of the deflection is a criterion for the safety or the behaviour of bridges if the factor of safety against the loads is sufficient and if the influence of possible stress oscillations due to vibrations on the ultimate strength is considered correctly. Of course, the structural design must be such that all deformations will be possible without damaging any members, especially those of the floor system.

Meanwhile, the writer designed numerous other bridges with similar or even larger slenderness, built of steel or of prestressed concrete without any unfavorable experience due to such slenderness. Many other European engineers have followed these lines of design and therefore, depth-span ratios of 1/30 to 1/40 are quite common and the deflections may be as high as 1/300 of the span for steel girders. Most of these structures are continuous over many spans.

The vibrations of the main girders become usually more moderate by the larger slenderness and for large spans the frequency of vibration can become so slow that these primary vibrations cannot be felt by pedestrians. Only the secondary vibrations of transverse girders or of stringers may be "annoying" to pedestrians.

In the writer's opinion, passengers of vehicles can usually not feel the vibrations of the bridges, so that in the United States, this point of view should be almost neglectable, having so few pedestrians.

In German design practise, the composite action between the floor system and the main girders is commonly used and the whole structure is considered as an unity in the longitudinal and in the transversal direction. Especially the transversal rigidity gives a good security against excessive vibration due to the damping effect against impacts, caused by loads which are not acting in the center of gravity of the whole cross section. In this way resonance oscillations are very rare.

The possible changes of stresses due to live load and impact are estimated and their influence on the fatigue strength of the material is considered, when

a. Proc. Paper 1633, May, 1958.

1. Consulting and Municipal Engr., Stuttgart, N. Germany.

the allowable stresses or the factor of safety against ultimate load capacity is chosen.

The Rhinebridge of Cologne-Deutz shows not a single damage to its steel structure after more than 10 years of heavy traffic service, under the perhaps heaviest traffic loads for highway bridges due to a high sequence of rapid transit rail cars and a high percentage of heavy trucks amongst the road vehicles. Measurements of the strain oscillations have shown, that the maximum stresses do usually not exceed about 20% of the design stresses due to live load.

With these experiences, in Germany the depth-span ratio is no longer a design criterion for highway bridges.

SPECIFICATIONS FOR PRESERVATIVE TREATMENT OF TIMBER: PROGRESS REPORT OF THE SUB-COMMITTEE ON TIMBER STRUCTURES OF THE STRUCTURAL DIVISION[a]

Discussion by W. H. O'Brien

W. H. O'BRIEN,[1] A. M. ASCE.—Most of the material in this specification is excellent and presents in a very orderly and concise manner pertinent information on the subject. We cannot help but feel, however, that it reflects experience primarily with some of the West Coast species.

Under the paragraph "Preparation of Treatment," it is stated that some species "may be slightly more refractory than others." In the table of Recommended Minimum Net Retentions which conform to the AWPA standards the committee shows 20# for Southern Pine in coastal waters and 14# creosote for Douglas Fir. This difference is due entirely to the treatable characteristics of the two species. The fact is that 14# is practically a limit of the amount of creosote that can be injected into Douglas Fir. This ratio of 14-20 can hardly be referred to as a slight difference.

Under the paragraph heading entitled "Incising," the statement is made "To insure uniform penetration, all sawn material 3" or thicker should be incised on all faces." The way this paragraph reads incising would be required on all species. This is not the case, however, as it is only the refractory species that require incising. The 20# treatment can be obtained in Southern Pine without incising.

The writer is sure that there was no intention to minimize the differences in the treatment characteristics of the species and to leave the impression that any difficulty is encountered in treating Southern Pine. Railroads, Public Service companies and many others with experience in treating of various kinds of lumber will confirm this relationship.

a. Proc. Paper 1637, May, 1958.

1. Chf. Technical Div., Southern Pine Assn., New Orleans, La.

WIND FORCES ON STRUCTURES: NATURE OF THE WIND[a]

Corrections

CORRECTIONS.—On page 1 of Proceedings Paper 1708 please change the word "Girdus" in the listing of Proceedings Paper 1711 to "Girders".

On page 1, in footnote 1, please delete the words "From Master File."

The present Fig. 2A on page 8 is actually Fig. 3 and should, therefore, have been printed on page 13. Fig. 3 on page 13 is actually Fig. 2A and, similarly, should have been printed on page 8.

a. Proc. Paper 1708, July, 1958, by Robert H. Sherlock.

PROCEEDINGS PAPERS

The technical papers published in the past year are identified by number below. Technical-division sponsorship is indicated by an abbreviation at the end of each Paper Number, the symbols referring to: Air Transport (AT), City Planning (CP), Construction (CO), Engineering Mechanics (EM), Highway (HW), Hydraulics (HY), Irrigation and Drainage (IR), Pipeline (PL), Power (PO), Sanitary Engineering (SA), Soil Mechanics and Foundations (SM), Structural (ST), Surveying and Mapping (SU), and Waterways and Harbors (WW), divisions. Papers sponsored by the Board of Direction are identified by the symbols (BD). For titles and order coupons, refer to the appropriate issue of "Civil Engineering." Beginning with Volume 82 (January 1956) papers were published in Journals of the various Technical Divisions. To locate papers in the Journals, the symbols after the paper numbers are followed by a numeral designating the issue of a particular Journal in which the paper appeared. For example, Paper 1449 is identified as 1449 (HY 6) which indicates that the paper is contained in the sixth issue of the Journal of the Hydraulics Division during 1957.

VOLUME 83 (1957)

SEPTEMBER: 1352(IR2), 1353(ST5), 1354(ST5), 1355(ST5), 1356(ST5), 1357(ST5), 1358(ST5), 1359(IR2), 1360 (IR2), 1361(ST5), 1362(IR2), 1363(IR2), 1364(IR2), 1365(WW3), 1366(WW3), 1367(WW3), 1368(WW3), 1369 (WW3), 1370(WW3), 1371(HW4), 1372(HW4), 1373(HW4), 1374(HW4), 1375(PL3), 1376(PL3), 1377(IR2)[c],1378 (HW4)[c], 1379(IR2), 1380(HW4), 1381(WW3)[c], 1382(ST5)[c], 1383(PL3)[c], 1384(IR2), 1385(HW4), 1386(HW4).

OCTOBER: 1387(CP2), 1388(CP2), 1389(EM4), 1390(EM4),1391(HY5), 1392(HY5), 1393(HY5), 1394(HY5), 1395 (HY5), 1396(PO5), 1397(PO5), 1398(PO5), 1399(EM4), 1400(SA5), 1401(HY5), 1402(HY5), 1403(HY5), 1404 (HY5), 1405(HY5), 1406(HY5), 1407(SA5), 1408(SA5), 1409(SA5), 1410(SA5), 1411(SA5), 1412(EM4), 1413 (EM4), 1414(PO5), 1415(EM4)[c], 1416(PO5)[c], 1417(HY5)[c], 1418(EM4), 1419(PO5), 1420(PO5), 1421(PO5), 1422(SA5)[c], 1423(SA5), 1424(EM4), 1425(CP2).

NOVEMBER: 1426(SM4), 1427(SM4), 1428(SM4), 1429(SM4), 1430(SM4)[c]. 1431(ST6), 1432(ST6), 1433(ST6), 1434(ST6), 1435(ST6), 1436(ST6), 1437(ST6), 1438(SM4), 1439(SM4), 1440(ST6), 1441(ST6), 1442(ST6)[c], 1443(SU2), 1444(SU2), 1445(SU2), 1446(SU2), 1447(SU2), 1448(SU2)[c].

DECEMBER: 1449(HY6), 1450(HY6), 1451(HY6), 1452(HY6), 1453(HY6), 1454(HY6), 1455(HY6), 1456(HY6)[c], 1457(PO6), 1458(PO6), 1459(PO6), 1460(PO6)[c], 1461(SA6), 1462(SA6), 1463(SA6), 1464(SA6), 1465(SA6), 1466(SA6)[c], 1467(AT2), 1468(AT2), 1469(AT2), 1470(AT2), 1471(AT2), 1472(AT2), 1473(AT2), 1474(AT2), 1475(AT2), 1476(AT2), 1477(AT2), 1478(AT2), 1479(AT2), 1480(AT2), 1481(AT2), 1482(AT2), 1483(AT2), 1484(AT2), 1485(AT2)[c], 1486(BD2), 1487(BD2), 1488(PO6), 1489(PO6), 1490(BD2), 1491(BD2), 1492(HY6), 1493(BD2).

VOLUME 84 (1958)

JANUARY: 1494(EM1), 1495(EM1), 1496(EM1), 1497(IR1), 1498(IR1), 1499(IR1), 1500(IR1), 1501(IR1), 1502 (IR1), 1503(IR1), 1504(IR1), 1505(IR1), 1506(IR1), 1507(IR1), 1508(ST1), 1509(ST1), 1510(ST1), 1511(ST1), 1512(ST1), 1513(WW1), 1514(WW1), 1515(WW1), 1516(WW1), 1517(WW1), 1518(WW1), 1519(ST1), 1520 (EM1)[c], 1521(IR1)[c], 1522(ST1)[c], 1523(WW1)[c], 1524(HW1), 1525(HW1), 1526(HW1)[c], 1527(HW1).

FEBRUARY: 1528(HY1), 1529(PO1), 1530(HY1), 1531(HY1), 1532(HY1), 1533(SA1), 1534(SA1), 1535(SM1), 1536(SM1), 1537(SM1), 1538(PO1)[c], 1539(SA1), 1540(SA1), 1541(SA1), 1542(SA1), 1543(SA1), 1544(SM1), 1545(SM1), 1546(SM1), 1547(SM1), 1548(SM1), 1549(SM1), 1550(SM1), 1551(SM1), 1552(SM1), 1553(PO1), 1554(PO1), 1555(PO1), 1556(PO1), 1557(SA1)[c], 1558(HY1)[c], 1559(SM1)[c].

MARCH: 1560(ST2), 1561(ST2), 1562(ST2), 1563(ST2), 1564(ST2), 1565(ST2), 1566(ST2), 1567(ST2), 1568 (WW2), 1569(WW2), 1570(WW2), 1571(WW2), 1572(WW2), 1573(WW2), 1574(PL1), 1575(PL1), 1576(ST2)[c], 1577(PL1), 1578(PL1)[c], 1579(WW2)[c].

APRIL: 1580(EM2), 1581(EM2), 1582(HY2), 1583(HY2), 1584(HY2), 1585(HY2), 1586(HY2), 1587(HY2), 1588 (HY2), 1589(IR2), 1590(IR2), 1591(IR2), 1592(SA2), 1593(SU1), 1594(SU1), 1595(SU1), 1596(EM2), 1597(PO2), 1598(PO2), 1599(PO2), 1600(PO2), 1601(PO2), 1602(PO2), 1603(HY2), 1604(EM2), 1605(SU1)[c],1606(SA2), 1607(SA2), 1608(SA2), 1609(SA2), 1610(SA2), 1611(SA2), 1612(SA2), 1613(SA2), 1614(SA2)[c], 1615(IR2)[c], 1616 (HY2)[c], 1617(SU1), 1618(PO2)[c], 1619(EM2)[c], 1620(CP1).

MAY: 1621(HW2), 1622(HW2), 1623(HW2), 1624(HW2), 1625(HW2), 1626(HW2), 1627(HW2), 1628(HW2), 1629 (ST3), 1630(ST3), 1631(ST3), 1632(ST3), 1633(ST3), 1634(ST3), 1635(ST3), 1636(ST3). 1637(ST3), 1638(ST3), 1639(WW3), 1640(WW3), 1641(WW3), 1642(WW3), 1643(WW3), 1644(WW3), 1645(SM2), 1646(SM2), 1647 (SM2), 1648(SM2), 1649(SM2), 1650(SM2), 1651(HW2), 1652(HW2)[c], 1653(WW3)[c], 1654(SM2), 1655(SM2), 1656(ST3)[c], 1657(SM2)[c].

JUNE: 1658(AT1), 1659(AT1), 1660(HY3), 1661(HY3), 1662(HY3), 1663(HY3), 1664(HY3), 1665(SA3), 1666 (PL2), 1667(PL2), 1668(PL2), 1669(AT1), 1670(PO3), 1671(PO3), 1672(PO3), 1673(PL2), 1674(PL2), 1675 (PO3), 1676(PO3), 1677(SA3), 1678(SA3), 1679(SA3), 1680(SA3), 1681(SA3), 1682(SA3), 1683(PO3), 1684 (HY3), 1685(SA3), 1686(SA3), 1687(PO3), 1688(SA3)[c], 1689(PO3)[c], 1690(HY3)[c], 1691(PL2)[c].

JULY: 1692(EM3), 1693(EM3), 1694(ST4), 1695(ST4), 1696(ST4), 1697(SU2), 1698(SU2), 1699(SU2), 1700(SU2), 1701(SA4), 1702(SA4), 1703(SA4), 1704(SA4), 1705(SA4), 1706(EM3), 1707(ST4), 1708(ST4), 1709(ST4), 1710 (ST4), 1711(ST4), 1712(ST4), 1713(SU2), 1714(SA4), 1715(SA4), 1716(SU2), 1717(SA4), 1718(EM3), 1719 (EM3), 1720(SU2), 1721(ST4)[c], 1722(ST4), 1723(ST4), 1724(EM3)[c].

AUGUST: 1725(HY4), 1726(HY4), 1727(SM3), 1728(SM3), 1729(SM3), 1730(SM3), 1731(SM3), 1732(SM3), 1733 (PO4), 1734(PO4), 1735(PO4), 1736(PO4), 1737(PO4), 1738(PO4), 1739(PO4), 1740(PO4), 1741(PO4), 1742 (PO4), 1743(PO4), 1744(PO4), 1745(PO4), 1746(PO4), 1747(PO4), 1748(PO4), 1749(PO4).

SEPTEMBER: 1750(IR3), 1751(IR3), 1752(IR3), 1753(IR3), 1754(IR3), 1755(ST5), 1756(ST5), 1757(ST5), 1758(ST5), 1759(ST5), 1760(ST5), 1761(ST5), 1762(ST5), 1763(ST5), 1764(ST5), 1765(WW4), 1766(WW4), 1767(WW4), 1768(WW4), 1769(WW4), 1770(WW4), 1771(WW4), 1772(WW4), 1773(WW4), 1774(IR3), 1775 (IR3), 1776(SA5), 1777(SA5), 1778(SA5), 1779(SA5), 1780(SA5), 1781(WW4), 1782(SA5), 1783(SA5), 1784 (IR3)[c], 1785(WW4)[c], 1786(SA5)[c], 1787(ST5)[c], 1788(IR3), 1789(WW4).

c. Discussion of several papers, grouped by divisions.

AMERICAN SOCIETY OF CIVIL ENGINEERS

OFFICERS FOR 1958

PRESIDENT

LOUIS R. HOWSON

VICE-PRESIDENTS

Term expires October, 1958:
FRANCIS S. FRIEL
NORMAN R. MOORE

Term expires October, 1959:
WALDO G. BOWMAN
SAMUEL B. MORRIS

DIRECTORS

Term expires October, 1958:
JOHN P. RILEY
CAREY H. BROWN
MASON C. PRICHARD
ROBERT H. SHERLOCK
R. ROBINSON ROWE
LOUIS E. RYDELL
CLARENCE L. ECKEL

Term expires October, 1959:
CLINTON D. HANOVER, Jr.
E. LELAND DURKEE
HOWARD F. PECKWORTH
FINLEY B. LAVERTY
WILLIAM J. HEDLEY
RANDLE B. ALEXANDER

Term expires October, 1960:
PHILIP C. RUTLEDGE
WESTON S. EVANS
TILTON E. SHELBURNE
CRAIG P. HAZELET
DONALD H. MATTERN
JOHN E. RINNE

PAST PRESIDENTS

Members of the Board

ENOCH R. NEEDLES

MASON G. LOCKWOOD

EXECUTIVE SECRETARY

WILLIAM H. WISELY

TREASURER

CHARLES E. TROUT

ASSISTANT SECRETARY

E. LAWRENCE CHANDLER

ASSISTANT TREASURER

CARLTON S. PROCTOR

PROCEEDINGS OF THE SOCIETY

HAROLD T. LARSEN
Manager of Technical Publications

PAUL A. PARISI
Editor of Technical Publications

COMMITTEE ON PUBLICATIONS

HOWARD F. PECKWORTH, *Chairman*

PHILIP C. RUTLEDGE, *Vice-Chairman*

E. LELAND DURKEE
TILTON E. SHELBURNE
R. ROBINSON ROWE
LOUIS E. RYDELL